# Synthesis and Characterization of Platinum(II) Complexes with diazine ligands

Julien R.L. Priqueler

Department of Chemistry

McGill University

Montreal (Qc), Canada

September 2010

## A thesis submitted to the Graduate and Postdoctoral Studies Office in partial fulfillment of the requirement of the degree of

## **Doctor of Philosophy**

© Julien R.L. Priqueler 2010

## **Abstract**

Several series of platinum(II) based complexes have been synthesized. The ligands used include halides and sulfoxides, but also pyrazine and 2,5-dimethylpyrazine. Both diazines were also employed as bridging ligands to prepare dimeric compounds, such as trans, trans-Pt(TMSO)Cl<sub>2</sub>( $\mu$ -pz)Pt(R<sub>2</sub>SO)Cl<sub>2</sub> or trans, trans-{Pt(DEtSO)Cl<sub>2</sub>}<sub>2</sub>( $\mu$ -pz). The complexes have been characterized by IR, Raman and multinuclear magnetic resonance spectroscopies (<sup>1</sup>H, <sup>13</sup>C and <sup>195</sup>Pt). <sup>195</sup>Pt-NMR spectroscopy, a key technique of this project, has been studied more in details in the form of a review paper. The reaction of 2,5-dimethylpyrazine with K[Pt(R<sub>2</sub>SO)Cl<sub>3</sub>] has been investigated and the crystal structures of two dimeric complexes, trans, trans-{Pt(DEtSO)Cl<sub>2</sub>}<sub>2</sub>( $\mu$ -Me<sub>2</sub>pz) and trans, trans-{Pt(DBuSO)Cl<sub>2</sub>}<sub>2</sub>( $\mu$ -Me<sub>2</sub>pz), were determined. Pyrazine was also employed in monomeric compounds, such as cis- Pt(R<sub>2</sub>SO)(pz)l<sub>2</sub>, cis-Pt(pz)<sub>2</sub>X<sub>2</sub> and trans-Pt(pz)<sub>2</sub>X<sub>2</sub>, (X = Cl, I, Br, NO<sub>2</sub>) and trans-Pt(DEtSO)(pz)Cl<sub>2</sub>.

## Résumé

Plusieurs séries de complexes de platine(II) ont été synthétisées. Les ligands employés pour ces synthèses incluent des halogénures, des sulfoxydes, mais aussi la pyrazine et la 2,5-dimethylpyrazine. Les deux diazines ont également été utilisées comme ligands pontées dans la préparation de composés dimériques, tels les *trans,trans*-Pt(TMSO)Cl<sub>2</sub>(μ-pz)Pt(R<sub>2</sub>SO)Cl<sub>2</sub> et les trans, trans-{Pt(DEtSO)Cl<sub>2</sub>}<sub>2</sub>( $\mu$ -pz). Les complexes ont, par la suite, été caracterisés par spectroscopies IR, Raman et RMN multinoyaux (1H, 13C et <sup>195</sup>Pt). La spectroscopie RMN du platine-195, une technique clé de ce projet, a été étudiée plus en détails et a fait l'objet de la publication d'une revue. La réaction de la 2,5-dimethylpyrazine avec le complexe monosubstitué K[Pt(R<sub>2</sub>SO)Cl<sub>3</sub>] a été étudiée et la structure cristalline de deux complexes dimériques, le *trans*, *trans*-{Pt(DEtSO)Cl<sub>2</sub>}<sub>2</sub>(μ-Me<sub>2</sub>pz) le et trans, trans-{Pt(DBuSO)Cl<sub>2</sub>}<sub>2</sub>(μ-Me<sub>2</sub>pz), ont pu être résolues. La pyrazine a également été utilisée dans la synthèse de monomères, tells les cis- Pt(R<sub>2</sub>SO)(pz)I<sub>2</sub>, les cis- $Pt(pz)_2X_2$  et trans- $Pt(pz)_2X_2$ , (X = Cl, I, Br, NO<sub>2</sub>) et les trans- $Pt(DEtSO)(pz)Cl_2$ .

## Acknowledgements

I would first like to thank my research directors, Professor Ian S. Butler and Fernande D. Rochon for their support and encouragement throughout this work. They have been particularly helpful in guiding me for the writing of the review paper on <sup>195</sup>Pt NMR spectroscopy.

I would also like to acknowledge:

- The Department of Chemistry, at McGill University, for the financial support in the form of teaching scholarship.
- Dre. Mirela Barsan for her support, advice, encouragement and friendship over the last five years.
- Dr Majd Fahkfahk for his support and always useful advices
- Dr Christian Tessier for his time with the crystal resolution.
- Martin Baril for his assistance with the Raman spectrometer.

- Mrs. Chantal Marotte for solving any administrative issues so efficiently over the time.
- My colleagues from the laboratory OM335 (McGill University) and from the laboratory CB3475 (UQAM), past and present, who made my experience in the universities unforgettable.
- And finally many thanks to my wife and my kids, Christine, Kyan and MayLee, for their continuous presence, support and encouragement, even in difficult moments.

## **Table of Contents**

Abstract	iiii
Résumé	iv
Acknowledgements	v
Table of Contents	viiii
List of Tables	x
List of Figures	xiii
Note on Units	xvi
List of Abbreviations	xvii
Chapter 1: Introduction	1
1.1-Platinum	1
1.2-Electronic structure of Pt(II) complexes (different theories)	3
1.3-Substitution reactions of the platinum(II) complexes	8
1.4- Trans effect - trans influence	10
1.5-Sulfoxides	18
1.6-Anticancer activity	20
1.7-Raman spectroscopy	30
1.8-Goal of the project	41
References	45
Chapter 2: 195-Pt NMR Spectroscopy	52
2.1-Introduction	54
2.2-Theoretical aspects	57
2.3-Empirical approach	59
2.4-Other considerations	62
2.5-Coupling constants	66
2.6-Liquid state spectroscopy	70
2.7-Solid-state technique	87
2.8-Conclusions	94
References	121
Chapter 3: Pyrazine-bridged mixed-sulfoxides Pt(II) complexes: Synthesis, vibrational (IR	
and Raman) and multinuclear (195Pt, 13C, 1H) NMR spectroscopies of trans-trans-	
Pt(TMSO)Cl <sub>2</sub> (µ-pyrazine)Pt(R <sub>2</sub> SO)Cl <sub>2</sub>	129
3.1-Introduction	129
3.2-Experimental	133

3.3-Result and Discussion	137
3.4-Conclusions	153
References	155
Chapter 4: <i>Trans-trans</i> -{Pt(R <sub>2</sub> SO)Cl <sub>2</sub> } <sub>2</sub> (μ-Me <sub>2</sub> pyrazine)	
R <sub>2</sub> SO = DMSO, TMSO, DEtSO, DPrSO, DBuSO, DBzSO, DPhSO and MeBzSO	167
4.1-Preparation	168
4.2-195Pt, 13C, 1H NMR spectroscopies	177
4.3-IR, Raman	194
4.4-Crystal structures of ({Pt(DEtSO)Cl}_2) $_2$ ( $\mu$ -Me $_2$ pyrazine) and {Pt(DBuSO)Cl}_2) $_2$ ( $\mu$ -	
Me <sub>2</sub> pyrazine))	202
4.5-{Pt(R <sub>2</sub> SO)Cl <sub>2</sub> } <sub>2</sub> (μ-quinoxaline)	224
References	226
Chapter 5: <i>Trans-trans</i> -{Pt(DEtSO)Cl <sub>2</sub> } <sub>2</sub> (μ-pyrazine) and <i>trans</i> -Pt(pyrazine)(DEtSO)Cl <sub>2</sub>	232
5.1-Preparation	233
5.2-195Pt, 13C, 1H NMR spectroscopies	235
5.3-IR, Raman	245
References	251
Chapter 6: Pt(R <sub>2</sub> SO)(pz)I <sub>2</sub> , R <sub>2</sub> SO = DMSO, TMSO, DPrSO, DBuSO, DBzSO	253
6.1-Preparation	254
6.2-195Pt, 13C, 1H NMR spectroscopies	257
6.3-IR, Raman	268
6.4-other attempts	274
References	276
Chapter 7: $Cis$ -Pt(pz) <sub>2</sub> X <sub>2</sub> and $trans$ -Pt(pz) <sub>2</sub> X <sub>2</sub> , X = Cl, I, Br, NO <sub>2</sub>	278
7.1-Preparation	279
7.2- <sup>195</sup> Pt, <sup>13</sup> C, <sup>1</sup> H NMR spectroscopies	282
7.3-Raman	287
References	294
Conclusions, contribution to original knowledge and suggestion for future work	295
References	302

## List of Tables

Table 1.4.1 Rates of substitution of Cl <sup>-</sup> ( <i>trans</i> to Lt) by H <sub>2</sub> O in [PtCl <sub>3</sub> Lt] <sup>n-</sup> complexes]	14
Table 1.4.2 Bond lengths Pt-Cl for several platinum complexes	15
Table 1.6.1 Proportion of the species present in blood plasma and inside the cell during a	
cisplatin injection	23
Table 2.3 Chemical shift summary based on published papers	62
Table 2.6.8 Structure of $Pt_5(\mu\text{-CO})_5(CO)(PCy_3)_4$ (the cyclohexyl rings are omitted for clarity), v	vith
a symmetry plane passing through Pt5-Pt2-Pt1 and the 195Pt-NMR data	83
Table 3.1 Raman spectra of the symmetric dimers Pt(R <sub>2</sub> SO)Cl <sub>2</sub> (μ-pz)Pt(R <sub>2</sub> SO)Cl <sub>2</sub> (5 first	
compounds) and the mixed-ligands dimers Pt(TMSO)Cl <sub>2</sub> (μ-pz) Pt(R <sub>2</sub> SO)Cl <sub>2</sub>	159
Table 3.2 v(Pt-Cl) and v(Pt-S) (cm-1) (1st line IR, 2nd line Raman and symmetric dimer in	
parentheses)	162
Table 3.3 <sup>195</sup> Pt chemical shifts (ppm) of the complexes Pt(TMSO)Cl <sub>2</sub> (μ-pz)Pt(R <sub>2</sub> SO)Cl <sub>2</sub> ,	
compared to the $\delta$ (195Pt) of the symmetric dimer	163
Table 3.4 $\delta(^{1}H)$ and $\delta(^{13}C)$ (ppm) of pyrazine in Pt(TMSO)Cl <sub>2</sub> ( $\mu$ -pz)Pt(R <sub>2</sub> SO)Cl <sub>2</sub> and in the	
symmetric dimer Pt(R <sub>2</sub> SO)Cl <sub>2</sub> (μ-pz)Pt(R <sub>2</sub> SO)Cl <sub>2</sub>	164
Table 3.5 $^{1}\text{H NMR}\ \Delta\delta\ (\delta_{\text{complex}}-\delta_{\text{sulfoxide}})$ (ppm) of the sulfoxide ligands in the complexes	
Pt(TMSO)Cl <sub>2</sub> (µ-pz)Pt(R <sub>2</sub> SO)Cl <sub>2</sub>	165
Table 3.6 $^{13}$ C NMR $\Delta\delta$ ( $\delta$ complex- $\delta$ sulfoxide) (ppm) of the TMSO and R <sub>2</sub> SO in the complexes	
(TMSO)Cl <sub>2</sub> Pt(μ-pz)Pt(R <sub>2</sub> SO)Cl <sub>2</sub>	166
Table 4.1 Experimental conditions and synthesis yields for the $\textit{trans-trans}$ -{Pt(R <sub>2</sub> SO)Cl <sub>2</sub> } <sub>2</sub> ( $\mu$ -	
Me <sub>2</sub> pyrazine) complexes	175
Table 4.2.2.1 <sup>1</sup> H-NMR signals (ppm) and coupling constants (Hz) of the free sulfoxide molecu	ıles
in CDCl <sub>3</sub>	180
Table 4.2.2.2 <sup>13</sup> C NMR (ppm) of the free sulfoxide molecules in CDCl <sub>3</sub>	182
Table 4.2.3.1 $^{195}$ Pt- and $^{1}$ H-NMR chemical shifts and $\Delta\delta$ ( $\delta_{complex}$ - $\delta_{dmpz}$ ) (ppm) of dmpz in the	
complexes {Pt(R <sub>2</sub> SO)Cl <sub>2</sub> } <sub>2</sub> (μ-Me <sub>2</sub> pz)	183
Table 4.2.3.2 $^{13}$ C- NMR chemical shifts and $\Delta\delta$ ( $\delta_{complex}$ - $\delta_{dmpz}$ ) (ppm) of dmpz in the complexes	3
{Pt(R <sub>2</sub> SO)Cl <sub>2</sub> } <sub>2</sub> (μ-Me <sub>2</sub> pz)	188
Table 4.2.3.3 $\delta(^{1}H)$ , $\Delta\delta$ ( $\delta_{complex}$ - $\delta_{sulfoxide}$ ) (ppm) of the sulfoxide ligands in the complexes	
{Pt(R <sub>2</sub> SO)Cl <sub>2</sub> } <sub>2</sub> (μ-Me <sub>2</sub> pz)	190
Table 4.2.3.4 $^{13}$ C NMR $\Delta\delta$ ( $\delta_{complex}$ - $\delta_{sulfoxide}$ ) (ppm) of the sulfoxide ligands in the complexes	
{Pt(R <sub>2</sub> SO)Cl <sub>2</sub> } <sub>2</sub> (μ-2,5-Me <sub>2</sub> pz)	192
Table 4.3.1 Infrared assignments (cm <sup>-1</sup> ) of the complexes {Pt(R <sub>2</sub> SO)Cl <sub>2</sub> } <sub>2</sub> (μ-2,5-Me <sub>2</sub> pz)	195

Table 4.3.2 Raman assignments (cm <sup>-1</sup> ) of the complexes $\{Pt(R_2SO)Cl_2\}_2(\mu-2,5-Me_2pz)$	199
Table 4.4.1.1 Crystal data and structure refinement for {Pt(DEtSO)Cl <sub>2</sub> }(μ-2,5-Me <sub>2</sub> pz)	204
Table 4.4.1.2 Atomic partitioning for the two possible conformations in the crystal framework of	of
{Pt(DEtSO)Cl <sub>2</sub> }(μ-2,5-Me <sub>2</sub> pz)	205
Table 4.4.1.3 Atomic coordinates (x104) and equivalent isotropic displacement parameters (Å	<sup>2</sup> X
10³) for {Pt(DEtSO)Cl <sub>2</sub> }(μ-2,5-Me <sub>2</sub> pz)	206
Table 4.4.1.4 Bond lengths [Å] and angles [°] for {Pt(DEtSO)Cl <sub>2</sub> }(µ-2,5-Me <sub>2</sub> pz)	208
Table 4.4.1.5 Torsion angles [°] for {Pt(DEtSO)Cl₂}(μ-2,5-Me₂pz)	209
Table 4.4.2.1 Crystal data and structure refinement for {Pt(DBuSO)Cl₂}(μ-2,5-Me₂pz)	218
Table 4.4.2.2 Atomic coordinates (x104) and equivalent isotropic displacement parameters (Å	.2 <b>X</b>
10³) for {Pt(DBuSO)Cl <sub>2</sub> }(µ-2,5-Me <sub>2</sub> pz)	219
Table 4.4.2.3 Bond lengths [Å] and angles [°] for {Pt(DBuSO)Cl₂}(μ-2,5-Me₂pz)	221
Table 4.4.2.4 Torsion angles [°] for {Pt(DBuSO)Cl₂}(μ-2,5-Me₂pz)	221
Table 5.2.1 <sup>195</sup> Pt-NMR chemical shifts (ppm) of the Pt(R <sub>2</sub> SO)(pz)Cl <sub>2</sub> and {Pt(R <sub>2</sub> SO)Cl <sub>2</sub> }(μ-	
pz){Pt(R <sub>2</sub> SO)Cl <sub>2</sub> } complexes	236
Table 5.2.2.1 $\delta(^{1}H)$ (ppm), $^{3}J(^{1}H-^{195}Pt)$ (Hz) and $\delta(^{13}C)$ (ppm) of pyrazine in the symmetrical	
{Pt(R <sub>2</sub> SO)Cl <sub>2</sub> }(μ-pz){Pt(R <sub>2</sub> SO)Cl <sub>2</sub> } dimeric compounds	238
Table 5.2.2.2 $^{1}$ H NMR $\Delta\delta$ ( $\delta_{complex}$ - $\delta_{sulfoxide}$ ) (ppm) of the sulfoxide ligands in the <i>trans,trans</i> -	
{Pt(R <sub>2</sub> SO)Cl <sub>2</sub> }(μ-pz){Pt(R <sub>2</sub> SO)Cl <sub>2</sub> } complexes	239
Table 5.2.2.3 $^{13}$ C NMR $\Delta\delta$ ( $\delta_{complex}$ - $\delta_{sulfoxide}$ ) (ppm) of the sulfoxide ligands in the <i>trans,trans</i> -	
{Pt(R <sub>2</sub> SO)Cl <sub>2</sub> }(μ-pz){Pt(R <sub>2</sub> SO)Cl <sub>2</sub> } complexes	240
Table 5.2.3.1 $\delta(^{1}H)$ (ppm), $^{3}J(^{1}H_{a^{-1}}H_{b})$ (Hz) and $\delta(^{13}C)$ (ppm) of pyrazine carbon atoms in the	
trans-Pt(R <sub>2</sub> SO)(pz)Cl <sub>2</sub> monomeric compounds	242
Table 5.2.3.2 $^{1}$ H-NMR $\Delta\delta$ ( $\delta$ <sub>complex</sub> - $\delta$ <sub>sulfoxide</sub> ) (ppm) of the sulfoxide ligands in the Pt(R <sub>2</sub> SO)(pz)C	Cl <sub>2</sub>
complexes	244
Table 5.2.3.3 $^{13}$ C NMR $\Delta\delta$ ( $\delta_{complex}$ - $\delta_{sulfoxide}$ ) (ppm) of the sulfoxide ligands in the Pt(R <sub>2</sub> SO)(pz)( $^{13}$ C NMR $^{1$	Cl <sub>2</sub>
complexes	245
Table 5.3.1 Infrared spectra observed for the coordinated pyrazine and sulfoxide ligands in th	е
DEtSO compounds (cm-1) and assignment of the bands. The Pt-Cl, Pt-N and Pt-S vibrations a	re
also indicated	246
Table 5.3.2 Raman vibrations observed in the <i>trans,trans</i> -{Pt(DEtSO)Cl <sub>2</sub> } <sub>2</sub> (μ-pz) and <i>trans</i> -	
Pt(DEtSO)(pz)Cl <sub>2</sub> compounds	248
Table 6.2.2 <sup>195</sup> Pt NMR chemical shifts (ppm) in the <i>cis</i> -Pt(R <sub>2</sub> SO)(pz)I <sub>2</sub> complexes	258
Table 6.2.3.1 <sup>1</sup> H NMR chemical shifts (ppm) and coupling constants (Hz) of the pyrazine ligan	ıd in
the complexes <i>cis</i> -Pt(R <sub>2</sub> SO)(pz)I <sub>2</sub>	260
Table 6.2.3.2 <sup>13</sup> C NMR chemical shifts (ppm) of the pyrazine ligand in the complexes <i>cis</i> -	
Pt(R <sub>2</sub> SO)(pz)I <sub>2</sub>	261

Table 6.2.4.1 <sup>1</sup> H NMR chemical shifts (ppm) and coupling constants (Hz) of the free sulfoxide	<b>;</b>
ligands in CD <sub>3</sub> COCD <sub>3</sub>	263
Table 6.2.4.2 <sup>13</sup> C NMR chemical shifts (ppm) of the free sulfoxide ligands in CD <sub>3</sub> COCD <sub>3</sub>	264
Table 6.2.4.3 <sup>1</sup> H-NMR chemical shifts (ppm), coupling constants (Hz) of the sulfoxide ligands	in
the <i>cis</i> -Pt(R <sub>2</sub> SO)(pz)I <sub>2</sub> complexes	265
Table 6.2.4.4 <sup>13</sup> C-NMR chemical shifts (ppm) of the sulfoxide ligands in the <i>cis</i> -Pt(R <sub>2</sub> SO)(pz)I	2
complexes	267
Table 6.3.1.1 Vibrations observed for the coordinated pyrazine ligand in the <i>cis-</i> Pt(R <sub>2</sub> SO)(pz)	<b>l</b> <sub>2</sub>
compounds (cm <sup>-1</sup> ) and assignment of the bands	268
Table 6.3.1.2 Comparison between the v(S-O) vibration (cm <sup>-1</sup> ) of the free ligands and the	
$Pt(R_2SO)(pz)X_2$ complexes (X = CI, I)	269
Table 6.3.2 Vibrations observed in the Raman spectra of the coordinated pyrazine ligand in the	ne
$\emph{cis-Pt}(R_2SO)(pz)I_2 \ compounds \ (cm^{-1}) \ and \ assignment \ of \ the \ bands$	271
Table 7.2.2 $^{195}$ Pt-NMR chemical shifts (ppm) for <i>cis</i> - and <i>trans</i> -Pt(pz) <sub>2</sub> (X) <sub>2</sub> , (X = CI, Br, I, NO <sub>2</sub> )	)283
Table 7.2.3 Pyrazine <sup>1</sup> H-NMR chemical shifts (ppm) and coupling constants (Hz) for the <i>cis</i> - a	and
trans-Pt(pz) <sub>2</sub> (X) <sub>2</sub> , (X = CI, Br, I, NO <sub>2</sub> ) complexes	285
Table 7.2.4 Pyrazine <sup>13</sup> C NMR chemical shifts (ippm) in the complexes <i>cis</i> and <i>trans</i> -Pt(pz) <sub>2</sub> (λ	X) <sub>2</sub> ,
(X = CI, Br, I)	287
Table 7.3 Raman bands (in cm <sup>-1</sup> ) of the complexes $cis$ and $trans$ -Pt(pz) <sub>2</sub> (X) <sub>2</sub> (X = Cl, Br, I, NO	<b>)</b> <sub>2</sub> )
	289

## List of Figures

Figure 1.2.1.1 Sketch of square-planar geometry (D <sub>4h</sub> symmetry) for Pt(II)	3
Figure 1.2.1.2 Diagram representing the hybridization of Pt(II) according to the valence bond	
theory.	4
Figure 1.2.2 Energy diagram of the d-orbitals (D <sub>4h</sub> geometry) for Pt(II) complexes	5
Figure 1.2.3 Energy level diagram in square-planar $Pt(II)$ complexes, without any $\pi$ -bonding	7
Figure 1.3.1 Proposed mechanism for nucleophilic substitution in square-planar Pt(II) complex	xes.
	8
Figure 1.3.2 Simplified energy diagram for a substitution reaction in a square-planar Pt(II)	
complex as a function of time.	9
Figure 1.4.1 Simplified sketch of reaction of [PtCl <sub>4</sub> ] <sup>2-</sup> with NH <sub>3</sub> .	11
Figure 1.4.2 Mechanism of formation of <i>cis</i> and <i>trans</i> -Pt(NH <sub>3</sub> ) <sub>2</sub> Cl <sub>2</sub>	. 12
Figure 1.4.3 Approximate order of the <i>trans</i> effect for platinum(II) complexes in water	. 13
Figure 1.4.4 <i>Trans</i> -influence series.	. 16
Figure 1.4.5 Transition state representation of the reaction of trans-PtL(NH <sub>3</sub> )Cl <sub>2</sub> with the Cl-	
ligand.	. 18
Figure 1.5.1 Representation of the different resonance forms of the sulfoxide ligands	. 18
Figure 1.5.2 Representation of the overlap between a sulfur $sp^3$ orbital and the oxygen $2p_x$ or	bital
	. 19
Figure 1.5.3 Representation of the overlap between the sulfur $3d_{xz}$ orbital and the oxygen $2p_z$	
orbital.	. 19
Figure 1.6.1 Monoaquation reaction proposed by Rosenberg in 1978	. 22
Figure 1.6.2 Diaquation reaction proposed by the Miller group.	. 23
Figure 1.6.3 Mechanism of physiological action proposed by House et al	. 25
Figure 1.6.4 Structure of the complex $cis$ -(NH <sub>3</sub> ) <sub>2</sub> Pt{d(pGpG)}, where d(pGpG) = guanine	
desoxyribose phosphate dinucleoside	. 26
Figure 1.6.5 Sketch of the Pt(II) unit binding on two adjacent guanines	. 27
Figure 1.7.1 Light scattered from a molecule.	. 31
Figure 1.7.2 Jablonksi Energy Diagram for Raman Scattering	. 32
Figure 1.7.3 Example of a Raman spectrum.	. 33
Figure 1.7.4 Normal vibrations of CH <sub>3</sub> Cl – Only side views and only one component of each	
degenerate vibration are given.	. 39
Figure 1.7.5 Green, red and NIR 785 nm laser excitation of a fluorescent sample	. 41
Figure 2.1 Examples of platinum-195 NMR chemical shifts	55

Figure 2.4 195Pt chemical shifts of cis-[Pt(HNCOR) <sub>2</sub> (Am) <sub>2</sub> ] in MeOH6	38
Figure 2.6.1 Molecules proposed as CDA and ethylene exchange reaction of complex 1 with	
unsaturated molecules 3	73
Figure 2.6.2 Ethylene exchange reactions with trisubstituted allenes and <sup>195</sup> Pt-NMR analysis of	
the diastereoisomeric mixtures formed from 1c with (a) (RS)-2 and (b) (S)-2 (ee 65%)	74
Figure 2.6.3 Functionalities of the compounds $PtX(2,6-(CH_2NMe_2)_2-4-RC_6H_2)$ (X = halo ligantic properties of the compounds $PtX(2,6-(CH_2NMe_2)_2-4-RC_6H_2)$ ) (X = halo ligantic properties of the compounds $PtX(2,6-(CH_2NMe_2)_2-4-RC_6H_2)$ ) (X = halo ligantic properties of the compounds $PtX(2,6-(CH_2NMe_2)_2-4-RC_6H_2)$ ) (X = halo ligantic properties of the compounds $PtX(2,6-(CH_2NMe_2)_2-4-RC_6H_2)$ ) (X = halo ligantic properties of the compounds $PtX(2,6-(CH_2NMe_2)_2-4-RC_6H_2)$ ) (X = halo ligantic properties of the compounds $PtX(2,6-(CH_2NMe_2)_2-4-RC_6H_2)$ ) (X = halo ligantic properties of the compounds $PtX(2,6-(CH_2NMe_2)_2-4-RC_6H_2)$ ) (X = halo ligantic properties of the compounds $PtX(2,6-(CH_2NMe_2)_2-4-RC_6H_2)$ ) (X = halo ligantic properties of the compounds $PtX(2,6-(CH_2NMe_2)_2-4-RC_6H_2)$ ) (X = halo ligantic properties of the compounds $PtX(2,6-(CH_2NMe_2)_2-4-RC_6H_2)$ ) (X = halo ligantic properties of the compounds $PtX(2,6-(CH_2NMe_2)_2-4-RC_6H_2)$ ) (X = halo ligantic properties of the compounds $PtX(2,6-(CH_2NMe_2)_2-4-RC_6H_2)$ ) (X = halo ligantic properties of the compounds $PtX(2,6-(CH_2NMe_2)_2-4-RC_6H_2)$ ) (X = halo ligantic properties of the compounds $PtX(2,6-(CH_2NMe_2)_2-4-RC_6H_2)$ ) (X = halo ligantic properties of the compounds $PtX(2,6-(CH_2NMe_2)_2-4-RC_6H_2)$ ) (X = halo ligantic properties of the compounds $PtX(2,6-(CH_2NMe_2)_2-4-RC_6H_2)$ ) (X = halo ligantic properties of the compounds $PtX(2,6-(CH_2NMe_2)_2-4-RC_6H_2)$ ) (X = halo ligantic properties of the compounds $PtX(2,6-(CH_2NMe_2)_2-4-RC_6H_2)$ ) (X = halo ligantic properties of the compounds $PtX(2,6-(CH_2NMe_2)_2-4-RC_6H_2)$ ) (X = halo ligantic properties of the compounds $PtX(2,6-(CH_2NMe_2)_2-4-RC_6H_2)$ ) (X = halo ligantic properties of the compounds $PtX(2,6-(CH_2NMe_2)_2-4-RC_6H_2)$ ) (X = halo ligantic properties of the compounds $PtX(2,6-(CH_2NMe_2)_2-4-RC_6H_2)$ )	ıd,
R = amino acid or peptide).	75
Figure 2.6.4 Reaction with $SO_2$ and the $^{195}\text{Pt-NMR}$ chemical shifts of the different compounds. $^{75}$	77
Figure 2.6.5 Some thiazole compounds prepared by the group of Farrell	78
Figure 2.6.6 Preparation of Pt(II) complexes with methyl derivatives of thiourea	79
Figure 2.6.7 Water-soluble compound [Pt(terpy)(S-carborane)](OTf)2 for potential use as a BNC	T
agent	80
Figure 2.6.8 Structure of $Pt_5(\mu\text{-CO})_5(CO)(PCy_3)_4$ , with a symmetry plane passing through Pt5-	
Pt2-Pt1 and the <sup>195</sup> Pt-NMR data	82
Figure 2.6.9 (A) Reaction with GSH as monitored by $^{195}$ Pt-NMR spectroscopy from t = 0.5-7.5 h	۱.
(B) Spectrum of the final product $[{trans-Pt(SG)(NH_3)_2}_2\mu-(SG)]^+$ (VI) at t = 12 h. Proposed	
reaction pathway in the reaction of the dinuclear platinum drugs with glutathione (X = Cl, $H_2O$ or	
H <sub>2</sub> N(CH <sub>2</sub> ) <sub>6</sub> NH <sub>3</sub> <sup>+</sup> )	86
Figure 2.7.1 Position of the <sup>195</sup> Pt-NMR resonances for several compounds	89
Figure 2.7.2 General form of line shapes expected for a sample of small platinum particles which	:h
are clean (a) and coated (b) with adsorbed molecules.	90
Figure 2.7.3 Point-by-point <sup>195</sup> Pt-NMR spectra (solid circles) and simulation of 2.5-nm carbon-	
supported Pt electrocatalysts with and without adsorbates.	92
Figure 2.7.4 Relationship between the healing length and electronegativity as determined from	
the equation.	93
Figure 3.3.4 Scheme of the complexes	47
Figure 4.1 Mechanism for the possible formation of the monomeric compound	77
Figure 4.2.1.1 <sup>1</sup> H-NMR spectrum of free 2,5-dimethylpyrazine	78
Figure 4.2.1.2 <sup>13</sup> C-NMR spectrum of free 2,5-dimethylpyrazine	79
Figure 4.2.3 $^{13}\text{C}$ NMR spectrum of the $\{Pt(DEtSO)Cl_2\}_2(\mu\text{-Me}_2pz)$ taken in CDCl3	89
Figure 4.4.1.1 ORTEP view of (I) (disorder, 2 orientations) showing the numbering scheme	
adopted	ე7
Figure 4.4.1.2 ORTEP view of (I) (conformation 1) showing the numbering scheme adopted 2	10
Figure 4.4.1.3 ORTEP view of (I) (conformation 2) showing the numbering scheme adopted 2	10
Figure 4.4.1.4 ORTEP view of (I) (conformations 1 and 2) showing the numbering scheme	
adopted	12
Figure 4.4.2.1 ORTEP view of (II) showing the numbering scheme adopted	20

Figure 5.2.1 $^{195}$ Pt NMR spectrum of the {Pt(DEtSO)Cl <sub>2</sub> }( $\mu$ -pz){Pt(DEtSO)Cl <sub>2</sub> } compound	237
Figure 5.2.2 Sketch of the electronic inverse polarization of the S-O $\pi$ bond in <i>trans,trans</i> -	
$Pt(R_2SO)Cl_2$ ( $\mu$ -pz) $Pt(R_2SO)Cl_2$ complexes.	241
Figure 6.2.4.3 <sup>1</sup> H NMR spectrum of the <i>cis</i> -Pt(DMSO)(pz)I <sub>2</sub> complex in the sulfoxide region	
$(^{3}J(^{195}Pt^{-1}H) = 23.4Hz)$	266
Figure 7.3 Raman spectra of <i>cis</i> -Pt(pz) <sub>2</sub> Br <sub>2</sub> between 950 and 175cm <sup>-1</sup>	388
Figure 8 Sketch of the ORTEP structure of the mixed-geometry dimeric species cis,trans-	
{Pt(DPrSO)Cl <sub>2</sub> } <sub>2</sub> (μ-pz)	298

## Note on Units

The following units have been used in this thesis for historical reasons. Their definitions and SI equivalents are given below.

Physical Quantity	Symbol	SI Units	Units Used
wavenumber	ν	m <sup>-1</sup>	cm <sup>-1</sup> ( = 100 m <sup>-1</sup> )
pressure	р	Pa (N m <sup>-2</sup> )	kbar ( = 10 <sup>8</sup> Pa)
cell constants	a,b,c	m	Å ( = 10 <sup>-10</sup> m)

## List of Abbreviations, Acronyms and Symbols

°C degree Celsius

Å angstrøm (equivalent to 10<sup>-10</sup> m)

δ chemical shift (in ppm)

ρ density

acac acetylacetonate

acenap acenaphthene

Asp L-aspartate

AT acquisition time

Boh 2-(3-hydroxypropylamino)-6-benzylamino-9-isopropylpurine

bpy 2,2'-bipyridine

bpydicar 2,2'-bipyridine-5,5'-dicarboxylate

cm<sup>-1</sup> centimetre<sup>-1</sup> (frequency unit)

COD 1,5-cyclooctadiene

dach 1,2-diaminocyclohexane

damch 1,1-di(aminomethyl)cyclohexane

DBuSO di-n-butylsulfoxide

**DBzSO** dibenzylsulfoxide

dcpe bis(dicyclohexylphosphino)ethane

decomposition (temperature) decomp.

Diethylsulfoxide **DEtSO** 

6,8-dimethylimidazo-1,3,5-triazin-4(3H)-one diMe-4-O-

IMT

6,8-dimethyl-2-thioxo-2,3-dihydroimidazo-1,3,5-triazin-4(1H)diMe-4-O-2-S-

IMT one

DMF N,N'-dimethylformamide

dimethylsulfoxide **DMSO** 

diphenylsulfoxide DPhSO

**DPrSO** di-n-propylsulfoxide

dppa bis(diphenylphosphino)acetylene dppam bis(diphenylphosphino)ammine

dppe bis(diphenylphosphino)ethane

dppf bis(diphenylphosphino)ferrocene

dppm bis(diphenylphosphino)methane

dppn bis(diphenylphosphino)naphthalene

en ethylenediamine

FB filter bandwidth

Glu L-glutamate

GMP guanosine 5'-monophosphate

Guo guanosine

Hbph- $\eta^1$ -byphenylmonanion

Hz hertz (cycle by second)

HOMO highest occupied molecular orbital

IR infrared spectroscopy

coupling constant between two nucleus separated by y bonds

PrOc 2-(2-hydroxyethylamino)-6-benzylamino-9-isopropylpurine

LUMO lowest unoccupied molecular orbital

M molarity (number of mols by litre)

MeBzSO methylbenzylsulfoxide

nap naphthalene

non<sub>2</sub>bpy 4,4'-dinonyl-2,2'-bpyridine

NT number of transients

Oc 2-(2-hydroxyethylamino)-6-benzylamino-9-methylpurine

 $\pi_h$  Orbitals orbitals in the plane of the complex having the optimum

symmetry to undergo a  $\pi$  interaction

 $\pi_v$  Orbitals orbitals perpendicular to the plane of the complex having the

optimum symmetry to undergo a  $\pi$  interaction

pdn pyridazine

phen 1,10-phenanthroline

phenan phenanthrene

pic picoline

pm pyrimidine

ppm part per million

PW pulse width

py pyridine

pz pyrazine (1,4-diazine)

quin quinoline

qx quinoxaline

R1 reliability factor

Ref reference

Ros 2-(R)-(1-ethyl-2-hydroxyethylamino)-6-benzylamino-9-

isopropylpurine

SW spectral width

TMSO tetramethylenesulfoxide

tmtu tetramethylthiourea

wR2 weighted reliability factor

Z number of formula per unit cell

#### **CHAPTER I**

#### **INTRODUCTION**

#### 1.1 Platinum

Platinum was discovered in South America in the 16<sup>th</sup> century. The coordination chemistry of the element began to develop following the preparation of Zeise's salt, K[PtCl<sub>3</sub>(C<sub>2</sub>H<sub>4</sub>)]'H<sub>2</sub>O, around 1830, one of the first organometallic compounds to be reported (1,2). Its inventor, W.C. Zeise, a professor at the University of Copenhagen, prepared this salt while investigating the reaction of K<sub>2</sub>[PtCl<sub>4</sub>] with boiling ethanol. The structure could not be explained until the advent of X-ray diffraction, showing the nature of the platinum-ethylene bond. Platinum chemistry became even more popular after the wide-scale acceptance of the so-called *trans effect*, which was originally proposed by the Russian scientist Chernayev at the beginning of the 20<sup>th</sup> century (3). Platinum is a noble transition metal and *aqua regia* 

(royal water, a mixture of nitric and hydrochloric acids in a 1:3 volumetric ratio) is the only reagent that dissolves the metal leading to the formation of  $H_2[PtCl_6]$ . This platinum(IV) salt can be reduced to give the anionic platinum(II) complex,  $[PtCl_4]^2$ -(4), which is frequently used as a starting reagent in platinum coordination chemistry. Platinum has 32 isotopes, of which only three have non-negligible natural abundances. These are Pt-194, Pt-195 and Pt-196 with abundances of 32.9, 33.8 and 25.3%, respectively. Platinum exists in the oxidation states 0, +2 and +4. The most stable form in aqueous solution is the divalent state. The +1 and +3 states are also known, but these are quite rare.

Stable mononuclear platinum(II) complexes can be prepared with  $\sigma$ - and  $\pi$ -donor ligands. These ligands can be monodentate anions, such as halides (with the exception of fluoride), nitrates, nitrites, sulphites and carboxylates, and they can also be neutral ligands containing groups IV, V and VI donor atoms. Generally, heavy atoms have free d-orbitals that can accept electrons from the  $d_{xy}$ ,  $d_{xz}$  and  $d_{yz}$  platinum orbitals to form multiple character bonds (i.e.,  $\sigma$ -bond formation by ligand-to-platinum donation  $L \to M$  and  $\pi$ -bond formation by platinum-to-ligand retrodonation  $M \to L$ ). Like the fluorine atom, oxygen does not have any d-orbitals, and so it only has a very weak affinity for platinum. This situation explains why the sulfoxide–platinum bond occurs through the sulfur atom. Platinum(II) complexes can also be prepared with bidentate, tridentate or tetradentate ligands, even if the latter have a tendency to increase the platinum coordination from four to five.

#### 1.2 Electronic structure of platinum(II) in coordination complexes

## 1.2.1 Valence bond theory

The ground-state electronic configuration of Pt(II) is  $[Xe]4f^{14}5d^8$  and there are eight paired d-electrons. Among the nine available orbitals (5d, 6s and 6p), those used to form  $\sigma$ -bonds, for symmetry reasons, are the  $5d_{x}^{2}$ - $_{y}^{2}$ ,  $6p_{x}$ ,  $6p_{y}$  and a combination of the 6s and  $5d_{z}^{2}$  orbitals. The contribution of the  $5d_{z}^{2}$  orbital is very weak, because it is perpendicular to the coordination plane and the resulting orbital has a predominant s character (4). According to the valence bond theory, the consequence of this situation is  $dsp^{2}$  hybridization, which leads to Pt(II) complexes having square-plane geometry (Fig. 1.2.1.1).

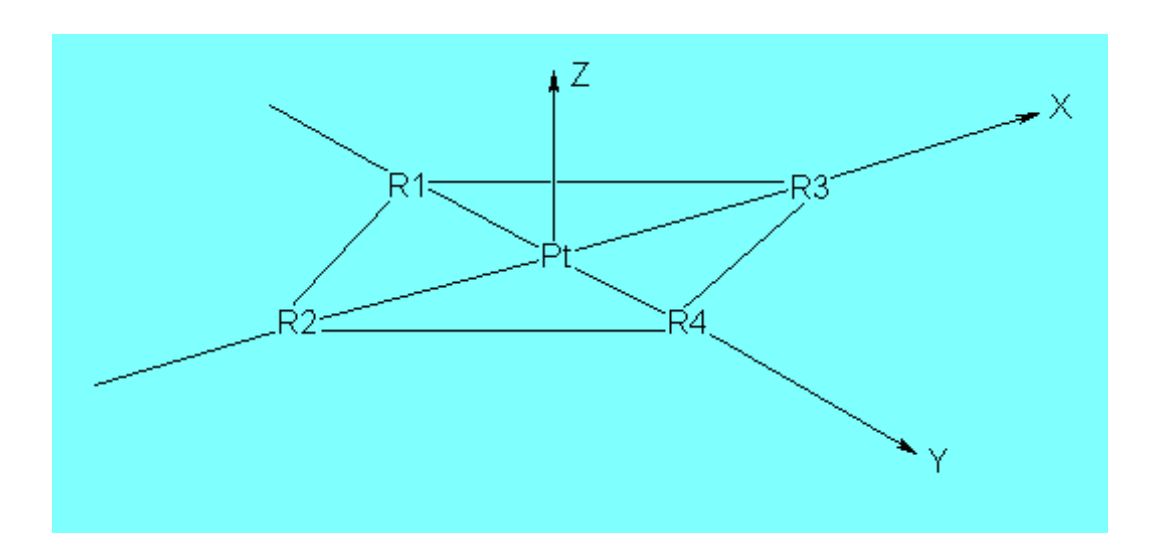
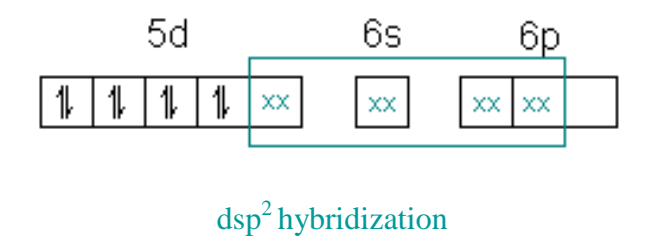


Figure 1.2.1.1 Sketch of square-planar geometry ( $D_{4h}$  symmetry) for Pt(II).

Therefore, valence bond theory indicates that the square-planar geometry of Pt(II) is the result of  $dsp^2$  hybridization  $(d_x^2)_y^2$ , s,  $p_x$  and  $p_y$ ) (Fig. 1.2.1.2). The metal has four hybridized orbitals in which the lobes point towards the corners of a square, all in the same plane.



**Figure 1.2.1.2** Diagram representing the hybridization of Pt(II) according to the valence bond theory.

This representation explains the fact that such Pt(II) complexes are diamagnetic (magnetic moment equal to zero). The hybridization, however, involves only the external orbitals (or valence orbitals). It does not take into account the other orbitals, in particular, the antibonding orbitals. Therefore, valence bond theory is useless in interpreting the electronic spectra of coordination complexes. On the other hand, crystal field theory does permit the explanation of the electronic spectra of some simple molecules.

#### 1.2.2 Crystal field theory

When ligands get close to the Pt d-orbitals, an electrostatic field is created and this is the origin of the crystal field theory. The five d-orbitals are no longer degenerate (5). Those orbitals which point towards the ligands will be the most energetic (Fig. 1.2.2). The greater the electrostatic field caused by the ligands, the larger will be the energy gap between the  $d_{xy}$  and  $d_{x-y}^{2}$  orbitals. According to the Spectrochemical Series, the sulfoxide and diazine (pyrazine, dimethylpyrazine, quinoxaline) ligands, which were used in this thesis work, lead to strong and medium crystal fields, respectively. Whatever the situation, however, Pt(II) having eight paired d-electrons means that square planar Pt(II) complexes are always diamagnetic.

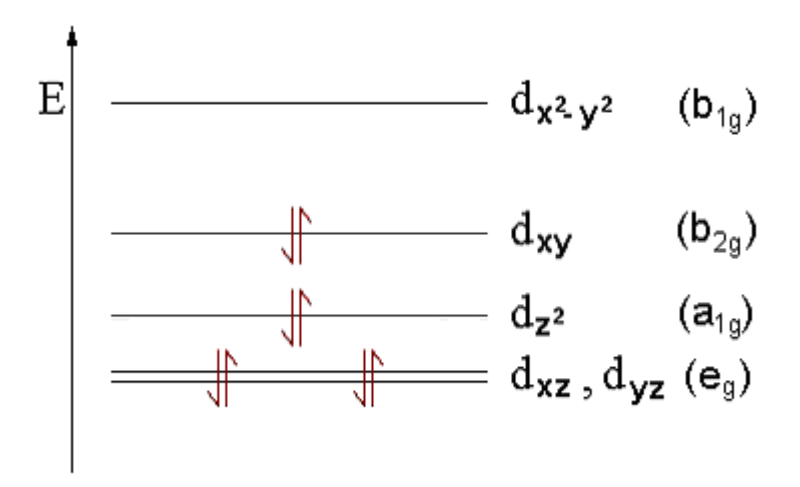
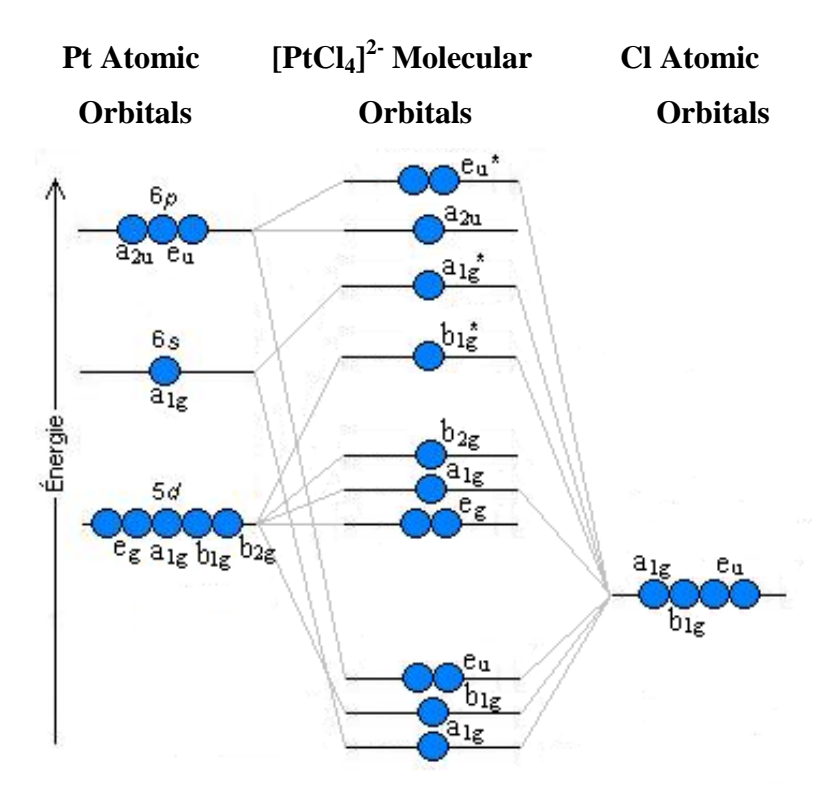


Figure 1.2.2 Energy diagram of the d-orbitals ( $D_{4h}$  geometry) for Pt(II) complexes.

Crystal field theory can explain the electronic spectra of some simple molecules quite well. Three electronic transitions are expected for Pt(II) complexes, but the intensities are weak.

### 1.2.3 Molecular orbital theory

Molecular orbital theory is the most complete bonding theory. It is based on the overlap of the metal and ligand orbitals, when the orbital symmetries permit it. When metal atomic orbitals combine with  $\sigma$ -bonding orbitals of ligands,  $\sigma$ -bonding molecular orbitals are produced. The simplified diagram below describes the bonding in the square-planar [PtCl<sub>4</sub>]<sup>2</sup>-structure; any possible  $\pi$ -bonding interactions have been omitted (Fig. 1.2.3).



**Figure 1.2.3** Energy level diagram in square-planar Pt(II) complexes, without any  $\pi$ -bonding.

In  $[PtCl_4]^{2-}$ , the metal d-orbitals lose their degeneracy leading to five molecular orbitals with the following symmetries:  $e_g(d_{xz}, d_{yz})$ ,  $a_{1g}(d_z^2)$ ,  $b_{2g}(d_{xy})$  and  $b_{1g}(d_x^2)$ . In the same way, the p-level leads to three molecular orbitals with the symmetries:  $a_{2u}(p_z)$  and  $e_u(p_x, p_y)$ . The orbital symmetries of the four chloride ligands used in creating the  $\sigma$  bonds are  $a_{1g}$ ,  $b_{1g}$  and  $e_u$ .

Possible bonding interactions of the  $\pi$ -type could also been considered, and this makes the structural description of the complexes much more complicated (6). The  $b_{2g}$ ,  $e_g$  and  $a_{2u}$  molecular orbitals are non- $\sigma$ -bonding, but they could overlap with ligand  $\pi$ -orbitals to form bonding and antibonding molecular orbitals of the type  $\pi_1$ .

## 1.3 Substitution reactions of the platinum(II) complexes

In square-planar Pt(II) complexes, the  $d_x^2$ ,  $p_x^2$ , s,  $p_x$  and  $p_y$  orbitals are  $dsp^2$  hybridized and are all occupied. The  $p_z$  orbital is empty. Huheey *et al.* (7) have suggested a bimolecular nucleophilic  $S_N2$  mechanism for substitution reactions of square-planar Pt(II) complexes. The metal center is attacked by a nucleophile  $P_x$ 0 Nu, which leads to a square-pyramidal intermediate (Fig. 1.3.1 b), where the  $p_z$ 1 orbital is occupied. To reduce the steric hindrance, this intermediate changes to a trigonal bipyramid (Fig. 1.3.1 c). The ligands,  $P_x^2$ 1 and  $P_x^2$ 2 retain their axial position, whereas the entering nucleophile ( $P_x^2$ 2 nucleophile ( $P_x^2$ 3 nucleophile ( $P_x^2$ 4 nucleophile ( $P_x^2$ 5 nucleophile ( $P_x^2$ 6 nucleophile ( $P_x^2$ 6 nucleophile ( $P_x^2$ 7 nucleophile ( $P_x^2$ 8 nucleophile ( $P_x^2$ 8 nucleophile ( $P_x^2$ 9 nucleophile (P

**Figure 1.3.1** Proposed mechanism for nucleophilic substitution in square-planar Pt(II) complexes.

The trigonal bipyramidal species can occur as an activated complex or as a reaction intermediate. The life-time of each species allows a distinction to be made between the two cases. The energy profile of such a reaction is given in Fig. 1.3.2.

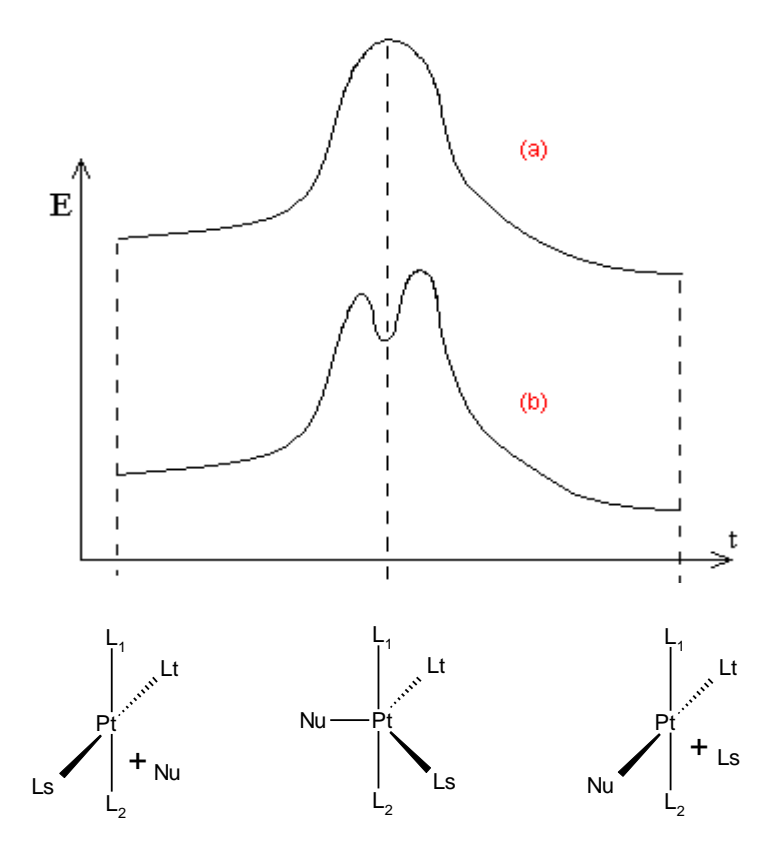


**Figure 1.3.2** Simplified energy diagram for a substitution reaction in a square-planar Pt(II) complex as a function of time.

The activated complex (a) is related to the transition state at the vertex of the energy curve, whereas the reaction intermediate (b) indicates that the species has a measurable life-time. Furthermore, this latter is more stable than is the activated complex formed during the reaction.

There are numerous factors that could influence the substitution reactions in Pt(II) complexes. Among these factors, the most important are probably the nature of the entering and leavings groups, the solvent effect, the chelate effect, the steric hindrance and the *trans* effect, which will be discussed in the next section.

#### 1.4 Trans effect and trans influence

As mentioned earlier, the discovery of important deposits of platinum minerals in Russia was the starting point of an intensive study of platinum compounds. A consequence of these studies by the Russian school was the identification of the first stereospecific substitution reaction, and the first example of the *trans* effect. The concept of *trans* effect was introduced by Chernyaev in 1926 to explain the experimental results obtained for several square-planar Pt(II) complexes (3). These results included kinetic and thermodynamic data. Chernyaev noticed that the rate of substitution of a group bound to the Pt center was strongly influenced by the nature of the group which was located diagonally to it, i.e. the group in the *trans* position. In the example given below (Fig. 1.4.1), the second NH<sub>3</sub> molecule goes preferentially into the *cis* position to the other NH<sub>3</sub> group, which is already bound to the Pt center. This situation is the consequence of the larger *trans* effect of Cl<sup>-</sup> in comparison with that of NH<sub>3</sub>.

CI CI CI NH<sub>3</sub>

$$+ NH_3 + NH_3 + NH_3$$
CI CI NH<sub>3</sub>

$$+ NH_3 + NH_3 + NH_3$$
CI NH<sub>3</sub>

**Figure 1.4.1** Simplified sketch of reaction of [PtCl<sub>4</sub>]<sup>2-</sup> with NH<sub>3</sub>.

Soon after the introduction of the *trans*-effect concept by Chernyaev, Grinberg *et al.* put forward the first hypothesis as to its origin (8). They considered the polarizabilities of the various groups coordinated to the central platinum atom. Any asymmetry in the charge distribution will result in a polarization of the platinum atom. The bond most affected by this result will be the bond *trans* to the most polarizable group. This explanation can satisfactorily account for the *trans* effects of the halides, but it is insufficient for other ligands.

Another hypothesis takes into account  $\pi$ -bonding to explain the larger *trans* effects of ligands such as  $C_2H_4$ ,  $CN^-$  and CO. A stronger  $\pi$ -bond with the ligand Lt (Fig. 1.3.1) will weaken the bond with the group Ls located in the *trans* position, thereby stabilizing the pentacoordinated intermediate (c). The position of  $C_2H_4$ ,  $CN^-$  and CO on the left-hand side of the Spectrochemical Series (Fig. 1.4.3) suggests that the increase of the reaction rates observed for these ligands stems from their ability to decrease the energy of the transition state. The Pt-Lt  $\pi$ -bond diminishes the  $\pi$ -electronic density in the position opposite. Ligands which are good  $\pi$ -acceptors also facilitate the equatorial position of the trigonal bipyramidal intermediate.

A more recent theory takes into account reaction mechanisms - this is the electrostatic kinetic theory. For the nucleophilic substitution mechanism (see Fig. 1.3), Cardwell suggested that the most rapidly formed trigonal bipyramid (Fig. 1.3.1 (c)) is the one with the most electroattracting ligands located at the vertices of the bipyramid ( $L_1$  and  $L_2$ ). The formation of *cisplatin* and *transplatin* will serve to illustrate this theory.

Figure 1.4.2 Mechanism of formation of *cis* and *trans*-Pt(NH<sub>3</sub>)<sub>2</sub>Cl<sub>2</sub>.

Because of its charge, the Cl<sup>-</sup> ligand is less electroattracting than is NH<sub>3</sub>, and so the approach of the HOMO orbital of NH<sub>3</sub> is facilitated if the Cl<sup>-</sup> ion in the *trans* position moves away from the entering ligand. Therefore, in the formation of *cisplatin*, the NH<sub>3</sub> ligand receives more resistance from the two Cl<sup>-</sup> ligands *trans* to each other than from the NH<sub>3</sub>-Cl pair. The entering NH<sub>3</sub> ligand will then move away

from the two chlorides in the plane, where there is less repulsion (angles = 120°), and NH<sub>3</sub> will be located at the vertex of the bipyramid. In the case of *transplatin*, the Cl-NH<sub>3</sub> pair provides more resistance to the entering Cl<sup>-</sup> ligand than does the NH<sub>3</sub>-NH<sub>3</sub> pair. NH<sub>3</sub>-Cl will be part of the trigonal plane whereby the *trans* complex is formed.

Nowadays, the *trans* effect is defined by the ability of a ligand to generate a labilization to the group located in a position *trans* to it (9). The *trans* effect can be used, for instance, to explain the chemical reactivity between the *cis* and *trans* isomers of PtL<sub>2</sub>X<sub>2</sub>. The *cis*-Pt(NH<sub>3</sub>)<sub>2</sub>Cl<sub>2</sub> complex reacts with thiourea (tu) to give [Pt(tu)<sub>4</sub>]Cl<sub>2</sub>, whereas its *trans* analogue gives the *trans*-Pt(tu)<sub>2</sub>Cl<sub>2</sub> complex (6). The approximate order of the *trans* effect, especially based on the synthesis of platinum(II) complexes and their reactions, is given on the Figure 1.4.3 (10).

**Figure 1.4.3** Approximate order of the *trans* effect for platinum(II) complexes in water.

The *trans* effect spreads over several orders of magnitude. This situation can be illustrated by the rate of substitution of the  $Cl^-$  ion by  $H_2O$  in  $[PtCl_3L]^{n-}$  complexes (Table 1.4.1). The *trans* effect is thus a kinetic effect.

$$\begin{array}{c|cccc}
CI & & & CI \\
 & & & & \\
\hline
CI & & & & \\
Pt & & Lt & & \\
\hline
CI & & & & & \\
CI & & & \\
\hline
CI & & & \\
CI & & & \\
\hline
CI & & & \\
CI & & & \\
\hline
CI & & & \\
CI & & & \\
\hline
CI & & & \\
CI & & & \\
\hline
CI & & & \\
CI & & & \\
\hline
CI & & & \\
CI & & & \\
\hline
CI & & & \\
CI & & & \\
\hline
CI & & & \\
CI & & & \\
\hline
CI & & & \\
CI & &$$

**Table 1.4.1** Rates of substitution of Cl<sup>-</sup> (*trans* to Lt) by H<sub>2</sub>O in [PtCl<sub>3</sub>Lt]<sup>n</sup>-complexes.

Ligand Lt	Rate of substitution	
H <sub>2</sub> O	1	
$NH_3$	200	
CI <sup>-</sup>	330	
Br <sup>-</sup>	3000	
DMSO	$2 \times 10^6$	
$C_2H_4$	$10^{11}$	

The hypotheses, used to explain the *trans* effect, describe the electronic effects generated by the *trans* directing ligand, through the metal and towards the leaving group. They are essentially based on inductive (11) and mesomeric effects

(12). These effects do not take into account the nature of the fundamental state. These effects, arising from a ligand L, are for instance a tendency to weaken the bond M-X being in *trans* (13). A distinction can then be made between the properties at equilibrium (*trans* influence) and the kinetic effects (*trans* effect). The bond lengths seem to explain better the *trans* influence concept (14). Several examples of interatomic lengths Pt-Cl are summarized in Table 1.4.2.

**Table 1.4.2** Bond lengths Pt-Cl for several platinum complexes.

Complex	Ligand in trans position	Pt-Cl (Å)	Reference
[Pt(acac)Cl <sub>2</sub> ] <sup>2-</sup>	$O^{2-}$	$2.28 \pm 0.01$	15
cis-Pt(py) <sub>2</sub> Cl <sub>2</sub>	ру	$2.30 \pm 0.01$	16
trans-Pt(PEt <sub>3</sub> ) <sub>2</sub> Cl <sub>2</sub>	Cl	$2.30 \pm 0.01$	17
$[Pt(C_{12}H_{17})Cl]_2$	C=C	$2.31 \pm 0.01$	18
cis-Pt(PMe <sub>3</sub> ) <sub>2</sub> Cl <sub>2</sub>	$PR_3$	$2.37 \pm 0.01$	19
trans-Pt(PPh <sub>2</sub> Et) <sub>2</sub> HCl	H <sup>-</sup>	$2.42 \pm 0.01$	20
trans-Pt(PPhMe <sub>2</sub> ) <sub>2</sub> (SiPh <sub>2</sub> Me)Cl	$[SiR_3]^{-}$	$2.45 \pm 0.01$	21
trans-Pt(PPh <sub>2</sub> Et) <sub>2</sub> HCl	H <sup>-</sup>	$2.42 \pm 0.01$	20

In general, the *trans* influence increases as the electronegativity decreases. Similar conclusions were obtained by Chatt *et al.* in 1955 on the basis of IR absorbance data for the complexes (22). So, the *trans* influence is defined as the influence of the ligands L on the properties, at the fundamental level, of the groups X, to which they are *trans* (23). These properties can be studied through variations in

the bond stretching vibrations or force constants, metal-ligand bond lengths and coupling constants in NMR spectroscopy. The *trans* influence series has been determined from structural data and is presented in Fig. 1.4.4 below (24,25).

$$R_2SO$$
 
$$R_3Si > Ph > \sigma\text{-}R > carbenes > AsR_3 > CO > I^- > Br^- > Cl^- > NH_3 > O^{2\text{-}} > F^-$$
 
$$H^- PR_3 \qquad RCN \qquad C=C$$

**Figure 1.4.4** *Trans*-influence series.

An interpretation of the *trans*-influence is based on the overlapping of  $\sigma$ orbitals associated with the M-L and M-X bonds. If the  $\sigma$ -orbital of the ligand L
overlaps the p $\sigma$  orbital of the metal more than it does the  $\sigma$ -orbital for *trans* ligand
X, then the M-L bond strength increases while the M-X bond strength decreases
(26). Therefore, the best  $\sigma$ -donating ligands and the weakest  $\pi$ -accepting ligands
have the higher *trans* influence. In fact, ethylene has a relatively low *trans*influence. The *trans*-influence of a tertiary phosphine group is larger, but less than
that of an alkyl group. This situation is probably due to the fact that the  $\pi$ -accepting
ligands are in direct competition with the ligand X for the electronic charge on the
metal. On the other hand, the *trans*-effect of ethylene is essentially due to the
stabilization of the transition states rather than the labilization of the fundamental
state of the *trans* ligand (27,12).

There is a possible relationship between the kinetic trans-effect and the trans-influence. The latter would be defined as the effect of a ligand on the bond strength M-L, located in a trans position in the fundamental state of the complex (28). In trans-PtL(NH<sub>3</sub>)Cl<sub>2</sub>, the ligand L efficiency to weaken the trans bond Pt-N increases as L becomes a better trans-director, whereas the overlapping degree in the bond Pt-N decreases. So, a relationship can be established between the ability of L to act as trans-director and its trans influence. As L is a better trans-director, the bond strength cis Pt-Cl, deducted from the overlapping degree Pt-Cl, decreases. This decrease is slightly smaller than is the weakening of the bond located in the trans position. Molecular orbital calculations show that the Pt-N bond strength does not change significantly between a very weak (H<sub>2</sub>O) and a very strong trans-director (H<sup>-</sup> ), the difference being only 10% of the total strength. These facts suggest that the kinetic trans effect is due more to stabilization of the transition state than to weakening of the link in the *trans* position. Making the assumption that Cl<sup>-</sup> is the entering group in the reaction with trans-PtL(NH<sub>3</sub>)Cl<sub>2</sub>, the entering and leaving groups of the activated complex (respectively, Cl and NH<sub>3</sub>) are not linked to the metal center by the 6p<sub>y</sub> orbital (fig. 1.4.5). In this way, the *trans*-director ligand L is left with more than half of the  $6p_y$  orbital. The activated complex, as a consequence, will be stabilized only if L is a good  $\boldsymbol{\sigma}$  donor and will use the  $p_y$  empty orbital. Consequently the energy difference between the fundamental and transition states will be small.

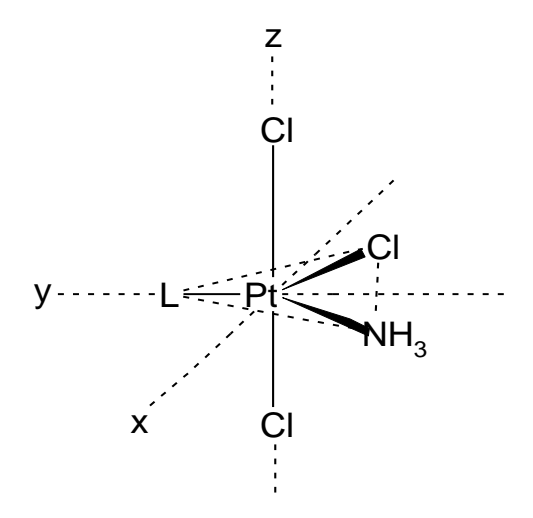


**Figure 1.4.5** Transition state representation of the reaction of *trans*-PtL(NH<sub>3</sub>)Cl<sub>2</sub> with the Cl<sup>-</sup> ligand.

## 1.5 Sulfoxide Ligands

In the sulfoxide ligands, the central sulfur atom has four sp<sup>3</sup> hybridized orbitals, an unshared electron pair and a double bond with the oxygen atom. The unshared electron pair allows a resonance of the sulfoxide molecule, as suggested by Cotton, Francis and Horrocks (fig. 1.5.1) (29).

**Figure 1.5.1** Representation of the different resonance forms of the sulfoxide ligands.

Mesomer II is the most commonly accepted - it includes a double bond between the oxygen atom and the sulfur atom. The  $\sigma$ -link is obtained by overlapping a sulfur sp<sup>3</sup> orbital with an oxygen 2p<sub>x</sub> orbital (Fig. 1.5.2) (30).

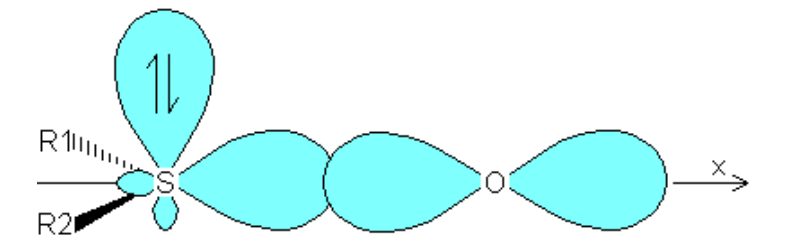


**Figure 1.5.2** Representation of the overlap between a sulfur  $sp^3$  orbital and the oxygen  $2p_x$  orbital.

The sulfur  $3d_{xy}$  or  $3d_{xz}$  orbitalcan then accept, by overlapping, the electrons from the filled oxygen  $2p_y$  or  $2p_z$  orbitals to form the  $p\pi$ -d $\pi$  bond (fig. 1.5.3).

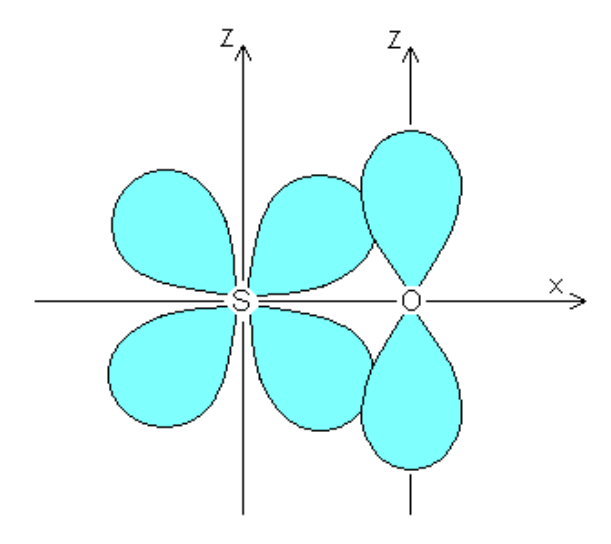


**Figure 1.5.3** Representation of the overlap between the sulfur  $3d_{xz}$  orbital and the oxygen  $2p_z$  orbital.

If resonance forms I and III (Fig. 1.5.1) exist in equal proportions, a bond order equal to 2 should be observed; this can be shown by studying the bond lengths and the bonds energies. The sulfoxide ligands bind to metals either through the oxygen atom (mesomer I) or through the sulfur atom (mesomer III). In the case of platinum, which is a soft metal, the bond is made through the sulfur atom. An exception can be noticed with the compound, *trans*-[Pt(DMSO)<sub>2</sub>(DMSO)<sub>2</sub>]<sup>2+</sup>, for which steric hindrance leads to a structure with two DMSO ligands linked through the oxygen atoms and the two others through the sulfur atoms. Thus, for platinum compounds, the resonance form III is favored (Fig. 1.5.1) and the link between the oxygen and the sulfur atoms is reinforced compared to the free molecule. And, an increase in the vibrational wavenumber of this bond is observed in the IR spectrum, when coordinated to platinum(II).

### 1.6 Anticancer activity of platinum(II) compounds

The anticancer activity of platinum(II) compounds was discovered by Rosenberg and his research team in 1967. They noticed an inhibition of the cell division in a culture of *Escherichia coli* bacteria when an electrical current was applied to it (31). This phenomenon was not only the result of the electrical current. Later, Rosenberg's group concluded that the electrical current was responsible for a slight dissolution of the platinum electrodes, forming platinum compounds in solution, namely *cis*-Pt(NH<sub>3</sub>)Cl<sub>2</sub>, which is known nowadays as *cisplatin* (32). This

experiment was the starting point of numerous research studies on the synthesis of new platinum compounds and, more particularly, *cisplatin* analogues. Other studies were also made on equivalent *trans* compounds (33), but the majority of the compounds investigated did not show any anticancer activity. This inactivity could be the consequence, at least in part, of their low cytotoxicity (34). From a molecular point of view, a possible explanation for this isomeric selectivity lies in the fact that the *cis* compounds form platinum-DNA complexes more easily and more rapidly than do their *trans* analogues, thereby inhibiting replication (35). Furthermore, the platinum-DNA compounds formed by the *trans* analogues would be more rapidly destroyed by biological repair mechanisms (36).

The majority of the active complexes exhibit some properties in common, such as electrical neutrality, the presence of two labile ligands in *cis* positions (chlorides, for instance) and the presence of two inert neutral ligands. *Cisplatin*, currently the most commonly used anticancer agent, has all of these features (37). It is prescribed today in the treatment of hormonal cancers (testicules, ovaries, prostate), bladder and lung cancers, and almost always combined with other medicines (38). The anticancer activity observed is generally related to the lability of the anionic ligands, the steric factors associated with the neutral ligands and their capacities to create strong hydrogen bonds with DNA. Charged complexes cannot easily penetrate inside cells and most of the time such complexes are found to be inactive.

Some platinum(II) complexes, even if they are structurally different than the ones discussed above, have displayed some interesting anticancer activity, but today, none of them has yet been accepted by the health care systems.

The mechanism of action of *cisplatin* is not completely understood and is still the center of controversy, especially with respect to the nature of the species which react with the DNA bases. In 1978, Rosenberg proposed a mechanism (based on the following experiment (39). *Cisplatin* was injected into a patient in low concentration (in the order of a few mM, since the complex is not very soluble) and remains unchanged in the blood, taking into account the high concentration of chloride ions (~100 mM). The neutrality of the complex is important for penetration through the cell membrane by a mechanism of active or passive diffusion (40). In the cells, the concentration in chloride ions is ca. 4 mM, which permits the following aquation reaction (Fig. 1.6.1) to take place.

**Figure 1.6.1** Monoaquation reaction proposed by Rosenberg in 1978 (39).

The monoaqua species is much more reactive than is *cisplatin* itself. It is sufficiently labile to allow platinum(II) to bind to the DNA bases, but most researchers working in this area topic believe more in the hypothesis of a reaction involving a diaqua species (41). A subsequent reaction is then necessary (Fig. 1.6.2).

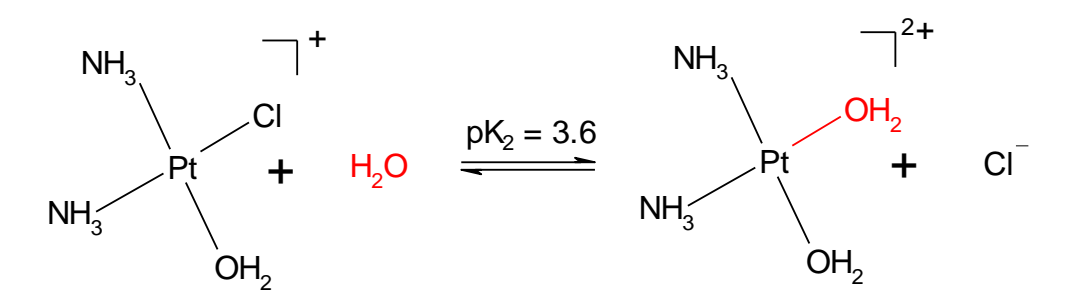


**Figure 1.6.2** Diagnation reaction proposed by the Miller group (41).

In more recent studies, however, the House research group has shown that the *cisplatin* aquation and hydrolysis reactions are much more complex (41-43). According to them, it is possible to estimate the quantity of species present at equilibrium in the blood plasma and the cell medium, as shown in Table 1.6.1.

**Table 1.6.1** Proportion of the species present in blood plasma and inside the cell during a *cisplatin* injection.

Species	Blood plasma	Inside the cellule
cis-Pt(NH <sub>3</sub> ) <sub>2</sub> Cl <sub>2</sub>	68 %	31 %
cis-Pt(NH <sub>3</sub> ) <sub>2</sub> (OH)Cl	24 %	32 %
cis-[Pt(NH <sub>3</sub> ) <sub>2</sub> (OH <sub>2</sub> )Cl] <sup>+</sup>	7 %	28 %
cis-[Pt(NH <sub>3</sub> ) <sub>2</sub> (OH <sub>2</sub> )(OH)] <sup>+</sup>	traces	7 %
cis-[Pt(NH <sub>3</sub> ) <sub>2</sub> (OH <sub>2</sub> ) <sub>2</sub> ] <sup>2+</sup>	traces	traces
cis-Pt(NH <sub>3</sub> ) <sub>2</sub> (OH) <sub>2</sub>	traces	traces

The equilibrium in the blood plasma is reached in six hours. It is important to note that the pH, in the blood plasma or inside the cell, is close to 7.4. This is why the diaqua and the dihydroxo species are essentially absent. The difference in the proportions of the species in the two media can be understood if the concentration of the chloride ions, which goes from 100 mM in the blood to 4 mM inside the cell, is taken into account. The hydrolysis of *cisplatin* has relatively slow kinetics. It appears reasonable, therefore, to believe that a non-negligible quantity of it goes directly through the cell membrane. It is possible that the monohydroxomonochloro species, being neutral, also goes across the membrane. Furthermore, it appears more or less certain that all the other species remain in the plasma because of their charges.

Since the diaqua and dihydroxo species are only present in low concentrations in the cellular medium, their reactions with DNA are not as

important. On the other hand, the monoaquamonochloro species seems capable of such an interaction. But, as a species is used up, there will be a rearrangement in the equilibria taking place. House *et al.* proposed the following mechanism for the physiological action of *cisplatin* (Fig. 1.6.3).

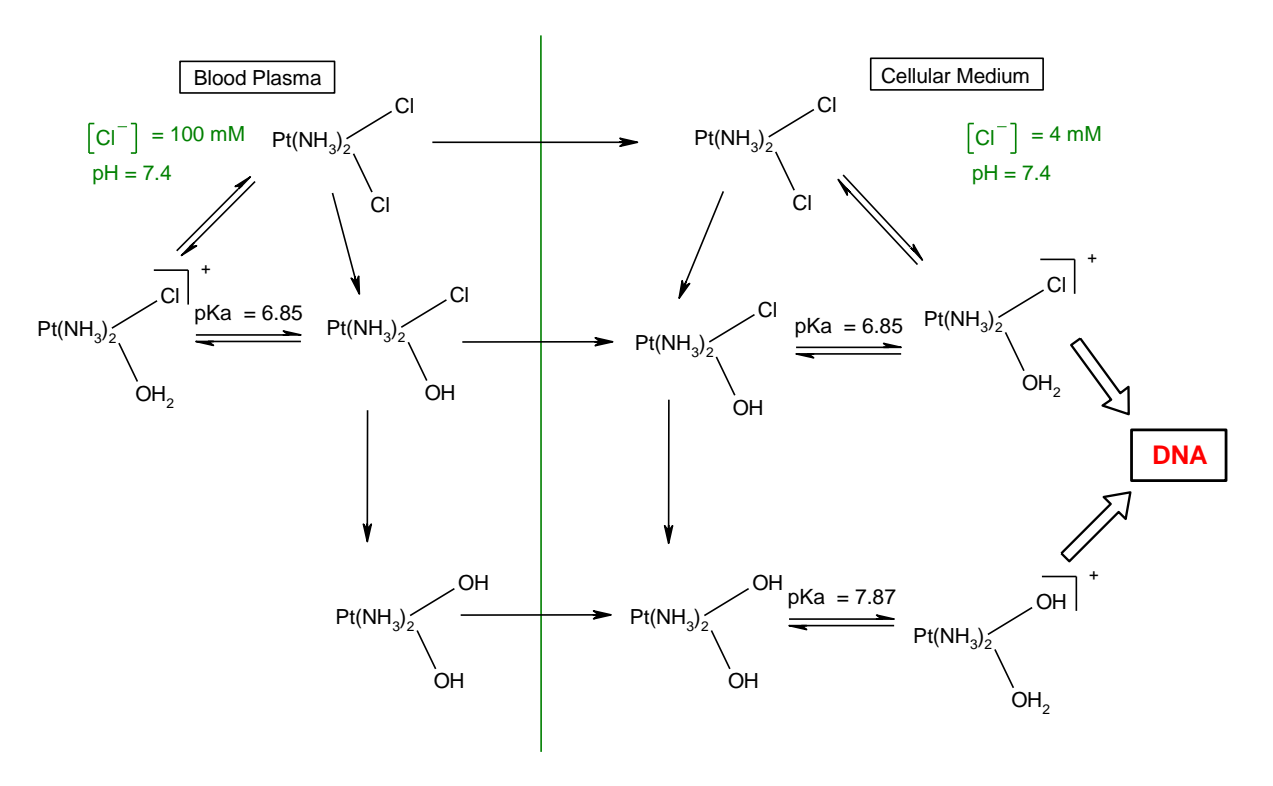


**Figure 1.6.3** Mechanism of physiological action proposed by House *et al.* (adapted from ref. 43).

Some studies have also been made using platinum-195 NMR spectroscopy, which have shown the presence of dimeric and trimeric compounds, the platinum units being bridged by hydroxo ligands (39,44). House *et al.* omitted these species from their proposed mechanism, which can be explained by the fact that their results were base d mainly on UV-visible spectroscopy, a technique that cannot detect the

presence of oligomers. Some authors have claimed these oligomeric species to be, at least in part, the cause of the toxicity of *cisplatin* and its derivatives (45,46). The structures of several dimers (47-50), trimers (49,50) and tetramers have been determined by X-ray diffraction. It would appear judicious then to check if such oligomers are being produced when a new medicine is developed.

Whatever is the active species in the physiological medium, several authors (51-53) have suggested that the active platinum complexes create intrachain and irreversible bonds with DNA, using active sites of the nucleotide bases (54,55). They have shown that the guanine N7 position is the most probable coordination site for platinum. The *cis*-diammine part can create links with groups which are about 2.80 Å distant. *In vitro* studies on di- and polynucleosides have supported this hypothesis withthe most important interaction being *internal* bridging of two guanine bases of the DNA chain by a platinum group (Fig. 1.6.4). *In vivo* studies have confirmed this hypothesis.

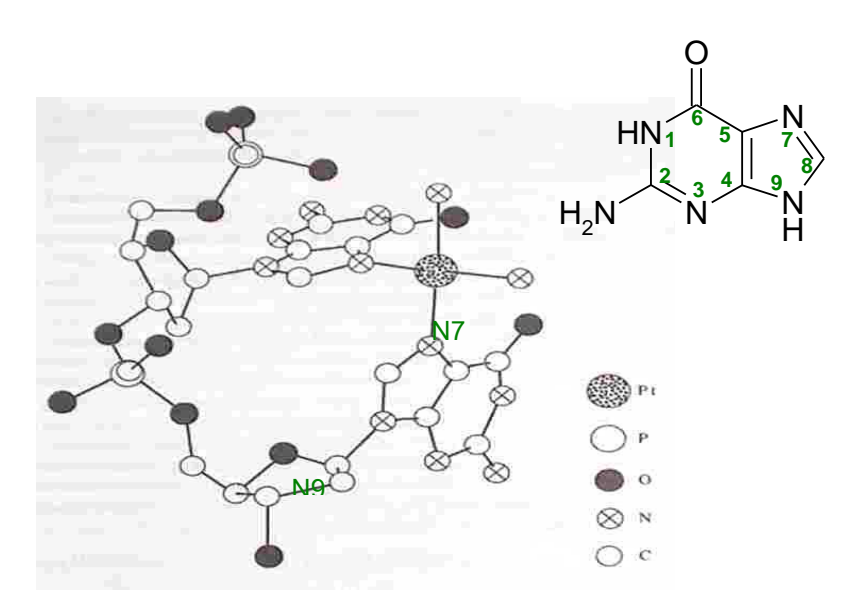


**Figure 1.6.4** Structure of the complex cis-(NH<sub>3</sub>)<sub>2</sub>Pt{d(pGpG)}, where d(pGpG) = guanine desoxyribose phosphate dinucleoside (adapted from ref. 56).

The relative inactivity of *transplatin* can be attributed to its spatial inability to bind to the DNA molecule, as illustrated in Fig. 1.6.4. It can, however, bind to two groups, at much larger distances, which come close to platinum from two opposite directions. The *cisplatin* binding to DNA strongly interfers with the ability of the Watson-Crick bases to pair (57). And so, when a DNA strand reacts with the *cis* Pt(II) isomer, through two adjacent guanines, the bases pairing is interrupted (Fig 1.6.5).

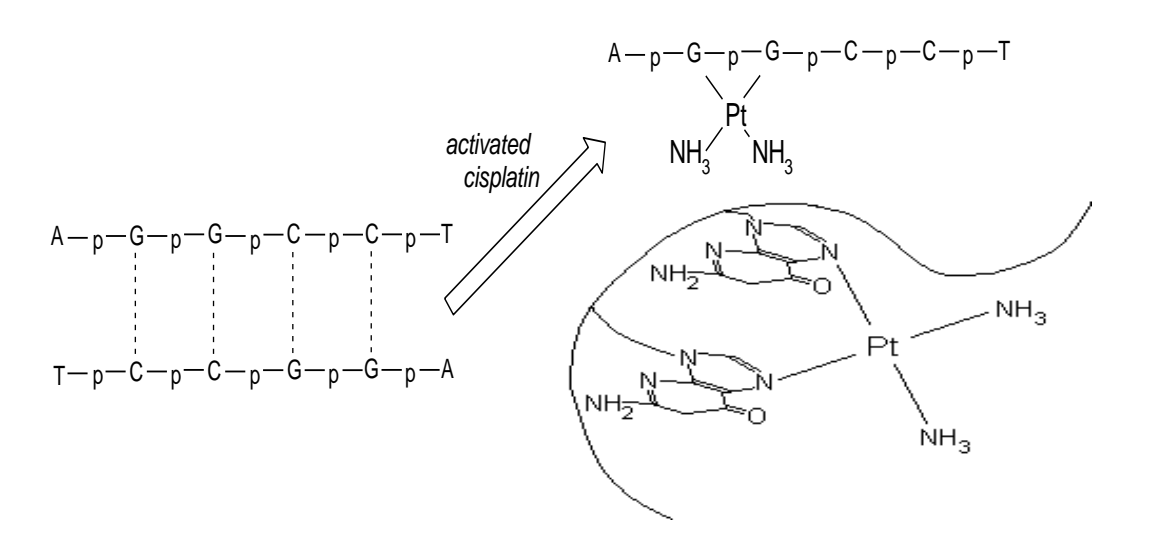


**Figure 1.6.5** Sketch of the Pt(II) unit binding on two adjacent guanines (adapted from ref. 58).

The *cis*-Pt—DNA bond induces a severe kink in the molecule leading to some tensions and the rupture of several hydrogen bonds in the base pairs. The double helix unwinds and, during the cellular division and reproduction, errors in the bases pairing are generated. In healthy cells, the lesions will be rapidly repaired before cell reproduction by an autocorrector mechanism. But, this will not happen in cancer cells, the mechanism being defective (59). A mutation then occurs, with the possible destruction of the cancer cell.

Other hypotheses on the link between *cisplatin* and DNA have also been formulated. These include intrachain bonding, but also interchain bonding between the hydrolysed complex and the DNA bases (60). It also seems also that sulfurcontaining molecules may play a non-negligible role in the transfer process of platinum to DNA (61-63).

One aspect of the chemotherapeutic use of *cis*-diamminedichloroplatinum(II) and this family of medicines is their negative side effects, especially nephrotoxicity. This situation is probably the consequence of enzyme inactivation by coordination of thiol groups to Pt(II) or Hg(II). The soft and hard acids and bases theory suggests the protection of these thiols by the use of "saving agents" having soft sulfur atoms (7). For example, two typical saving agents would be diethyldithiodicarbamate,  $Et_2NCS^-$ , and the thiosulfate ion,  $S_2O_3^{2-}$ .

A decade ago, some complexes with amine ligands in the *trans* position were found to show anticancer activity for very specific organs (64). Furthermore, neutral ligands having a donating atom different than nitrogen, such as sulfur, can also give active complexes (65). Several platinum(II) complexes with sulfoxide ligands have

anticancer activity, depending on the nature of the coordinated sulfoxide. So, the activity is not only function of the amine ligands, monodentate (*cis*) or bidentate, as in the case of 1,2-diaminocyclohexane (dach) and 1,1-bis(aminomethyl) cyclohexane (damch). According to Farrell *et al.*, the most active complexes in the Pt(R<sub>2</sub>SO)(diamine)Cl<sub>2</sub> series are those with the most labile sulfoxide ligand (66). And, the cytotoxicities of the *cis*- and *trans*-Pt(R<sub>2</sub>SO)(quinoline)Cl<sub>2</sub> compounds are similar to *cisplatin*, with even an increase for the less hindered sulfoxides (67). Furthermore, the chirality of sulfur, in the case of asymmetric sulfoxides, can also play a role in the activity. At physiological conditions, platinum complexes with sterically hindered sulfoxide ligands hydrolyse more rapidly than do their equivalents with less hindered ligands.

So, it appears that the mode of action of the complexes is quite diverse. For instance, Farrell's research group has shown that *cis*- and *trans*-Pt(py)<sub>2</sub>Cl<sub>2</sub> have a similar cytotoxicities (as determined by the required concentration for a growth inhibition of 50% of cells, IC<sub>50</sub>) to that of *cisplatin* (68). It is admitted that links with DNA take place thanks to hydrogen bonds. But, bound pyridine cannot form any hydrogen bonds, which is verified since these complexes show 5-fold less links with DNA than does *cisplatin*. And, the anticancer activity of the *trans* and *cis* complexes is caused by different mechanisms.

When present in the human body, platinum complexes can react with molecules other than DNA, especially those containing sulfur (69). Examples of such biomolecules are the amino acids cysteine and methionine, the peptides glutathion and the protein metallothionine. It is also possible that these interactions

are responsible for several biological effects, such as the activity diminution of platinum(II) complexes or the development of a cellular resistance toward platinum, and toxic effects like nephrotoxicity (70). So, when an anticancer medicine is developed, it is always very important to study and account for the possible negative effects on other physiological molecules.

#### 1.7 Raman Spectroscopy

Raman spectroscopy is a very powerful technique that can help in understanding the physical structure of a specific molecular system. Since this is a less conventional technique that has been used to characterize the new materials synthesized as part of this thesis work, it is appropriate to explain more about the technique itself here.

When monochromatic radiation is incident upon a molecular system, this light will interact with the system in different ways. It may be reflected, absorbed or scattered. It is the scattering of the radiation that occurs which can tell the Raman spectroscopist something about the structure of the molecular system. If the wavelength of the scattered radiation is analyzed, not only is the incident radiation wavelength seen, known as Rayleigh scattering, but a small amount of the radiation is also scattered at several different wavelengths both below and above the incident radiation wavelength. This latter scattering is referred to as Stokes and Anti-Stokes Raman scattering, respectively. Only 10<sup>-7</sup> of the scattered light is associated with Raman scattering. Some chemical and structural information can be extracted from the change in wavelength of the scattered photons (Figure 1.7.1).

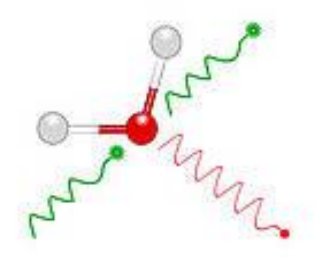


Figure 1.7.1 Light scattered from a molecule

In molecular systems, the observed Raman frequencies are mainly associated with rotational, vibrational and electronic transitions. The scattered radiation occurs over all directions and can also have observable changes in its polarization:

- As mentioned already, the scattering process without a change of wavelength or frequency ( $\lambda = h\nu$ ) is called Rayleigh scattering, and is the same process described by John William Strutt, also known as Lord Rayleigh, and which accounts for the blue color of the sky (71).
- A change in the wavelength or frequency of the light is called Raman scattering.

  Raman shifted photons of light can be either of higher or lower energy, depending upon the vibrational state of the molecule.

Photons interact with molecules to induce transitions between energy states. A photon is scattered by the molecular system. Most photons are elastically scattered, i.e., Rayleigh scattering. Raman spectroscopy is based on the Raman effect, which is the inelastic scattering of photons by molecules. The effect was discovered by the Indian physicist, C.V. Raman in 1928 (72). A simplified energy diagram that illustrates these concepts is in the figure 1.7.2.

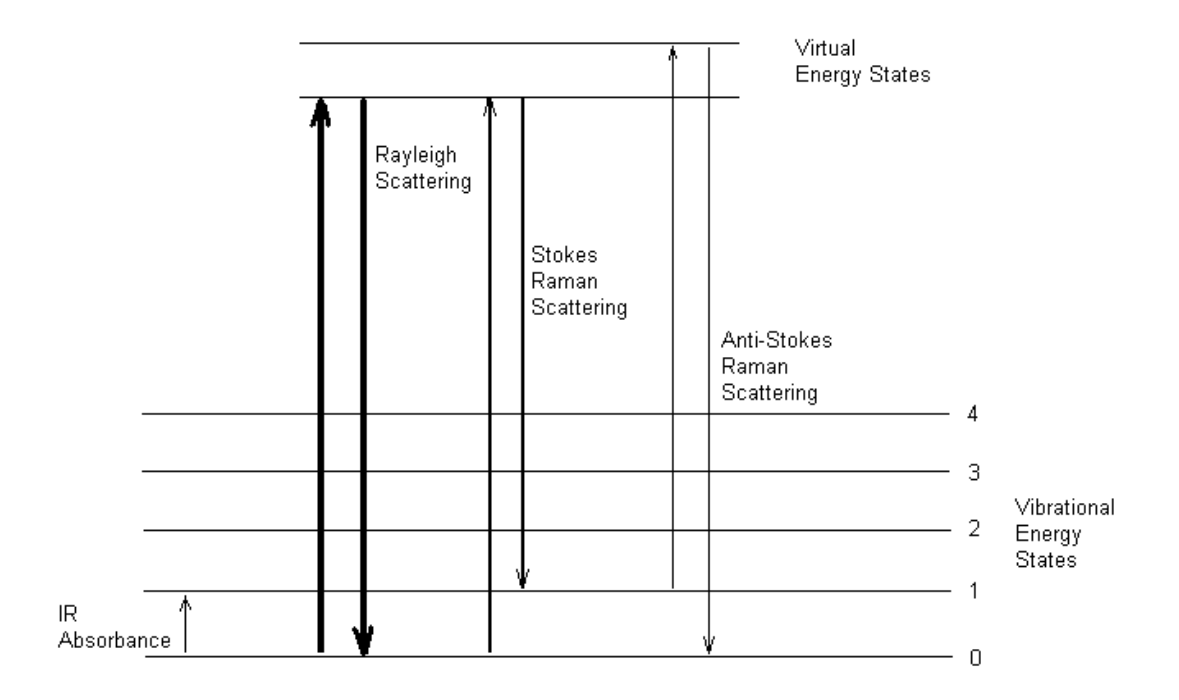


Figure 1.7.2. Jablonksi Energy Diagram for Raman Scattering

The energy of the scattered radiation is less than the incident radiation for the Stokes line and the energy of the scattered radiation is more than the incident radiation for the anti-Stokes line. The energy increase or decrease from the excitation is related to the vibrational energy spacing in the ground electronic state of the molecule and, therefore, the wavenumber of the Stokes and anti-Stokes lines are a direct measure of the vibrational energies of the molecule. A schematic Raman spectrum may appear as represented in figure 1.7.3.

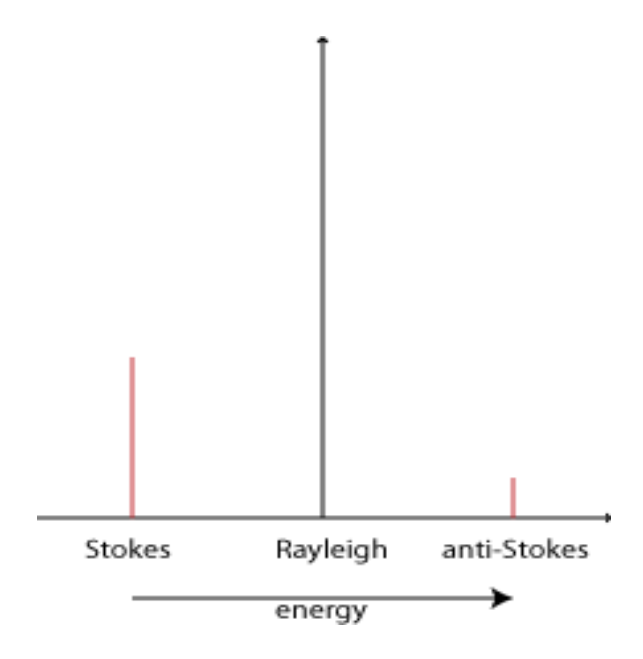


Figure 1.7.3 Example of a Raman spectrum

In the example spectrum, the Stokes and anti-Stokes lines are equally displaced from the Rayleigh line. This occurs, because in either case, one vibrational quantum of energy is gained or lost. Also, the anti-Stokes line is much less intense than is the Stokes line. This situation occurs because only molecules that are vibrationally excited prior to irradiation can give rise to the anti-Stokes line. Hence, in Raman spectroscopy, only the more intense Stokes line is normally measured at room temperature.

Both infrared and Raman spectroscopy measure the vibrational energies of molecules, but these methods rely on different selection rules. For a vibrational motion to be IR active, the dipole moment of the molecule must change during the vibration. Therefore, the symmetric stretch in  $CO_2$  is not IR active because there is

no net change in dipole moment during the vibration. The asymmetric stretch is IR active due to a change in dipole moment.

For a transition to be Raman active, there must be a change in the polarizability of the molecule during the vibration. The symmetric stretch in CO<sub>2</sub> is Raman active because the polarizability of the molecule changes. This can be seen by comparing the ellipsoid at the equilibrium bond length to the ellipsoid for the extended and compressed symmetric motions. For a vibration to be Raman active, the polarizability of the molecule must have change with the vibrational motion. Thus, Raman spectroscopy complements IR spectroscopy.

Experimentally, only the Stokes shifts are normally measured in a Raman spectrum. The Stokes lines will be at lower wavenumbers than the exciting light. Since Raman scattering is not very efficient, a high power excitation source, such as a laser, is necessary. And, since the interest is in the energy difference between the excitation and the Stokes lines, the excitation source should be monochromatic. This is a property of many laser systems.

Vibrational spectroscopy of molecules can be relatively complicated. Quantum mechanics requires that only certain well-defined frequencies and atomic displacements are allowed. These are known as the normal modes of vibration of the molecule (73). A linear molecule with N atoms has 3N-5 normal modes, and a non-linear molecule has 3N-6 normal modes of vibration. There are several types of motion that contribute to the normal modes. Some examples are:

- stretching motion between two bonded atoms
- bending motion between three atoms connected by two bonds

- out-of-plan deformation modes that change an otherwise planar structure into a non-planar one

Infrared spectroscopy allows one to characterize vibrations in molecules by measuring the absorption of light of certain energies that correspond to the vibrational excitation of the molecule from  $v = 0 \rightarrow v = 1$  (or higher) states. As indicated above, not all of the normal modes of vibration can be excited by IR radiation. There are selection rules that govern the ability of a molecule to be detected by IR spectroscopy (74).

The Raman effect is due to the interaction of the electromagnetic field of the incident radiation,  $E_i$ , with a molecule. The electric field may induce an electric dipole in the molecule, given by the relationship:

$$p = \alpha Ei$$
.

where  $\alpha$  is referred to as the polarizability of the molecule and p is the induced dipole. The electric field due to the incident radiation is a time-varying quantity of the form

$$E_i = E_0 \cos(2\pi v_i t)$$

For a vibrating molecule, the polarizability is also a time-varying term that depends on the vibrational frequency of the molecule,  $v_{\rm vib}$ 

$$\alpha = \alpha_{\rm o} + \alpha_{\rm vib}\cos(2\pi v_{\rm vib}t)$$

Multiplication of these two time-varying terms,  $E_i$  and  $\alpha$ , gives rise to a cross product term of the form:

$$\frac{\alpha_{\text{vib}}E_0}{2} = [\cos 2\pi t(\nu_i + \nu_{\text{vib}}) + \cos 2\pi t(\nu_i - \nu_{\text{vib}})]$$

This cross term in the induced dipole represents light that can be scattered at both higher and lower energy than the Rayleigh (elastic) scattering of the incident radiation. The incremental differences from the frequency of the incident radiation,  $v_i$ , are the vibrational frequencies of the molecule,  $v_{vib}$ . As we know already, these lines are referred to as the "anti-Stokes" and "Stokes" lines, respectively. The ratio of the intensity of the Raman anti-Stokes and Stokes lines is predicted to be:

$$\frac{I_A}{I_S} = \left(\frac{v_i + v_{vib}}{v_i - v_{vib}}\right)^4 e^X$$

$$X = (-hv_{vib}) / (kT)$$

The Boltzmann exponential factor is the dominant term in the equation, which makes the anti-Stokes features of the spectra much weaker than the corresponding Stokes lines at normal temperatures.

Infrared spectroscopy and Raman spectroscopy are complementary techniques, because the selection rules are different. For example, homonuclear diatomic molecules do not have an infrared absorption spectrum, because they have no dipole moment, but do have a Raman spectrum, since stretching and contraction of the bond changes the interactions between electrons and nuclei, thereby changing the molecular polarizability. For highly symmetric polyatomic molecules possessing

a center of inversion (such as benzene), it is observed that bands that are active in the IR spectrum are not active in the Raman spectrum (and vice-versa). In molecules with little or no symmetry, modes are likely to be active in both IR and Raman spectroscopy.

The distortion of a molecule in an electric field and, therefore, the vibrational Raman cross section, is determined by its polarizability.

A Raman transition from one state to another and, therefore, a Raman shift, can be activated optically only in the presence of non-zero polarizability derivative with respect to the normal coordinate (that is, the vibration or rotation):

$$\left| \frac{\partial \alpha}{\partial Q} \right| > 0$$

Raman-active vibrations/rotations can be identified by using group theory. Molecules can be classified according to symmetry elements or operations that leave at least one common point unchanged. This classification gives rise to the point group representation for the molecule. Raman-active modes can be found for molecules or crystals that show symmetry by using the appropriate character table for that symmetry group (75).

**Infrared Transitions.** For a fundamental transition to occur by absorption of infrared radiation the transition moment integral must be nonzero. The transition moment integrals are of the form:

$$\int \psi_{v}^{o} X \psi_{v}^{f} \delta \tau \qquad \qquad \int \psi_{v}^{o} Y \psi_{v}^{f} \delta \tau \qquad \qquad \int \psi_{v}^{o} Z \psi_{v}^{f} \delta \tau$$

where  $\psi_v^o$  is the wave function for the initial state involved in the transition (the ground state), and  $\psi_v^f$  is the wave function for the final state involved in the transition (the excited state). The x, y and z involved in the integrals refer to the Cartesian components of the oscillating electric vector of the radiation. If any of these three integrals is nonzero, then the transition moment integral is nonzero and the transition is allowed.

A fundamental transition will be IR active (that is, give rise to an absorption band) if the normal mode involved belongs to the same symmetry representation as any one or several of the Cartesian coordinates.

**Raman Transitions.** For a fundamental transition to occur by Raman scattering of radiation, the transition moment integral must be nonzero. The transition moment integrals are of the form:

$$\int \psi_{v}^{o} \alpha \psi_{v}^{f} \delta \tau$$

where  $\alpha$  represents the polarizability of the molecule. The symmetry representations for the polarizability is the same as that of quadratic terms involving the Cartesian coordinates,  $x^2$ ,  $y^2$ ,  $z^2$ , xy, yz, and xz.

A fundamental transition will be Raman active (that is, give rise to a Raman shift) if the normal mode involved belongs to the same symmetry representation as any one or more of the Cartesian components of the polarizability tensor of the molecule.

**Normal Modes of Vibration.** The normal modes of vibration for CH<sub>3</sub>Cl and CHCl<sub>3</sub> (both molecules have the same symmetry) are shown, as an example, in Figure 1.8.4.

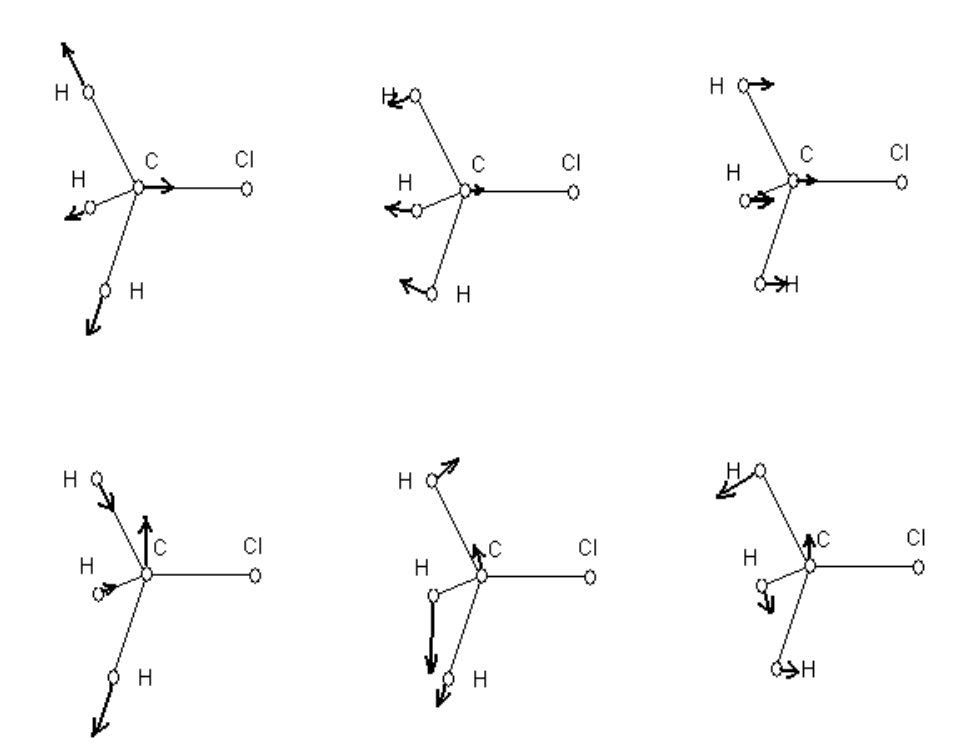


**Figure 1.7.4** Normal vibrations of CH<sub>3</sub>Cl – Only side views and only one component of each degenerate vibration are given (adapted from ref. 76).

This figure shows that the first three vibrations for these  $C_{3\nu}$  symmetry molecules are of  $A_1$  symmetry, and that the other three are doubly degenerate E symmetry vibrations.

**Raman Instrumentation.** Best suited laser wavelength - The correct selection of the laser wavelength can be an important consideration for Raman spectroscopy. With

modern equipment, often several laser wavelengths may be employed so as to achieve the best detection of the Raman signal.

For instance, many organic and biological samples are quite fluorescent species. Exciting these samples with a laser operating in the green region (532 nm) can promote this fluorescence, which can swamp any underlying Raman spectrum to such an extent that it is no longer detectable. In cases like this one, the use of a laser in the red region (633 nm) or NIR (785 nm) can provide a better solution. With the lower photon energy, a red or NIR laser may not promote the electronic transition (and hence the fluorescence) and so the Raman scattering may be far easier to detect. Conversely, as one increases the wavelength, from green to red to NIR, the scattering efficiency will decrease, so longer integration times or higher power lasers will be required in the experiment.

Thus, it is often most practical to have a number of laser wavelengths available to match the various sample properties one may encounter, be it resonance enhancements, penetration depth of fluorescence (Fig. 1.7.5).

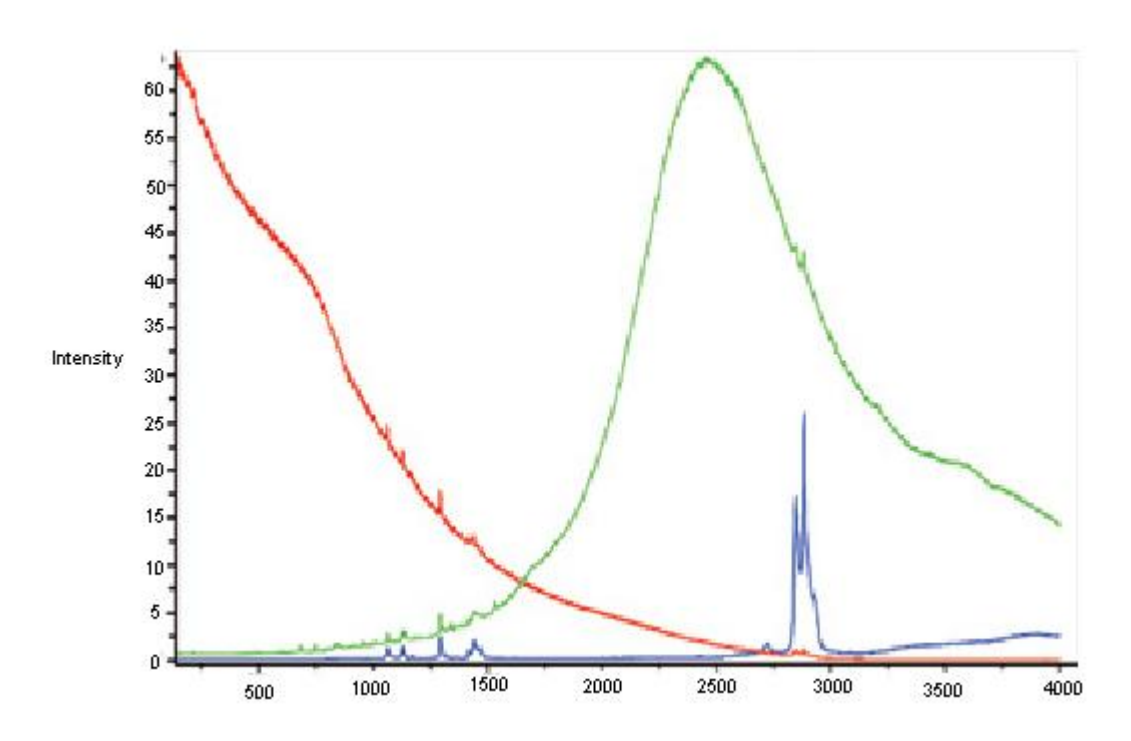


Figure 1.7.5 Green, red and NIR 785 nm laser excitation of a fluorescent sample.

The strong background seen with the green and red lasers swamps the Raman signal, whereas the 785 nm excitation is outside of the fluorescence range, enabling the Raman spectrum to be detected (77).

## 1.8 Goal of the project

The antitumor activity of platinum(II) complexes of the type *cis*-Pt(amine)<sub>2</sub>Cl<sub>2</sub> is now well established. Nowadays, *cisplatin* still remains the most used anticancer agent in chemotherapy. It is efficient, but its side effect are dramatic and numerous (vomiting, hair loss, taste, audition, kidney alteration, infertility, diarrhoea) (78), even if several methods have been developed to reduce them. This is one of the reasons which stimulate the current research in the area, the medicine

resistance being another reason. The search for improved platinum-based drugs continues with the goals of reducing toxic side-effects and broadening the spectrum of activity to tumors resistant to *cisplatin*. The curative solution would be to develop a medicine having an effect only on cancer cells, without affecting the other cells.

A good way to reach that goal would be to attach an active medicinal molecule to a second inert 'carrying' molecule, which could put it down specifically at the tumor site. The side effects would also be drastically reduce to the minimum. This method could be used efficiently for all hormonal-dependent cancers, such as prostate or breast cancers. For breast cancer in particular, a medicine focused on an estrogenic molecule could be located only on breast cells, considering estrogens are located mainly in the breast. And so, the other body parts would be little affected.

Complexes with a *trans* geometry are not generally well known for their antitumor activity. But when the ammine (of *cisplatin*) is replaced with a planar ligand, such as pyridine, the cytotoxicity of the *trans* complexes is dramatically enhanced in comparison with *cisplatin* and *transplatin*, this latter remaining inactive at usual biological concentrations (34). This result is fundamental in the sense that complexes structurally different from *cisplatin* and its analogues can have a very different clinical activity and toxicity, due to different cell pharmacology (79). This is what led us believe that complexes with pyrazine ligands, which are also planar, could show an activity irrespective of their stereo-geometry is. It has been suggested that platinum(II) complexes had to have at least one hydrogen atom on the amine nitrogen to be able to bind to DNA (80). However, recent studies have shown examples of active complexes having neither primary nor secondary amines (81-83).

A major focus of current research is the investigation of "non-classical" platinum antitumor compounds, including *trans*- and polynuclear platinum(II) derivatives, which act by a different biological mechanism to that of *cisplatin* resulting in a different profile of activity.

Sulfoxide ligands have been of interest to us since they can accept  $\pi$ -electron density from a metallic center. For this type of ligand, cis geometry complexes are usually more stable than are their trans analogues (unlike amine systems). Recently, mixed complexes with pyrimidine and sulfoxide ligands (84,85) have been investigated. Pyrimidine has also free  $\pi^*$  orbitals, which could accept electron density from platinum. The reactions of the  $[Pt(R_2SO)Cl_3]^-$  complexes with pyrimidine produces first the trans isomers, which can then isomerize to the cis compounds.

It appeared interesting to us to determine the influence of the pyrimidine ligand in these reactions. Consequently, a new direction was begun recently on preparing mixed complexes with sulfoxide and pyrazine ligands (86,87). Unlike pyrimidine, pyrazine (1,4-diazine) is a symmetrical molecule but it also has vacant  $\pi^*$  orbitals, which could form  $\pi$  bonds with platinum. The main interest in coordinated pyrazine is the possibility of transferring electronic effects through the heterocycle (88,89) and its ability to create bridges between two platinum atoms (90,91,95,96). Polynuclear platinum(II) complexes, linked by dinitrogenized ligands, are finding more success among antitumor agents, some of which are in final-phase clinical tests (92-94). In addition to pyrazine, two similar ligands will be used in this

project, 2,5-dimethylpyrazine and quinoxaline. We expected that these ligands would also act as bridging ligands.

The sulfoxide ligands used in this project exhibited different steric hindrances. This is the reason why they show slightly different behavior from each other. Complexes formed with dimethylsulfoxide (DMSO), diethylsulfoxide (DEtSO), tetramethylenesulfoxide (TMSO), di-*n*-propylsulfoxide (DPrSO), di-*n*-butylsulfoxide (DBuSO), dibenzylsulfoxide (DBzSO), diphenylsulfoxide (DPhSO) and methylbenzylsulfoxide (MeBzSO) will be studied. Characterization of the synthesized platinum(II) complexes will be achieved mainly by multinuclear-NMR spectroscopy (<sup>1</sup>H, <sup>13</sup>C and <sup>195</sup>Pt) and by IR and Raman spectroscopy. When crystals are obtained, their crystallographic structures will be solved by X-ray diffraction methods.

#### References

- (1) W. C. Zeise. *Pogg. Ann.* **1827**, 9, 632.
- (2) W. C. Zeise. *Pogg. Ann.* **1831**, *21*, 497.
- (3) I. I. Chernyaev. Ann. Inst. Platine SSSR. 1926, 4, 261.
- (4) H. G. Gray and C. J. J. Ballhausen. J. Am. Chem. Soc. 1963, 85, 260.
- (5) D. S. Martin, M. A. Tucker and A. G. Kassman. *Inorg. Chem.* **1965**, *4*, 1682.
- (6) U. Belluco. Organometallic and coordination chemistry of platinum. Academic Press, 1974. Chapter 1.
- (7) J. E. Huheey, E. A. Keiter and R. L. Keiter, Inorganic Chemistry: Principles of Structure and Reactivity, 4th ed.; HarperCollins College Publishers: New York, 1993.
- (8) A. A. Grinberg. Ann. Inst. Platine SSSR. 1927, 5, 109.
- (9) F. Basolo and R. G. Pearson. Prog. *Inorg. Chem.* **1962**, *4*, 381.
- (10) J. E. Huheey. Inorganic Chemistry, Principles of structure and reactivity. 2<sup>nd</sup> ed., Harper and Row Publishers, 1978. page 491.
- (11) A. A. Grinberg. *Acta Physicochim. SSSR.* **1935**, *3*, 573.
- (12) J. Chatt, L. A. Duncanson and L. M. Venanzi. *Chem. Ind.* (London) **1955**, 749.
- (13) W. McFarlane. *Chem. Comm.* **1968**, 393.
- (14) R. McWeeny, R. Mason and A. D. C. Towl. *Discuss. Faraday Soc.* **1969**, *47*, 20.
- (15) R. Mason, G. B. Robertson and P. J. Pauling, P.J. J. Chem. Soc. (A) 1969, 485.
- (16) P. Colamarino and P. L. Orioli. J. Chem. Soc., Dalton Trans. 1975, 1656.

- (17) G. G. Messmer and E. L. Amma. *Inorg. Chem.* **1966**, *5*, 1775.
- (18) R. Mason, G. B. Robertson, P. O. Whimp, B. L. Shaw and G. Shaw. *Chem. Comm.* **1968**, 868.
- (19) G. G. Messmer, E. L. Amma and J. A. Ibers. *Inorg. Chem.* **1967**, *6*, 725.
- (20) R. Eisenberg and J. A. Ibers. *Inorg. Chem.* **1965**, *4*, 773.
- (21) J. Chatt, C. Eaborn, S. Ibekwe and P. N. Kapoor. *Chem. Comm.* **1967**, 869.
- (22) J. Chatt, L. A. Duncanson and L. M. Venanzi. *J. Chem. Soc.* **1955**, 4456.
- (23) A. Pidcock, R. E. Richards and L. M. J. Chem. Soc. (A) **1966**, 1707.
- (24) University of Oxford, Department of Chemistry, Oxford, United Kingdom.

  www.chem.ox.ac.uk/icl/dermot/mechanism1/lecture1/ligands.html
- (25) M. H. Johansson, Thesis, 2002, Packing effect in Pd(II) and Pt(II) compounds, X-ray crystallography, Inorganic Chemistry, Chemical Center, P.O. Box 124, S-22100 Lund, Sweden.
- (26) The University of Alaska Fairbanks, Department of Chemistry, Alaska, USA. www.uaf.edu/chem/howard/402 webs/402 menu.htm
- (27) L. E. Orgel. J. Inorg. Nucl. Chem. 1956, 2, 137.
- (28) S. Otto and M. H. Johansson. *Inorg. Chim. Acta.* **2002**, *329*, 135.
- (29) F. A. Cotton, R. Francis and W. D. Horrocks. J. Phys. Chem. 1960, 64, 1534.
- (30) A. L. Ternay. Contemporary organic chemistry. 2<sup>nd</sup> ed., Saunders Company, Philadelphia, 1979. Chapter 24.
- (31) B. Rosenberg, E. Renshaw, L. Van Camp, J. Hartwick and J. Drobnik. *J. Bacteriol.* **1967**, *93*, 716.

- (32) B. Rosenberg, L. Van Camp, E. B. Grinly and A. J. Thomson. J. Biol. Chem. 1967, 242, 1347.
- (33) M. J. Cleare and J. D. Hoeschele. *Bioinorg. Chem.* **1974**, 2, 187.
- (34) N. Farrell, T. T. B. Ha, J.-P. Souchard, F. L. Wimmer, S. Cros and N. P. Johnson. J. Med. Chem. 1989, 32, 2240.
- (35) N. P. Johnson, P. Lapetoule, H. Razaka, G. Villani, D. C. H. McBrien et T. Slater. Biological Mechanisms of Platinum Drugs. IRL Press Oxford, 1986. Chapter 1.
- (36) R. B. Ciccarelli, M. J. Solomon, A. Varshavsky and S. J. Lippard. *J. Biochemistry.* **1985**, *24*, 7533.
- (37) S. J. Lippard. Platinum, gold and other metal chemotherapeutic agents, ACS Symposium Series 209, American Chemical Society, Washington, DC, 1985.
- (38) J. Reedijk. J. Chem. Soc., Chem. Commun. 1996, 7, 801.
- (39) B. Rosenberg. *Biochimie*. **1978**, *60*, 859.
- (40) A. Eastman. Cancer Cells. 1990, 2, 275.
- (41) S. E. Miller and D. A. House. *Inorg. Chim. Acta.* **1990**, *173*, 53.
- (42) E. Koubeck and D. A. House. *Inorg. Chim. Acta.* **1992**, *191*, 103.
- (43) C. J. Abraham, K. J. Gerard and D. A. House. *Inorg. Chim. Acta.* 1993, 209, 119.
- (44) C. J. Boreham, J. A. Broomhead and D. P. Fairlie. Aust. J. Chem. **1981**, 34, 659.
- (45) J. A. Broomhead, D. P. Fairlie and M. W. Whitehouse. *Chem. Biol. Interact.* 1980, 31, 113.

- (46) S. K. Aggarwal, J. A. Broomhead, D. P. Fairlie and M. W. Whitehouse. *Cancer Chemother. Pharmacol.* **1980**, *4*, 249.
- (47) R. Faggiani, B. Lippert, C. J. L. Lock and B. Rosenberg. J. Am. Chem. Soc. 1977, 99, 777.
- (48) B. Lippert, C. J. L. Lock, B. Rosenberg and M. Zvagulis. *Inorg. Chem.* 1978, 17, 2971.
- (49) R. Faggiani, B. Lippert, C. J. L. Lock and B. Rosenberg. *Inorg. Chem.* 1977, 16, 1192.
- (50) R. Faggiani, B. Lippert, C. J. L. Lock and B. Rosenberg, B. *Inorg. Chem.* 1978, 17, 1941.
- (51) J. P. Caradonna and S. J. Lippard. J. Am. Chem. Soc. 1982, 104, 5793.
- (52) P. M. Takahara, A. C. Rosenzweig, C. A. Frederick and S. J. Lippard. *Nature* 1995, 377, 649.
- (53) T. Uemura, T. Shimura, H. Nakanishi and H. Y. Okuno. *Inorg. Chim. Acta*. 1991, 181, 11.
- (54) S. Mansy, G. Y. H. Chu, R. E. Duncan and R. S. Tobias. J. Am. Chem. Soc. 1978, 100, 607.
- (55) H. Basch, M. Krauss, W. J. Stevens and D. Cohen. *Inorg. Chem.* **1986**, 25, 684.
- (56) S. E. Sherman, D. Gibson, A. H. J. Wang and S. J. Lippard. *Science*. **1985**, 203, 412.
- (57) J. D. Watson and F. H. C. Crick. *Nature*. **1953**, *171*, 737.
- (58) S. J. Lippard and W. I. Sundquist. Coord. Chem. Rev. 1990, 100, 293.
- (59) B. Rosenberg. *Cancer.* **1985**, 2303.

- (60) J. K. Barton and S. J. Lippard. Annals N. Y. Acad. Sci. 1978, 313, 686.
- (61) S. S. G. E. van Boom and J. Reedijk. J. Chem. Soc., Chem. Commun. 1993, 1397.
- (62) K. J. Barnham, M. I. Djuran, P. S. Murdoch and P. J. Sadler. J. Chem. Soc., Chem. Commun. 1994, 721.
- (63) S. S. G. E. van Boom, PhD Thesis, Leiden University, 1995.
- (64) M. Caluccia, A. Nassi, F. Loseto, A. Boccarelli, M. A. Mariggio, D. Giordano,
  F. D. Intini, P. Caputo and G. J. Natile. *Med. Chem.* 1993, 36, 510.
- (65) K. J. Barnham, M. I. Djuran, P. S. Murdoch, J. D. Ranford and P. J. Sadler. *Inorg. Chem.* 1996, 35, 1065.
- (66) N. Farrell, D. M. Kiley, W. Schmidt and M. P. Hacker. *Inorg. Chem.* 1990, 29, 397.
- (67) M. van Beusichem and N. Farrell. *Inorg. Chem.* **1992**, *31*, 634.
- (68) N. Farrell, L. R. Kelland, J. D. Roberts and M. van Beusichem. *Cancer Res.* 1992, 52, 5065.
- (69) K. J. Barnham, M. I. Djuran, P. S. Murdoch, J. D. Ranford and P. J. Sadler. *Inorg. Chem.* 1996, 35, 1065.
- (70) E. L. M. Lempers and J. Reedijk. *J. Adv. Inorg. Chem.* **1992**, *37*, 175.
- (71) Phil. Mag. **1899**, 47, 375.
- (72) "A new radiation", *Indian J. Phys.* **1928**, 2, 387.
- (73) J. C. de Paula, <a href="http://www.haverford.edu/chem/302/Raman.pdf">http://www.haverford.edu/chem/302/Raman.pdf</a>
- (74) D. P. Shoemaker, C. W. Garland and J. W. Nibler, Experiments in Physical Chemistry, 6<sup>th</sup> ed., McGraw-Hill, New York, NY, pp. 389 397.

- (75) F. A. Cotton, Chemical Applications of Group Theory, Wiley Interscience, New York, NY, 1963.
- (76) G. Herzberg, Infrared and Raman Spectra of Polyatomic Molecules, Van Nostrand Reinhold, New York, NY, 1945.
- (77) Horiba scientific, 2 Miyanohigashi, Kisshoin, Minami-ku Kyoto 601-8510 Japan. www.horiba.com
- (78) CancerBACUP (British Association of Cancer United Patients), 3 Bath Place, Rivington Street, London EC2A 3JR, UK. <a href="https://www.cancerbacup.org.uk">www.cancerbacup.org.uk</a>
- (79) Coordination Chemistry Reviews 2008, 252, 2239.
- (80) J. Reedijk, A. M. J. Fichtinger-Schepman, A. T. van Oosterom and P. van de Putte. *Struc. Bonding.* **1987**, *67*, 53.
- (81) A. Gund and B. K. Keppler. *Angew. Chem., Int. Ed. Engl.* **1994**, *33*, 186.
- (82) L. K. Webster, G. B. Deacon, D. P. Buxton, B. L. Hillcoat, A. M. James, I. A. G. Roos, R. J. Tomson, L. P. G. Wakelin and T. L. J. William. *J. Med. Chem.* 1992, 35, 3349.
- (83) M. J. Bloemink, H. Engelking, S. Karent Zopoulos, B. Krebs and J. Reedijk. *Inorg. Chem.* **1996**, *35*, 619.
- (84) N. Nédélec and F. D. Rochon. *Inorg. Chim. Acta* **2001**, *319*, 95.
- (85) N. Nédélec and F. D. Rochon. *Inorg. Chem.* **2001**, *40*, 5236.
- (86) J. R. L. Priqueler and F. D. Rochon. *Inorg. Chim. Acta* **2004**, *357*, 2167.
- (87) J. R. L. Priqueler and F. D. Rochon. *Can. J. Chem.* **2004**, *80*, 649.
- (88) C. Creutz and H. Taube. J. Am. Chem. Soc. **1969**, 91, 3988.
- (89) C. Creutz and H. Taube. J. Am. Chem. Soc. **1973**, 95, 1086.

- (90) N. J. S. Salt, J. P. Rourke and P. M. Maitlis. 3<sup>rd</sup> International Symposium on Platinum Group Chemistry, 1987, Sheffield, UK.
- (91) P. J. Stang, D. H. Cao, S. Saito and A. M. Arif. J. Am. Chem. Soc. 1995, 117, 6273.
- (92) P. M. G. Calvert, A. N. Hughes, E. R. Plummer, A. S. T. Azzabi, M. W. Verrill, M. G. Camboni, E. Verdi, A. Berareggi, M. Zuchetti, A. M. Robinson, J. Carmichael and A. H. Calvert. *Clinical Cancer Res.* 1999, 5, 3796.
- (93) Y. Qu, H. Rauter, A. P. S. Fontes, R. Bandarage, L. R. Kelland and N. Farrell.
  J. Med. Chem. 2000, 43, 3189.
- (94) A. Hegmans, Y. Qu, L. R. Kelland, J. D. Roberts and N. Farrell. *Inorg. Chem.* **2001**, 40, 6108.
- (95) A. Albinati, F. Isaia, W. Kaufmann, C. Sorato and L. M. Venanzi. *Inorg. Chem.* 1989, 28, 1112.
- (96) W. Lu, M. C. W. Chan, K.-K. Cheung and C.-M. Che. *Organometallics*. **2001**, 20, 2477.

## **CHAPTER II**

# <sup>195</sup>Pt NUCLEAR MAGNETIC RESONANCE SPECTROSCOPY

This chapter was published in the form of a review in 2006, and then updated since:

An Overview of 195 Pt Nuclear Magnetic Resonance Spectroscopy

Priqueler, Julien; Butler, Ian; Rochon, Fernande

Applied Spectroscopy Reviews

Volume 41, Number 3, 2006, pp. 185-226(42).

Taylor and Francis Ltd Publishing.

2.1 Introduction	55
2.2 Theoretical aspects	58
2.3 Empirical approach	60
2.4 Other considerations	63
2.5 Coupling constants	67
2.6 Selected applications of liquid-state <sup>195</sup> Pt-NMR spectroscopy	71
a. Determination of enantiomeric composition and absolute configuration	on <b>71</b>
<b>b.</b> Biosensors and diagnostic biomarkers	75
c. Research in the anticancer field	78
d. Cluster chemistry	82
e. Kinetic studies	84
2.7 Solid-state <sup>195</sup> Pt-NMR spectroscopy	88
2.8 Conclusions	95
References	122
δ( <sup>195</sup> Pt) NMR chemical shifts	Appendix A
J( <sup>195</sup> Pt- <sup>1</sup> H) coupling constants	Appendix B

#### 2.1 Introduction

Platinum chemistry encompasses many areas including homogeneous catalysis for organic and industrial chemistry, heterogeneous catalysis for the automobile industry (catalytic convectors) and anticancer drugs. It is not surprising, therefore, that many laboratories throughout the world are now showing an increasing interest in <sup>195</sup>Pt-NMR spectroscopy as a routine analytical method. Multinuclear magnetic resonance spectroscopy is a very powerful technique for the characterization of platinum complexes in solution. The <sup>195</sup>Pt nucleus has a spin of ½, while the other isotopes have a zero spin. The relatively high natural abundance of <sup>195</sup>Pt (33.8%), combined with a large magnetogyric ratio (5.768 x 10<sup>7</sup> rad T<sup>-1</sup> s<sup>-1</sup>) leads to a receptivity of 3.4 x 10<sup>-3</sup> relative to the proton, i.e., 19 times that of <sup>13</sup>C (1). The NMR frequency, relative to a 100-MHz <sup>1</sup>H instrument is 21.4 MHz, not very far from the NMR frequency of <sup>13</sup>C (25.1 MHz).

Platinum-195 NMR spectroscopy is now an important, non-destructive analytical technique. While it is a relatively old method, it was not initially particularly useful because of the non-availability of suitable instrumentation. With the advent of Fourier-transform NMR spectroscopy for the <sup>1</sup>H and <sup>13</sup>C nuclei in the 1970s, it became evident that what was possible for these nuclei should also be feasible for the <sup>195</sup>Pt nucleus. The introduction of superconducting magnets in modern NMR instruments has increased the signal-to-noise ratio considerably, which was in fact one of the major limitations in the routine use of <sup>195</sup>Pt NMR spectroscopy, for which the signals are usually quite broad. This present chapter

presents an overview of the <sup>195</sup>Pt-NMR technique, together with descriptions of some selected liquid- and solid-state applications. Platinum-195 NMR spectra are generally measured for solutions. Unlike <sup>1</sup>H-NMR spectroscopy though, each species normally gives a unique signal, except for polymetallic species, where coupling between different Pt centers can be observed. For these types of compounds, the technique is an excellent source of information for metal-metal bonds. In general, however, a single signal is observed for each Pt atom. If a molecule contains two different Pt environments, two different resonances are detected. Therefore, different Pt signals can result from distinct molecules (Figs. 2.1 (a) and (b)), or from different environments in the same molecule (Fig. 2.1 (c)).

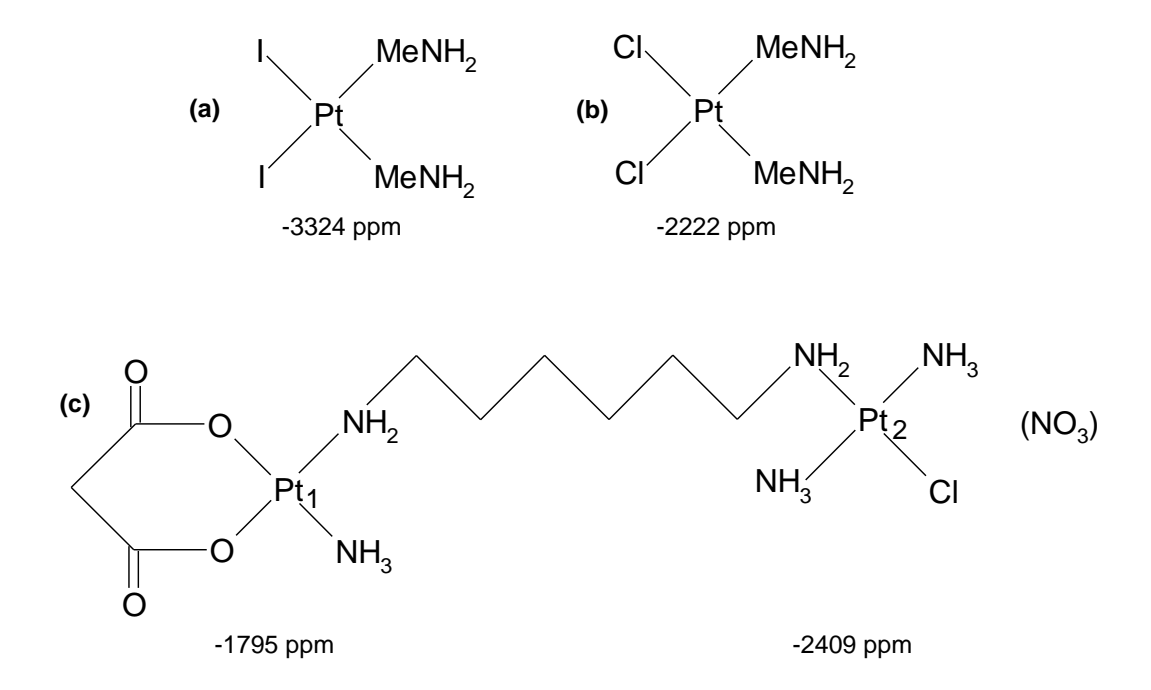


**Figure 2.1** Examples of platinum-195 NMR chemical shifts.

By convention,  $^{195}$ Pt-NMR resonances are reported in terms of a chemical shift ( $\delta(Pt)$ ), in ppm, from a reference compound rather than specifying the absolute

frequency. The reference compound used in most of the cases is Na<sub>2</sub>[PtCl<sub>6</sub>] in D<sub>2</sub>O where  $\delta(Pt) = 0$  ppm. This compound is commercially available, relatively cheap and quite stable. Its 195Pt-NMR spectrum can be measured in a few minutes. The spectrum of a less soluble compound can usually be obtained in an hour or so. Many neutral Pt compounds are not very soluble and overnight measurements are often required. The <sup>195</sup>Pt-NMR resonance window is very large, ~15,000 ppm, whereas it is only 300 ppm for <sup>13</sup>C and 15 ppm for <sup>1</sup>H (diamagnetic compounds). Most commonly used instruments have a more limited working window, usually about 1500-1600 ppm. It is therefore important to know approximately where to expect the signal of the compound under investigation, in order to prevent the observation of fold-over peaks, caused by signals outside the selected frequency range. The existence of such fold-over peaks can be confirmed, for example, by either changing the spectral width (SW) on a Varian instrument or by changing the TO value (transmitter offset position) on a Bruker spectrometer. It is important to calibrate an instrument by measuring the spectrum of a standard compound, whose signal is preferably in the working window and whose  $\delta(Pt)$  value is known relative to Na<sub>2</sub>[PtCl<sub>6</sub>] in D<sub>2</sub>O. The most common external standard used in the literature is K<sub>2</sub>[PtCl<sub>4</sub>] in D<sub>2</sub>O, which has a resonance at -1628 ppm. The aqueous solution of this material shows a second peak at -1194 ppm, corresponding to K[Pt(H<sub>2</sub>O)Cl<sub>3</sub>], which can be reduced by adding KCl. Therefore, great care should be taken in order to calibrate the frequency of the instrument by using the correct signal. Other reference materials are often used for other windows, e.g. K[Pt(DMSO)Cl<sub>3</sub>] in D<sub>2</sub>O (δ(Pt) = -2998 ppm), cis-Pt(tetramethylenesulfoxide)<sub>2</sub>Cl<sub>2</sub> in CDCl<sub>3</sub> ( $\delta$ (Pt) = -3450 ppm) and  $K_2[Pt(CN)_4]$  in  $D_2O(\delta(Pt) = -4705 \text{ ppm})$ .

The <sup>195</sup>Pt chemical shift is influenced by the presence of all the ligands in the coordination sphere of the Pt atom. The  $\delta(^{195}\text{Pt})$  values are highly sensitive to the nature of the binding atoms. The  $\sigma$  bond (L $\rightarrow$ M) reduces the electron density on the ligand and increases it on the Pt atom. If there is a back-donation of  $\pi$  electrons (M $\rightarrow$ L), the electron density is then reduced on the Pt atom and is increased on the ligand. For most ligands,  $\pi$  -bonding is not very important, and a deshielding effect is observed on the ligand. <sup>195</sup>Pt-NMR spectroscopy should be combined with <sup>1</sup>H, <sup>13</sup>C and other nuclei spectroscopy in order to gain maximum information. There is usually an inversed relationship between the chemical shifts observed in, for example, <sup>1</sup>H-NMR and <sup>195</sup>Pt-NMR. Important information on the nature of the Pt-ligand bond can thus be obtained from the multinuclear magnetic resonance spectra. Nowadays,  $\delta(^{195}\text{Pt})$  signals have been reported for many compounds and several trends have been noted, especially in the excellent 1982 review by Pregosin (2). This NMR research has provided considerable structural information on Pt complexes.

# 2.2 Theoretical aspects

The total contribution to a heavy metal shielding constant ( $\sigma$ ) for a nucleus like <sup>195</sup>Pt, is indicated by the expression (3):

$$\sigma = \sigma_p + \sigma_d + \sigma_x$$

where  $\sigma_d$  represents the diamagnetic screening contribution and is the same for all Pt(II) complexes. This component describes the local electronic density around the nucleus that is orthogonal to the instrument magnetic field,  $H_0$ . The extraneous

component  $(\sigma_x)$  corresponds to different anisotropic contributions, while changes in the paramagnetic constant  $\sigma_p$  represent the variable factors, which are due to the nucleus non-symmetry, a consequence of the orbital geometry. Its magnetic vector is opposed to the diamagnetic component vector, which in turn, induces a displacement to lower field. The component  $\sigma_p$  can be determined from the Ramsey equation (4), which was later adapted for <sup>195</sup>Pt (5-6).

$$\sigma_{\rm p} = \frac{-e^2 h^2}{2m^2c^2} < r^{-3} > Ca_{\rm lg}^2 [8 Ca_{2g}^2 \Delta E_{\rm A}^{-1} + 4 Ce_{\rm g}^2 \Delta E_{\rm E}^{-1}]$$

The terms e, h, m, c and  $< r^{-3} >$  are all constants. They denote, respectively, the electron charge, Planck's constant, electron mass, speed of light and r is an average distance of a 5d electron from the nucleus. The expressions  $\Delta E$  indicate the energy differences between the occupied molecular orbitals and the empty orbitals (LUMO) accessible for a one-electron transition. The values Ceg, Calg and Ca2g correspond to the coefficients of the metallic character of the Pt d-orbitals in the molecular orbitals involved in the electronic transitions. If there is no covalent bonding, the molecular orbitals are pure d-orbitals ( $Ce_g = Ca_{lg} = Ca_{2g} = 1$ ). The  $\sigma$ -bonds involve mainly the  $d_{x^2-y^2}$  orbital whose metal coefficient will decrease, while back-donation of  $\pi$ electrons from Pt to the ligands will also decrease mainly the Ceg and Ca2g values In theory, the 195Pt chemical shift could be calculated approximately from the electronic spectral data of the compound under study and by estimating the C coefficients. At the moment, the d-d electronic spectra of Pt compounds are not easy to obtain and interpret. Most compounds absorb close to the UV region where other much more intense bands are usually observed. Extensive theoretical calculations

will undoubtedly be undertaken in the future. Meanwhile, many coordination chemists are continuing to use empirical information to determine the approximate Pt frequency of a compound or to relate its chemical shift to its structure.

#### 2.3 Empirical approach

Since theoretical interpretations are still not very successful for the prediction of Pt chemical shifts, Pt scientists have used an empirical approach, based on the available <sup>195</sup>Pt chemical shift data in the literature. The seminal review by Pregosin (2) has proved to be particularly useful over the past 20 years. The most important observations are summarized below.

i) For a series of Pt complexes, the resonance is shifted towards higher fields when the donor atom varies in the following order:

$$O < Cl < N \sim Br < S \sim I < As \sim CN \sim CO \sim P$$

For example, for  $[Pt(L)Cl_3]^-$ :  $L = H_2O -1194$ ,  $MeNH_2 -1842$ , DMSO -2998 and  $PPh_3$  -3513 ppm, For cis-Pt(pyrazine)<sub>2</sub>X<sub>2</sub> :  $X = Cl^-$  -2009,  $NO_2^-$  -2255,  $Br^-$  -2355 and  $I^-$  -3260 ppm.

ii) The chemical shifts are usually dependent on the oxidation state of the metal. Pt(II) complexes are generally more shielded than the Pt(IV) compounds. Pt(0) complexes have chemical shifts at approximately the same fields as do Pt(II) species.

For example, some typical chemical shifts are:  $K_2[PtCl_4]$  -1628,  $K_2[PtCl_6]$  0,  $K_2[Pt(CN)_4]$  -4746 and  $K_2[Pt(CN)_6]$  -3866 ppm.

iii) The chemical shifts usually increase (more negative) when going down in

a group in the Periodic Table (except for group 15).

For example, the  $\delta(Pt)$  for  $[Pt(NH_3)_3Cl]^+$ ,  $[Pt(NH_3)_3Br]^+$  and  $[Pt(NH_3)_3I]^+$  are -2353, -2492 and -2819 ppm, respectively (7).

iv) The  $\delta(Pt)$  values for complexes of the type  $PtL_2X_2$  depend on the geometry of the complexes. *Cis* and *trans* square planar complexes often have similar signals, but they are usually still distinct. The solvent is important, since the difference between the chemical shifts of the isomers might depend on the solvent.

For example, *cis*-Pt(Me<sub>2</sub>SO)(py)Cl<sub>2</sub> -2856 ppm and *trans*-Pt(Me<sub>2</sub>SO)(py)Cl<sub>2</sub> -2957 ppm (8); *cis*-Pt(cyclobutylamine)<sub>2</sub>I<sub>2</sub> -3378 ppm in acetone, -3346 ppm in DMF-d<sub>7</sub> and *trans*-Pt(cyclobutylamine)<sub>2</sub>I<sub>2</sub> -3400 ppm in acetone, -3384 in DMF-d<sub>7</sub> (9). The difference between the two latter isomers is 22 ppm in acetone and 38 ppm in DMF-d<sub>7</sub>.

- The  $\delta(Pt)$  values for (R) and (S) stereoisomers are usually different. In the case of Pt(Me<sub>2</sub>NCH(Me)CH<sub>2</sub>Se)(PEt<sub>3</sub>)Cl, a signal at -4211 was observed for the (R) form and at -4315 ppm for the (S) form (10). Another example where geometric isomers has been observed is for the bidentate ligand N,N'-dimethylethylenediamine. In the *meso* form, the two -CH<sub>3</sub> groups are on the same side of the Pt plane, while in the dl structure, the two -CH<sub>3</sub> groups are on opposite sides of the plane. For the complex  $[Pt(N,N'-Me_2en)(D_2O)_2]^{2+}$ , the signals for the *meso* and dl isomers were detected at -1977 and -1952 ppm (11).
- vi) The  $\delta(Pt)$  values of simple complexes containing non- $\pi$ -bonding ligands, like amines can sometimes be related to the basicity of the ligands or the pKa

values of the protonated ligands. In a related series of complexes, other factors that affect chemical shifts, such as solvent influence or steric hindrance should not be different. For complexes of the type *trans*-Pt(pyridine derivative)<sub>2</sub>Cl<sub>2</sub>, there is a slight increase in the Pt shielding as the pKa of the protonated ligands increase (12). Similar results were obtained for *cis*- and *trans*-Pt(amine)<sub>2</sub>I<sub>2</sub> (13). The basicity of a ligand can also be evaluated by its proton affinity in the gas phase, but there are not many such values available in the literature. A good linear relationship was reported for complexes of the types *cis*- and *trans*-Pt(amine)<sub>2</sub>I<sub>2</sub>. The proton affinity value in the gas phase seems a better basicity indicator than are the pKa values. The latter are measured in a solvent, which participates in the reaction and the results depend on many factors like the bulkiness around the protonated atom.

A tabulation of published  $\delta(^{195}\text{Pt})$  values for Pt(II) complexes is given in the table 2.3. Three main chemical shift regions are noted: the -5500 to -3500 ppm region, which is dominated by  $\pi$ -acceptor, P- and S-bonded ligands, the -3500 to -1500 ppm region, where N-bonded ligands are observed and finally below -1500 ppm, where the signals of O-bonded ligands appear, e.g.,  $[\text{Pt}(D_2O)_4]^{2+}$  (31 ppm) and trans-Pt(D<sub>2</sub>O)<sub>2</sub>Cl<sub>2</sub> (-630 ppm) (14).

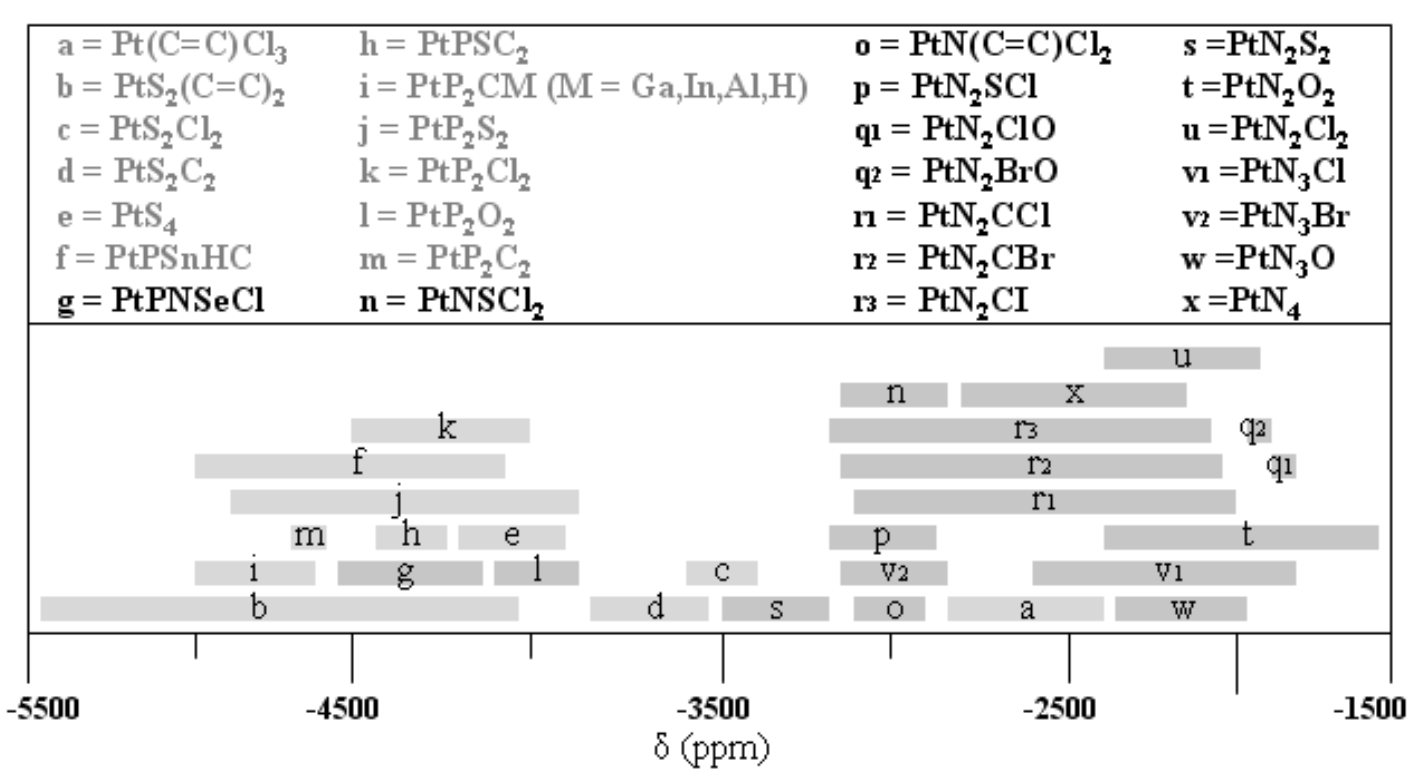


**Table 2.3** Chemical shift summary based on published papers.

Based on available NMR data in the literature, it is sometimes possible to identify a new compound in solution. In this way, Mahalakshmi *et al.* have assigned a new signal observed at -4319 ppm in their work on  $PtX_2(PPh_2(C_6H_4CHO))_2$  complexes (15). They observed  $\delta(Pt)$  signals at -4026 (X=Cl) and -4621 (X=Br) ppm. And they deduced that the new resonance at -4319 ppm was caused by the presence of the mixed-halo complex  $PtClBr(PPh_2(C_6H_4CHO))_2$ .

#### 2.4 Other considerations

There are several other factors which affect  $^{195}$ Pt chemical shifts. Often the solvent used in  $^{195}$ Pt-NMR spectroscopy influences the  $\delta(Pt)$  value. For instance, a 400-ppm difference was observed for (9-methyladeninium)<sub>2</sub>[PtCl<sub>6</sub>]·2H<sub>2</sub>O depending on whether it was dissolved in water or DMSO (16). DMSO is a strong S-binding ligand for Pt(II) complexes and should be used as a solvent with care, especially for chloro compounds and never with aqua complexes, since coordination of DMSO will be rapid. It should be used only when no other solvent can be found and the spectra should be measured rapidly. Dimethylformamide (DMF) is also a good bonding ligand in solution and has been shown to react with chloro-bridged Pt(II) dimers to produce stable DMF complexes (17). For neutral complexes, the  $\delta(Pt)$  value often does not vary very much in different organic solvents, but the signal will be shifted to higher fields when measured in water. For example, the signal of *cis*-Pt(cyclobutylamine)<sub>2</sub>Cl<sub>2</sub> was reported at -2225 ppm in DMF-d<sub>7</sub>, while it is observed at -2290 ppm in D<sub>2</sub>O. Water is a small molecule which can more easily approach the

Pt atom on both sides of the square plane and therefore increase the electron density in the environment of the metal atom.

As mentioned earlier, the geometry of the complex is an important factor in determining the  $\delta(Pt)$  value. The position of the resonance results partly from the extent of  $\sigma$  and  $\pi$  bonding involving the metal atom. For square-planar pyridine compounds of the type  $Pt(Ypy)_2X_2$ , the  $\Delta\delta$  between the signals for the two isomers is  $\sim$ 50 ppm for X = Cl and  $\sim$ 90 ppm for X = I (12). This difference has been related to the relative order of the iodo, chloro and pyridine ligands in the trans influence series. For primary amine complexes of the type  $Pt(amine)_2X_2$ , the  $\Delta\delta$  value for iodo complexes are less than 18 ppm in CD<sub>3</sub>COCD<sub>3</sub> and about 25 ppm in DMF-d<sub>7</sub>, while it is even lower for the chloro complexes (13). When  $X = H_2O$  and  $NO_3$ , the  $\Delta\delta$  values are much larger, i.e., ~190 ppm and ~130 ppm respectively. In these compounds, the signals of the cis isomers are usually observed at higher fields than are those for the trans compounds. For ligands forming  $\pi$ -bonds with the metal, the situation is reversed. Back-donation of electrons  $(M \rightarrow L)$  will decrease the electronic density on the Pt atom. Because of the geometry of the d orbitals,  $\pi$ bonding will be more efficient in the cis configuration than in the trans one. Therefore, the cis configuration will result in a much greater decrease in electronic the Pt atom than will the trans configuration. For the Pt(R<sub>2</sub>SO)(pyrimidine)Cl<sub>2</sub> complexes, the cis isomers were detected at around -2950 ppm, while the trans isomers were observed at higher fields, at around -3060 ppm (18).

Steric hindrance around the ligand donor atom is also an important factor in

the determination of the chemical shift. It will cause a signal displacement generally towards lower fields. This can be explained by the solvent effect and it is a very important factor for solvents which can bind the Pt atom in solution. It has also been termed the "ortho effect" when the ligands are, for example, pyridine derivatives. The presence of a methyl group in *ortho* positions will increase the steric hindrance around the binding N atom of the ligand. For normal complexes, the molecules of solvent can approach the Pt atom on both sides of the square plane, which increases the electron density around the central metal atom. This increase will cause a shielding effect on the <sup>195</sup>Pt-NMR spectra. A large steric hindrance on the binding atom of the ligands will prevent the approach of solvent molecules, thus reducing the electron density in the close environment of the Pt atom. This effect is very important for solvents with electron-donating groups such as water. For example the signal of cis-Pt(MeNH<sub>2</sub>)<sub>2</sub>Cl<sub>2</sub> in DMF-d<sub>7</sub> was reported at -2224 ppm, while the one for the secondary amine compound cis-Pt(Me<sub>2</sub>NH)<sub>2</sub>Cl<sub>2</sub> appeared at -2188 ppm. Other examples include a series of complexes of the type K[Pt(Ypy)Cl<sub>3</sub>] measured in  $D_2O$ , where Ypy is a derivative of pyridine. For unsubstituted pyridine, the  $\delta(Pt)$ value of the complex was at -1816 ppm, while it was reduced to -1796 ppm for the 2-picoline compound and further reduced to -1754 ppm when Ypy = 2,6-lutidine. In order to verify the cause of the observed shift towards lower fields with increasing steric hindrance in the *ortho* position of the ligand, these data were compared to the signal of complexes containing pyridine ligands with -CH<sub>2</sub>OH groups in ortho positions. These groups were thought to mimic the approach of water molecules towards the metal center and increase the electron density around the Pt atom. As

expected, the  $\delta(Pt)$  value for K[Pt(2-HOCH<sub>2</sub>pyridine)Cl<sub>3</sub>] was found at -1820 ppm, while it was increased to -1839 for K[Pt(2,6-(HOCH<sub>2</sub>)<sub>2</sub>pyridine)Cl<sub>3</sub>] (19).

The chelate effect has also an influence on the chemical shifts. The presence of a metal-chelate shifts the resonance to higher fields. For a N<sub>2</sub>Cl<sub>2</sub>Pt(II) environment, the chemical shifts of the following compounds in D<sub>2</sub>O are: *cis*-Pt(NH<sub>3</sub>)<sub>2</sub>Cl<sub>2</sub> -2168 ppm, *cis*-Pt(cyclobutylamine)<sub>2</sub>Cl<sub>2</sub> -2290 ppm and Pt(N,N-Me<sub>2</sub>en)Cl<sub>2</sub> -2355 ppm (11). The same observations can be made for the following compounds in MeOD: *cis*-[Pt(HNCO<sup>t</sup>Bu)<sub>2</sub>(NH<sub>2</sub>CH<sub>3</sub>)<sub>2</sub>]·H<sub>2</sub>O -2593 ppm, *cis*-[Pt(HNCO<sup>t</sup>Bu)<sub>2</sub>(NH<sub>2</sub><sup>t</sup>Bu)<sub>2</sub>]·H<sub>2</sub>O -2599 ppm and *cis*-[Pt(HNCO<sup>t</sup>Bu)<sub>2</sub>(en)]·H<sub>2</sub>O -2692 ppm (Fig. 2.4) (56).

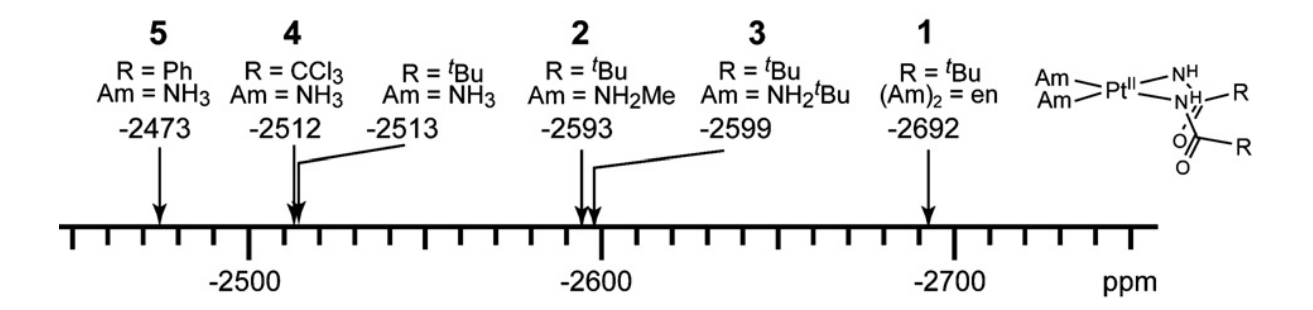


**Figure 2.4** <sup>195</sup>Pt chemical shifts of cis-[Pt(HNCOR)<sub>2</sub>(Am)<sub>2</sub>] in MeOH (56).

The temperature at which the spectra are measured is also a factor influencing the chemical shifts. A variation of 1°C modifies the observed signal by 0.1-1.0 ppm (20). When the temperature is increased by 100°C, the shift can vary by 50 ppm. Since most spectra are measured at room temperature, this factor is less important. Finally, the resonance frequency can also be slightly influenced by the complex concentration. Most Pt complexes are not very soluble, except for the simple salts, and often their lack of solubility is a major problem. Long accumulation times are often required, which might bring changes of the different species in solution. These changes with time can be studied by <sup>195</sup>Pt-NMR spectroscopy, provided that the changes are not too rapid.

#### 2.5 Coupling constants

The study of the  $^{1}$ H,  $^{15}$ N,  $^{31}$ P and  $^{13}$ C NMR spectra of Pt complexes is very useful and can bring further information on the structure of the compounds. The chemical shift differences between the free molecules and the bonded ligands give important information on the binding sites of the ligands to the platinum center. Atoms closer to the donor site will be more affected by coordination than are the other atoms. Usually, a deshielding effect is observed on the ligand, unless  $\pi$ -bonding is important. The  $\sigma$  bond (L $\rightarrow$ M) reduces the electron density on the ligand and increases it on the Pt atom. As mentioned already, if there is a back-donation of  $\pi$  electrons (M $\rightarrow$ L), the electron density is then reduced on the Pt atom and is increased on the ligand. Further information is also obtained from the splittings in

the NMR resonances produced by spin-spin couplings to other magnetically active nuclei in the molecule. Couplings between <sup>195</sup>Pt and isotopes such as <sup>1</sup>H, <sup>13</sup>C, <sup>15</sup>N and <sup>31</sup>P can confirm the position of the binding sites and have been reported through one to four bonds (<sup>1</sup>J, <sup>2</sup>J, <sup>3</sup>J or <sup>4</sup>J). Coupling with <sup>1</sup>H is the most common and a list of coupling constants J(<sup>195</sup>Pt-<sup>1</sup>H) is given in Appendix B.

Since the natural abundance of <sup>195</sup>Pt is 33.8%, signals in the <sup>1</sup>H or <sup>13</sup>C NMR spectra appear as normal signals for the <sup>194</sup>Pt and <sup>196</sup>Pt isotopes, flanked with satellites, due to coupling with the <sup>195</sup>Pt isotope. On a low-field spectrometer, the two satellites each have 17% intensity, a consequence of the relative abundance of <sup>195</sup>Pt. If the signal is a singlet, it will appear as a singlet and a doublet with 1:4:1 relative intensities. From a practical point-of-view, the triplet will show a 1:5:1 ratio on a 60-MHz, a 1:7:1 ratio on a 100-MHz and about a 1:10:1 ratio on a 300-MHz spectrometer (21). The intensity of the satellites due to coupling with <sup>195</sup>Pt decreases as the field of the spectrometer is increased. This result is a consequence of the chemical shift anisotropy (22). Therefore, provided that the sample is reasonably soluble, it is preferable to use a lower field instrument in order to obtain good values of coupling constants. If the solubility is low, long accumulation times should be used in order to reduce the background noise.

Couplings through one bond have been reported on <sup>15</sup>N amine Pt(II) complexes. The coupling constants vary with the nature of the ligand located in trans position to the amine ligand. These <sup>1</sup>J(<sup>195</sup>Pt-<sup>15</sup>N) values are in the 150-350 Hz range and give important information on the trans influence. The couplings can be

observed in both <sup>195</sup>Pt- and <sup>15</sup>N-NMR spectra. Couplings of the type <sup>1</sup>J(<sup>195</sup>Pt-<sup>14</sup>N) are not usually observed in <sup>195</sup>Pt-NMR spectroscopy, since the signals are much wider. The relaxation time caused by the quadrupolar  $(I = 1)^{-14}N$  nucleus bonded to platinum is too fast for the coupling to be observed, and too slow to decouple completely from the platinum atom (22). <sup>1</sup>J(<sup>195</sup>Pt-<sup>13</sup>C) coupling constants have also been reported on CH<sub>3</sub> complexes and are in the 500-600 Hz range (23). These values are increased to 1000-1800 Hz in carbonyl complexes (24). A <sup>31</sup>P-NMR study of compounds of the type cis- and trans-Pt(PR<sub>3</sub>)<sub>2</sub>Cl<sub>2</sub> has shown that the <sup>1</sup>J(<sup>195</sup>Pt-<sup>31</sup>P) coupling constant increases when the extent of  $\pi$ -bonding increases. The  ${}^{1}J({}^{195}Pt-{}^{31}P)$ values are usually quite large especially for the trans isomers. These couplings are usually observed in <sup>31</sup>P-NMR, but sometimes they can be observed in the <sup>195</sup>Pt-NMR spectra. For instance, a doublet of doublets was reported for a prismatic molecular rotor produced from the assembly of the biphenyl rod [Ph<sub>2</sub>P(CH<sub>2</sub>)<sub>3</sub>PPh<sub>2</sub>Pt-C<sub>6</sub>H<sub>4</sub>-C<sub>6</sub>H<sub>4</sub>-PtPh<sub>2</sub>P(CH<sub>2</sub>)<sub>3</sub>PPh<sub>2</sub>]<sup>2+</sup> with 4,4'-bipyridine forming a molecular rectangle  $({}^{1}J({}^{195}Pt - {}^{31}P) = 3629$  and 1535 Hz) (25). These values are consistent with the Pt satellites observed in the  $^{31}$ P-NMR spectrum ( $^{1}J = 3646$  and 1538 Hz). Some <sup>1</sup>J(<sup>195</sup>Pt-<sup>195</sup>Pt) couplings have also been observed in clusters. There are many values summarized in the two reviews by Pregosin (2,26) and these vary between about 60 and 9000 Hz.

Coupling through two or three bonds is more common and the coupling values can give important information on the geometry of the complexes. Usually, these values are larger for cis compounds than for trans ones. For example in  $Pt(amine)_2I_2$  complexes, the average  $^2J(^{195}Pt^{-1}H)$  values were found to be 69 Hz (cis)

and 60 Hz (trans), (13) while in Pt(amine)<sub>2</sub>(NO<sub>3</sub>)<sub>2</sub>, they are 67 Hz (cis) and 58 Hz (trans) (27). Couplings of the type  ${}^2J({}^{195}Pt^{-1}H)$  have been observed for amine complexes even when measured in D<sub>2</sub>O, but sometimes the pH is important. For example for the ionic compound K[Pt(MeNH<sub>2</sub>)Cl<sub>3</sub>], the coupling was observed in D<sub>2</sub>O at pD=4 but not at pD=7, where exchange of the amine protons with the solvent is too rapid. The  ${}^2J({}^{195}Pt^{-13}C)$  couplings are often smaller than expected. For example, in Pt(amine)<sub>2</sub>I<sub>2</sub> compounds, they are around 17 Hz (cis) and 12 Hz (trans) (9,13). When the amine is a pyridine derivative, the couplings are too small to be observed. These small couplings are probably due to inadequate orientation of the orbitals. But in Pt-R<sub>2</sub>SO complexes, the  ${}^2J({}^{195}Pt^{-13}C)$  are more normal and are about the same for cis and trans isomers (~55 Hz) (18).

Coupling of the types  ${}^{3}J({}^{195}Pt^{-1}H)$  and  ${}^{3}J({}^{195}Pt^{-13}C)$  are common. Again the values are greater for cis diamine compounds (~40 Hz) than for the corresponding trans isomers (~30 Hz). Some authors have identified the configuration of a complex based on the coupling constants. For instance, *cis* and *trans*-Pt(py)<sub>2</sub>X<sub>2</sub> (py = pyridine derivative, X = uninegative ligand) have been differentiated by Ha *et al.* (28) by the  ${}^{3}J({}^{195}Pt^{-1}H)$  coupling observed in  ${}^{1}H$ -NMR spectroscopy. For sulfoxide complexes, the difference is smaller, about 25 and 22 Hz respectively. In *cis*-Pt(2,4-lutidine)<sub>2</sub>(NO<sub>3</sub>)<sub>2</sub>, the  ${}^{3}J({}^{195}Pt^{-13}C)$  coupling with the C atom in the pyridine ring is larger (48 Hz) than is the one with the methyl group in the *ortho* position (31 Hz). Couplings through four bonds are more difficult to calculate, especially on higher fields instruments. These couplings are usually 9-16 Hz and have been reported only on singlets. One example where the  ${}^{4}J({}^{195}Pt^{-1}H)$  could be calculated with a good

precision was done on a 60 MHz instrument. The coupling constant for K[Pt(CH<sub>3</sub>CN)Cl<sub>3</sub>] was found to be 14.5 Hz, while the corresponding values for *cis*-and *trans*-Pt(amine)(CH<sub>3</sub>CN)Cl<sub>2</sub> were calculated as 13 and 15 Hz respectively (29). Therefore, these coupling constants are also dependent on the geometry of the compounds, but a good precision is required. A few other <sup>4</sup>J(<sup>195</sup>Pt-<sup>1</sup>H) values have been reported with larger errors (300 MHz instrument). For examples, values between 11-13 Hz for compounds of the types Pt(pyridine)<sub>2</sub>(NO<sub>3</sub>)<sub>2</sub> (30), [Pt(pyridine)<sub>2</sub>(H<sub>2</sub>O)<sub>2</sub>](NO<sub>3</sub>)<sub>2</sub> and Pt(pyridine)<sub>2</sub>(OH)<sub>2</sub> (31) were reported. A few examples of <sup>4</sup>J(<sup>195</sup>Pt-<sup>13</sup>C) were noted. For the ionic complexes K[Pt(pyridine)Cl<sub>3</sub>] and K[Pt(3,5-lutidine)Cl<sub>3</sub>], the coupling constants are 11.8 and 14.7 Hz (20.15 MHz) (19).

# 2.6 Selected applications of liquid-state <sup>195</sup>Pt-NMR spectroscopy

Multinuclear magnetic resonance is a method which is developing rapidly in the study of Pt compounds, especially in view of recent instrumentation developments. Examples of the more recent interesting applications are discussed below.

### i) Determination of enantiomeric composition and absolute configuration

The most outstanding use of <sup>195</sup>Pt-NMR spectroscopy is in the study of enantiomers and the determination of their absolute configuration. Uccello-Baretta and coworkers have employed the technique for several years to determinate the enantiomeric composition of chiral compounds. The use of chiral derivatizing agents

(CDAs) in NMR spectroscopy is one of the most effective answers to the growing demand for the study of the configuration of chiral substrates. The compounds *cis*-and *trans*-Pt(ethylene)((S)- $\alpha$ -methylbenzylamine)Cl<sub>2</sub> (**1'b** in Fig. 2.6.1) were suggested as CDAs for the analysis of unsaturated compounds (32-33) and trisubstituted allenes (34-35) by <sup>195</sup>Pt-NMR spectroscopy. More recently, the use of the ionic organometallic complex [PtCl<sub>3</sub>(C<sub>2</sub>H<sub>4</sub>)]<sup>+</sup>[(S,S)-(PhMeCH)<sub>2</sub>NH<sub>2</sub>]<sup>+</sup> (**1a**) was also suggested (36). Compound **1a** seems to have a large applicability to several types of chiral unsaturated molecules, such as vinyl ethers, cyclic and acyclic allyl ethers and simple olefins. In solution, the Pt-coordinated C<sub>2</sub>H<sub>4</sub> ligand is exchanged with the unsaturated compound (**3** in Fig. 2.6.1), which is a diastereoisomeric mixture. Distinct <sup>195</sup>Pt-NMR resonances for all the complexed enantiomers were observed, which permitted the quantitative determination of the different enantiomers or their purity.

In 2001, the same research group reported the use of a similar ionic complex [PtCl<sub>3</sub>(C<sub>2</sub>H<sub>4</sub>)]<sup>-</sup>[(1*S*, *I* '*S*)-bis(1-(1naphthyl)ethyl)amineH]<sup>+</sup> (**1c** in Fig. 2.6.1) as an efficient CDA for the complete stereocharacterization of trisubstitued allenes, including the determination of the enantiomeric purities and their absolute configuration (37-38). The complexation of the trisubstituted allenes occurs by the two prochiral faces of the less substituted double bond, the one bearing the hydrogen atom (Fig. 2.6.2). Therefore, each enantiomer can lead to two diastereoisomers.

195 Pt-NMR spectroscopy is an easy way to determine the relative isomer ratio, each of them giving rise to a single 195 Pt resonance. The enantiomeric composition can be evaluated by comparing the intensity of the signals produced by each isomer. An

example can be given by the complexation of the racemic allene (tbutyl)MeC=C=CHBr (2) which produced two distinct <sup>195</sup>Pt resonances of equal intensities at -2392 and at -2397 ppm (Fig. 2.6.2a). The relative proportion of the enantiomers determined by integration was in good agreement with the results obtained when using known enantiomeric compositions and determined by gas chromatography. The complex containing a known (S) enantiomeric excess of 65% showed a prevalence of the -2397 ppm signal (Fig. 2.6.2b). The resonances were thus easily assigned. The ratio of the integrated signals showed the expected enantiomeric composition of the corresponding allenes. Only two <sup>195</sup>Pt-NMR resonances have also been observed for other complexed racemic allenes containing a tert-butyl group. The <sup>195</sup>Pt-NMR resonances of the diastereoisomeric derivatives exhibited well separated signals with those of the (R)-enantiomers appearing at lower fields than do those of the (S) analogues. Therefore, the <sup>195</sup>Pt-NMR method gives not only the enantiomeric proportions, but also their absolute configuration. The technique has faced some remarkable limitations when using trans-disubstituted CDAs containing secondary amines. The diastereoisomeric mixtures obtained from trans-PtCl<sub>2</sub>(C<sub>2</sub>H<sub>4</sub>)(1S,1'S)-bis(1-(1-Np)Et)NH and trans-PtCl<sub>2</sub>(C<sub>2</sub>H<sub>4</sub>)(1S,1'S)-N-(1'-(1-Np)Et)-1-PhEtNH (Np = naphthyl) gave very complicated <sup>195</sup>Pt-NMR spectra, because of the presence of slow-exchanging rotamers for each platinum(II) compound.

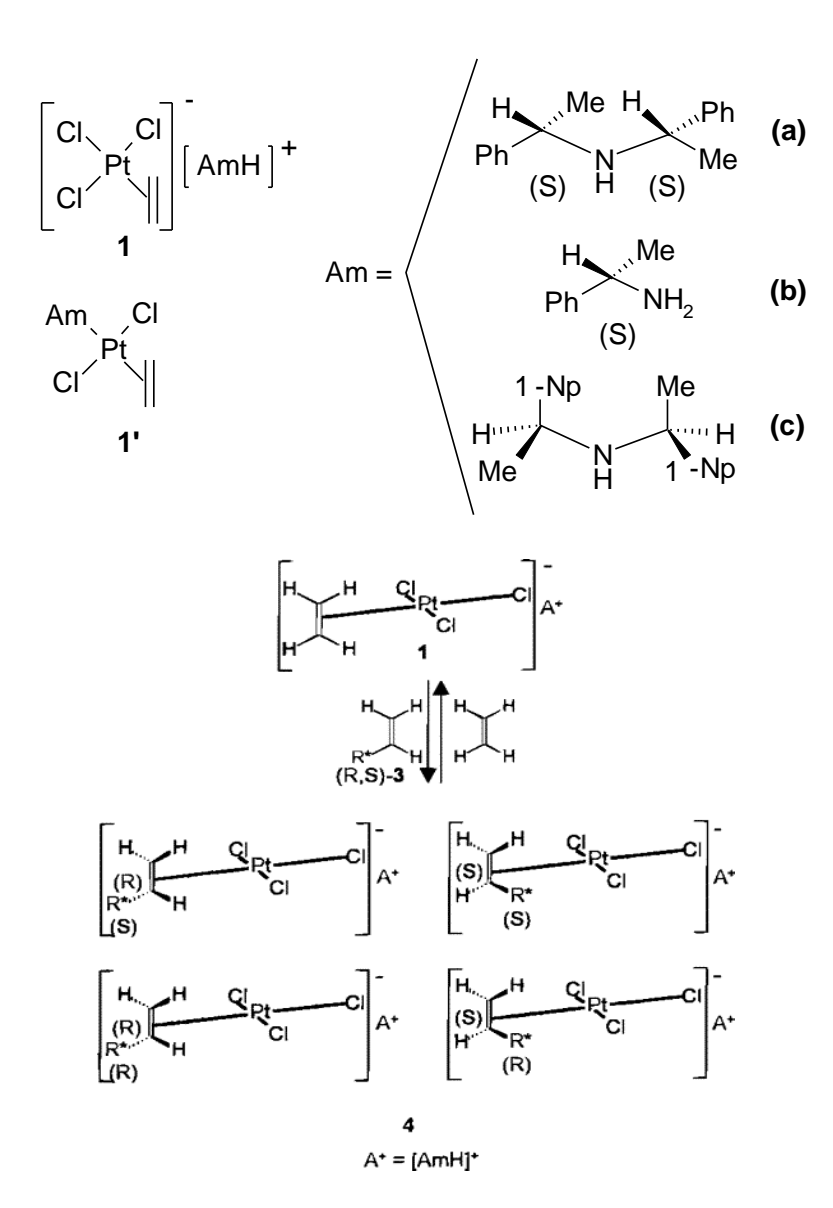


**Figure 2.6.1** Molecules proposed as CDA and ethylene exchange reaction of complex **1** with unsaturated molecules **3**. Reprinted with permission from Uccello-Barretta, G.; Bernardini, R.; Lazzaroni, R.; Salvadori, P. [PtCl<sub>3</sub>(C<sub>2</sub>H<sub>4</sub>)]<sup>-</sup>[(*S*,*S*)-(PhMeCH)<sub>2</sub>NH<sub>2</sub>]<sup>+</sup>. Org. Lett. 2000, 2, 1795-1798. Copyright (2000) American Chemical Society.

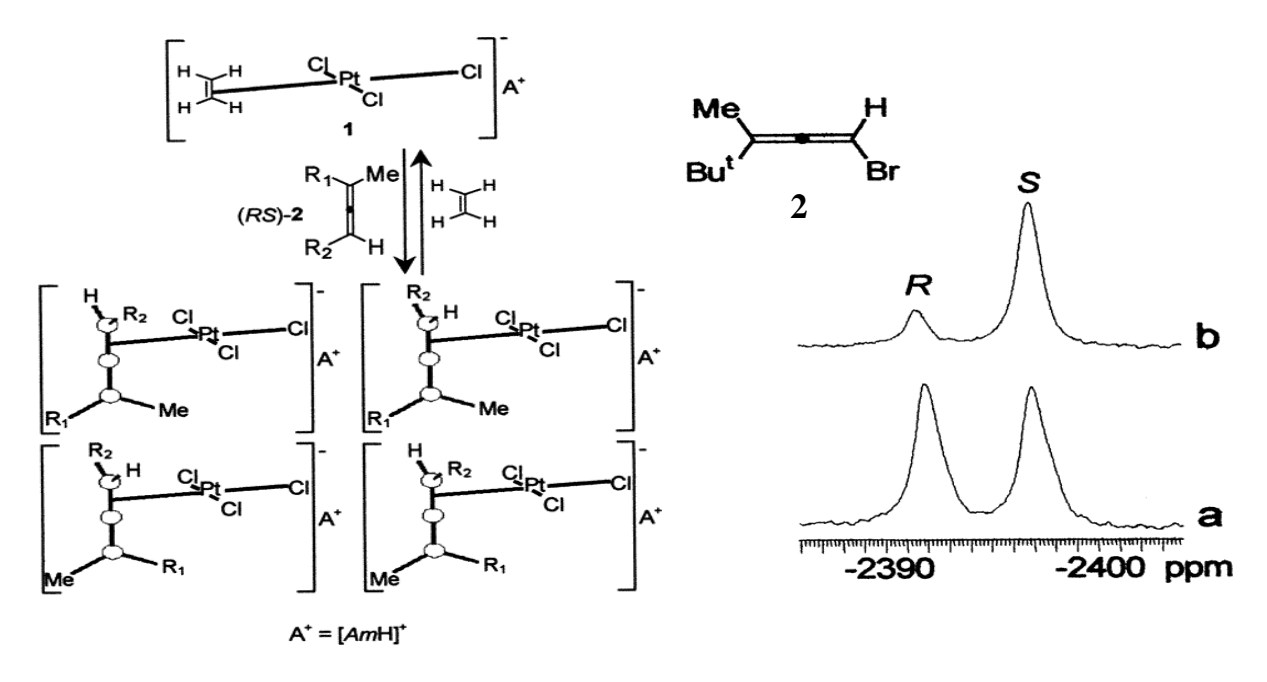


**Figure 2.6.2** Ethylene exchange reactions with trisubstituted allenes and <sup>195</sup>Pt-NMR analysis of the diastereoisomeric mixtures formed from **1c** with (a) (*RS*)-**2** and (b) (*S*)-**2** (ee 65%). Reprinted with permission from Uccello-Barretta, G.; Bernardini, R.; Balzano, F.; Caporusso, A.M.; Salvadori, P. Org. Lett. 2001, 3, 205-207. Copyright (2001) American Chemical Society.

#### ii) Biosensors and diagnostic biomarkers for peptide labelling

The specific folding of peptide sequences which determines the three-dimensional structure of the molecule and its functionalities is or great importance in protein chemistry. Details of the folding process are still not fully understood. The structures of the biomolecules bring important information on the mechanism of action of proteins and enzymes. Peptide labelling is an interesting concept to monitor such folding processes. Appropriate biomarkers may be introduced either by peptide side-chain modification or by labelling the terminal amino acid of the protein. Van Koten and his research group (39) have shown the broad application potential of organoplatinum(II) complexes of the type PtX(2,6-(CH<sub>2</sub>NMe<sub>2</sub>)<sub>2</sub>-4-

RC<sub>6</sub>H<sub>2</sub>) (Fig. 2.6.3), where R can be an amino acid sequence. Peptide functionalization of the Pt(II) compounds provides a diagnostic biomarker for medical and biochemical applications. The <sup>195</sup>Pt nucleus displays a characteristic magnetic resonance imaging (MRI) activity, which has been much used in the medical field to produce high quality images of the inside of the human body. The chemical shifts and <sup>195</sup>Pt coupling constants in <sup>1</sup>H-NMR spectra are direct consequences of the steric and electronic environment around the Pt nucleus and provide additional information on the structures of the biomolecules. The method used for the covalent binding of the PtBr(2,6-(CH<sub>2</sub>NMe<sub>2</sub>)<sub>2</sub>-4-RC<sub>6</sub>H<sub>2</sub>) complex to the peptides is described in the publication. Metalation of the intermediate organic biomolecule was monitored by <sup>1</sup>H- and <sup>195</sup>Pt-NMR spectroscopy. A single resonance was observed at -3183 ppm in <sup>195</sup>Pt-NMR spectroscopy for the methoxy L-valine product.

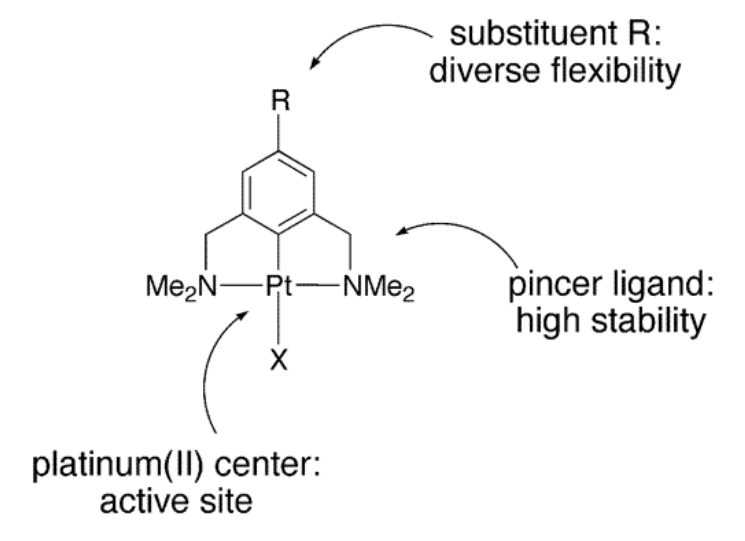


**Figure 2.6.3** Functionalities of the compounds PtX(2,6-(CH<sub>2</sub>NMe<sub>2</sub>)<sub>2</sub>-4-RC<sub>6</sub>H<sub>2</sub>) (X = halo ligand, R = amino acid or peptide). Reprinted with permission from Albrecht, M.; Rodríguez, G.; Schoenmaker, J.; Van Koten, G. Org. Lett. 2000, 2, 3461-3464. Copyright (2000) American Chemical Society.

Beside their potential biomarking property, these biofunctionalized Pt(II) complexes can display biosensor activity, since the Pt center selectively and reversibly binds SO<sub>2</sub>. The reaction with SO<sub>2</sub> produces a strong change of color from colorless to bright orange. The SO<sub>2</sub> recognition process can be followed by various spectroscopic methods such as IR, NMR or UV-VIS spectroscopy. Addition of SO<sub>2</sub> induces a low-field shift of the signals for both the NMe<sub>2</sub> and -CH<sub>2</sub>N protons in the <sup>1</sup>H-NMR spectra of the compounds shown in Fig. 2.6.4 ( $\Delta\delta \sim 0.2$  ppm). Furthermore, <sup>195</sup>Pt-NMR spectroscopy revealed a very dramatic effect, the resonances were shifted downfield by ~1150 ppm after reaction with SO<sub>2</sub>. The strong deshielding effect on the platinum center is in accordance with a Pt-L charge-transfer process. These results suggest strongly that <sup>195</sup>Pt-NMR spectroscopy can be used as a diagnostic probe for the presence of the  $PtX(C_6H_2(CH_2NMe_2)_2-2,6-R-4)$  unit at a given position in the structure of the peptide and also for its physical location by labeling the platinum position as the corresponding Pt-SO<sub>2</sub> complex. Therefore organo-Pt(II) labeled peptides have promising applications, both as SO<sub>2</sub> biosensors and as diagnostic biomarkers. This type of Pt(II) compounds combines an effective labeling system with a selective molecular recognition site for the detection of SO<sub>2</sub> gas, thus providing functional biomarkers, which may concomitantly be used also as biosensors.

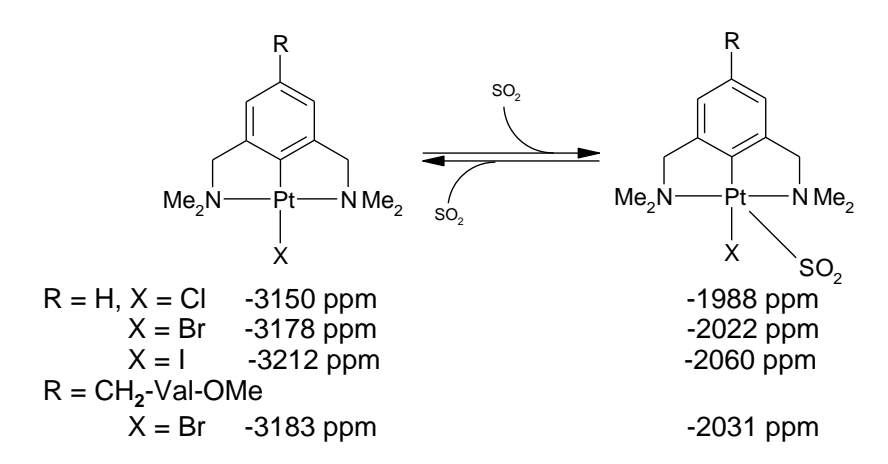


**Figure 2.6.4** Reaction with SO<sub>2</sub> and the <sup>195</sup>Pt-NMR chemical shifts of the different compounds. Adapted with permission from Albrecht, M.; Rodríguez, G.; Schoenmaker, J.; Van Koten, G. Org. Lett. 2000, 2, 3461-3464. Copyright (2000) American Chemical Society.

# iii) Research in the anticancer field

The antitumor properties of *cis*-Pt(NH<sub>3</sub>)<sub>2</sub>Cl<sub>2</sub> (*cisplatin*) have been known for several decades and it is one of the compounds most commonly used in chemotherapy. The work of Farrell *et al.* is a good example of the use of <sup>195</sup>Pt-NMR spectroscopy in the field of cancer research. The group has synthesized several new Pt(II) compounds and evaluated their antitumor activities. Platinum(II) complexes, such as *trans*-Pt(NH<sub>3</sub>)<sub>2</sub>Cl<sub>2</sub> have been historically considered inactive in biological media. However, Farrell's group demonstrated the biological activity of such complexes when using cyclic planar ligands, which greatly enhanced the cytotoxicity (40). They prepared several compounds with thiazole (Tz) (Fig. 2.6.5). Calculations on the electronic structures suggested that the thiazole negative charge was more important on the nitrogen atom and, therefore, the nitrogen is a better donor to platinum. The <sup>195</sup>Pt chemical shifts and the <sup>3</sup>J(<sup>195</sup>Pt-<sup>1</sup>H) coupling constants

confirmed the hypothesis that the ligand was bonded through the nitrogen atom.

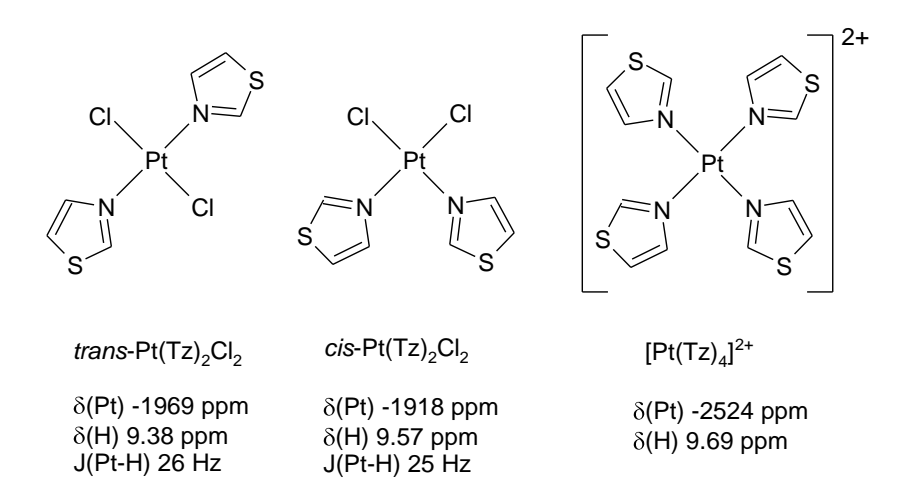


**Figure 2.6.5** Some thiazole compounds prepared by the group of Farrell.

In the late 1990s, Pt(II) complexes with 1,1,3,3-tetramethylthiourea (tmtu) were prepared from the *cisplatin* analogues Pt(en)Cl<sub>2</sub> and Pt(dach)Cl<sub>2</sub> (41). A high field shift of ~600 ppm was observed in the <sup>195</sup>Pt-NMR spectra of the tmtu complexes, as expected for a substitution of a chloro ligand by a sulfur donor (Fig. 2.6.6). Some dinuclear compounds were also synthesized and their  $\delta$ (<sup>195</sup>Pt) values are consistent with a [PtN<sub>2</sub>SCl] coordination sphere. A secondary product was also obtained, with a signal in the -3400 ppm region, where a [PtN<sub>2</sub>S<sub>2</sub>] environment is expected. This product was identified as [Pt(en)(tmtu)<sub>2</sub>]<sup>2+</sup>. When the tmtu monomeric species (**8a** and **8b**, Fig. 8) were reacted with 5'-GMP and r(GpG), the products Pt(en)(5'-GMP-*N7*)(tmtu) and Pt(dach)(5'-GMP-*N7*)(tmtu) were found to be slightly more shielded in their <sup>195</sup>Pt-NMR spectra ( $\delta$ (<sup>195</sup>Pt) = -3003 and -2982 ppm respectively) (42). This observation is consistent with a [N<sub>3</sub>S] environment for Pt(II).

PtACl<sub>2</sub> 
$$\xrightarrow{AgNO_3/DMF}$$
  $\left[PtA(DMF-O)C\right]^+$  L  $\xrightarrow{N}$  Pt Cl  $\xrightarrow{N}$   $\times$  S  $\xrightarrow{N}$  Pt Cl  $\times$  S  $\times$ 

Figure 2.6.6 Preparation of Pt(II) complexes with methyl derivatives of thiourea.

Water-soluble Pt(II) compounds containing a dodecarborane ligand were recently reported as a novel means of delivering boron atoms close to DNA in tumour cells. The effective delivery of boron-containing complexes to tumour sites for Boron Neutron Capture Therapy (BNCT) is dependent on the solubility on the compounds in aqueous media. The success of BNCT relies mainly on the presence of large cellular concentration of boron. In order to solubilize the carborane cage, some authors (43) have use polar hydrophilic functional groups derived from glycerol as a pendant group and a thiopropyl group bonded to a Pt(II) atom (Fig. 2.6.7). The Pt coordination sphere is completed by a tridentate terpyridine ligand. The new compound could not be characterized by crystallographic methods since it

is very hygroscopic, but it was characterized by multinuclear magnetic resonance spectroscopy. The  $^{195}\text{Pt}$  signal at  $\delta=\text{-}3072$  ppm confirmed the presence of a PtSN $_3$  core.

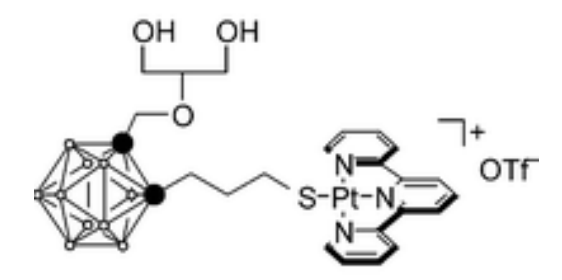


**Figure 2.6.7** Water-soluble compound [Pt(terpy)(S-carborane)](OTf)<sub>2</sub> for potential use as a BNCT agent. Reproduced by permission of The Royal Society of Chemistry.

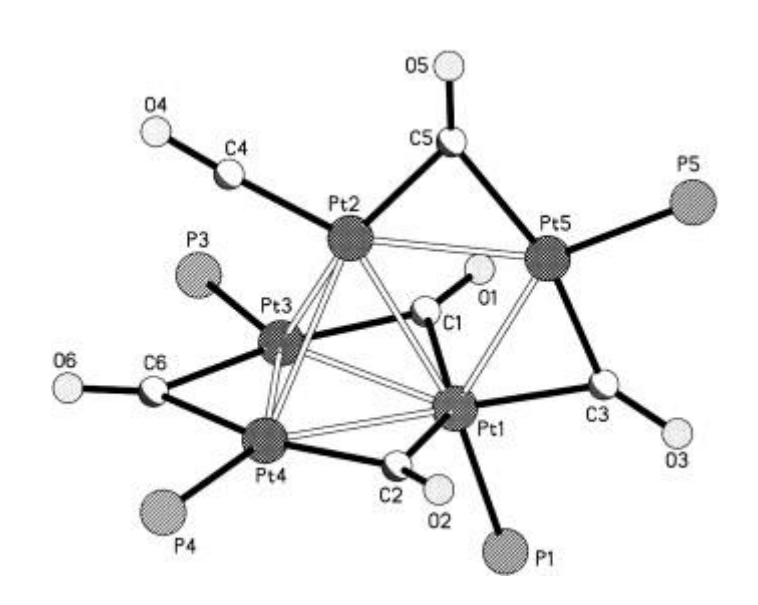
Another example showing the power of this technique to detect the presence of different species in solution has been published on a study of the products of hydrolysis of Pt(en)X<sub>2</sub> where *en* is ethylenediamine or its methyl derivatives (44). Compounds of this type have good antitumor properties. In order to understand the reactions of similar compounds inside the cells where the pH is neutral and the chloride concentration is relatively low, the dihalo ligands were removed with a silver salt and the pH of the resulting solution was adjusted to about 7. The <sup>195</sup>Pt-NMR spectrum of the resulting mixture exhibited nine signals. All the signals except one were attributed to various species in solution, including aqua complexes and hydroxo-bridged dimers, trimers and tetramers. These results are particularly interesting since hydroxo-bridged dimers of this type have been shown to be very toxic and this could explain partially the toxicity of *cisplatin* and its analogues.

#### iv) Cluster chemistry

Roulet's group has been publishing their results on platinum clusters for more than a decade. They have been especially interested in studying the intramolecular dynamics of cluster reactivity by using mainly 195Pt-NMR spectroscopy. Recently, they have focused their attention on the reactivity of triangular platinum clusters towards oxidative addition (45). Their lastest compound  $Pt_3(\mu-CO)_2(\mu-SnCl_2)_2(PCy_3)_3$  (Cy = cyclohexyl) is the first example in the literature where SnCl<sub>2</sub> acts as edge-bridging ligands. The cluster was studied in solution by multinuclear magnetic resonance. The results have shown that, at low temperature, it has the same structure in solution as in the solid state. Two distinct <sup>195</sup>Pt chemical shifts were observed at -50°C, one at -4351 ppm for the two equivalent metallic centers and another at slightly lower field (-4096 ppm) due to the third Pt atom. The <sup>195</sup>Pt signals are quite broad, but the values of the <sup>1</sup>J(<sup>195</sup>Pt-<sup>195</sup>Pt) coupling constants could be estimated from simulation (2159 and 1198 Hz). The cluster decomposes slowly in solution at -30°C and rapidly at room temperature, producing two dinuclear species and other unidentified products.

Pentanuclear Pt clusters have been shown however, to be more stable than are trinuclear clusters. The  $Pt_5(\mu\text{-CO})_5(CO)L_4$  (L =  $PPh_3$ ,  $PPh_2Bz$ ,  $AsPh_3$ ,  $PEt_3$  and  $PCy_3$ ) complexes have been synthesized (46). The crystal structure of  $Pt_5(\mu\text{-CO})_5(CO)(PCy_3)_4$  was determined by X-ray diffraction methods (Fig. 2.6.8). The  $^{195}Pt\text{-NMR}$  spectrum of the  $PCy_3$  compound could not be measured due to its low solubility, but data were reported for the other four compounds (Fig. 2.6.8), which

showed four distinct signals (Pt3 and Pt4 are magnetically equivalent). Because of the complexity of the signals and considering all the 32 isotopomers for pentaplatinum species, assignments were made with the aid of simulations of the <sup>195</sup>Pt, <sup>31</sup>P and <sup>13</sup>C (99% enriched <sup>13</sup>CO) NMR spectra using the gNMR 4.1 program. For the four complexes, Pt5 was found to be the most shielded and Pt1 was the least shielded by about 1000 ppm. The metallic centers were assigned at fields Pt5 > Pt3 = Pt4 > Pt2 > Pt1. The J(<sup>195</sup>Pt-<sup>195</sup>Pt) coupling constants calculated using the simulations are also shown in Fig. 10. The <sup>195</sup>Pt-NMR solution study confirmed that the four pentanuclear platinum complexes exhibit stereochemistries identical to the one of the PCy<sub>3</sub> compound studied in the solid state. In other words, the C<sub>s</sub> symmetry observed in the solid state is preserved in solution.



L	PPh <sub>3</sub>	PPh <sub>2</sub> Bz	AsPh <sub>3</sub>	PEt <sub>3</sub>
$\delta_{Pt1}$	-3571	-3621	-3734	-3628
$\delta_{Pt2}$	-4066	-3960	-4172	-3874
$\delta_{\text{Pt3,4}}$	-4305	-4256	-4468	-4206

L	PPh <sub>3</sub>	PPh <sub>2</sub> Bz	AsPh <sub>3</sub>	PEt <sub>3</sub>		
$\delta_{Pt5}$	-4725	-4575	-4785	-4517		
$^{1}J_{\mathrm{Pt1-Pt2}}$	1854	1497	1787	1695		
$^{1}J_{\mathrm{Pt1-Pt3,4}}$	866	879	632	944		
$^{1}J_{\mathrm{Pt1-Pt5}}$	1132	1180	221	1187		
$^{1}J_{\mathrm{Pt2-Pt5}}$	1875	1866	2010	1781		
$^{1}J_{\mathrm{Pt3-Pt4}}$	1906	1950	1950	1840		
$^{1}J_{\mathrm{Pt3,4-Pt2}}$	824	957	918	926		
$^2J_{\mathrm{Pt3,4-Pt5}}$	-333	-328	-398	-268		

**Figure 2.6.8** Structure of  $Pt_5(\mu\text{-CO})_5(CO)(PCy_3)_4$  (the cyclohexyl rings are omitted for clarity), with a symmetry plane passing through Pt5-Pt2-Pt1 and the <sup>195</sup>Pt-NMR data (δ in ppm, *J* in Hz). Reprinted from Inorg. Chim. Acta, Vol. 358, 497-503. Z. Béni, R. Ros, A. Tassan, R. Scopelliti and R. Roulet. Copyright (2005), with permission from Elsevier.

#### v) Kinetics studies

<sup>195</sup>Pt-NMR spectroscopy can also be used for monitoring a reaction over a period of time. The chemical reactions can sometimes be studied directly in the NMR tube. Fontes and co-workers (47) have studied the profile of the solvolysis reactions of cis-PtA<sub>2</sub>Cl<sub>2</sub> (A = pyridine or picoline) in dimethylsulfoxide (DMSO).

$$cis$$
-PtA<sub>2</sub>Cl<sub>2</sub> + DMSO  $\longrightarrow cis$ -PtA(DMSO)Cl<sub>2</sub> + A



#### trans-PtA(DMSO)Cl<sub>2</sub>

The signals of the starting material were observed at -1954 and -1961 ppm, respectively, for cis-Pt(py)<sub>2</sub>Cl<sub>2</sub> and cis-Pt(pic)<sub>2</sub>Cl<sub>2</sub>, and these started to decrease after 1 h. Two new signals appeared at about -2855 and -3020 ppm due to formation of the cis- and trans-PtA(DMSO)Cl<sub>2</sub> complexes. A similar study with trans-PtA<sub>2</sub>Cl<sub>2</sub> in DMSO did not show any solvolysis, even after a long time and under more drastic conditions. The <sup>195</sup>Pt-NMR signals of only the starting compounds were observed. An excellent example has also been published by Kerrison and Sadler (48), in which the chemical reactions were studied in an NMR tube as a function of time. The study has also shown the importance of the solvent used in these reactions. Using <sup>195</sup>Pt-NMR spectroscopy the reaction of cis-Pt(NH<sub>3</sub>)<sub>2</sub>Cl<sub>2</sub> with glycine in DMSO was investigated. Eleven different species were detected, including eight DMSO complexes (one being a trans compound) and four compounds containing the ligand glycine. All eleven species were identified in the study. This research has shown how the solvent influences the structure of Pt(II) complexes in solution. This was a particularly important study, since in the 1970s, many antitumor tests were performed in DMSO solutions, because neutral complexes are not very soluble. Furthermore, the presence of trans isomers has confirmed the isomerization of cis

complexes to the trans analogues in DMSO and other organic solvents. The antitumor properties of most Pt(II) complexes are related to the cis configuration of the compounds.

Cisplatin and its analogues are believed to react with the sulfur-containing tripeptide glutathione (GSH). Two thirds of administrated *cisplatin* has been found to coordinate to GSH and only a small fraction is available for antitumor activity. Recently, the reaction of *transplatin* with GSH was investigated by <sup>195</sup>Pt-NMR spectroscopy (49). A study of the profile of the reaction with time showed the slow formation of an intermediate compound after 30 minutes ( $\delta(^{195}\text{Pt}) = -3226 \text{ ppm}$ ), and then the final product, *trans*-[(Pt(SG)(NH<sub>3</sub>)<sub>2</sub>)<sub>2</sub>- $\mu$ -SG]<sup>+</sup> (VI) was formed after 12 h ( $\delta(^{195}\text{Pt}) = -3186 \text{ ppm}$ ). The intermediate complex was identified as *trans*-Pt(SG)<sub>2</sub>(NH<sub>3</sub>)<sub>2</sub> (V) and the simplified reaction V  $\rightarrow$  VI followed a first-order kinetic model (k ~ 0.4 s<sup>-1</sup>). *Transplatin* was replaced by two 'nonclassical' complexes currently in clinical trial, [{*trans*-Pt(NH<sub>3</sub>)<sub>2</sub>Cl}<sub>2</sub>- $\mu$ -(H<sub>2</sub>N(CH<sub>2</sub>)<sub>6</sub>NH<sub>2</sub>)<sub>2</sub>](NO<sub>3</sub>)<sub>4</sub>. The same NMR pattern was obtained and the suggested pathway of the [(*trans*-Pt(SG)(NH<sub>3</sub>)<sub>2</sub>)<sub>2</sub>- $\mu$ -SG]<sup>+</sup> formation is shown in Fig. 2.6.9.

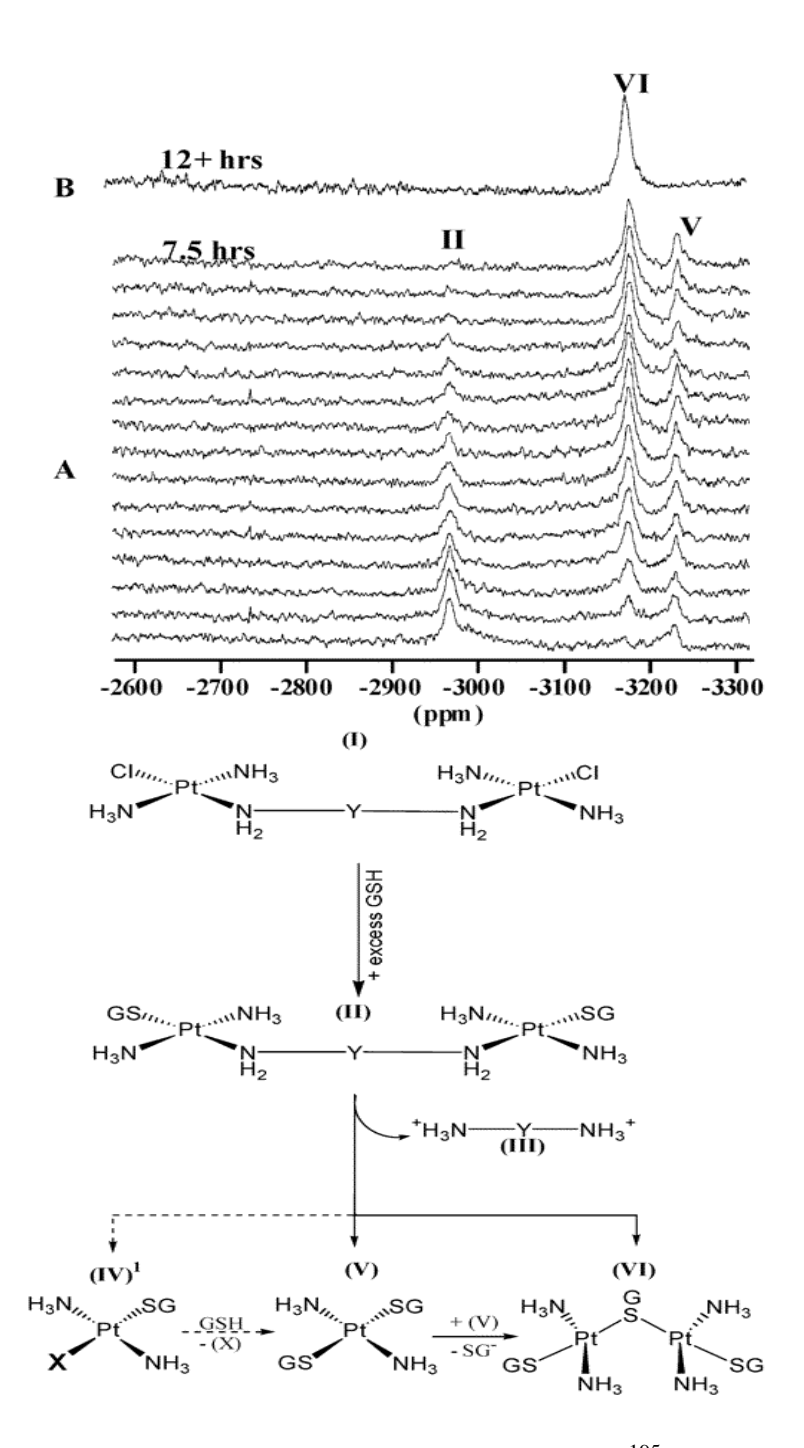


**Figure 2.6.9** (A) Reaction with GSH as monitored by  $^{195}$ Pt-NMR spectroscopy from t = 0.5-7.5 h. (B) Spectrum of the final product  $[\{trans-Pt(SG)(NH_3)_2\}_2\mu-(SG)]^+$  (VI) at t = 12 h. Proposed reaction pathway in the reaction of the dinuclear platinum drugs with glutathione (**X** = Cl, H<sub>2</sub>O or H<sub>2</sub>N(CH<sub>2</sub>)<sub>6</sub>NH<sub>3</sub><sup>+</sup>). Reprinted with permission from Oehsen, M.E.; Qu, Y.; Farrell, N. Inorg. Chem. 2003, 42, 5498-5506. Copyright (2003) American Chemical Society.

<sup>195</sup>Pt-NMR spectroscopy was used as a fingerprint for other GSH interactions. For instance, the formation of the product  $[(trans-Pt(SG)(NH_3)_2)_2-\mu-(SG)]^+$  was found to be complete after only 4h using  $[(trans-Pt(NH_3)_2Cl)_2-\mu-(H_2N(CH_2)_3(NH_2^+)(CH_2)_4NH_2)]$  (NO<sub>3</sub>)<sub>3</sub>.

# 2.7 Solid-State <sup>195</sup>Pt-NMR Spectroscopy

While liquid-state <sup>195</sup>Pt-NMR spectroscopy encompasses a wide range of areas, the parallel solid-state technique has been used mainly in studies of heterogeneous catalysis and is more industrially oriented. Over the past 20 years, NMR spectroscopy has become an efficient and powerful technique to investigate catalytic materials, such as clays, silicas and zeolites. Nowadays, the technique is being focused more on small metallic particles (50). Such particles are of great interest because they have very high surface areas and, therefore, high specific activity. The surfaces are not always suitable for investigations using standard molecular spectroscopic technique, and solid-state NMR spectroscopy appears to be an excellent method. Metallic particles typically contain more than a hundred atoms corresponding, in the case of Pt, to about a thousand valence electrons.

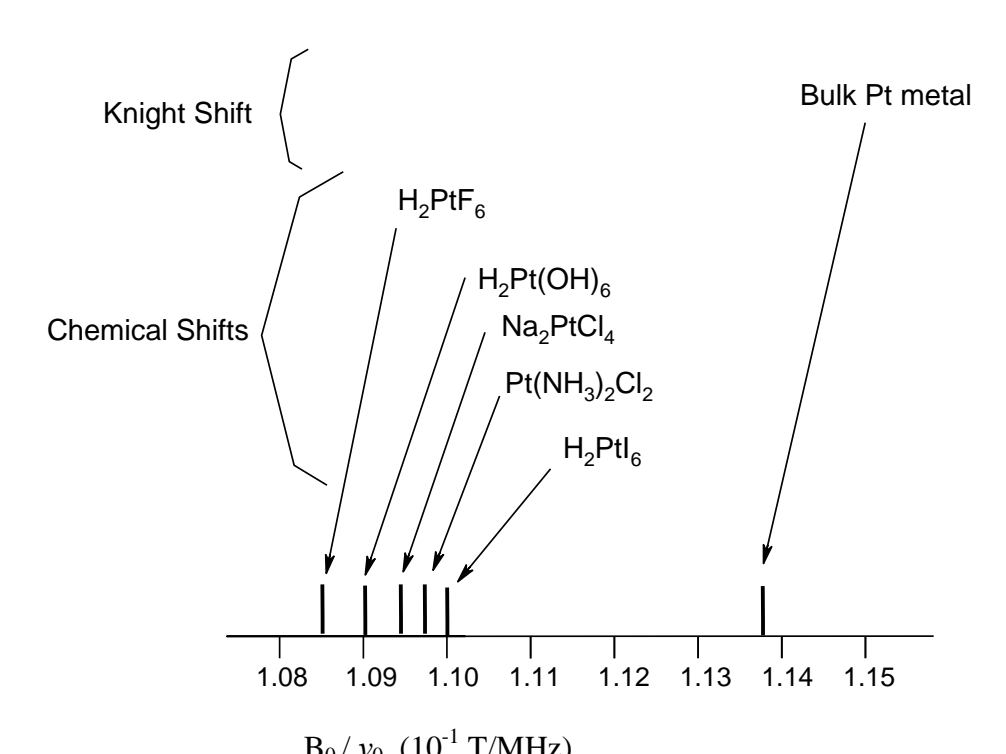
Platinum is a highly suitable element for the study of metal particles, due once again to its natural isotopic abundance (33.8%), high gyromagnetic ratio  $\gamma$  (9 MHz in 10 kG) and nuclear spin ( $I = \frac{1}{2}$ ), which eliminate the complexity of the structure on the NMR line shape, due to the electronic quadrupolar moment. For diamagnetic compounds, the NMR frequency,  $v_0$ , of a nuclear spin in a fixed

external magnetic field  $B_0$ , varies according to the following law for a substance i:

$$2\pi v_0 = \gamma (1 + \sigma_i) B_0$$

where  $B_0/2\pi$  is the NMR frequency of a 'bare' nucleus and  $\sigma_i$  is the chemical shift. Here,  $\sigma_i$  has its origin in magnetic fields produced at the nucleus by currents induced in the surrounding electrons on the application of  $B_0$ . It is also associated with the electron orbital motion induced by  $B_0$ . In metals, the conduction-electron spins are polarised by  $B_0$ , giving rise to an additional shift in  $v_0$ , called the Knight shift, K. This latter parameter also follows the same relationship mentioned above. While chemical shifts are related to orbital magnetism, the Knight shift arises from spin magnetism. It is governed only by the inverse of the energy level separation around the highest occupied orbital or, in a band picture, by the density of states at the Fermi energy level. It is also governed by the modulus of the corresponding wavefunctions at the site of the nucleus being investigated. In a metal like platinum,  $\sigma_i$  is the sum of the chemical and the Knight shifts. Generally, the Knight shift is much greater than is the chemical shift. The NMR spectrum can give information on one single point in the electronic energy spectrum, at the Fermi energy level.

As for liquid-state NMR spectroscopy, Na<sub>2</sub>[PtCl<sub>6</sub>] is the most common reference material used to measure the shifts. Fig. 2.7.1 shows the  $^{195}$ Pt-NMR chemical shifts in various molecules and in bulk metal (51). The compounds on the downfield side of the figure exhibit small chemical shifts; they all fall within a range of  $\pm 0.7\%$  around the value of the accepted reference. Bulk platinum metal has a large negative Knight shift ( $\sigma_i = -3.4\%$ ), which makes it possible to resolve the Knight shift of atoms in surface layers from that of atoms in the bulk.



 $B_0/\nu_0~(10^{\text{-1}}~\text{T/MHz})$  Figure 2.7.1 Position of the  $^{195}\text{Pt-NMR}$  resonances for several compounds.

Considering a small particle of platinum metal (Fig. 2.7.2), it would be expected that the central Pt nuclei in this particle, far from the surface, would be in an environment like that of bulk Pt. On the other hand, surface Pt nuclei would be expected to be in a different environment, since they lack neighbours on one side. They should show different Knight shifts for this reason. Finally, Pt nuclei in the interior layers near the surface would be expected to have intermediate Knight shift values. When the particle is covered with absorbed molecules, the chemical shift of surface Pt nuclei will depend mainly on the nature of the adsorbed molecules.

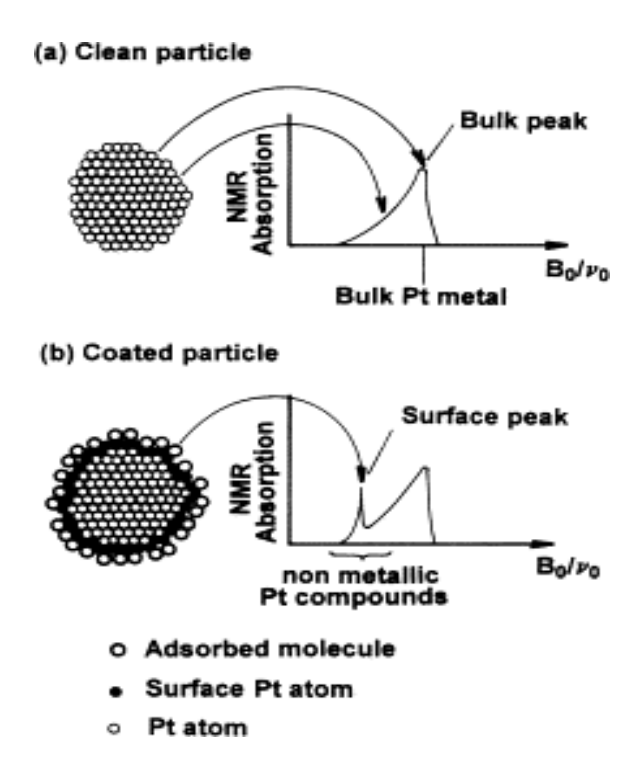


**Figure 2.7.2** General form of line shapes expected for a sample of small platinum particles which are clean (a) and coated (b) with adsorbed molecules. Reprinted Fig. 3 with permission from H. E. Rhodes, P.-K. Wang, H. T. Stokes, C. P. Slichter, and J. H. Sinfelt, Phys. Rev. B Vol. 26, 3559-3568, 1982. Copyright (1982) by the American Physical Society.

Since the observed NMR spectra cover a large range of frequencies (or fields), they have to be obtained by a point-by-point method. Generally, the area of the spin echo is measured at different values of  $B_0$ , with stabilised  $v_0$ . Since the spin echoes from the sample are generally quite small, each point is obtained by signal averaging a spin every 50,000 times or more. The peak position and width reflect the Fermi level local density of states ( $E_f$ -LDOS) and its spatial distribution (50). The dynamic coupling of the nuclear spins to their surroundings is expressed by the spin-lattice relaxation time ( $T_1$ ). Measurement of the various  $T_1s$  provides added insight into the dynamic coupling between the nuclear spin system and the low-lying

electronic excitations, while spin-spin relation time  $(T_2)$  measurements serve as an effective means to estimate the strengths of the various couplings between different nuclear spins.

Oldfield and his research group have used solid-state <sup>195</sup>Pt-NMR spectroscopy for many years to understand how submonolayer adsorbates modify the physical and the chemical properties of metal surfaces. For instance, the technique was used to show a correlation between adsorbate electronegativity  $(\gamma)$ and metal surface electronic properties (52). Different species (Ru, H, CO, CN, S and O) were electrochemically adsorbed on clean carbon-supported nanoscale platinum particles. A series of point-by-point <sup>195</sup>Pt-NMR spectra, of carbonsupported nanoscale electrode materials, was obtained, with and without adsorbates (Fig. 2.7.3). A linear relationship was observed between the <sup>195</sup>Pt-NMR Knight shifts of the surface and subsurface platinum atoms and the electronegativity of the adsorbate. This result implied an interesting linear correlation between the chemical nature of the ligand and changes in the physical properties of the Pt substrate. The frequency shifts of the metal atoms located deeper than the third layer were unaffected by the surface adsorbate electronegativity. This observation demonstrates the applicability of the Friedel-Heine invariance of the LDOS in such nanoscale electrocatalyst systems. According to theory and the correlation values obtained for the systems, the healing length, m, can be expressed as a function of the electronegativity ( $\chi$ ):

$$m = \frac{1}{\text{Ln} [(23.2+5.3\chi)/(11.9+5.8\chi)]}$$

Knowing that 0.229 m is the layer thickness for platinum particles, a plot of the healing length (0.229 m) as a function of  $\chi$  (Fig. 2.7.4) shows that the larger the electronegativity, the longer the healing length, i.e., the deeper the influence of the adsorbate goes. These results will lead to useful correlations between electronic properties (Knight shifts, relaxation rates, local density of states, healing length) and more conventional chemical properties, such as ligand electronegativity. These properties may be helpful in understanding the electronic structure interfaces and the catalytic processes in general.

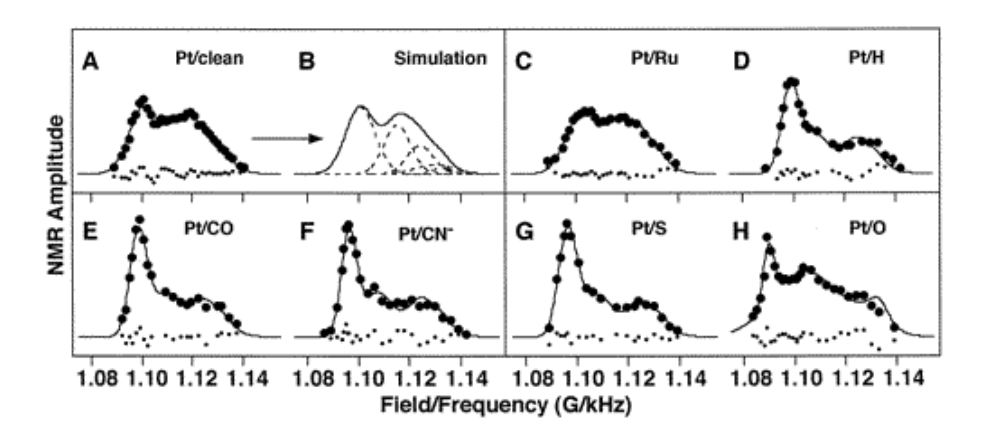


**Figure 2.7.3** Point-by-point <sup>195</sup>Pt-NMR spectra (solid circles) and simulation of 2.5-nm carbon-supported Pt electrocatalysts with and without adsorbates. The simulations (solid lines) and the variances between the experimental and fitted values (small dots) are also shown. Reprinted with permission from Tong, Y.Y.; Rice, C.; Wieckowski, A.; Oldfield, E. J. Am. Chem. Soc. 2000, 122, 11921-11924. Copyright (2000) American Chemical Society.

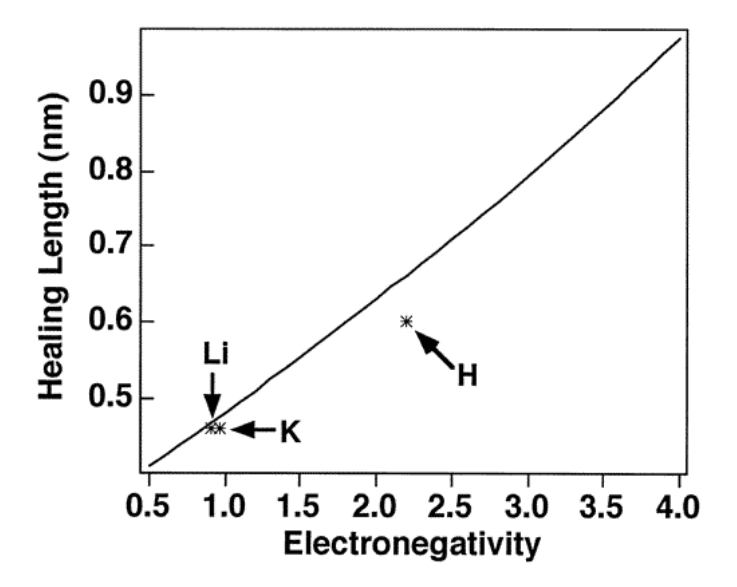


**Figure 2.7.4** Relationship between the healing length and electronegativity as determined from the equation. Reprinted with permission from Tong, Y.Y.; Rice, C.; Wieckowski, A.; Oldfield, E. J. Am. Chem. Soc. 2000, 122, 11921-11924. Copyright (2000) American Chemical Society.

Even if solid-state <sup>195</sup>Pt-NMR spectroscopy appears to have been devoted mainly to industrial studies, the recent exploitation of some of the modern NMR techniques may well generate interest in academic laboratories. For instance, Harris *et al.* have used cross-polarization (CP) and magic-angle spinning (MAS) techniques to set up solid-state experiments on heavy-metal spin-1/2 nuclei, including <sup>195</sup>Pt (53). The K<sub>2</sub>[Pt(OH)<sub>6</sub>] standard used appeared to be the best compound for such a <sup>195</sup>Pt-CP-MAS experiment. A very large chemical shift anisotropy (csa) is usually associated with the <sup>195</sup>Pt nucleus. This fact has proved to be the major stumbling block to making solid-state <sup>195</sup>Pt-NMR spectroscopy an easy technique to use. In cases, like [Pt(CN)<sub>6</sub>]<sup>2-</sup>, the csa is minimized, because the Pt nucleus occupies a high-symmetry site (54). Very high spinning speeds are usually required, as in the case of the work of Duer *et al.*, where speeds above 11 kHz were used for the *trans*-

{PtCl(PBu<sub>3</sub>)<sub>2</sub>}<sub>2</sub>( $\mu$ -(C $\equiv$ C-p-C<sub>6</sub>H<sub>4</sub>-C $\equiv$ C)) compound (55). Under this condition, the shielding tensor is averaged out as much as possible. The results were found to be in agreement with the main shielding values of cis-Pt(PMe<sub>3</sub>)<sub>2</sub>Cl<sub>2</sub>, suggesting a strong  $\sigma$ -bond interaction between Pt and P. The data also showed that both PBu<sub>3</sub> and C $\equiv$ C-R ligands are good  $\pi$ -acceptors.

#### 2.8 Conclusions

Platinum-195 NMR spectroscopy is a very versatile technique in fundamental research as well as for industrial applications. The method permits the determination of the binding sites of ligands and allows a chemical differentiation to be made between two geometrical isomers, on the basis of both the chemical shifts and the <sup>195</sup>Pt coupling constants. It can also be used to determine the chirality of a compound and determine the relative proportions of the different enantiomers. It has been used to monitor the kinetics of transformation reactions in solution, including isomerization or enantioneric reactions. It is also becoming a useful tool in the biological sciences, especially with large molecules like peptides. For example, it seems to be a good diagnostic probe for the presence of a Pt atom at a given position in a peptide structure and its location can be further determined by labelling the Pt atom with SO<sub>2</sub>. When side- or by-products are obtained, the <sup>195</sup>Pt chemical shifts give important information on the metallic coordination sphere. For example, in Pt-R<sub>2</sub>SO complexes, the chemical shifts for Pt-O and Pt-S bonds are quite different. Moreover, it provides purity estimations of the synthesized compounds and, for mixtures, the relative intensity of each Pt signal is directly related to its quantity in

the mixture. It can commonly confirm information suggested by classical analytical techniques, such as <sup>1</sup>H- and <sup>13</sup>C-NMR, UV-Visible and IR spectroscopy.

In summary, the chemical shifts are sensitive parameters, which are often used to identify the type, the number and the geometrical arrangement of the coordinated ligands to a platinum center. The coupling constants appear to be pertinent additional information in understanding the geometry of the complexes and in the study of the nature of the Pt-L bonds.

## **Appendix A** – <sup>195</sup>Pt(II) NMR Chemical Shifts

Compound	δ( <sup>195</sup> Pt)	Ref.
Pt(C=C)Cl <sub>3</sub>		
$[PtCl_3(C_2H_4)]^{-}[(1S,1'S)-bis(1-PhEt)NH_2]^{+}$	-2825	37
$[PtCl_3(C_2H_4)]^-[(1S,1'S)-bis[1-(1-Np)Et]NH_2]^+$	-2827	37
[PtCl <sub>3</sub> (C <sub>2</sub> H <sub>4</sub> )] <sup>-</sup> [(1 <i>S</i> ,1' <i>S</i> )-N-[1'-(1-Np)Et]-1-PhEtNH <sub>2</sub> ] <sup>+</sup>	-2826	37
$[PtCl_3(C_2H_4)]^{-}[(1S,1'S)-bis(1-PhEt)NH_2]^{+}$	-2825	37
$[PtCl_3(C_2H_4)]^-[(S)-1-(1-Np)EtNH_2]^+$	-2843	37
[PtCl <sub>3</sub> (CMe <sup>t</sup> Bu=CHPh)] <sup>-</sup> [( <i>S,S</i> )-(PhMeCH) <sub>2</sub> NH <sub>2</sub> ] <sup>+</sup>	-2417 (S)	36
[PtCl <sub>3</sub> (CMe <sup>t</sup> Bu=CHBr)]⁻[(S,S)-(PhMeCH) <sub>2</sub> NH <sub>2</sub> ] <sup>+</sup>	-2411 (R) -2397 (S)	38
[PtCl <sub>3</sub> (CMe <sup>t</sup> Bu=CH( <i>o</i> -OMePh))] <sup>-</sup> [( <i>S,S</i> )-(PhMeCH) <sub>2</sub> NH <sub>2</sub> ] <sup>+</sup>	-2392 ( <i>R</i> ) -2438 ( <i>S</i> )	38
[PtCl <sub>3</sub> (CMe <sup>t</sup> Bu=CH( <i>p</i> -OMePh))] <sup>-</sup> [( <i>S,S</i> )-(PhMeCH) <sub>2</sub> NH <sub>2</sub> ] <sup>+</sup>	-2434 (R) -2413 (S)	38
$[PtCl_3(CMe^tBu=CH(p-FPh))]^-[(S,S)-(PhMeCH)_2NH_2]^+$	-2405 (R) -2427 (S)	38
[PtCl <sub>3</sub> (CMe <sup>t</sup> Bu=CH(1-Np))] <sup>-</sup> [(S,S)-(PhMeCH) <sub>2</sub> NH <sub>2</sub> ] <sup>+</sup>	-2417 (R) -2455 (S)	38
[PtCl <sub>3</sub> (CMe <sup>t</sup> Bu=CHBu <sup>t</sup> )] <sup>-</sup> [( <i>S,S</i> )-(PhMeCH) <sub>2</sub> NH <sub>2</sub> ] <sup>+</sup>	-2450 (R) -2444 (S)	38
$[PtCl_3(CMe^tBu=CH(CH_2)_3OH)]^-[(S,S)-(PhMeCH)_2NH_2]^+$	-2440 (R) -2454 (S) -2435 (R)	38
PtC <sub>2</sub> O <sub>2</sub>	-2433 (N)	
$K[Pt(O,O'-acac)(\gamma-acac)_2]$	-2555	57
PtSO <sub>2</sub> Cl		

Pt(Me <sub>2</sub> SO)( <i>O,O</i> ′-acac)Cl	-2399	57
PtSO <sub>2</sub> C		
Pt(DMSO)( $O$ , $O$ '-acac)( $\gamma$ -acac)	-3198	57
PtS <sub>2</sub> PC		
Pt(Ph <sub>3</sub> P)(CO)(5,5-dihydro-1,4-dithiin-2,3-dithiolate)	-4467	58
PtS <sub>2</sub> (C=C) <sub>2</sub>		
Pt(COD)(5,5-dihydro-1,4-dithiin-2,3-dithiolate)	-5322	58
Pt(COD)(ethylene-1,2-dithiolate)	-5414	58
Pt(COD)(maleonitrile-1,2-dithiolate)	-5253	58
Pt(COD)(ethane-1,2-dithiolate)	-4070	58
PtS <sub>2</sub> Cl <sub>2</sub>		
trans-Pt(Me <sub>2</sub> S) <sub>2</sub> Cl <sub>2</sub>	-3409	59
cis-Pt(tetramethylenesulfoxyde) <sub>2</sub> Cl <sub>2</sub>	-3449	unpublished result
cis-Pt(di-n-propylsulfoxyde) <sub>2</sub> Cl <sub>2</sub>	-3512	unpublished result
trans-Pt(di-n-propylsulfoxyde)₂Cl₂	-3516	unpublished result
cis-Pt(di-n-butylsulfoxyde) <sub>2</sub> Cl <sub>2</sub>	-3518	unpublished result
Pt(1,4,7-trithiacyclononane)Cl <sub>2</sub>	-3605	60
PtS <sub>2</sub> Br <sub>2</sub>		
Pt(1,4,7-trithiacyclononane)Br <sub>2</sub>	-3779	60
PtS <sub>2</sub> I <sub>2</sub>		
Pt(1,4,7-trithiacyclononane)I <sub>2</sub>	-4147	60
PtS <sub>2</sub> C <sub>2</sub>		
$Et_4N[ReS_4(PtMe_2)]$	-3825	61

$Et_4N[ReS_4(PtMe_2)_2]$	-3597	61
$Et_4N[ReS_4(PtMe_2)_4]$	-3541	61
PtS <sub>3</sub> P		
$Pt(\kappa^2 S, S'-PCy_2S_2)(\kappa S-PCy_2S_2)(PHCy_2)$	-4052	102
PtS <sub>4</sub>		
[Pt(1,4,7,10,13,16-hexathiacyclooctadecane)](BF <sub>4</sub> ) <sub>2</sub>	-4152	62
$[Pt(1,4,7-trithiacyclononane)_2](PF_6)_2$	-4147	60
$[Pt(1,5,9-trithiacyclododecane)_2](PF_6)_2 \cdot 2CH_3NO_2$	-4201	63
$[Pt((C_6H_5)SO_2N=CS_2)_2](Bu_4N)_2$	-3857	64
$[Pt((4-BrC_6H_4)SO_2N=CS_2)_2](Bu_4N)_2$	-3872	64
$Pt(\kappa^2 S, S'-PCy_2S_2)_2$	-3025	102
PtPSnHC		
PtH(CO)(P <sup>t</sup> Bu <sub>3</sub> )(SnPh <sub>3</sub> )	-5152	65
PtPNSeCl		
[Pt(SeCH <sub>2</sub> CH <sub>2</sub> NMe <sub>2</sub> )(PMePh <sub>2</sub> )Cl]	-4293	66
[Pt(Me <sub>2</sub> NCH(Me)CH <sub>2</sub> Se)(PEt <sub>3</sub> )Cl]	-4315 <i>(S)</i>	10
[Pt(Me <sub>2</sub> NCH(Me)CH <sub>2</sub> Se)(P <sup>n</sup> Bu <sub>3</sub> )Cl]	-4211 (R) -4182 (S)	10
[Pt(Me <sub>2</sub> NCH(Me)CH <sub>2</sub> Se)(PMe <sub>2</sub> Ph)Cl]	-4286 (R) -4267 (S)	10
[Pt(Me <sub>2</sub> NCH(Me)CH <sub>2</sub> Se)(P <sup>n</sup> Pr <sub>3</sub> )Cl]	-4165 <i>(R)</i> -4569 <i>(S)</i>	10
PtPSC <sub>2</sub>	-4425 <i>(R)</i>	
$cis, cis$ -[Ph <sub>2</sub> Pt( $\mu$ -SMe <sub>2</sub> )( $\mu$ -dppm)Pt( $o$ -MeC <sub>6</sub> H <sub>4</sub> ) <sub>2</sub> ] <sup>-</sup>	-4295	67
$cis, cis$ -[ $(p$ -MeC <sub>6</sub> H <sub>4</sub> $)_2$ Pt $(\mu$ -SMe <sub>2</sub> $)(\mu$ -dppm)Pt $(o$ -MeC <sub>6</sub> H <sub>4</sub> $)_2$ ] <sup>-</sup>	-4283 -4274	67
$cis, cis$ -[ $(m$ -MeC <sub>6</sub> H <sub>4</sub> ) <sub>2</sub> Pt( $\mu$ -SMe <sub>2</sub> )( $\mu$ -dppm)Pt( $o$ -MeC <sub>6</sub> H <sub>4</sub> ) <sub>2</sub> ]	-4287 -4296 -4283	67

$cis, cis$ -[( $o$ -MeC <sub>6</sub> H <sub>4</sub> ) <sub>2</sub> Pt( $\mu$ -SMe <sub>2</sub> )( $\mu$ -dppm)PtMe <sub>2</sub> ] <sup>-</sup>	-4340 -4264	67
PtPSn <sub>3</sub>		
[Pt2Sn9(PPh3)]2-	-5270	68
PtPCl <sub>3</sub>		
$[Pt(P(m-C_6H_4SO_3Na)_3)CI_3]^T$	-3916	69
PtP <sub>2</sub> NSe		
[Pt <sub>2</sub> (SeCH <sub>2</sub> CH <sub>2</sub> NMe <sub>2</sub> ) <sub>2</sub> (dppp) <sub>2</sub> ](BF <sub>4</sub> ) <sub>2</sub>	-4534	66
PtP <sub>2</sub> NS		
[Pt(2-mercaptopyridine)Fe( $\eta^5$ -C <sub>5</sub> H <sub>4</sub> PPh <sub>2</sub> ) <sub>2</sub> ](BF <sub>4</sub> )	-3500	70
PtP <sub>2</sub> CM (M = Ga,In,Al,H)		
Pt(dcpe)(Ga(CH <sub>2</sub> SiMe <sub>3</sub> ) <sub>2</sub> )(CH <sub>2</sub> SiMe <sub>3</sub> )	-4735	71
Pt(dcpe)(In(CH2-tBu)2)(CH2-tBu)	-4611	71
Pt(dcpe)(Al(CH <sub>2</sub> - <sup>t</sup> Bu) <sub>2</sub> )(CH <sub>2</sub> - <sup>t</sup> Bu)	-4970	71
$Pt(dcpe)(\mu_2-H)CH_2SiMe_2CH_2Ga(CH_2SiMe_3)_2\}$	-5004	71
$Pt(dcpe)(\mu_2-H)CH_2CMe_2CH_2Al(CH_2-^tBu)_2$	-4974	71
PtP <sub>2</sub> OCI		
cis-[Pt(P( $m$ -C <sub>6</sub> H <sub>4</sub> SO <sub>3</sub> Na) <sub>3</sub> ) <sub>2</sub> (OH <sub>2</sub> )Cl] <sup>-</sup>	-4280	69
cis-Pt(PHCy <sub>2</sub> ) <sub>2</sub> (Cl)(OPh)	-4323	107
PtP <sub>2</sub> BrCl		
$[PtBrCl\{PPh_2(C_6H_4CHO)\}_2]$	-4319	15
PtP <sub>2</sub> SSe		
Pt(1-S,8-Se-nap)(PPh <sub>3</sub> ) <sub>2</sub>	-4820	108
Pt(1-S,8-Se-nap)(PMe <sub>3</sub> ) <sub>2</sub>	-4716	108

### PtP<sub>2</sub>S<sub>2</sub>

Pt(Ph <sub>3</sub> P) <sub>2</sub> (5,5-dihydro-1,4-dithiin-2,3-dithiolate)	-4735	58
Pt(Ph <sub>3</sub> P) <sub>2</sub> (ethylene-1,2-dithiolate)	-4792	58
Pt(Ph <sub>3</sub> P) <sub>2</sub> (maleonitrile-1,2-dithiolate)	-4551	58
Pt(Ph <sub>3</sub> P) <sub>2</sub> (ethane-1,2-dithiolate)	-4881	58
(cyanide-1,2-dithiolate) $Pt(\mu$ -dppa) <sub>2</sub> $Pt(cyanide-1,2$ -dithiolate)	-4742	72
$(MeS-1,2-dithiolate)Pt(\mu-dppa)_2Pt(MeS-1,2-dithiolate)$	-4742	72
(1,4-dithiin ring-1,2-dithiolate)Pt(μ-dppa) <sub>2</sub> Pt(1,4-dithiin ring-1,2-	-4663	72
dithiolate) (tetrathiafulvalene-1,2-dithiolate)Pt( $\mu$ -dppa) <sub>2</sub> Pt(tetrathiafulvalene-1,2-dithiolate)	-4506	72
$[Pt2(\mu-SC6H4CH3-4)2(dppm)2](CF3SO3)2$	-3813	73
$[Pt_2(\mu-SC_6H_4Cl-4)_2(dppm)_2](CF_3SO_3)_2$	-3811	73
[Pt(trithiacyclononane)(PPh <sub>3</sub> ) <sub>2</sub> ](PF <sub>6</sub> ) <sub>2</sub>	-4347	60
[Pt(trithiacyclononane)(dppe)](PF <sub>6</sub> ) <sub>2</sub>	-4069	60
[Pt(trithiacyclononane)(bis(PPh <sub>2</sub> )benzene)](PF <sub>6</sub> ) <sub>2</sub>	-4618	60
[Pt(trithiacyclononane)(1,1'-bis(PPh <sub>2</sub> )ferrocene)](PF <sub>6</sub> ) <sub>2</sub>	-4407	60
Pt(2-mercaptopyridine) <sub>2</sub> Fe( $\eta^5$ -C <sub>5</sub> H <sub>4</sub> PPh <sub>2</sub> ) <sub>2</sub>	-4684	70
$[Pt(\kappa^2S,S'-PS_2Cy_2)(PHCy_2)_2]CI$	-4596	102
$Pt(\kappa^2 S, S'-PS_2Cy_2)\{\kappa P-P(S)Cy_2\}(PHCy_2)$	-4522	102
Pt(1,8-S <sub>2</sub> -nap)(PPh <sub>3</sub> ) <sub>2</sub>	-4799	108
Pt(1,8-S <sub>2</sub> -nap)(PMe <sub>3</sub> ) <sub>2</sub>	-4663	108
Pt(1,2-S <sub>2</sub> -acenap)(PPh <sub>3</sub> ) <sub>2</sub>	-4836	108
Pt(4,5-S <sub>2</sub> -phenan)(PPh <sub>3</sub> ) <sub>2</sub>	-4736	108
Pt(1,8-S <sub>2</sub> -2- <sup>t</sup> Bu-nap)(PPh <sub>3</sub> ) <sub>2</sub>	-4664	108

Pt(1-S,8-{S(O)}-nap)(PPh <sub>3</sub> ) <sub>2</sub>	-4530	108
Pt(1-S,8-{S(O) <sub>2</sub> }-nap)(PPh <sub>3</sub> ) <sub>2</sub>	-4529	108
Pt(1-{S(O)},8-{S(O) <sub>2</sub> }-nap)(PPh <sub>3</sub> ) <sub>2</sub>	-4097	108
$Pt(1,8-\{S(O)_2\}_2-nap)(PMe_2Ph)_2\cdot 0.5CH_2Cl_2$	-4352	108
Pt(1,8-{S(O) <sub>2</sub> } <sub>2</sub> -nap)(PPh <sub>3</sub> ) <sub>2</sub>	-4250	108
PtP <sub>2</sub> Cl <sub>2</sub>		
cis-Pt(P( $m$ -C <sub>6</sub> H <sub>4</sub> SO <sub>3</sub> Na) <sub>3</sub> ) <sub>2</sub> Cl <sub>2</sub>	-4437	69
trans-Pt(P( $m$ -C <sub>6</sub> H <sub>4</sub> SO <sub>3</sub> Na) <sub>3</sub> ) <sub>2</sub> Cl <sub>2</sub>	-4072	69
$Cl_2Pt(\mu-dppa)_2PtCl_2$	-4431	72
$Pt(o-C_6H_4(CH_2PPh_2)_2)CI_2$	-4503	74
$PtCl_2(PPh_2(C_6H_4CHO))_2$	-4026	15
$PtAu_{2}(tris[2-(diphenylphosphino)ethyl]phosphine)Cl_{4}\cdot 2H_{2}O$	-4565	110
PtP <sub>2</sub> Te <sub>2</sub>		
Pt(Te <sub>2</sub> C <sub>5</sub> H <sub>8</sub> O)(dppn)	-4955	97
PtP <sub>2</sub> Br <sub>2</sub>		
PtBr2(PPh2(C6H4CHO))2	-4621	15
PtP <sub>2</sub> O <sub>2</sub>		
$[Pt_2(P(m-C_6H_4SO_3Na)_3)_4(\mu-OH)_2]^{2+}$	-4083	69
cis-[Pt(P( $m$ -C <sub>6</sub> H <sub>4</sub> SO <sub>3</sub> Na) <sub>3</sub> ) <sub>2</sub> (OH <sub>2</sub> ) <sub>2</sub> ](CF <sub>3</sub> SO <sub>3</sub> ) <sub>2</sub>	-3839	69
cis-Pt(PHCy <sub>2</sub> ) <sub>2</sub> (OPh) <sub>2</sub>	-4155	107
PtP <sub>2</sub> C <sub>2</sub>		
$cis, cis$ -Me <sub>2</sub> (Ph <sub>3</sub> P)Pt( $\mu$ -dppam)Pt(PPh <sub>3</sub> )Me <sub>2</sub>	-4672	75
$cis, cis$ -Me <sub>2</sub> {( $^{i}$ Pr- $O$ ) <sub>3</sub> P}Pt( $\mu$ -dppam)Pt{( $O$ - $^{i}$ Pr) <sub>3</sub> P}Me <sub>2</sub>	-4599	75

$cis, cis$ -Me <sub>2</sub> (Ph <sub>3</sub> P)Pt( $\mu$ -dppm)Pt(PPh <sub>3</sub> )Me <sub>2</sub>	-4718	75
$cis, cis$ -Me <sub>2</sub> {( $^{i}$ Pr- $O$ ) <sub>3</sub> P}Pt( $\mu$ -dppm)Pt{( $O$ - $^{i}$ Pr) <sub>3</sub> P}Me <sub>2</sub>	-4635	75
PtP <sub>2</sub> Se <sub>2</sub>		
cis-[Pt(PPh <sub>3</sub> ) <sub>2</sub> (SePh) <sub>2</sub> ]	-4904	76
trans-[Pt(PPh <sub>3</sub> ) <sub>2</sub> (SePh) <sub>2</sub> ]	-5040	76
$[Pt_2(\mu\text{-SePh})_2(dppm)_2](CF_3SO_3)_2$	-4085	73
trans-Pt(PPh <sub>3</sub> ) <sub>2</sub> (SeCC- $n$ -C <sub>5</sub> H <sub>11</sub> ) <sub>2</sub>	-4985	77
cis-Pt(dppf) <sub>2</sub> (SeCC- $n$ -C <sub>5</sub> H <sub>11</sub> ) <sub>2</sub>	-5009	77
Pt(1,8-Se <sub>2</sub> -nap)(PPh <sub>3</sub> ) <sub>2</sub>	-4912	108
Pt(1,8-Se <sub>2</sub> -nap)(PMe <sub>3</sub> ) <sub>2</sub>	-4767	108
PtP <sub>3</sub> Cl		
$[Pt(P(m-C_6H_4SO_3Na)_3)_3CI]CI$	-4731	69
$cis$ -Pt(PHCy <sub>2</sub> ) <sub>2</sub> {P(S)Cy <sub>2</sub> }Cl	-5329	102
$trans$ -[Pt(PHCy <sub>2</sub> )Cl( $\mu$ -PCy <sub>2</sub> )] <sub>2</sub>	-4014	107
[PtAu(tris[2-(diphenylphosphino)ethyl]phosphine)Cl <sub>2</sub> ]Cl·4H <sub>2</sub> O	-4795	110
PtP <sub>3</sub> Pt		
$\{(Cy_2PH)Pt(\mu\text{-PC}y_2)_2Pt'[Cy_2(MeO)P]\}$	-5530(Pt)	107
$\{[Cy_2(MeO)P]Pt(\mu-PCy_2)\}_2$	-5570(Pt') -5570	107
$\{[Cy_2(EtO)P]Pt(\mu-PCy_2)\}_2$	-5567	107
$\{[Cy_2(PhO)P]Pt(\mu-PCy_2)\}_2$	-5524	107
$\{(Cy_2PH)Pt(\mu-PCy_2)_2Pt'[Cy_2(^tBuO)P]\}$	-5492(Pt)	107
PtNSeCl <sub>2</sub>	-5445(Pt')	
Pt(PhSe(CH <sub>2</sub> ) <sub>2</sub> NH <sub>2</sub> )Cl <sub>2</sub>	-3088	105

Pt(BzSe(CH2)2NH2)Cl2	-3057	105
PtNSI <sub>2</sub>		
cis-Pt(tetramethylenesulfoxyde)(pz)I <sub>2</sub>	-4407	unpublished result
cis-Pt(DMSO)(pz)I <sub>2</sub>	-4356	unpublished result
cis-Pt(di-n-propylsulfoxyde)(pz)I <sub>2</sub>	-4373	unpublished result
cis-Pt(di-n-butylsulfoxyde)(pz)l <sub>2</sub>	-4371	unpublished result
cis-Pt(dibenzylsulfoxyde)(pz)I <sub>2</sub>	-4398	unpublished result
PtNSCl <sub>2</sub>		
cis-Pt(Me <sub>2</sub> SO)(pyr)Cl <sub>2</sub>	-2851	47
cis-Pt(Me <sub>2</sub> SO)(pic)Cl <sub>2</sub>	-2862	47
trans-Pt(Me <sub>2</sub> SO)(pyr)Cl <sub>2</sub>	-3014	47
trans-Pt(Me <sub>2</sub> SO)(pic)Cl <sub>2</sub>	-3023	47
trans-Pt(Me <sub>2</sub> S)(pyr)Cl <sub>2</sub>	-2821	59
trans-Pt(Me <sub>2</sub> S)(NHEt <sub>2</sub> )Cl <sub>2</sub>	-3139	59
trans-Pt(Me <sub>2</sub> SO)(diMe-4-O-IMT)Cl <sub>2</sub>	-3059	78
cis-Pt(Me <sub>2</sub> SO)(diMe-4-O-IMT)Cl <sub>2</sub>	-2991	78
trans-Pt(Me <sub>2</sub> SO)(diMe-4-O-2-S-IMT)Cl <sub>2</sub>	-3054	78
cis-Pt(Me <sub>2</sub> SO)(diMe-4-O-2-S-IMT)Cl <sub>2</sub>	-2994	78
$\{trans-Pt(Me_2SO)Cl_2\}_2(\mu-pz)$	-3049	79
$\{trans\text{-Pt}(diethylsulfoxyde)Cl_2\}_2(\mu\text{-pz})$	-3076	unpublished result
$\{trans\text{-Pt}(tetramethylenesulfoxyde)Cl_2\}_2(\mu\text{-pz})$	-3041	79
$\{trans-Pt(di-n-propylsulfoxyde)Cl_2\}_2(\mu-pz)$	-3048	79
$\{trans-Pt(di-n-buty sulfoxyde)Cl_2\}_2(\mu-pz)$	-3051	79

$\{trans\text{-Pt}(diphenylsulfoxyde)Cl_2\}_2(\mu\text{-pz})$	-3113	79
trans-Pt(Me <sub>2</sub> SO)(pz)Cl <sub>2</sub>	-3045	80
trans-Pt(tetramethylenesulfoxyde)(pz)Cl <sub>2</sub>	-3042	80
cis-Pt(di-n-propylsulfoxyde)(pz)Cl <sub>2</sub>	-3046	80
trans-Pt(diphenylsulfoxyde)(pz)Cl <sub>2</sub>	-3121	80
$ \{ \textit{trans}\text{-Pt(tetramethylenesulfoxyde)Cl}_2 \} (\mu - pz) \{ \textit{trans}\text{-Pt'(dibenzylsulfoxyde)Cl}_2 \} $	-3044 (Pt) -3059 (Pt')	unpublished result
$\label{eq:constraint} $$ \{trans-Pt(tetramethylenesulfoxyde)Cl_2\}(\mu-pz)\{trans-Pt'(di-n-propylsulfoxyde)Cl_2\}$$	-3042 (Pt) -3048 (Pt')	unpublished result
$\{\textit{trans}-Pt(\textit{tetramethylenesulfoxyde})Cl_2\}(\mu-pz)\{\textit{trans}-Pt'(\textit{di-}\textit{n-butylsulfoxyde})Cl_2\}$	-3043 (Pt) -3050 (Pt')	unpublished result
$\{trans$ -Pt(tetramethylenesulfoxyde)Cl <sub>2</sub> $\}_2(\mu$ -Me <sub>2</sub> pz)	-3059	unpublished result
$\{trans$ -Pt(diethylsulfoxyde)Cl <sub>2</sub> $\}_2(\mu$ -Me <sub>2</sub> pz)	-3103	unpublished result
$\{trans-Pt(di-n-propylsulfoxyde)Cl_2\}_2(\mu-Me_2pz)$	-3073	unpublished result
$\{trans-Pt(methylbenzylsulfoxyde)Cl_2\}_2(\mu-Me_2pz)$	-3097	unpublished result
$\{\textit{trans}\text{-Pt}(\text{tetramethylenesulfoxyde})\text{Cl}_2\}_2(\mu\text{-quinoxaline})$	-3044	unpublished result
$\{trans-Pt(Me_2SO)Cl_2\}_2(\mu-quinoxaline)$	-3103	unpublished result
PtN(C=C)CI <sub>2</sub>		
trans-PtCl <sub>2</sub> (C <sub>2</sub> H <sub>4</sub> )(1S,1'S)-bis(1-PhEt)NH	-2917	37
trans-PtCl <sub>2</sub> (C <sub>2</sub> H <sub>4</sub> )(1S,1'S)-bis[1-(1-Np)Et]NH	-2917	37
trans-PtCl <sub>2</sub> (C <sub>2</sub> H <sub>4</sub> )(1S,1'S)-N-[1'-(1-Np)Et]-1-PhEtNH	-2917 (S)	37
trans-PtCl <sub>2</sub> (C <sub>2</sub> H <sub>4</sub> )(S)-1-(1-Np)EtNH	-2910 ( <i>R</i> ) -3069	37
PtNCl <sub>3</sub>		
[Pt(NH=C(Et)ON=CMe <sub>2</sub> )Cl <sub>3</sub> ](Ph <sub>2</sub> PCH <sub>2</sub> Ph)	-1811	59

$[Pt(NH=C(Et)ON=C(C_4H_8))Cl_3](Ph_2PCH_2Ph)$	-1808	59
[Pt(NH=C(Et)ON=C(C5H10))Cl3](Ph2PCH2Ph)	-1807	59
PtN <sub>2</sub> Scl		
[Pt(en)(tmtu)Cl] <sup>+</sup>	-2929	41
[Pt(dach)(tmtu)Cl] <sup>+</sup>	-2895	41
trans-[Pt(Me <sub>2</sub> SO)(NH <sub>3</sub> ) <sub>2</sub> Cl](NO <sub>3</sub> )	-3123	47
trans-[Pt(MeBzSO)(NH <sub>3</sub> ) <sub>2</sub> Cl](NO <sub>3</sub> )	-3143	47
trans-[Pt(MePhSO)(NH <sub>3</sub> ) <sub>2</sub> Cl](NO <sub>3</sub> )	-3159	47
trans-[Pt(Me <sub>2</sub> SO)(pyr) <sub>2</sub> Cl](NO <sub>3</sub> )	-2902	47
cis-[Pt(Me <sub>2</sub> SO)(pyr) <sub>2</sub> Cl](NO <sub>3</sub> )	-2957	47
trans-[Pt(MeBzSO)(pyr) <sub>2</sub> Cl](NO <sub>3</sub> )	-2891	47
trans-[Pt(Me <sub>2</sub> SO)(pic) <sub>2</sub> Cl](NO <sub>3</sub> )	-2909	47
cis-[Pt(Me <sub>2</sub> SO)(pic) <sub>2</sub> Cl](NO <sub>3</sub> )	-2964	47
trans-[Pt(MeBzSO)(pic) <sub>2</sub> Cl](NO <sub>3</sub> )	-2890	47
cis-[Pt(2,3-diaminotoluene)(DMSO)CI] <sup>+</sup>	-3181	81
cis-[Pt(3,4-diaminotoluene)(DMSO)CI] <sup>+</sup>	-3185	81
cis-[Pt(4,5-diaminoxylene)(DMSO)CI] <sup>+</sup>	-3121	81
cis-[Pt(4,5-diaminophenol)(DMSO)Cl] <sup>+</sup>	-3134	81
PtN <sub>2</sub> SO		
cis-[Pt(NH <sub>3</sub> ) <sub>2</sub> (Me <sub>2</sub> SO)(H <sub>2</sub> O)](NO <sub>3</sub> ) <sub>2</sub>	-2813	7
PtN <sub>2</sub> ClO		
cis-[Pt(NH <sub>3</sub> ) <sub>2</sub> (H <sub>2</sub> O)Cl] <sup>+</sup>	-1841	7
cis[Pt(NH <sub>3</sub> ) <sub>2</sub> (OH)Cl	-1826	7

PtN <sub>2</sub> BrO		
cis-[Pt(NH <sub>3</sub> ) <sub>2</sub> (H <sub>2</sub> O)Br] <sup>+</sup>	-1934	7
cis-Pt(NH <sub>3</sub> ) <sub>2</sub> (OH)Br	-1915	7
PtN <sub>2</sub> IO		
cis-[Pt(NH <sub>3</sub> ) <sub>2</sub> (H <sub>2</sub> O)I](NO <sub>3</sub> )	-2224	7
cis-Pt(NH <sub>3</sub> ) <sub>2</sub> (OH)I	-2199	7
PtN <sub>2</sub> CBr		
$PtBr(C_6H_2(CH_2NMe_2)_2-2,6-(CH_2-Val-OMe)-4)$	-3183	39
PtBr(C6H3(CH2NMe2)2-2,6)	-3178	39
PtN <sub>2</sub> CCI		
PtCI(C6H3(CH2NMe2)2-2,6)	-3150	39
PtN <sub>2</sub> CI		
PtI(C6H3(CH2NMe2)2-2,6)	-3212	39
PtN <sub>2</sub> S <sub>2</sub>		
$[Pt(en)(tu)_2](NO_3)_2$	-3454	42
cis-[Pt(NH <sub>3</sub> ) <sub>2</sub> (tu) <sub>2</sub> ] <sup>2+</sup>	-3400	7
Pt(ethylene-1,2-dithiolate)(bpy) <sub>2</sub>	-3506	58
trans-Pt(SG) <sub>2</sub> (NH <sub>3</sub> ) <sub>2</sub>	-3226	82
$trans$ -[(Pt(SG)(NH <sub>3</sub> ) <sub>2</sub> ) <sub>2</sub> $\mu$ -(SG)] <sup>+</sup>	-3186	82
[Pt(1,4,7-trithiacyclononane)(bpy)](PF <sub>6</sub> ) <sub>2</sub>	-3261	60
[Pt(1,4,7-trithiacyclononane)(Me <sub>2</sub> bpy)](PF <sub>6</sub> ) <sub>2</sub>	-3279	60
[Pt(1,4,7-trithiacyclononane)( <sup>t</sup> Bu <sub>2</sub> bpy)](PF <sub>6</sub> ) <sub>2</sub>	-3289	60
[Pt(1,4,7-trithiacyclononane)(non <sub>2</sub> bpy)](PF <sub>6</sub> ) <sub>2</sub>	-3284	60

[Pt(1,4,7-trithiacyclononane)(phen)](PF <sub>6</sub> ) <sub>2</sub>	-3292	60
[Pt(1,4,7-trithiacyclononane)(Me <sub>4</sub> phen)](PF <sub>6</sub> ) <sub>2</sub>	-3313	60
PtN <sub>2</sub> O <sub>2</sub>		
cis-[Pt(NH <sub>3</sub> ) <sub>2</sub> (H <sub>2</sub> O) <sub>2</sub> ] <sup>2+</sup>	-1584	83
trans- $[Pt(NH_3)_2(H_2O)_2]^{2+}$	-1374	7
cis-Pt(NH <sub>3</sub> ) <sub>2</sub> (OH) <sub>2</sub>	-1572	7
cis-Pt(NH <sub>3</sub> ) <sub>2</sub> (OSO <sub>3</sub> )(H <sub>2</sub> O)	-1550	7
$trans$ -[Pt(NH <sub>3</sub> ) <sub>2</sub> Cl- $\mu$ -(NH <sub>2</sub> (CH <sub>2</sub> ) <sub>6</sub> NH <sub>2</sub> )Pt'(mal)(NH <sub>3</sub> )](NO <sub>3</sub> )	-2409 (Pt) -1795 (Pt')	84
Pt(dach)(acetylGlu)	-1864	85
Pt(dach)(propionylGlu)	-1847	85
Pt(dach)(pivaloylGlu)	-1861	85
Pt(dach)(O,O'-Glu)	-1918	85
cis-Pt(cyclobutylamine) <sub>2</sub> (NO <sub>3</sub> ) <sub>2</sub>	-1706	9
trans-Pt(cyclobutylamine) <sub>2</sub> (NO <sub>3</sub> ) <sub>2</sub>	-1572	9
cis-Pt(cyclohexylamine) <sub>2</sub> (NO <sub>3</sub> ) <sub>2</sub>	-1682	9
trans-Pt(cyclohexylamine) <sub>2</sub> (NO <sub>3</sub> ) <sub>2</sub>	-1542	9
cis-Pt(cyclopentylamine) <sub>2</sub> (NO <sub>3</sub> ) <sub>2</sub>	-1690	9
trans-Pt(cyclopentylamine) <sub>2</sub> (NO <sub>3</sub> ) <sub>2</sub>	-1569	9
cis-[Pt(cyclobutylamine) <sub>2</sub> (D <sub>2</sub> O) <sub>2</sub> ](NO <sub>3</sub> ) <sub>2</sub>	-1747	9
trans-[Pt(cyclobutylamine) <sub>2</sub> (D <sub>2</sub> O) <sub>2</sub> ](NO <sub>3</sub> ) <sub>2</sub>	-1541	9
cis-[Pt(cyclopentylamine) <sub>2</sub> (D <sub>2</sub> O) <sub>2</sub> ](NO <sub>3</sub> ) <sub>2</sub>	-1721	9
trans-[Pt(cyclopentylamine) <sub>2</sub> (D <sub>2</sub> O) <sub>2</sub> ](NO <sub>3</sub> ) <sub>2</sub>	-1536	9
cis-[Pt(cyclohexylamine) <sub>2</sub> (D <sub>2</sub> O) <sub>2</sub> ](NO <sub>3</sub> ) <sub>2</sub>	-1711	9

trans-[Pt(cyclohexylamine) <sub>2</sub> (D <sub>2</sub> O) <sub>2</sub> ](NO <sub>3</sub> ) <sub>2</sub>	-1513	9
cis-[Pt(cyclohexylamine) <sub>2</sub> (D <sub>2</sub> O)(NO <sub>3</sub> )](NO <sub>3</sub> )	-1724	9
trans-[Pt(cyclopropylamine) <sub>2</sub> (D <sub>2</sub> O)(NO <sub>3</sub> )](NO <sub>3</sub> )	-1549	9
cis-Pt(cyclobutylamine) <sub>2</sub> (OD) <sub>2</sub>	-1722	9
trans-Pt(cyclobutylamine)₂(OD)₂	-1564	9
cis-Pt(cyclohexylamine) <sub>2</sub> (OD) <sub>2</sub>	-1694	9
trans-Pt(cyclohexylamine) <sub>2</sub> (OD) <sub>2</sub>	-1550	9
cis-[Pt(cyclobutylamine) <sub>2</sub> (OD)(OD <sub>2</sub> )] <sup>+</sup>	-1733	9
$trans$ -[Pt(cyclobutylamine) $_2$ (OD)(OD $_2$ )] $^+$	-1551	9
cis-[Pt(cyclohexylamine) <sub>2</sub> (OD)(OD <sub>2</sub> )] <sup>+</sup>	-1693	9
$trans$ -[Pt(cyclohexylamine) $_2$ (OD)(OD $_2$ )] $^+$	-1539	9
$trans$ -[Pt(cyclopentylamine) $_2$ (OD)(OD $_2$ )] $^+$	-1556	9
$cis$ -[(Pt(cyclobutylamine) <sub>2</sub> ) <sub>2</sub> ( $\mu$ -OD) <sub>2</sub>	-1350	9
$cis$ -[(Pt(cyclohexylamine) <sub>2</sub> ) <sub>2</sub> ( $\mu$ -OD) <sub>2</sub>	-1375	9
trans-Pt(3-Acpy) <sub>2</sub> (NO <sub>3</sub> ) <sub>2</sub>	-1474	101
PtN <sub>2</sub> I <sub>2</sub>		
cis-Pt(NH <sub>3</sub> ) <sub>2</sub> I <sub>2</sub>	-3264	7
cis-Pt(MeNH <sub>2</sub> ) <sub>2</sub> I <sub>2</sub>	-3342	13
trans-Pt(MeNH <sub>2</sub> ) <sub>2</sub> I <sub>2</sub>	-3360	13
cis-Pt(nBuNH <sub>2</sub> ) <sub>2</sub> I <sub>2</sub>	-3349	13
trans-Pt(nBuNH <sub>2</sub> ) <sub>2</sub> I <sub>2</sub>	-3363	13
cis-Pt(Me <sub>2</sub> NH) <sub>2</sub> I <sub>2</sub>	-3247	13
trans-Pt(Me <sub>2</sub> NH) <sub>2</sub> I <sub>2</sub>	-3057	13

cis-Pt(cyclopropylamine) <sub>2</sub> l <sub>2</sub>	-3353	9
trans-Pt(cyclopropylamine)₂l₂	-3362	9
cis-Pt(cyclobutylamine) <sub>2</sub> I <sub>2</sub>	-3378	9
trans-Pt(cyclobutylamine) <sub>2</sub> l <sub>2</sub>	-3400	9
cis-Pt(pyridine) <sub>2</sub> I <sub>2</sub>	-3199	7
trans-Pt(pyridine)₂I₂	-3133	103
cis-Pt(2-picoline) <sub>2</sub> I <sub>2</sub>	-3281	12
trans-Pt(2-picoline) <sub>2</sub> l <sub>2</sub>	-3264	12
trans-Pt(3-Acpy)I <sub>2</sub>	-3224	101
trans-Pt(pz) <sub>2</sub> I <sub>2</sub>	-3269	unpublished result
cis-Pt(pz) <sub>2</sub> I <sub>2</sub>	-3260	unpublished result
PtN <sub>2</sub> Br <sub>2</sub>		
cis-Pt(NH <sub>3</sub> ) <sub>2</sub> Br <sub>2</sub>	-2459	7
Pt(bipy)Br <sub>2</sub>	-1896	106
trans-Pt(pz) <sub>2</sub> Br <sub>2</sub>	-2393	unpublished result
cis-Pt(pz) <sub>2</sub> Br <sub>2</sub>	-2355	unpublished result
PtN <sub>2</sub> Cl <sub>2</sub>		
trans-Pt(NH <sub>3</sub> ) <sub>2</sub> Cl <sub>2</sub>	-2101	47
cis-Pt(NH <sub>3</sub> ) <sub>2</sub> Cl <sub>2</sub>	-2104	7
cis-Pt(pyr) <sub>2</sub> Cl <sub>2</sub>	-1998	47
trans-Pt(pyr) <sub>2</sub> Cl <sub>2</sub>	-1948	47
trans-Pt(2-pic) <sub>2</sub> Cl <sub>2</sub>	-1973	47
cis-Pt(2-pic) <sub>2</sub> Cl <sub>2</sub>	-2021	47

cis-Pt(MeNH <sub>2</sub> ) <sub>2</sub> Cl <sub>2</sub>	-2222	103
cis-Pt(Me <sub>2</sub> NH) <sub>2</sub> Cl <sub>2</sub>	-2188	103
trans-Pt(Me <sub>2</sub> NH) <sub>2</sub> Cl <sub>2</sub>	-2181	103
Pt(2,2'bpyr) <sub>2</sub> Cl <sub>2</sub>	-2315	86
$Pt(NH=C(Me)ON=CMe_2)_2Cl_2$	-2040	59
Pt(NH=C(Me)ON=CMeEt) <sub>2</sub> Cl <sub>2</sub>	-2088	59
$Pt(NH=C(Me)ONMe_2)_2Cl_2$	-2047	59
Pt(NH=C(Me)ONEt <sub>2</sub> ) <sub>2</sub> Cl <sub>2</sub>	-2028	59
Pt(NH=C(Me)ON(CH2Ph)2)2Cl2	-2033	59
trans-Pt(NH <sub>3</sub> )(2-pyridinyl-acetato- <i>N,O</i> )Cl <sub>2</sub>	-1930	87
$[cis-Pt(NH_3)_2Cl-(\mu-NH_2(CH_2)_6NH_2)-cis-Pt'(NH_3)Cl_2]Cl$	-2416 (Pt)	88
cis-Pt(2,3-diaminotoluene)Cl <sub>2</sub>	-2202 (Pt') -2248	81
cis-Pt(3,4-diaminotoluene)Cl <sub>2</sub>	-2213	81
cis-Pt(4,5-diaminoxylene)Cl <sub>2</sub>	-2238	81
cis-Pt(2,3-diaminophenol)Cl <sub>2</sub>	-2212	81
cis-Pt(5,7-diphenyl-1,2,4-triazolopyrimidine) <sub>2</sub> Cl <sub>2</sub>	-2072	89
cis-Pt(5,7-ditertbutyl-1,2,4-triazolopyrimidine) <sub>2</sub> Cl <sub>2</sub>	-2096	89
cis-Pt(5,7-diphenyl-1,2,4-triazolopyrimidine)(NH <sub>3</sub> )Cl <sub>2</sub>	-2090	89
cis-Pt(5,7-di <sup>t</sup> butyl-1,2,4-triazolopyrimidine)(NH <sub>3</sub> )Cl <sub>2</sub>	-2091	89
cis-Pt(cyclopropylamine) <sub>2</sub> Cl <sub>2</sub>	-2190	9
trans-Pt(cyclopropylamine) <sub>2</sub> Cl <sub>2</sub>	-2211	9
cis-Pt(cyclobutylamine) <sub>2</sub> Cl <sub>2</sub>	-2225	9
trans-Pt(cyclobutylamine) <sub>2</sub> Cl <sub>2</sub>	-2237	9

cis-Pt(cyclopentylamine) <sub>2</sub> Cl <sub>2</sub>	-2204	9
trans-Pt(cyclopentylamine) <sub>2</sub> Cl <sub>2</sub>	-2222	9
Pt(bpydicar)Cl <sub>2</sub>	-1831	98
$Pt(ArN=(CO_2CD_3)C(CO_2CD_3)=NAr)Cl_2$	-1559	99
Pt(ArN=HCH=NAr)=NAr)Cl <sub>2</sub>	-2100	99
Pt(ArN=C(Me)C(Me)=NAr)=NAr)Cl <sub>2</sub>	-2179	99
$trans$ -Pt{N=C(CH <sub>2</sub> CO <sub>2</sub> Me)ON(Me)C(H)(4-MeC <sub>6</sub> H <sub>4</sub> )} <sub>2</sub> Cl <sub>2</sub>	-2290	100
$trans-Pt\{N=C(CH_2CI)ON(Me)C(H)(2,4,6-Me_3C_6H_2)\}_2CI_2$	-2191	100
cis-Pt(Boh) <sub>2</sub> Cl <sub>2</sub>	-2050	109
cis-Pt(Oc) <sub>2</sub> Cl <sub>2</sub>	-2055	109
cis-Pt(Ros) <sub>2</sub> Cl <sub>2</sub>	-2051	109
cis-Pt( <sup>i</sup> PrOc) <sub>2</sub> Cl <sub>2</sub>	-2052	109
cis-[Pt(BohH) <sub>2</sub> Cl <sub>2</sub> ]Cl <sub>2</sub>	-2080	109
cis-[Pt(OcH) <sub>2</sub> Cl <sub>2</sub> ]Cl <sub>2</sub>	-2071	109
cis-[Pt(RosH) <sub>2</sub> Cl <sub>2</sub> ]Cl <sub>2</sub>	-2072	109
cis-[Pt( <sup>i</sup> PrOcH) <sub>2</sub> Cl <sub>2</sub> ]Cl <sub>2</sub>	-2065	109
trans-Pt(pz) <sub>2</sub> Cl <sub>2</sub>	-2036	unpublished result
cis-Pt(pz) <sub>2</sub> Cl <sub>2</sub>	-2009	unpublished result
PtN <sub>3</sub> Cl		
$[\{\textit{trans}-Pt(NH_3)_2Cl\}_2-\mu-(H_2N(CH_2)_2NH_2)]Cl_2$	-2401	90
$[\{\textit{trans}-Pt(NH_3)_2Cl\}_2-\mu-(H_2N(CH_2)_3NH_2)]Cl_2$	-2421	90
$[\{trans\text{-Pt}(NH_3)_2Cl\}_2\text{-}\mu\text{-}(H_2N(CH_2)_6NH_2)]Cl_2$	-2425	90
$[\{trans-Pt(NH_3)_2Cl\}_2-\mu-(H_2N(CH_2)_6NH_2)](NO_3)_2$	-2397	90

$[\{trans-Pt(NH_3)_2Cl\}_2-\mu-(H_2N(CH_2)_7NH_2)]Cl_2$	-2418	90
$[\{trans\text{-Pt}(NH_3)_2Cl\}_2-\mu\text{-}(H_2N(CH_2)_8NH_2)]Cl_2$	-2431	90
[Pt(NH <sub>3</sub> ) <sub>3</sub> Cl](NO <sub>3</sub> )	-2353	7
cis-[Pt(NH <sub>3</sub> ) <sub>2</sub> (GMP)Cl]	-2295	91
$[\{cis\text{-Pt}(NH_3)_2Cl\}_2\text{-}(\mu\text{-pz})]Cl_2$	-2302	92
$[\{cis\text{-Pt}(NH_3)_2Cl\}_2\text{-}(\mu\text{-pm})]Cl_2$	-2323	92
$[\{cis\text{-Pt}(NH_3)_2CI\}_2\text{-}(\mu\text{-pdn})](NO_3)_2$	-2251	92
$[trans-Pt(NH_3)_2Cl-\mu-(NH_2(CH_2)_6NH_2)Pt'(mal)(NH_3)]NO_3$	-2409 (Pt)	84
$[cis-Pt(NH_3)_2Cl-\mu-(NH_2(CH_2)_6NH_2)-cis-Pt'(NH_3)Cl_2]Cl$	-1795 (Pt') -2416 (Pt)	88
$[(trans-Pt(NH_3)_2CI)_2-\mu(H_2N(CH_2)_6NH_2)_2\}]^{2+}$	-2202 (Pt') -2397	82
$[(trans-Pt(NH_3)_2CI)_2-\mu-(H_2N(CH_2)_3(NH_2^+)(CH_2)_4NH_2)]^{3+}$	-2418	82
[Pt(dach)(adenine)Cl](NO <sub>3</sub> )	-2537	93
[Pt(dach)(guanine)Cl](NO <sub>3</sub> )	-2519	93
[Pt(dach)(hypoxanthine)Cl](NO <sub>3</sub> )	-2515	93
[Pt(dach)(cytosine)Cl](NO <sub>3</sub> )	-2549	93
[Pt(dach)(adenosine)Cl](NO <sub>3</sub> )	-2579	93
[Pt(dach)(guanosine)Cl](NO <sub>3</sub> )	-2519	93
[Pt(dach)(inosine)Cl](NO <sub>3</sub> )	-2519	93
[Pt(dach)(methylcytosine)Cl](NO <sub>3</sub> )	-2545	93
$Pt(NCEt)(\underline{N}H=C(Et)NC(Ph)\underline{N}Ph)CI$	-2295	94
$Pt(NCH_2Ph)(\underline{N}H=C(CH_2Ph)NC(Ph)=\underline{N}Ph)Cl$	-2296	94
$Pt(NCPh)(\underline{N}H=C(Ph)NHC(Ph)=\underline{N}Ph)CI$	-2256	94
$Pt(NCNEt_2)(\underline{N}H=C(NEt_2)NC(Ph)=\underline{N}Ph)Cl$	-2273	94

PtN <sub>3</sub> Br		
$[Pt(NH_3)_3Br]^+$	-2492	7
PtN <sub>3</sub> I		
$[Pt(NH_3)_3I]^+$	-2819	7
PtN₃S		
[Pt(NH3)3(Me2SO)]2+	-3213	7
$[Pt(NH_3)_3SCN]^+$	-2798	7
$[Pt(NH_3)_3(tu)]^+$	-2962	7
[Pt(en)(GMP)tmtu)] <sup>2+</sup>	-3003	42
[Pt(dach)(GMP)tmtu)] <sup>2+</sup>	-2982	42
$trans$ -[(Pt(NH <sub>3</sub> ) <sub>2</sub> GS) <sub>2</sub> - $\mu$ -(H <sub>2</sub> N(CH <sub>2</sub> ) <sub>6</sub> NH <sub>2</sub> )] <sup>2+</sup>	-2987	82
PtN <sub>3</sub> O		
$[Pt(NH_3)_3H_2O]^{2+}$	-2070	7
$[Pt(NH_3)_3OH]^+$	-2062	7
Pt(NH <sub>3</sub> ) <sub>3</sub> SO <sub>4</sub>	-2035	7
cis-[Pt(NH <sub>3</sub> ) <sub>2</sub> (NO <sub>2</sub> )(H <sub>2</sub> O)] <sup>+</sup>	-1981	7
Pt(dach)(O,N-Glu)	-2410	85
PtN <sub>4</sub>		
[Pt(en)(GMP) <sub>2</sub> ] <sup>2+</sup>	-2648	42
trans-[Pt(NH <sub>3</sub> ) <sub>2</sub> (GMP) <sub>2</sub> ] <sup>2+</sup>	-2467	42
trans-[Pt(pic) <sub>2</sub> (GMP) <sub>2</sub> ] <sup>2+</sup>	-2331	42
trans-[Pt(NH <sub>3</sub> ) <sub>2</sub> (H <sub>2</sub> N(CH <sub>2</sub> ) <sub>5</sub> NH <sub>2</sub> )]Cl <sub>2</sub>	-2655	90
cis-[Pt(NH <sub>3</sub> ) <sub>2</sub> (en)]Cl <sub>2</sub>	-2795	90

$[Pt(NH_3)_4]^{2+}$	-2580	7
$[Pt(NH_3)_3NO_2]^+$	-2390	7
cis-Pt(NH <sub>3</sub> ) <sub>2</sub> (NO <sub>2</sub> ) <sub>2</sub>	-2214	7
cis-[Pt(NH <sub>3</sub> ) <sub>2</sub> (Guo) <sub>2</sub> ] <sup>2+</sup>	-2455	91
$[\{trans\text{-Pt}(NH_3)_2Cl\}_2 - \mu - \{trans\text{-Pt}(NH_3)_2(H_2N(CH_2)_6NH_2)_2\}](NO_3)_4$	-2648 [PtN <sub>4</sub> ]	95
cis-[Pt(NH <sub>3</sub> ) <sub>2</sub> (9-MeAdenine-N6)(9-MeAdenine-N7)] <sup>2+</sup>	-2417 [PtN₃Cl] -2530	96
cis-[Pt(NH <sub>3</sub> ) <sub>2</sub> (9-MeAdenine-N6)(9-MeHypoxanthine-N7)] <sup>2+</sup>	-2524	96
$Pt(\underline{N}H=C(Et)NC(Ph)\underline{N}Ph)_2$	-2145	94
$Pt(\underline{N}H=C(CH_2Ph)NC(Ph)=\underline{N}Ph)_2$	-2261	94
$Pt(\underline{N}H=C(Ph)NC(Ph)=\underline{N}Ph)_2$	-2270	94
$Pt(\underline{N}H=C(NEt_2)NC(Ph)=\underline{N}Ph)_2$	-2259	94
cis-Pt(HNCOPh) <sub>2</sub> (NH <sub>3</sub> ) <sub>2</sub>	-2473	56
cis-Pt(HNCOCCl <sub>3</sub> ) <sub>2</sub> (NH <sub>3</sub> ) <sub>2</sub>	-2512	56
cis-Pt(HNCO <sup>t</sup> Bu) <sub>2</sub> (NH <sub>3</sub> ) <sub>2</sub>	-2513	56
cis-Pt(HNCO <sup>t</sup> Bu) <sub>2</sub> (NH <sub>2</sub> CH <sub>3</sub> ) <sub>2</sub>	-2593	56
cis-Pt(HNCO <sup>t</sup> Bu) <sub>2</sub> (NH <sub>2</sub> <sup>t</sup> Bu) <sub>2</sub>	-2599	56
Pt(HNCO <sup>t</sup> Bu) <sub>2</sub> (en)	-2692	56
[Pt(MeNH <sub>2</sub> ) <sub>4</sub> ]I <sub>2</sub>	-2769	103
[Pt(EtNH <sub>2</sub> ) <sub>4</sub> ]I <sub>2</sub>	-2753	103
$[Pt(n-PrNH_2)_4]I_2$	-2741	103
$[Pt(n-BuNH_2)_4]I_2$	-2743	103
[Pt(iso-PrNH <sub>2</sub> ) <sub>4</sub> ]I <sub>2</sub>	-2724	103
[Pt(iso-BuNH <sub>2</sub> ) <sub>4</sub> ]I <sub>2</sub>	-2748	103

[Pt(cyclo-PrNH <sub>2</sub> ) <sub>4</sub> ]I <sub>2</sub>	-2715	103
[Pt(cyclo-BuNH <sub>2</sub> ) <sub>4</sub> ]I <sub>2</sub>	-2766	103
[Pt(PhMeNH <sub>2</sub> ) <sub>4</sub> ]I <sub>2</sub>	-2868	104
[Pt(PhEtNH <sub>2</sub> ) <sub>4</sub> ]I <sub>2</sub>	-2855	104
[Pt(PhPrNH <sub>2</sub> ) <sub>4</sub> ]I <sub>2</sub>	-2858	104
[Pt(PhBuNH <sub>2</sub> ) <sub>4</sub> ]I <sub>2</sub>	-2909	104
trans-Pt(pz) <sub>2</sub> (NO <sub>2</sub> ) <sub>2</sub>	-2255	unpublished result
cis-Pt(pz) <sub>2</sub> (NO <sub>2</sub> ) <sub>2</sub>	-2366	unpublished result

# **Appendix B** – <sup>195</sup>Pt-<sup>1</sup>H NMR coupling constants

Compound	<sup>3</sup> J( <sup>195</sup> Pt- <sup>1</sup> H)	Ref.
$PtS_2(C=C)_2$		
Pt(COD)(5,5-dihydro-1,4-dithiin-2,3-dithiolate)	57 (COD <sup>2</sup> J)	58
Pt(COD)(ethylene-1,2-dithiolate)	53 (COD, <sup>2</sup> J)	58
Pt(COD)(maleonitrile-1,2-dithiolate)	98 (dithiolate) 54 (COD, <sup>2</sup> J)	58
Pt(COD)(ethane-1,2-dithiolate)	52 (COD, <sup>2</sup> J) 51 (dithiolate)	58
PtS <sub>2</sub> Cl <sub>2</sub>	31 (ditinolate)	
cis-Pt(Me <sub>2</sub> S) <sub>2</sub> Cl <sub>2</sub>	42	unpublished result
cis-Pt(tetramethylenesulfoxyde) <sub>2</sub> Cl <sub>2</sub>	55	unpublished result
$Pt(C=C)_2C_2$		
Pt(Hbph) <sub>2</sub> (COD)	40 (COD, <sup>2</sup> J)	58

	69 (Hbph)	
PtC <sub>2</sub> S <sub>2</sub>		
cis-Pt(Hbph) <sub>2</sub> (DMSO) <sub>2</sub>	12 (DMSO)	111
cis-Pt(Hbph) <sub>2</sub> (SEt <sub>2</sub> ) <sub>2</sub>	73 (Hbph) 26 (CH₂) 79 (Hbph)	111
PtPSnHC	, ,	
PtH(CO)(P <sup>t</sup> Bu <sub>3</sub> )(SnPh <sub>3</sub> )	775 ( <sup>1</sup> J)	65
PtPNSeCl		
Pt(SeCH <sub>2</sub> CH <sub>2</sub> NMe <sub>2</sub> )(PMePh <sub>2</sub> )Cl	15	66
PtP <sub>2</sub> NCI		
trans-PtCl(NH(4-IC <sub>6</sub> H <sub>4</sub> ))(PEt <sub>3</sub> ) <sub>2</sub>	40 ( <sup>2</sup> J)	112
trans-PtCl(NH(4-ClC <sub>6</sub> H <sub>4</sub> ))(PEt <sub>3</sub> ) <sub>2</sub>	33 ( <sup>2</sup> J)	112
PtP <sub>2</sub> HC		
$(dcpe)Pt(\mu_2-H)(CH_2SiMe_2)CH_2Ga(CH_2SiMe_3)_2$	866 ( <sup>1</sup> J)	71
PtP <sub>2</sub> CIC		
$Pt(2,6-(Cy_2PCH_2)_2C_6H_3)CI$	18	72
PtP <sub>2</sub> IC		
$Pt(2,6-(Cy_2PCH_2)_2C_6H_3)I$	19	72
PtP <sub>2</sub> OC		
$Pt(2,6-(Cy_2PCH_2)_2C_6H_3)(OSO_2CF_3)$	21	72
PtP <sub>2</sub> S <sub>2</sub>		
Pt(ethylene-1,2-dithiolate)(Ph <sub>3</sub> P) <sub>2</sub>	84 (dithiolate)	58
Pt(ethane-1,2-dithiolate)(Ph <sub>3</sub> P) <sub>2</sub>	46 (dithiolate)	58
PtNSCl <sub>2</sub>		

$\{\textit{trans}\text{-Pt}(\textit{tetramethylenesulfoxyde}) \text{Cl}_2\}_2(\mu\text{-pz})$	34	79
$\{trans$ -Pt(diethylsulfoxyde)Cl <sub>2</sub> $\}_2(\mu$ -pz)	29	unpublished result
$\{\textit{trans}\text{-Pt}(\textit{di-}\textit{n}\text{-propylsulfoxyde}) Cl_2\}_2(\mu\text{-pz})$	28	79
$\{\textit{trans}\text{-Pt}(\textit{di-}\textit{n}\text{-butylsulfoxyde}) Cl_2\}_2(\mu\text{-pz})$	29	79
$\{trans$ -Pt(diphenylsulfoxyde)Cl <sub>2</sub> $\}_2(\mu$ -pz)	35	79
trans-Pt(Me <sub>2</sub> SO)(pz)Cl <sub>2</sub>	23	80
$\{\textit{trans}\text{-Pt}(\textit{tetramethylenesulfoxyde}) Cl_2\}_2(\mu\text{-Me}_2pz)$	38	unpublished result
$\{\textit{trans}\text{-Pt}(\textit{diethylsulfoxyde}) Cl_2\}_2(\mu\text{-Me}_2pz)$	25	unpublished result
$\{trans$ -Pt(di- $n$ -propylsulfoxyde)Cl <sub>2</sub> $\}_2(\mu$ -Me <sub>2</sub> pz)	26	unpublished result
$\{\textit{trans}\text{-Pt}(\textit{di-}\textit{n}\text{-butylsulfoxyde}) Cl_2\}_2(\mu\text{-Me}_2pz)$	29	unpublished result
$\{ trans\text{-Pt}(methylbenzylsulfoxyde) Cl_2 \}_2 (\mu\text{-Me}_2 pz)$	31	unpublished result
$\{trans\text{-Pt(tetramethylenesulfoxyde)Cl}_2\}_2(\mu\text{-quinoxaline)}$	38	unpublished result
$\{trans$ -Pt(di- $n$ -propylsulfoxyde)Cl <sub>2</sub> $\}_2$ ( $\mu$ -quinoxaline)	35	unpublished result
$\{trans$ -Pt(di- $n$ -butylsulfoxyde)Cl <sub>2</sub> $\}_2(\mu$ -quinoxaline)	42	unpublished result
PtN <sub>2</sub> SCI		
trans-[Pt(Me <sub>2</sub> SO)(NH <sub>3</sub> ) <sub>2</sub> Cl]NO <sub>3</sub>	28	47
trans-[Pt(MeBzSO)(NH <sub>3</sub> ) <sub>2</sub> Cl]NO <sub>3</sub>	29	47
trans-[Pt(MePhSO)(NH <sub>3</sub> ) <sub>2</sub> Cl]NO <sub>3</sub>	28	47
trans-[Pt(Me <sub>2</sub> SO)(pyridine) <sub>2</sub> Cl]NO <sub>3</sub>	28	47
trans-[Pt(Me <sub>2</sub> SO)(picoline) <sub>2</sub> Cl]NO <sub>3</sub>	30	47
PtN <sub>2</sub> CCI		
Pt(C <sub>6</sub> H <sub>2</sub> (CH <sub>2</sub> NMe <sub>2</sub> ) <sub>2</sub> -2,6-(OSiMe <sub>2</sub> - <i>t</i> -Bu)-4)Cl	38 (NMe <sub>2</sub> )	39
1,3,5-{Pt(C <sub>6</sub> H <sub>2</sub> (CH <sub>2</sub> NMe <sub>2</sub> ) <sub>2</sub> -2,6-O(CO)-4)Cl} <sub>3</sub> C <sub>6</sub> H <sub>3</sub>	47 (CH <sub>2</sub> ) 32 (NMe <sub>2</sub> ) 41 (CH <sub>2</sub> )	39

Pt(C <sub>6</sub> H <sub>2</sub> (CH <sub>2</sub> NMe <sub>2</sub> ) <sub>2</sub> -2,6-(SiMe <sub>3</sub> )-4-(NMe <sub>2</sub> ) <sub>2</sub> -3,5)Cl	36 (NMe <sub>2</sub> ) 45 (CH <sub>2</sub> )	39
PtN <sub>2</sub> C <sub>2</sub>	, <del>-</del> /	
Pt(Hbph) <sub>2</sub> (bpy)	23 (bpy)	111
Pt(Hbph)₂(phen)	71 (Hbph) 21 (phen) 72 (Hbph)	111
PtN <sub>2</sub> O <sub>2</sub>		
cis-[Pt(NH <sub>3</sub> ) <sub>2</sub> (H <sub>2</sub> O) <sub>2</sub> ] <sup>2+</sup>	71 ( <sup>2</sup> <i>J</i> )	83
cis-Pt(NH <sub>3</sub> ) <sub>2</sub> (OH) <sub>2</sub>	56 ( <sup>2</sup> <i>J</i> )	7
$cis$ -[Pt(NH <sub>3</sub> ) <sub>2</sub> ( $\mu$ -OH) <sub>2</sub> ](NO <sub>3</sub> ) <sub>2</sub>	66 ( <sup>2</sup> J)	7
cis-Pt(cyclobutylamine) <sub>2</sub> (NO <sub>3</sub> ) <sub>2</sub>	68 ( <sup>2</sup> J)	9
trans-Pt(cyclobutylamine) <sub>2</sub> (NO <sub>3</sub> ) <sub>2</sub>	60 ( <sup>2</sup> J)	9
cis-Pt(cyclopentylamine) <sub>2</sub> (NO <sub>3</sub> ) <sub>2</sub>	68 ( <sup>2</sup> J)	9
trans-Pt(cyclopentylamine) <sub>2</sub> (NO <sub>3</sub> ) <sub>2</sub>	61 ( <sup>2</sup> J)	9
cis-[Pt(cyclobutylamine) $_2(D_2O)_2$ ](NO $_3$ ) $_2$	33, 65 ( <sup>2</sup> J)	9
trans-[Pt(cyclobutylamine) <sub>2</sub> (D <sub>2</sub> O) <sub>2</sub> ](NO <sub>3</sub> ) <sub>2</sub>	26, 58 ( <sup>2</sup> J)	9
cis-[Pt(cyclopentylamine) <sub>2</sub> (D <sub>2</sub> O) <sub>2</sub> ](NO <sub>3</sub> ) <sub>2</sub>	61 ( <sup>2</sup> <i>J</i> )	9
trans-[Pt(cyclopentylamine) <sub>2</sub> (D <sub>2</sub> O) <sub>2</sub> ](NO <sub>3</sub> ) <sub>2</sub>	56 ( <sup>2</sup> <i>J</i> )	9
cis-Pt(cyclobutylamine) <sub>2</sub> (OD) <sub>2</sub>	33	9
trans-Pt(cyclobutylamine) <sub>2</sub> (OD) <sub>2</sub>	27	9
PtN <sub>2</sub> S <sub>2</sub>		
cis-[Pt(NH <sub>3</sub> ) <sub>2</sub> (tu) <sub>2</sub> ] <sup>2+</sup>	50 ( <sup>2</sup> <i>J</i> )	7
Pt(ethylene-1,2-dithiolate)(bpy) <sub>2</sub>	51	58
[Pt(1,4,7-trithiacyclononane)(bpy)](PF <sub>6</sub> ) <sub>2</sub>	36	60
[Pt(1,4,7-trithiacyclononane)(Me <sub>2</sub> bpy)](PF <sub>6</sub> ) <sub>2</sub>	36	60

[Pt(1,4,7-trithiacyclononane)( <sup>t</sup> Bu <sub>2</sub> bpy)](PF <sub>6</sub> ) <sub>2</sub>	36	60
[Pt(1,4,7-trithiacyclononane)(phen)](PF <sub>6</sub> ) <sub>2</sub>	37	60
[Pt(1,4,7-trithiacyclononane)(Me <sub>4</sub> phen)](PF <sub>6</sub> ) <sub>2</sub>	36	60
PtN <sub>2</sub> I <sub>2</sub>		
cis-Pt(MeNH <sub>2</sub> ) <sub>2</sub> I <sub>2</sub>	49, 69 ( <sup>2</sup> J)	13
cis-Pt(Et <sub>2</sub> NH) <sub>2</sub> I <sub>2</sub>	34, 68 ( <sup>2</sup> J)	13
$cis$ -Pt $(nBuNH_2)_2I_2$	43, 65 ( <sup>2</sup> <i>J</i> )	13
cis-Pt(Me <sub>2</sub> NH) <sub>2</sub> I <sub>2</sub>	43, 70 ( <sup>2</sup> <i>J</i> )	13
trans-Pt(MeNH <sub>2</sub> ) <sub>2</sub> I <sub>2</sub>	35, 61 ( <sup>2</sup> <i>J</i> )	13
$trans$ -Pt( $n$ BuNH $_2$ ) $_2$ I $_2$	58 ( <sup>2</sup> J)	13
trans-Pt(Me <sub>2</sub> NH) <sub>2</sub> I <sub>2</sub>	37, 62 ( <sup>2</sup> <i>J</i> )	13
cis-Pt(cyclobutylamine) <sub>2</sub> l <sub>2</sub>	70 ( <sup>2</sup> J)	9
trans-Pt(cyclobutylamine)₂I₂	61 ( <sup>2</sup> J)	9
trans-Pt(pz) <sub>2</sub> l <sub>2</sub>	36	unpublished result
cis-Pt(pz) <sub>2</sub> I <sub>2</sub>	42	unpublished result
PtN <sub>2</sub> Br <sub>2</sub>		
trans-Pt(pz) <sub>2</sub> Br <sub>2</sub>	33	unpublished result
cis-Pt(pz) <sub>2</sub> Br <sub>2</sub>	42	unpublished result
PtN <sub>2</sub> Cl <sub>2</sub>		
trans-Pt(pz) <sub>2</sub> Cl <sub>2</sub>	33	unpublished result
cis-Pt(pz) <sub>2</sub> Cl <sub>2</sub>	41	unpublished result
PtN <sub>4</sub>		
cis-[Pt(NH <sub>3</sub> ) <sub>2</sub> (en)]Cl <sub>2</sub>	41	90

$[Pt(NH_3)_4]^{2+}$	56 ( <sup>2</sup> <i>J</i> )	7
[Pt(PhMeNH <sub>2</sub> ) <sub>4</sub> ]I <sub>2</sub>	40	104
[Pt(MeNH <sub>2</sub> ) <sub>4</sub> ]I <sub>2</sub>	42	103
trans-Pt(pz) <sub>2</sub> (NO <sub>2</sub> ) <sub>2</sub>	47	unpublished result

### References

- (1) G. H. Fuller. J. Phys. Chem. Ref. Data. 1976, 5, 835.
- (2) Pregosin, P.S. Coord. Chem. Rev. 1982, 44, 247.
- (3) Appleton, T.G.; Clark, H.C.; Manzer, L.E. Coord. Chem. Rev. 1973, 10, 335.
- (4) Ramsey, N.F. Phys. Rev. 1950, 78, 699.
- (5) Dean, R.R.; Green. J.C. J. Chem. Soc. (A) **1968**, 3047.
- (6) Gill, D.S.; Rosenberg, B. J. Am. Chem. Soc. 1982, 104, 4598.
- (7) Appleton, T.G.; Hall, J.R.; Ralph, S.F. Inorg. Chem. 1985, 24, 4685.
- (8) Marzilli, L.G.; Hayden, Y.; Reily, M.D. Inorg. Chem. 1986, 25, 974.
- (9) Rochon, F.D.; Buculei, V. Inorg. Chim, Acta. 2005, 358, 2040.
- (10) Dey S.; Kumbhare L.B.; Jain V.K.; Schurr T.; Kaim W.; Klein A.; Belaj F. Eur.
  J. Inorg. Chem. 2004, 22, 4510.
- (11) Rochon, F.D.; Morneau, A. Mag. Res. Chem. 1991, 29, 120.
- (12) Rochon, F.D.; Tessier, C. Inorg. Chim. Acta. 1999, 295, 25.
- (13) Rochon, F.D.; Buculei, V. Inorg. Chim. Acta. 2004, 357, 2218.
- (14) Gröning, O.; Drakenberg, T.; Elding, L.I. *Inorg. Chem.* **1982**, *21*, 1820.
- (15) Mahalakshmi, H.; Phadnis, P.P.; Jain, V.K.; Tiekink, E.R.T. *Indian J. Chem.*, Sect A. **2004**, 43, 2287.
- (16) Gaballa, A.; Schmidt, H.; Hempel, G.; Reichert, D.; Wagner, C.; Rusanov, E.; Steinborn, D. *J. Inorg. Biochem.* **2004**, *98*, 439.
- (17) Rochon, F.D.; Melanson, R.; Doyon, M.; Butler, I.S. *Inorg. Chem.* **1994**, *33*, 4485.

- (18) Nédélec, N.; Rochon, F.D. Inorg. Chim. Acta. **2001**, *319*, 95.
- (19) Rochon, F.D.; Beauchamp, A.L.; Bensimon, C. Can. J. Chem. 1996, 74, 2121.
- (20) Freeman, W.; Pregosin, P.S.; Sze, S.N.; Venanzi, L.M. *J. Magn. Reson.* **1976**, 22, 473.
- (21) Clark, H.C.; Ward, J.E.H. J. Am. Chem. Soc. 1974, 96, 1741.
- (22) Ismail, I.M.; Kerrison, S.J.S.; Sadler, P.J. *Polyhedron.* **1982**, *1*, 57.
- (23) Chisholm, M.H.; Clark, H.C.; Manzer, L.E.; Stothers, J.B.; Ward, J.E.H. *J. Am. Chem. Soc.* **1973**, *95*, 8574.
- (24) Cherwinski, W. J.; Johnson, B.F.G.; Lewis, J.; Norton, J.R. *J. Chem. Soc.*, *Dalton Trans.* **1975**, *12*, 1156.
- (25) Caskey, D.C.; Shoemaker, R.K.; Michl, J. Org. Lett. 2004, 6, 2093.
- (26) Pregosin, P.S. Studies of Inorganic Chemistry, #13. Group 10, nickel to platinum. Transition metal nuclear magnetic resonance, ed. P.S. Pregosin, Elsevier, Amsterdam, The Netherlands, 1991, 216-263.
- (27) Rochon, F.D.; Buculei, V. Can. J. Chem. 2004, 82, 524.
- (28) Ha, T.B.T.; Souchard, J.-P.; Wimmer, F.L.; Johnson, N.P. *Polyhedron*. **1990**, *9*, 2647.
- (29) Rochon, F.D.; Fleurent, L. Inorg. Chim. Acta. 1988, 143, 81.
- (30) Rochon, F.D.; Tessier, C. *Inorg. Chim. Acta.* **2001**, *322*, 37.
- (31) Rochon, F.D.; Tessier, C. Can. J. Chem. 2002, 80, 379.
- (32) Salvadori, P.; Uccello-Barretta, G.; Bertozzi, S.; Settambolo, R.; Lazzaroni, R. J. Org. Chem. 1988, 53, 5768.
- (33) Uccello-Barretta, G.; Bernardini, R.; Lazzaroni, R.; Salvadori, P. J. Organomet.

- Chem. 2000, 598, 174.
- (34) Salvadori, P.; Uccello-Barretta, G.; Lazzaroni, R.; Caporusso, A.M. J. Chem. Soc., Chem. Comm. 1990, 16, 1121.
- (35) Uccello-Barretta, G.; Balzano, F.; Salvadori, P.; Lazzaroni, R.; Caporusso, A.M.; Menicagli, R. *Enantiomer.* **1996**, *1*, 365.
- (36) Uccello-Barretta, G.; Bernardini, R.; Lazzaroni, R.; Salvadori, P. Org. Lett. **2000**, 2, 1795.
- (37) Uccello-Barretta, G.; Bernardini, R.; Balzano, F.; Salvadori, P. *J. Org. Chem.* **2001**, *66*, 123.
- (38) Uccello-Barretta, G.; Bernardini, R.; Balzano, F.; Caporusso, A.M.; Salvadori, *P. Org. Lett.* **2001**, *3*, 205.
- (39) Albrecht, M.; Rodriguez, G.; Schoenmaker, J.; Van Koten, G. Org. Lett. 2000, 2, 3461.
- (40) Van Beusichem, M.; Farrell, N. *Inorg. Chem.* **1992**, *31*, 634.
- (41) Bierbach, U.; Hambley, T.W.; Farrell, N. Inorg. Chem. 1998, 37, 708.
- (42) Bierbach, U.; Roberts, J.D.; Farrell, N. *Inorg. Chem.* **1998**, *37*, 717.
- (43) Crossley, E.L.; Caiazza, D.; Rendina, L.M. *Dalton Trans.* **2005**, *17*, 2825.
- (44) Rochon, F.D.; Melanson, R.; Morneau, A. Mag. Res. Chem. 1992, 30, 697.
- (45) Béni, Z.; Scopelliti, R.; Roulet, R. Inorg. Chem. Comm. 2005, 8, 99.
- (46) Béni, Z.; Ros, R.; Tassan, A.; Scopelliti, R.; Roulet, R. *Inorg. Chim. Acta.* **2005**, *358*, 497.
- (47) Fontes, A.P.S.; Oskarsson, Å.; Lövqvist, K.; Farrell, N. *Inorg. Chem.* **2001**, *40*, 1745.

- (48) Kerrison, S.J.; Sadler, P.J. Chem. Comm. 1977, 861.
- (49) Oehlsen, M.E.; Qu, Y.; Farrell, N. Inorg. Chem. 2003, 42, 5498.
- (50) Tong, Y.Y.; Wieckowski, A.; Oldfield, E. J. Phys. Chem. B. 2002, 106, 2434.
- (51) Bucher, J.P.; Buttet, J.; Van der Klink, J.J.; Graetzel, M.; Newson, E.; Truong, T.B. *Colloids and Surface*. **1989**, *36*, 155.
- (52) Tong, Y.Y.; Rice, C.; Wieckowski, A.; Oldfield, E. J. Am. Chem. Soc. 2000, 122, 11921.
- (53) Harris, R.K.; Sebald, A. Magn. Reson. Chem. 1987, 25, 1058.
- (54) Wasylishen, R.E.; Britten, J.F. Magn. Reson. Chem. 1988, 26, 1075.
- (55) Duer, M.J.; Khan, M.S.; Kakkar, A.K. *Solid State Nucl. Magn. Reson.* **1992**, *1*, 13.
- (56) Uemura, K.; Yamasaki, K.; Fukui, K.; Matsumoto, K. *Inorg. Chim. Acta.* **2007**, *360*, 2623.
- (57) De Pascali, S.A.; Papadia, P.; Ciccarese, A.; Pacifico, C.; Fanizzi, F.P. First Eur. J. Inorg. Chem. 2005, 788.
- (58) Keefer, C.E.; Bereman, R.D.; Purrington, S.T.; Knight, B.W.; Boyle, P.D. *Inorg. Chem.* 1999, 38, 2294.
- (59) Wagner, G.; Pakhomova, T.B.; Bokach, N.A.; Fraústo da Silva, J.J.R.; Vicente, J.; Pombeiro, A.J.L.; Kukushkin, V.Y. *Inorg. Chem.* 2001, 40, 1683.
- (60) Grant, G.J.; Patel, K.N.; Helm, M.L.; Mehne, L.F.; Klinger, D.W.; Van Derveer, D.G. *Polyhedron*. **2004**, *23*, 1361.
- (61) Yao, H.J.; Rauchfuss, T.B.; Wilson, S.R. J. Organomet. Chem. 2005, 690, 193.
- (62) Grant, G.J.; Chen, W.N.; Goforth, A.M.; Baucom, C.L.; Patel, K.; Repovic, P.;

- Van Derveer, D.G.; Pennington, W.T. Eur. J. Inorg. Chem. 2005, 479.
- (63) Grant, G.J.; Goforth, A.M.; Van Derveer, D.G.; Pennington, W.T. *Inorg. Chim. Acta.* **2004**, *357*, 2107.
- (64) Oliveira, M.R.L.; Rubinger, M.M.M.; Guilardi, S.; Franca, F.D.D.; Ellena, J.; De Bellis, V.M. *Polyhedron.* **2004**, *23*, 1153.
- (65) Beni Z.; Scopelliti R.; Roulet R. Inorg. Chem. Comm. 2004, 7, 935.
- (66) Jain, V.K. Phosphorus, Sulfur Silicon Relat. Elem. 2005, 180, 913.
- (67) Hashemi, M.; Rashidi, M. J. Organomet. Chem. 2005, 690, 982.
- (68) Kesanli, B.; Fettinger, J.; Gardner, D.R.; Eichhorn, B. *J. Am. Chem. Soc.* **2002**, *124*, 4779.
- (69) Francisco, L.W.; Moreno, D.A.; Atwood, J.D. Organometallics. 2001, 20, 4237.
- (70) De Castro, V.D.; De Lima, G.M.; Porto, A.O.; Siebald, H.G.L.; De Souza Filho, J.D.; Ardisson, J.D.; Ayala, J.D.; Bombieri, G.*Polyhedron*. **2004**, *23*, 63.
- (71) Fischer, R.A.; Weiss, D.; Winter, M.; Muller, I.; Kaesz, H.D.; Frohlich, N.; Frenking, G. J. Organomet. Chem. 2004, 689, 4611.
- (72) Shin, K.S.; Noh, D.Y. Bull. Korean Chem. Soc. 2004, 25, 130.
- (73) Singhal, A.; Jain, V.K.; Klein, A.; Niemeyer, M.; Kaim, W. *Inorg. Chim. Acta.*2004, 357, 2134.
- (74) Brown, M.D.; Levason, W.; Reid, G.; Watts, R. Polyhedron. 2005, 24, 75.
- (75) Rashidi, M.; Kamali, K.; Jennings, M.C.; Puddephatt, R.J. *J. Organomet. Chem.* **2005**, *690*, 1600.
- (76) Hannu, M.S.; Oilunkaniemi, R.; Laitinen, R.S.; Ahlgen, M. Inor. Chem. Comm.

- **2000**, *3*, 397.
- (77) Schafer, S.; Moser, C.; Tirree, J. J.; Nieger, M.; Pietschnig, R. Inor. Chem. 2005, 44, 2798.
- (78) Lakomska, I.; Golankiewicz, B.; Wietrzyk, J.; Pelczynska, M.; Nasulewicz, A.; Opolski, A.; Sitkowski, J.; Kozerski, L.; Szlyk, E. *Inorg. Chim. Acta.* **2005**, *358*, 1911.
- (79) Priqueler, J.R.L.; Rochon, F.D. Inorg. Chim. Acta. 2004, 357, 2167.
- (80) Priqueler, J.R.L.; Rochon, F.D. Can. J. Chem. 2004, 82, 649.
- (81) Pérez-Cabré, M.; Cervantes, G.; Moreno, V.; Prieto, M.J.; Pérez, J.M.; Font-Bardia, M.; Solans, X. J. Inorg. Biochem. **2004**, 98, 510.
- (82) Oehsen, M.E.; Qu, Y.; Farrell, N. Inorg. Chem. 2003, 42, 5498.
- (83) Levason, W.; Pletche, D. *Platinum Metals Rev.* **1993**, *37*, 17.
- (84) Qu, Y.; Fitzgerald, J.A.; Rauter, H.; Farrell, N. Inorg. Chem. 2001, 40, 6324.
- (85) Kim, Y.S.; Song, R.; Chung, H.C.; Jun, M.J.; Sohn, Y.S. *J. Inorg. Biochem.* **2004**, 98, 98.
- (86) Hope, E.G.; Levason, W.; Powell, N.A. Inorg. Chim. Acta. 1986, 115, 187.
- (87) Bierbach, U.; Sabat, M.; Farrell, N. Inorg. Chem. 2000, 39, 1882.
- (88) Qu, Y.; Rauter, H.; Fontes, A.P.S.; Bandarage, R.; Kelland, L.R.; Farrell, N. J. Med. Chem. **2000**, 43, 3189.
- (89) Lakomska, I.; Szlyk, E.; Sitkowski, J.; Kozerski, L.; Wietrzyk, J.; Pelczynska, M.; Nasulewicz, A.; Opolski, A. J. Inorg. Biochem. 2004, 98, 167.
- (90) Qu, Y.; Farrell, N. Inorg. Chem. 1992, 31, 930.
- (91) Miller, S.K.; Marzilli, L.G. Inorg. Chem. 1985, 24, 2421.

- (92) Komeda, S.; Kalayda, G.V.; Lutz, M.; Spek, A.L.; Yamanaka, Y.; Sato, T.; Chikuma, M.; Reedijk, J. *J. Med. Chem.* **2003**, *46*, 1210.
- (93) Ali, M.S.; Khan, S.R.A.; Ojima, H.; Guzman, I.Y.; Whitmire, K.H.; Siddik, Z.H.; Khokhar, A.R. *J. Inorg. Biochem.* **2005**, *99*, 795.
- (94) Bokach, N.A.; Kuznetsova, T.V.; Simanova, S.A.; Haukka, M.; Pombeiro, A.J.L.; Kukushkin, V.Y. *Inorg. Chem.* **2005**, *44*, 5152.
- (95) Manzotti, C.; Torriani, D.; Randisi, E.; De Georgi, M.; Pezzoni, G.; Menta, E.; Spinelli, S.; Fiebig, H.H.; Farrell, N.; Giuliani. F.C. *Proc. Am. Assoc. Cancer Res.* **1997**, *38*, 22080.
- (96) Arpalahti J., Klika K.D. Eur. J. Inorg. Chem. 2003, 23, 4195.
- (97) Wagner, A.; Vigo, L.; Oilunkaniemi, R.; Laitinen, R.S.; Weigand, W. Dalton Trans. 2008, 27, 3535.
- (98) Szeto, K.C.; Kongshaug, K.O.; Jakobsen, S.; Tilset, M.; Lillerud, K.P. *Dalton Trans.* **2008**, *15*, 2054.
- (99) Lersch, M.; Krivokapic, A.; Tilset, M. Organometallics. 2007, 26, 1581.
- (100) Lasri, J.; Charmier, M.A.J.; Haukka, M.; Pombeiro, A.J.L. J. Org. Chem. 2007, 72, 750.
- (101) Tessier, C.; Rochon, F.D. Acta Cryst. C. 2006, C62, m620.
- (102) Gallo, V.; Latronico, M.; Mastrorilli, P.; Nobile, C.F.; Ciccarella, G.; Englert,U. Eur. J. Inorg. Chem. 2006, 13, 2634.
- (103) Rochon, F.D.; Tessier, C.; Buculei, V. Inorg. Chim. Acta. 2007, 360, 2255.
- (104) Rochon, F.D.; Bonnier, C. Inorg. Chim. Acta. 2007, 360, 461.
- (105) Carland, M.; Abrahams, B.F.; Rede, T.; Stephenson, J.; Murray, V.; Denny,

- W.A.; McFadyen, W.D. Inorg. Chim. Acta. 2006, 359, 3252.
- (106) Sartori, D.A.; Hurst, S.K.; Wood, N.; Larsen, R.D.; Abbott, E.H. *J. Chem. Cryst.* **2005**, *33*, 995.
- (107) Gallo, V.; Latronico, M.; Mastrorilli, P.; Nobile, C.F.; Suranna, G.P.; Ciccarella, G.; Englert, U. Eur. J. Inorg. Chem. 2005, 4607.
- (108) Aucott, S.M.; Milton, H.L.; Robertson, S.D.; Slawin, A.M.Z.; Walker, G.D.; Woollins, J.D. *Chem. Eur. J.* **2004**, *10*, 1666.
- (109) Malon, M.; Travnicek, Z.; Marek, R.; Strnad, M. J. Inorg. Biochem. 2005, 99, 2127.
- (110) Fernández, D.; García-Seijo, M.I.; Castiñeiras, A.; García-Fernández, M.E. Dalton Trans. 2004, 2526.
- (111) Plutino, M.R.; Scolaro, L.M.; Albinati, A.; Romeo, R. J. Am. Chem. Soc. 2004, 126, 6470.
- (112) Albéniz, A. C.; Calle, V.; Espinet, P.; Gómez, S. Inorg. Chem. 2001, 40, 4211.

#### **CHAPTER III**

Pyrazine-bridged mixed-sulfoxides Pt(II) complexes: Synthesis, vibrational and multinuclear-NMR spectroscopy of  $\it trans-trans-Pt(TMSO)Cl_2(\mu-pyrazine)Pt(R_2SO)Cl_2$ 

## 3.1 Introduction

The antitumor properties of Pt(II) complexes of the type *cis*-Pt(amine)<sub>2</sub>Cl<sub>2</sub> have been known for several decades. The platinum drug binds to DNA and in the process interferes probably with the repair mechanism of the cancer cells, causing ultimately the cell death. Nowadays, *cisplatin* (*cis*-Pt(NH<sub>3</sub>)<sub>2</sub>Cl<sub>2</sub>) is still one of the most commonly used anticancer agents in chemotherapy, even though it exhibits numerous and important side effects. *Carboplatin*, *cis*-Pt(NH<sub>3</sub>)<sub>2</sub>(1,1-

cyclobutanedicarboxylato), which is also used in several countries is slightly more soluble in water, but its effect is not as general as is that of *cisplatin*. The search for more specific and less toxic drugs is still continuing, especially in view of the significant cross-resistance of these drugs. A new rational approach is to design platinum drugs that will bind to DNA in a different way in order to reduce the drug resistance.

Platinum(II) complexes containing pyrazine (pz) are not common in the literature. Recently, the pyrazine-bridged dinuclear Pt(II) compound [{cis-Pt(NH<sub>3</sub>)<sub>2</sub>Cl}<sub>2</sub>(μ-pz)]Cl<sub>2</sub> was reported to possess good anticancer properties, especially since it seems to overcome the cross-resistance of *cisplatin* (1). The complex is ionic and should be more soluble in water than are conventional neutral antitumor compounds, which are normally quite insoluble. The crystal structure of the corresponding nitrate salt was determined (1). The pyrazine-bridged compound seems to possess the appropriate Pt---Pt distance and flexibility to provide cross-links with a minimal distortion of the DNA molecule. Other studies (2-4) have suggested that pyrazine-bridged complexes might be promising alternatives to *cisplatin* in chemotherapy.

A few other polynuclear Pt(II) complexes bridged by N-donors are becoming very popular as potent anticancer agents and some of them are in terminal clinical phases (5-8). These compounds do not always have the *cis* geometry and the *trans* complexes seem less toxic than are the *cis* compounds (9). Caluccia *et al.* have shown that *trans* complexes with amine ligands can exhibit antitumor properties for very specific organs (10). Furthermore, neutral ligands with non N-donors, such as

S-bonded ligands, produced several active compounds (11). Ionic or neutral Pt(II) complexes containing sulfoxide and amine ligands, such as [Pt(R<sub>2</sub>SO)(diamine)Cl]NO<sub>3</sub>, and *cis* and *trans*-Pt(R<sub>2</sub>SO)(quinoline)Cl<sub>2</sub> have been shown to exhibit some biological activity that seems to depend on the sulfoxide chain (12,13).

The chemistry of Pt(II)-sulfoxide complexes has been the subject of our research for several years. The soft Pt(II) center binds sulfoxides through the S atom, unless steric hindrance is very large, as in cis-[Pt(S-DMSO)<sub>2</sub>(O-DMSO)<sub>2</sub>]<sup>2+</sup> (14,15). Sulfoxide ligands have interesting coordinating behaviour, since they can accept  $\pi$ electron density from the Pt(II) center. For these types of ligands, the cis complexes are usually more stable than are the *trans* compounds (contrary to the amine system), unless the ligands are very sterically demanding. We have already studied mixedligand platinum(II) complexes containing pyrimidine (pm) or pyrazine and sulfoxide ligands. Pyrimidine and pyrazine are molecules which also contain empty  $\pi$ antibonding orbitals, which could accept electron density from the Pt(II) center. However, the multiple nature of the Pt-N bond in these species has not been studied. The reaction of the K[Pt(R<sub>2</sub>SO)Cl<sub>3</sub>] with pyrimidine (1:1 ratio) produces first trans-Pt(R<sub>2</sub>SO)(pm)Cl<sub>2</sub>, which then isomerizes to the *cis* isomer (16). When the Pt:pyrimidine ratio was 2:1, pyrimidine-bridged trans-trans dimers were isolated, which isomerize in dichloromethane to produce the cis-cis dimers (17). Similar reactions with pyrazine were quite different. The monomers trans-Pt(R<sub>2</sub>SO)(pz)Cl<sub>2</sub> (18) were obtained, but they did not isomerize except for the di-n-propylsulfoxide compound. Pyrazine-bridged dimers were also isolated and all the compounds

studied had the *trans-trans* geometry (19). No cis dinuclear species could be synthesized even with di-n-propylsulfoxide. Contrary to pyrimidine, pyrazine is a symmetric molecule, but it has also empty  $\pi^*$ -orbitals, which could form  $\pi$  bonds with Pt. The *trans* complexes should therefore isomerize to the *cis* compounds if the sulfoxide is not too bulky. The symmetries of the  $\pi^*$ -orbitals of pyrazine are probably quite different from those of pyrimidine and so their  $\pi$ -backaccepting properties might be reduced.

In the literature, the synthesis and IR spectroscopic characterization of cisand trans-Pt(pz)<sub>2</sub>X<sub>2</sub> (X = Cl, Br, I and NO<sub>2</sub>) were reported (20). But there are no reported studies on platinum compounds with sulfoxides and pyrazine, except for our two recent papers on the monomers cis- and trans-Pt(R<sub>2</sub>SO)(pz)Cl<sub>2</sub> (18) and the pyrazine-bridged dimers trans, trans-Pt(R<sub>2</sub>SO)Cl<sub>2</sub>(µ-pz)Pt(R<sub>2</sub>SO)Cl<sub>2</sub> (19). Only a few papers were found in the literature on mixed-ligands platinum compounds with non-substituted pyrazine ligands. Besides the compounds mentioned above, trans-Pt(phosphine)(pz)Cl<sub>2</sub> and trans, trans-Pt(phosphine)Cl<sub>2</sub>(μ-pz)Pt(phosphine)Cl<sub>2</sub>, were synthesized and characterized (20), while Hall et al. (22) have characterized by <sup>1</sup>H-NMR, IR UV spectroscopies dimer and the trans-trans, trans- $Pt(CO)Cl_2(\mu-pz)Pt(CO)Cl_2$ . The monomer trans- $Pt(C_2H_4)(pz)Cl_2$  and its derivatives were also synthesized and used as catalysts in hydrosylation reactions (23). The nature of the Pt(II)-pyrazine bond has not yet been investigated.

In this chapter, the synthesis and characterization of pyrazine-bridged dinuclear complexes containing two different sulfoxide ligands is described. All the compounds contain the cyclic tetramethylenesulfoxide ligand (TMSO). The second

Pt(II) atom is bonded to a different sulfoxide. Six sulfoxides with different steric hindrances were used: dimethylsulfoxide (DMSO), diethylsulfoxide (DEtSO), di-*n*-propylsulfoxide (DPrSO), di-*n*-butylsulfoxide (DBuSO), dibenzylsulfoxide (DBzSO) and diphenylsulfoxide (DPhSO). The (TMSO)Cl<sub>2</sub>Pt(μ-pz)Pt(R<sub>2</sub>SO)Cl<sub>2</sub> complexes were characterized in the solid state by IR and Raman spectroscopy and in solution by multinuclear-NMR (<sup>1</sup>H, <sup>13</sup>C and <sup>195</sup>Pt) spectroscopy.

### 3.2 Experimental

#### 3.2.1 Instrumentation and chemicals

The K<sub>2</sub>[PtCl<sub>4</sub>] starting material was obtained from Johnson Matthey Inc. and was purified by recrystallization in water before use. CDCl<sub>3</sub> was purchased from CDN Isotopes. Pyrazine and most of the sulfoxide ligands were obtained from Aldrich Chemical Co. Dimethylsulfoxide was bought from Anachemia Chemicals Ltd, diethylsulfoxide from Narchem Corp. and di-*n*-propylsulfoxide from Phillips Petroleum Co. The latter was purified by distillation before use.

The decomposition points were measured on a Fisher-Johns instrument and were not corrected. The IR spectra were recorded in the solid state (KBr pellets) on a Nicolet 4700 FTIR spectrometer between 4000 and 280 cm<sup>-1</sup>. The Raman spectra were measured between 4000 and about 200 cm<sup>-1</sup> on a Renishaw inVia spectrometer equipped with a microscope. Two laser excitation wavelengths were used: 514.5 nm (green) and 785 nm (near-IR) operating at 10-50% power level. Five spectral accumulations were made for each sample. All the NMR spectra were measured in CDCl<sub>3</sub> on a Varian Gemini 300BB spectrometer operating at 300.021, 75.454 and

64.321 MHz for  $^{1}$ H,  $^{13}$ C and  $^{195}$ Pt nuclei, respectively. The chloroform peaks were used as an internal standard for the  $^{1}$ H (7.24 ppm) and  $^{13}$ C (77.00 ppm) NMR spectra. For  $^{195}$ Pt, the external reference was K[Pt(DMSO)Cl<sub>3</sub>] in D<sub>2</sub>O, adjusted to -2998 ppm from K<sub>2</sub>[PtCl<sub>6</sub>] ( $\delta$ (Pt) = 0 ppm). The  $^{195}$ Pt-NMR spectra were measured between approximately -2500 and -4000 ppm.

## 3.2.2 Synthesis of Pt(TMSO)Cl<sub>2</sub>(µ-pyrazine)Pt(R<sub>2</sub>SO)Cl<sub>2</sub>

The monosubstituted complexes, K[Pt(R<sub>2</sub>SO)Cl<sub>3</sub>], were synthesized using slight modifications of the method published by Kukushkin *et al.* (24) and as recently described in the literature (25). The DBuSO, DBzSO and DPhSO complexes were obtained in low yields owing to the aqueous insolubility of the ligands and the very favorable formation of the insoluble disubstituted compound Pt(R<sub>2</sub>SO)<sub>2</sub>Cl<sub>2</sub>. For these ligands, the reactions were performed in a mixture of watermethanol or water-ethanol. *trans*-Pt(TMSO)(pz)Cl was synthesized as described in an earlier publication from our group (18).

The K[Pt(R<sub>2</sub>SO)Cl<sub>3</sub>] compound was dissolved in a minimum amount of a 1:1 chloroform-acetone mixture. A few drops of methanol were added for the DBuSO and DBzSO compounds and ethanol for the DPhSO complex. *trans*-Pt(TMSO)(pz)Cl<sub>2</sub> was also dissolved in the same chloroform-acetone mixture and added slowly to the previous K[Pt(R<sub>2</sub>SO)Cl<sub>3</sub>] solution at room temperature in a 1.0:1.1 proportion, i.e., a slight excess of the ionic salt was used. The mixture was stirred for 3 to 48 h depending on the ligand. The reactions were slower with the more hindered ligands. The solvent was evaporated to dryness at room temperature and a few mL of water were added to the resulting solid. After filtration, the

precipitate was washed with water, dried, washed with diethylether and finally dried in vacuum. The product was obtained as a yellow powder.

Pt(TMSO)Cl<sub>2</sub>(μ-pz)Pt(DMSO)Cl<sub>2</sub>: Yield 91%, dec. 192-212°C. IR (cm<sup>-1</sup>): pz [vibration number (26)] 3116m [v<sub>13</sub>(B<sub>1u</sub>)], 1419s [v<sub>19a</sub>(B<sub>1u</sub>)], 1400m [v<sub>19b</sub>(B<sub>3u</sub>)], 1107s [v<sub>3</sub>(B<sub>2g</sub>)], 1024w [v<sub>1</sub>(A<sub>g</sub>)], 808s [v<sub>11</sub>(B<sub>2u</sub>)]; ν(S-O) 1150s, ν(Pt-S) 442s, ν(Pt-Cl) 349s, other bands 1319w, 693m, 516m, 381m, 310m, 265w. <sup>1</sup>H NMR (ppm): H<sub>pz</sub> 9.091m, H<sub>αTMSO</sub> 4.05m 3.70m, H<sub>βTMSO</sub> 2.39m 2.21m, H<sub>αDMSO</sub> 3.52s 3.50s. <sup>13</sup>C NMR (ppm): C<sub>pz</sub> 148.26, C<sub>αDMSO</sub> 44.74, C<sub>αTMSO</sub> 57.37, C<sub>βTMSO</sub> 24.65.

Pt(TMSO)Cl<sub>2</sub>(μ-pz)Pt(DEtSO)Cl<sub>2</sub> : Yield 93%, dec. 153-181°C. IR (cm<sup>-1</sup>): pz: 3117m [v<sub>13</sub>(B<sub>1u</sub>)], 1420s [v<sub>19a</sub>(B<sub>1u</sub>)], 1402w [v<sub>19b</sub>(B<sub>3u</sub>)], 1109w [v<sub>3</sub>(B<sub>2g</sub>)], 805m [v<sub>11</sub>(B<sub>2u</sub>)]; v(S-O) 1136m, v(Pt-S) 419w, v(Pt-Cl) 351s, other bands 2923m, 2360m, 2339m, 1457w, 962w, 668m, 592w, 508w, 344w. <sup>1</sup>H NMR (ppm): H<sub>pz</sub> 9.106m, H<sub>αTMSO</sub> 4.02m 3.67m, H<sub>βTMSO</sub> 2.40m 2.21m, H<sub>αDEtSO</sub> 3.69m 3.36m, H<sub>βDEtSO</sub> 1.60m. <sup>13</sup>C NMR (ppm): C<sub>pz</sub> 148.26 148.18, C<sub>αTMSO</sub> 57.35, C<sub>βTMSO</sub> 24.63, C<sub>αDEtSO</sub> 49.46, 49.27, C<sub>βDEtSO</sub> 7.25.

Pt(TMSO)Cl<sub>2</sub>(μ-pz)Pt(DPrSO)Cl<sub>2</sub> : Yield 96%, dec. 149-186°C. IR (cm<sup>-1</sup>): pz: 3117m [v<sub>13</sub>B<sub>1u</sub>)], 1421s [v<sub>19a</sub>(B<sub>1u</sub>)], 1401m [v<sub>19b</sub>(B<sub>3u</sub>)], 1168m [v<sub>18a</sub>(B<sub>1u</sub>)], 1109m [v<sub>3</sub>(B<sub>2g</sub>)], 1076s [v<sub>14</sub>(B<sub>3u</sub>)], 1027w [v<sub>1</sub>(A<sub>g</sub>)], 810m [v<sub>11</sub>(B<sub>2u</sub>)]; v(S-O) 1146s, v(Pt-S) 447w, v(Pt-Cl) 352s, other band 510m.  $^{1}$ H NMR (ppm): H<sub>pz</sub> 9.097m, H<sub>αTMSO</sub> 4.02q (J=6.9 Hz) 3.65m, H<sub>βTMSO</sub> 2.40m 2.21m, H<sub>αDPrSO</sub> 3.65m 3.24m, H<sub>βDPrSO</sub> 2.21m, H<sub>γDPrSO</sub> 1.20t (J=7.3 Hz).  $^{13}$ C NMR (ppm): C<sub>pzTMSO</sub> 148.31, 148.21, C<sub>αTMSO</sub> 57.32, C<sub>βTMSO</sub> 24.64, C<sub>αDPrSO</sub> 56.97, C<sub>βDPrSO</sub> 16.66, C<sub>γDPrSO</sub> 12.87.

Pt(TMSO)Cl<sub>2</sub>(μ-pz)Pt(DBuSO)Cl<sub>2</sub>: Yield 94%, dec. 183-216°C. IR (cm<sup>-1</sup>): pz: 3115m [v<sub>13</sub>(B<sub>1u</sub>)], 1420s [v<sub>19a</sub>(B<sub>1u</sub>)], 1404s [v<sub>19b</sub>(B<sub>3u</sub>)], 1166 m [v<sub>18a</sub>(B<sub>1u</sub>)], 1110s [v<sub>3</sub>(B<sub>2g</sub>)], 1078s [v<sub>14</sub>(B<sub>3u</sub>)], 819m [v<sub>11</sub>(B<sub>2u</sub>)]; v(S-O) 1143s, v(Pt-S) 457w, v(Pt-Cl) 355s, other bands 2957m, 1465w, 923w, 875w, 661m, 563m, 513m. <sup>1</sup>H NMR (ppm): H<sub>pz</sub> 9.107m, H<sub>αTMSO</sub> 4.03m 3.67m, H<sub>βTMSO</sub> 2.40m 2.21m, H<sub>αDBuSO</sub> 3.67m 3.26m, H<sub>βDBuSO</sub> 2.18m 2.08m, H<sub>γDBuSO</sub> 1.60m, H<sub>δDBuSO</sub> 1.02t (J=7.2Hz). <sup>13</sup>C NMR (ppm): C<sub>pz</sub> 148.21 148.10, C<sub>αTMSO</sub> 57.32, C<sub>βTMSO</sub> 24.68, C<sub>αDBuSO</sub> 55.12, C<sub>βDBuSO</sub> 24.62, C<sub>γDBuSO</sub> 21.55, C<sub>δDBuSO</sub> 13.66.

Pt(TMSO)Cl<sub>2</sub>(μ-pz)Pt(DBzSO)Cl<sub>2</sub>: Yield 88%, dec. 165-189°C. IR (cm<sup>-1</sup>): pz: 3089w [v<sub>13</sub>(B<sub>1u</sub>)], 1424s [v<sub>19a</sub>(B<sub>1u</sub>)], 1406s [v<sub>19b</sub>(B<sub>3u</sub>)], 1168s [v<sub>18a</sub>(B<sub>1u</sub>)], 1116m [v<sub>3</sub>(B<sub>2g</sub>)], 1075m [v<sub>14</sub>(B<sub>3u</sub>)], 1030w [v<sub>1</sub>(A<sub>g</sub>)], 808m [v<sub>11</sub> (B<sub>2u</sub>)], ν(S-O) 1143s, ν(Pt-S) 416m, ν(Pt-Cl) 352s, other bands 1601w, 1495m, 1188m, 1075m, 922w, 697s, 583m, 563m, 515w, 482s.  $^{1}$ H NMR (ppm): H<sub>pz</sub> 9.104m, H<sub>αTMSO</sub> 4.05m 3.65m, H<sub>βTMSO</sub> 2.39m 2.21m, H<sub>αDBzSO</sub> 5.062m 4.576m, H<sub>orthoDBzSO</sub> 7.652m, H<sub>meta-paraDBzSO</sub> 7.447m.  $^{13}$ C NMR (ppm): C<sub>pz</sub> 148.26, C<sub>αTMSO</sub> 59.68, C<sub>βTMSO</sub> 25.01, C<sub>αDBzSO</sub> 59.68, aromatic C<sub>DBzSO</sub> 129.09, 129.40, 131.72, 132.24.

Pt(TMSO)Cl<sub>2</sub>(μ-pz)Pt(DPhSO)Cl<sub>2</sub>): Yield 94%; dec. 152-185°C; IR (cm<sup>-1</sup>): pz: 3115w [v<sub>13</sub>(B<sub>1u</sub>)], 1422s [v<sub>19a</sub>(B<sub>1u</sub>)], 1169m [v<sub>18a</sub>(B<sub>1u</sub>)], 1114m [v<sub>3</sub>(B<sub>2g</sub>)], 1075m [v<sub>14</sub>(B<sub>3u</sub>)], 1035w [v<sub>1</sub>(A<sub>g</sub>)], 807m [v<sub>11</sub>(B<sub>2u</sub>)], v(S-O) 1148s, v(Pt-S) 446w, v(Pt-Cl) 350s, other bands 3052w, 1444m, 1331w, 697m, 565s, 530m, 509m. <sup>1</sup>H NMR (ppm): H<sub>pzTMSO</sub> 9.106m, H<sub>pzDPhSO</sub> 9.137m, H<sub>αTMSO</sub> 4.03m 3.65m, H<sub>βTMSO</sub> 2.40m 2.21m, H<sub>orthoDPhSO</sub> 7.924dt (J = 7.8, 1.8 Hz), H<sub>meta-paraDPhSO</sub> 7.557m. <sup>13</sup>C NMR (ppm):

 $C_{pzTMSO}$  148.26,  $C_{pzDPhSO}$  148.53,  $C_{\alpha TMSO}$  57.35,  $C_{\beta TMSO}$  24.64,  $C_{DPhSO}$  140.67, 131.05, 127.42, 128.86, 133.18.

Pt(DEtSO)Cl<sub>2</sub>( $\mu$ -pz)Pt(DEtSO)Cl<sub>2</sub>: Yield 69%, dec. 180-190°C. IR (cm<sup>-1</sup>): pz: 3117m [ $\nu_{13}(B_{1u})$ ], 1420s [ $\nu_{19a}(B_{1u})$ ], 1402w [ $\nu_{19b}(B_{3u})$ ], 1109w [ $\nu_{3}(B_{2g})$ ], 805m [11( $B_{2u}$ )];  $\nu$ (S-O) 1136m,  $\nu$ (Pt-S) 419w,  $\nu$ (Pt-Cl) 351s, other band 508w. <sup>1</sup>H NMR (ppm):  $H_{pz}$  9.106s (<sup>195</sup>Pt-<sup>1</sup>H) = 29 Hz,  $H_{\alpha}$  4.51m 3.73m,  $H_{\beta}$  1.62m. <sup>13</sup>C NMR (ppm):  $C_{pz}$  148.18,  $C_{\alpha}$  49.31,  $C_{\beta}$  7.24.

#### 3.3 Results and discussion

## 3.3.1 Synthesis of the complexes

The reactions of  $K[Pt(R_2SO)Cl_3]$  with  $trans-Pt(TMSO)(pz)Cl_2$  (1.1:1.0 proportion) in a 1:1 chloroform-acetone mixture (a few drops of methanol were added for the DBuSO and DBzSO compounds and ethanol for the DPhSO complex) produced the pyrazine-bridged dimers,  $(TMSO)Cl_2Pt(\mu-pz)Pt(R_2SO)Cl_2$ . Compounds with  $R_2SO = DMSO$ , DEtSO, DPrSO, DBuSO, DBzSO and DPhSO were prepared. The  $Pt(TMSO)(pz)Cl_2$  solution must be added to the  $K[Pt(R_2SO)Cl_3]$  solution slowly in order to constantly have an excess of  $K[Pt(R_2SO)Cl_3]$ , which can easily be separated from the dimers since it is very soluble in water.

$$\begin{split} K[Pt(R_2SO)Cl_3] &+ \textit{trans-}Pt(TMSO)(pz)Cl_2 & \longrightarrow \\ & (TMSO)Cl_2Pt(\mu\text{-}pz)Pt(R_2SO)Cl_2 &+ KCl \end{split}$$

The mixed-sulfoxide dimers were obtained as yellow precipitates. The time of reaction varied with the bulkiness of the sulfoxide, from 3 h for DMSO to about 48 h for the more hindered sulfoxides (DBuSO, DBzSO and DPhSO). The yields

varied between 88% and 96%. These dinuclear species are very insoluble and this proved to be a major problem in the solution NMR characterization of the products. Very long accumulation times were required, especially for the <sup>195</sup>Pt- and <sup>13</sup>C-NMR spectra. The most insoluble is the DBzSO compound and its <sup>13</sup>C- and <sup>195</sup>Pt-NMR spectra contained significant background noise.

The reaction was first tested with the starting materials K[Pt(TMSO)Cl<sub>3</sub>] and trans-Pt(TMSO)(pz)Cl<sub>2</sub> and the expected compound, (TMSO)Cl<sub>2</sub>Pt(μ-pz)Pt(TMSO)Cl<sub>2</sub>, was obtained. The IR and NMR spectra of the product were identical to the *trans-trans* dimer, the crystal structure of which was reported earlier by our group (19). This result helped us in the interpretation of the IR and NMR spectra of the TMSO-R<sub>2</sub>SO mixed dimers, especially regarding their geometry.

Since the *trans* effect of sulfoxide ligands is much greater than that of chloride, *trans* isomers are expected to be formed first. Isomerization to the *cis* complexes was expected, especially for the less bulky sulfoxides as observed in the formation of *cis*-Pt(R<sub>2</sub>SO)<sub>2</sub>Cl<sub>2</sub> (14,27) For ligands capable of forming strong π-bonds with Pt(II), the *trans* complexes usually isomerize rapidly to the thermodynamically more stable *cis* compounds, unless the ligands are very sterically hindered. Nevertheless, isomerization was not detected in this work, as was observed for the symmetric sulfoxide dimers *trans-trans*-Pt(R<sub>2</sub>SO)Cl<sub>2</sub>(μ-pz)Pt(R<sub>2</sub>SO)Cl<sub>2</sub> (19). The characterization of the compounds has suggested that all the synthesized producs have the *trans-trans* geometry. Numerous attempts to obtain the *cis* complexes in different organic solvents were all unsuccessful. The pyrazine-bridged compounds seem to exhibit different reactivities compared to the pyrimidine-bridged

dimmers,  $Pt(R_2SO)Cl_2(\mu-pm)Pt(R_2SO)Cl_2$  (17), where isomerization of the *trans* compounds to the *cis* isomers was reported.

All the dinuclear pyrazine species were characterized in the solid state by IR and Raman spectroscopy and in CDCl<sub>3</sub> solution by multinuclear magnetic resonance (<sup>1</sup>H, <sup>195</sup>Pt and <sup>13</sup>C) spectroscopy.

## 3.3.2 IR and Raman Spectroscopy

The IR vibrational spectra of the mixed-sulfoxides complexes were measured in the solid state between 4000 and about 280 cm<sup>-1</sup>. Our assignments for the pyrazine ligand (experimental section) are based on those reported for the IR spectrum of pyrazine (26). A recent study of the IR vibrational spectrum of pyrazine in solid argon ( $10^{\circ}$ K) has also been published (28). Pyrazine exhibits a  $D_{2h}$  point group symmetry for which 24 vibrations are expected, 10 of which are IR active. The symmetry of the pyrazine-bridged ligand in the symmetric *trans-trans* dimers is not changed, but in the TMSO-R<sub>2</sub>SO dimers the symmetry is theoretically lowered, since the sulfoxides are different. Nevertheless, the results on these unsymmetrical dimers are almost identical to those observed for the symmetric dimers  $Pt(R_2SO)Cl_2(\mu-pz)Pt(R_2SO)Cl_2$  (19). All the pyrazine vibrations in the complexes are observed at identical or at slightly higher energies than those of free pyrazine.

As expected, the  $\nu$ (S-O) vibrations absorb at higher energy (between 1136 and 1150 cm<sup>-1</sup>) than in the free sulfoxides, since the ligands are bonded to Pt by the S atom and as reported in the literature (14,16-20,25,27,29). The sulfoxide S-O p $\pi$ -d $\pi$  bond is stronger when coordinated to the metal atom through the S atom than in the free sulfoxide or when there is a Pt-O coordination bond.

The IR spectra of the dinuclear species showed only one  $\nu(Pt-Cl)$  vibration mode between 349 and 355 cm<sup>-1</sup>, suggesting a trans-trans geometry. Two stretching bands are usually observed for cis-dichloro Pt(II) complexes. The v(Pt-S) and v(Pt-N) bands are difficult to assign, since they usually have low intensity and the v(Pt-N) vibrations often couple with other vibrations of the molecule. One absorption band observed between 415 and 460 cm<sup>-1</sup> was assigned to a v(Pt-S) vibration based on data in the literature (14,30-33). The  $\nu(Pt-N)$  vibrations have been assigned in different regions in the literature. For most Pt(II)-NH<sub>3</sub> and Pt-amine complexes, the absorption bands were reported in the ~500 cm<sup>-1</sup> region (34.35). Two studies on Pt(II)-pyrazine and Pt(II)-pyrazine-d<sub>4</sub> compounds have been published and surprisingly the v(Pt-N) vibrations were assigned at much lower energies. In cis- and trans-Pt(pz)<sub>2</sub>X<sub>2</sub>, the single v(Pt-N) vibration mode was assigned between 275 and 300 cm<sup>-1</sup> for the trans compounds and two bands were observed between 222 and 255 cm<sup>-1</sup> for the *cis* isomers (20). For the pyrazine-bridged *trans-trans*-Pt(CO)X<sub>2</sub>(μpz)PtX<sub>2</sub>(CO) dimers, the v(Pt-N) vibration was assigned at 186 cm<sup>-1</sup> for the Cl<sup>-</sup> compound and at 174 cm<sup>-1</sup> for the Br<sup>-</sup> analogue (22). In trans-Pt(C<sub>2</sub>H<sub>4</sub>)(py)Cl<sub>2</sub>, the  $\nu(Pt-N)$  vibration was also reported in this region (239 cm<sup>-1</sup>) (36). These energies seem very low for stretching  $\nu(Pt-N)$  vibrations, especially if the nature of the bond is slightly multiple. These vibrations are probably coupled with others and thus they might appear in an unexpected region. It is also possible that these reported vibrations (20,22,36) are not stretching modes, but are deformation modes. The IR spectrum of the cation [Pt(bpy)<sub>2</sub>]<sup>2+</sup> exhibits three bands at 235, 295 and 375 cm<sup>-1</sup>, which were assigned to  $\nu(Pt-N)$  and  $\nu(Pt-N)$  vibration modes (37). Our IR instrument has a lower limit of about 280 cm<sup>-1</sup>, therefore lower energy absorptions could not be detected. One band was observed in the 482-516 cm<sup>-1</sup> region, which could be assigned tentatively to the  $\nu(Pt-N)$  vibration.. In our previous publications on *cis*-and *trans*-Pt(pz)(R<sub>2</sub>SO)Cl<sub>2</sub> (18) and *trans*,*trans*-Pt(R<sub>2</sub>SO)Cl<sub>2</sub>( $\mu$ -pz)PtCl<sub>2</sub>(R<sub>2</sub>SO) (19), the  $\nu(Pt-N)$  vibration modes were also tentatively assigned around 500 cm<sup>-1</sup>.

The Raman spectra of the Pt(II) complexes were recorded in the solid state between 4000 and ~200 cm<sup>-1</sup>. A near-IR laser (785 nm) was used to excite the spectra, and the power used was 10 or 50%. The Raman spectrum of pyrazine has been published (38,39). Since the Raman spectra of the symmetric dinuclear species Pt(R<sub>2</sub>SO)Cl<sub>2</sub>(μ-pz)Pt(R<sub>2</sub>SO)Cl<sub>2</sub> have not been reported, they were recorded and the results are shown in Table 3.1 (the first five Pt complexes), while the Raman bands of the six new non-symmetric dinuclear species are shown in the following columns. The Raman spectra or both types of dimers are very similar and they will be discussed together.

This is the first Raman study on Pt(II) compounds containing Pt-pyrazine bonds and the second report on Pt-R<sub>2</sub>SO complexes. A study on K[Pt(R<sub>2</sub>SO)Cl<sub>3</sub>] and Pt(R<sub>2</sub>SO)<sub>2</sub>Cl<sub>2</sub> was published (29). Pyrazine has 24 vibrations of which 12 are active in Raman (2 are inactive in IR and Raman). We have remeasured the Raman spectrum of free pyrazine. The data on free pyrazine (our data) are also shown in Table 3.1. All the vibration modes of free pyrazine have been assigned (26,38,39). The well-accepted convention of Lord *et al.* (39) has been used in numbering the vibration modes with the z-axis through the two nitrogen atoms. The assignments of

the vibrations in the Pt(II) complexes are only tentative based on the spectrum of free pyrazine.

In the symmetrical dimers, the symmetry of pyrazine is the same as in the free molecule. In the unsymmetrical dimers, the symmetry of pyrazine is lowered, but the difference in environment is not large. Therefore, only very minor changes are expected between the symmetric and the non-symmetric compounds. Most of the bands of the Pt(II) complexes are very weak in intensity, partly because of the low laser power that had to be used, since the compounds decomposed in the laser radiation (785 nm). The green laser (514.5 nm) was tried, but the decomposition was much faster. ( $2v_{6a}$ ) on our instrument, probably because of the low intensity of the laser radiation, but we found a band in this region for several complexes. We have also observed the two missing bands

For the free ligand, we have observed 9 of the 10 bands reported by Tam and Cooney (38). We have not observed the very weak band at  $1226 \text{ cm}^{-1}$  ( $2v_{6a}$ ) on our instrument, probably because of the low intensity of the laser radiation, but we found a band in this region for several complexes. We have also observed the two missing bands from the work of Tam and Conney at 1358 and 596 cm<sup>-1</sup>. The former band was assigned to the  $v_{14}$  mode, as suggested by Foglizzo and Novak in a Raman study of the chloro and bromo pyrazinium salt (40). In our complexes, this vibration was found at about  $1405 \text{ cm}^{-1}$ . The band at  $596 \text{ cm}^{-1}$  in the free ligand has been assigned to the  $v_{6a(\text{ring})} - Ag$  mode, based on the work of Simmons *et al.* (26) who reported this vibration at  $598 \text{ cm}^{-1}$ . This vibration is shifted to slightly higher energy ( $\sim 60 \text{ cm}^{-1}$ ) in the Pt(II) complexes.

A relatively intense band was observed in all the complexes around 1050 cm<sup>-1</sup>, which seems consistent with the ring breathing mode ( $v_{1(ring)}$ ) observed at 1013 cm<sup>-1</sup> in free pyrazine. A strong band at around 694 cm<sup>-1</sup> in the dimers similarly seems consistent with an assignment to the  $v_{4(ring)}$  (B3g) vibration, observed at 699 cm<sup>-1</sup> in the free molecule (at 700 cm<sup>-1</sup> in (38)).

The v(S-O) bands were observed in the Raman spectra between 1125 and 1150 cm<sup>-1</sup>. in agreement with the IR spectra and in the region expected for Pt(II)-Sbonded sulfoxides. The vibrations involving the Pt(II) atom are usually observed in the region below 550 cm<sup>-1</sup>. The v(Pt-Cl) modes are easily identified, since they are strong vibrations in both the IR and Raman spectra and were observed in the Raman as a single band between 329 and 338 cm<sup>-1</sup>, i.e., at slightly lower energies than are those observed by IR spectroscopy (around 350 cm<sup>-1</sup>). The symmetric stretching vibration is probably observed in Raman, while the nonsymmetric stretching mode would be seen in IR only. For comparison, the v(Pt-Cl) vibration mode in trans-Pt(C<sub>2</sub>H<sub>4</sub>)(py)Cl<sub>2</sub> was observed in IR at 345 cm<sup>-1</sup> and at 335 cm<sup>-1</sup> in Raman (36). The observed IR and Raman vibrations for the symmetrical and unsymmetrical Pt(II) dimers are compared in Table 3.2. These bands are quite intense and fairly broad because of the different Cl isotopes. Therefore, it is not possible to observe the two different bands expected in the unsymmetrical dimers. Since there is only one stretching band for each compound, the complexes are assumed to have the transtrans configuration.

The other stretching vibration modes involving the Pt(II) atom are more difficult to assign, since they are weak bands and the IR data on v(Pt-N) modes are

not always in agreement. Based on a few IR (14,30-33) and Raman (29) studies in the literature, we have made the assignment of the v(Pt-S) bands between 416 and 478 cm<sup>-1</sup>, as listed in Table 3.2.

As discussed above in the IR section, the v(Pt-N) modes often couple with other vibrations, which makes their assignment even more difficult. In the literature, the Raman-active v(Pt-N) modes have been assigned in several regions. In trans-Pt(C<sub>2</sub>H<sub>4</sub>)(pv)Cl<sub>2</sub>, the v(Pt-N) mode was assigned at 239 cm<sup>-1</sup> in IR and at 227 cm<sup>-1</sup> in the Raman (36). For the cation [Pt(bpy)<sub>2</sub>]<sup>2+</sup>, the three bands observed between 230 and 378 cm<sup>-1</sup> in IR were assigned to deformation modes of the Pt-N bond. In the Raman, one band at 255 cm<sup>-1</sup> was assigned to the v(Pt-N) vibration and another band at 656 cm<sup>-1</sup> was also attributed to the same stretching mode (37). These data are listed in a table without comments and there might be some errors in the assignments. The data also seem contrary to the IR results published for the same compounds in the same paper, where bands between 230 and 378 cm<sup>-1</sup> were assigned to deformation modes of the Pt-N bonds. The same authors assign a Raman band at 262 cm<sup>-1</sup> to a  $\nu(Pt-N)$  vibration in the cation  $[Pt(NH_3)_4]^{2+}$  (37). Most  $\nu(Pt-N)$ IR data in the literature on Pt(II)-NH<sub>3</sub> complexes were reported in the 500 cm<sup>-1</sup> region (34,35). In our study, one vibration, which was observed between 507 and 533 cm<sup>-1</sup> could be tentatively assigned to a v(Pt-N) vibration mode in the spectra of the dinuclear species. This assignment seems more popular in the Pt(II)-amine chemistry field. Our Raman spectrometer was limited to about 200 cm<sup>-1</sup>. The two Raman bands observed around 370 and 215 cm<sup>-1</sup> can be respectively assigned to  $\delta$ (C-S-O) and  $\pi$ (Pt-N) vibrations, based on the literature (37,41,42).

## 3.3.3 <sup>195</sup>Pt-NMR Spectroscopy

Most pyrazine-bridged unsymmetrical dinuclear species are not very soluble, except the diethylsulfoxide compound, which is slightly more soluble than the others. The <sup>195</sup>Pt-NMR spectra of the complexes were measured in CDCl<sub>3</sub> and the chemical shifts are shown in Table 3.3. Two <sup>195</sup>Pt resonances of equal intensities were observed for all the products. For comparison, the <sup>195</sup>Pt resonances of the symmetrical compounds are also shown in Table 3.3.

A <sup>195</sup>Pt signal found around -3042 ppm was assigned to the TMSO moiety (Pt<sub>1</sub> in scheme 1). In the TMSO symmetric dimer, the resonance was detected at -3041 ppm in the same solvent (CDCl<sub>3</sub>). The second signal ( $\delta$ Pt<sub>2</sub>) was observed between -3048 and -3077 ppm, except for the DPhSO compound where it appeared at higher field (-3112 ppm). The results have shown that the  $\delta$ (Pt) of the second moiety (Pt<sub>2</sub>) is identical to the values of the corresponding symmetric dimer (Table 3.3). Therefore, the chemical shift of a Pt atom is influenced only by its four bonded ligands and not by the second sulfoxide bonded to the neighbouring Pt atom. This might suggest that the compounds have the *trans-trans* configuration (as shown in Scheme 1). In this geometry, the two sulfoxide ligands are farther from each other than in a *cis-cis* or *cis-trans* geometry.

The Pt-NMR spectrum of the symmetric dibenzylsulfoxide complex could not be measured since the compound is too insoluble for solution studies. But the unsymmetrical dimer is slightly more soluble and the  $\delta Pt_2$ ) signal was observed at -3059 ppm. Based on these results, we can predict that the resonance of the symmetric dimer should also be observed at around -3059 ppm.

The  $\delta(Pt_2)$  signal of the DPhSO complex, which contains two aromatic groups attached to the binding S atom, was observed at higher field than for the other compounds, as observed for the symmetric dimer (19), K[Pt(R<sub>2</sub>SO)Cl<sub>3</sub>] (25,43,44), trans-Pt(R<sub>2</sub>SO)(pz)Cl<sub>2</sub> (18), Pt(R<sub>2</sub>SO)(pm)Cl<sub>2</sub> (16) and the pyrimidinebridged dimers  $\{Pt(R_2SO)Cl_2\}_{2}(\mu-pm)$  (17). In all of these compounds, the chemical shifts for the DPhSO complexes were observed at higher fields than those for the others. The DPhSO ligand is the most sterically hindered, but it is also different from the other ligands, since it contains aromatic groups directly on the sulfur binding atom. These groups are probably responsible for the different electronic effects observed in this compound. The  $\delta(Pt)$  values show that the electronic density on the Pt atom is larger in the DPhSO complex compared to the other ligands. The shielded resonance is not caused by bulkiness on the bonding atom, since steric hindrance usually causes a deshielding effect. For the Pt-amine complexes, the  $\delta(Pt)$ resonances appeared at lower fields for amines containing bulky substituents on the binding atom (45,46). For  $K[Pt(R_2SO)Cl_3]$  (25) and  $Pt(R_2SO)_2Cl_2$  (25), the sulfoxide-pyrimidine complexes (16,17) and the sulfoxide-pyrazine compounds (18,19), we have suggested that the difference between the DPhSO complex and the others was due to inverse polarization of the  $\pi$ -electrons of the S=O bond. This phenomenon has been suggested in the literature to explain some <sup>13</sup>C-NMR results on Pt–C≡O (47) and Pt-carboxylato compounds (48). This effect would be present in all Pt-R<sub>2</sub>SO complexes, but would be more important for a ligand containing electron-attracting aromatic groups directly on the binding atom. This effect would increase the electron density on the Pt atom resulting in a higher field signal.

# 3.3.4 <sup>1</sup>H- and <sup>13</sup>C-NMR spectroscopy

The <sup>1</sup>H- and <sup>13</sup>C-NMR spectra of the complexes were measured in CDCl<sub>3</sub>. The chemical shifts are shown in the experimental section. The signals of the pyrazine ligand in the complexes will be discussed first. In its <sup>1</sup>H-NMR spectrum, free pyrazine has a single resonance at 8.585 ppm. In the symmetric dimers, pyrazine is also symmetric, contrary to monomeric species. Therefore, only one signal should be observed for the four H atoms. In the mixed-sulfoxides dimers, pyrazine is not symmetric but the difference is small. Theoretically the H<sub>2</sub> and H<sub>6</sub> protons should be different from the H<sub>3</sub> and H<sub>5</sub> protons, as shown in Scheme 3.3.4. The difference between the two signals should be very small, except if the sulfoxides are very different, as in the TMSO-DPhSO compound.

## **Scheme 3.3.4**

The region of the pyrazine protons is quite complex. Since  $H_2$  and  $H_6$  are only very slightly different from  $H_3$  and  $H_5$ , the signals will overlap. Furthermore, they will couple with each other to produce couplings of the types  ${}^3J(H_2-H_3)$  (around 3.2 Hz) and  ${}^5J(H_2-H_5)$  (around 1.1 Hz). In addition, each proton will couple with the  ${}^{195}Pt$  isotope. The probability of the dimer to contain two  ${}^{195}Pt$  atoms is quite low (11%), but the probability of the dimers containing one  ${}^{195}Pt$  atom is quite important

(44.5%). Since the two Pt atoms are not equivalent, the <sup>195</sup>Pt isotope can be located at position Pt<sub>1</sub> (22.3%) or on Pt<sub>2</sub> (22.3%). For each H atom on pyrazine, there will be couplings of the types <sup>3</sup>J(<sup>195</sup>Pt<sub>1</sub>-<sup>1</sup>H<sub>2,6</sub>), <sup>4</sup>J(<sup>195</sup>Pt<sub>1</sub>-<sup>1</sup>H<sub>3,5</sub>), <sup>3</sup>J(<sup>195</sup>Pt<sub>2</sub>-<sup>1</sup>H<sub>3,5</sub>) and <sup>4</sup>J(<sup>195</sup>Pt<sub>2</sub>-<sup>1</sup>H<sub>2,6</sub>). For all these reasons, the region is very complicated and the couplings could not be interpreted. The central signals are at approximately 9.10 ppm for most complexes (Table 3.4), while for the TMSO-DPhSO complex, there was another central signal at 9.13 ppm, where the resonance of the pyrazine protons was found in the symmetric DPhSO dimer (19).

Coordination of pyrazine to two platinum atoms causes a deshielding effect of the pyrazine protons of about 0.52 ppm for most of the complexes and 0.55 ppm for the DPhSO dimer. These results are in agreement with the <sup>195</sup>Pt-NMR data on the symmetric dimer, where the resonance of the DPhSO complex was found at higher fields than for the others. <sup>195</sup>Pt-NMR spectroscopy has shown a higher electron density on the Pt atom and a lower electron density on the pyrazine ligand (in <sup>1</sup>H NMR) for the DPhSO complex than with the other sulfoxide ligands. In the mixed-sulfoxide system, containing DPhSO, H<sub>3</sub> and H<sub>5</sub> were observed at slightly lower field than the others, which is in agreement with the <sup>195</sup>Pt-NMR results, where the DPhSO moiety (δPt<sub>2</sub>) was observed at higher field. When the electron density on the platinum atom increases, it should decrease on the ligand.

The <sup>1</sup>H chemical shifts of the pyrazine ligand are quite constant and do not vary much with the sulfoxide ligand (9.091-9.137 ppm). They can be compared with the values observed in the literature for the dinuclear symmetric complexes cis-[{Pt(NH<sub>3</sub>)<sub>2</sub>Cl}<sub>2</sub>( $\mu$ -pz)](NO<sub>3</sub>)<sub>2</sub> (9.04 ppm in D<sub>2</sub>O (1)), trans-{Pt(CO)Cl<sub>2</sub>}<sub>2</sub>( $\mu$ -pz)

(9.26 ppm in acetone) (22) and trans-{Pt(PEt<sub>3</sub>)Cl<sub>2</sub>}<sub>2</sub>( $\mu$ -pz) (9.19 ppm in CDCl<sub>3</sub>) (21). It seems that the second ligand and the geometry of the complexes have a small influence on the  $\delta(^1H)$  signal of the pyrazine bridging molecule, although the influence of the solvent should not be neglected.

Similar results were observed in <sup>13</sup>C-NMR spectroscopy. Free pyrazine has a solitary signal at 145.07 ppm in CDCl<sub>3</sub>. The  $\delta(^{13}\text{C})$  signals for bonded pyrazine in the complexes are shown in Table 3.4. The signals are deshielded upon coordination. For the TMSO, DEtSO, DPrSO and DBuSO symmetric dimers, the chemical shifts are almost constant ( $\delta = 148.2$  ppm). The DMSO compound was measured in DMF and cannot be compared with the others. Again, the signal for the DPhSO compound is slightly more deshielded ( $\delta = 148.41$  ppm) than for the others. The DBzSO symmetric dimer was synthesized, but its <sup>13</sup>C-NMR spectrum could not be measured because of its insolubility. For the mixed-sulfoxides dimers, only one signal was observed for all the pyrazine C atoms for the DMSO and the DBzSO compounds, probably because the two peaks are too close to be separated. Two resonances were observed for the other complexes. For most of these dimers, two very close signals are observed and it is difficult to assign the two resonances with certainly, although we have tried to make assignments, as shown in Table 3.4. The first value could correspond to  $\delta(C_2)$  and  $\delta(C_6)$  (between 148.21 and 148.31 ppm), since for the TMSO symmetric dimer it was observed at 148.25 ppm, while the second value could be assigned to  $\delta(C_3)$  and  $\delta(C_5)$ . For the TMSO-DPhSO compound, the assignment is more certain, since for the DPhSO ligand its chemical shift is observed at lower fields than the others. Therefore, the signal at 148.53 ppm was definitely assigned to  $C_3$  and  $C_5$ .

Coordination of pyrazine to two Pt atoms should considerably reduce the electronic density on the C atoms of pyrazine. The  $\Delta\delta$  values (3.0-3.46 ppm) are not as large as expected for N donors like amine ligands. The difference is caused by the presence of the sulfoxide ligands. As discussed previously, an inverse polarization effect on the S=O  $\pi$ -bond of the sulfoxide, would increase the electron density on the Pt atom and will also affect the electronic density on its *trans* pyrazine ligand.

The <sup>3</sup>J(<sup>195</sup>Pt-<sup>1</sup>H) coupling constants for the pyrazine protons were found to be between 28 and 35 Hz for the *trans,trans* symmetric complexes (19). For the mixed-sulfoxides compounds, they could not be observed due to the very low solubility of the dimers and especially because of the multiplicities of the signals as already discussed. For comparison, a value of 25 Hz was reported for the pyrazine-bridged dimeric compound, *trans*-{Pt(PMePh<sub>2</sub>)Cl<sub>2</sub>}<sub>2</sub>(μ-pz) (21). No couplings of the types <sup>2,3</sup>J(<sup>195</sup>Pt-<sup>13</sup>C) could be detected, owing to the very small solubility of the dimers which produced important background noise.

The  $^1H$  and  $^{13}C$  chemical shifts of the sulfoxide ligands in the mixed-dimers are shown in the experimental section and the  $\Delta\delta$  ( $\delta_{complex}$ - $\delta_{sulfoxide}$ ) values are listed in Tables 3.5 and 3.6. The  $^1H$  signals of the bonded ligands are observed at lower field than those of the free molecules. TMSO is a cyclic molecule and the protons on  $C_{\alpha}$  and  $C_{\beta}$  do not have the same environment. Therefore, the two geminal protons located on each C atom are not equivalent. Two different signals are observed for the protons located on  $C_{\alpha}$  and two for the protons on  $C_{\beta}$ . The protons closer in space to

the O atom are the most deshielded upon coordination. Two series of signals were also observed for most of the other bonded sulfoxides due to limited rotation around the S–C bonds. The separation between the signals of the geminal protons decreases as the distance from the coordination site increases, where the two chemical shifts become superimposable. Similar observations have already been reported for the pyrimidine-bridged dimeric complexes  $\{Pt(R_2SO)Cl_2\}_2(\mu-pm)$  (17) and the pyrazine symmetric dimers  $\{Pt(R_2SO)Cl_2\}_2(\mu-pz)$  (19). For the DMSO dimer, the two –CH<sub>3</sub> signals are quite close, because the rotation is less hindered in this small ligand.

The  $\delta(^1H)$  signals of the protons of the sulfoxide ligand close to the binding site are the most affected by its coordination to the Pt atom as expected, while the  $\Delta\delta$  values become negligible as the distance from the binding atom increases (Table 3.5). The  $^1H$  chemical shifts of the TMSO ligand are almost constant in all the compounds. For the other R<sub>2</sub>SO ligands (which do not contain an aromatic ring), the  $\Delta\delta$  average value for H<sub>\alpha</sub> seems to increase in the order DBuSO (0.73 ppm) < DPrSO (0.89 ppm)  $\approx$  DEtSO < DMSO (1.03 ppm)  $\approx$  TMSO (1.02 ppm). The angle C—S—C is the smallest ( $\sim$ 94°) in TMSO, which makes this ligand the least sterically hindered and its  $\Delta\delta$  H<sub>\alpha</sub> values are larger. The DPhSO (which is the most sterically demanding ligand) and the DBzSO compounds contain aromatic rings and these cannot be compared with the other complexes.

The signals of the C atoms (Table 3.6) in  $\alpha$  position to the S atom were observed at lower field than in the free molecule ( $\Delta\delta\approx3$  ppm), except for the DPhSO complex, which was observed at a very high field ( $\Delta\delta=-4.74$  ppm). The C atoms bonded to the S atom in the DPhSO dimer are highly shielded upon

coordination, indicating that the electron density has increased considerably upon coordination. Similar results were reported for the Pt(II) R<sub>2</sub>SO-pyrimidine complexes (16,17), the monomers and pyrazine-bridged symmetric dimers (18,19) and also for complexes of the types [Pt(R<sub>2</sub>SO)Cl<sub>3</sub>]<sup>-</sup> and Pt(R<sub>2</sub>SO)<sub>2</sub>Cl<sub>2</sub> (25). All the sulfoxides C atoms are less deshielded upon coordination than in other types of ligands (ex. amines). The presence of  $\pi$  bonding (Pt $\rightarrow$ S) increases the electronic density on the sulfoxide ligand. Furthermore, we have suggested in the past the presence of inverse polarization of the  $\pi(S=O)$  bond, which would explain the results observed in Pt-sulfoxide complexes (25) and carboxylato compounds (48). The coordination of the sulfoxide ligand to the Pt atom would reduce the  $\pi$ -electron density on the O atom ( $^{\delta+}O \rightarrow S^{\delta-}$ ) and increase it on the S atom and its neighbouring atoms, including the Pt atom. The inverse polarization effect of the  $\pi$  electrons in the S=O bond would be much more important in the DPhSO complex, since the two electron attracting phenyl groups are bonded directly on the S binding atom. The chemical shifts in <sup>13</sup>C-NMR spectroscopy are particularly sensitive to such mesomeric effects.

Satellites arising from the coupling of the sulfoxide protons with <sup>195</sup>Pt were not observed. The sulfoxide proton signals are usually multiplets of low intensity and consequently, the <sup>195</sup>Pt satellites are weak and overlap with the other signals. Furthermore, the low solubility of the complexes resulted in important background noise.

#### 3.4. Conclusions

The reaction of  $K[Pt(R_2SO)Cl_3]$  with trans-Pt(TMSO)(pz)Cl<sub>2</sub> in a 1.1:1.0 ratio gives the new dinuclear species Pt(TMSO)Cl<sub>2</sub>(µ-pz)Pt(R<sub>2</sub>SO)Cl<sub>2</sub>. The characterization of the compounds by IR and Raman spectroscopies seems to suggest a trans geometry for the six compounds studied in the solid state. The reaction of K[Pt(TMSO)Cl<sub>3</sub>] with trans-Pt(TMSO)(pz)Cl<sub>2</sub> has indeed produced  $trans, trans-Pt(TMSO)Cl_2(\mu-pz)Pt(TMSO)Cl_2$ , whose IR spectrum, **NMR** characterization and crystal structure were recently published by our group (19). The solution multinuclear magnetic resonance spectra of the new mixed-sulfoxides dimers were difficult to obtain because of the poor solubility of the complexes. No coupling constants  $J(^{195}Pt^{-1}H)$  or  $J(^{195}Pt^{-13}C)$  could be measured. The results seem to indicate that the geometry is identical to the one of the symmetric dimers reported earlier. The trans-trans configurations are therefore suggested for the new mixedligand dimers. Much time was devoted to attempts to recrystallize the compounds for crystallographic studies, but these complexes do not crystallize well.

The  $^{195}$ Pt-NMR spectra have shown two signals for the dimers. The resonance of the Pt-TMSO moiety was found at exactly the same field as in the TMSO symmetric dimer, while the signal of the R<sub>2</sub>SO-Pt moiety was observed at the same field as the symmetric R<sub>2</sub>SO dimers. The same observations were observed in the  $^{1}$ H- and  $^{13}$ C-NMR spectra.

Although we believe that the *cis* geometry should probably be thermodynamically more stable, the *trans-trans* dinuclear complexes did not isomerize in common organic solvents (even when heated), as did the pyrimidine-

bridged symmetric dimers (17). Our results seem to indicate potential  $\pi$ -backbonding from Pt to pyrazine, but to a much smaller extent than with sulfoxides and also probably less than with pyrimidine. The symmetries of the molecular orbitals of pyrazine and pyrimidine should be quite different. In fact, the symmetries of the pyrimidine ligand molecular orbitals might be more appropriate to accept  $\pi$ -electrons from Pt(II) than are those of pyrazine.

The inverse polarization of the sulfoxide  $\pi$ -bond  ${}^{\delta +}O \rightarrow S^{\delta -}$  was suggested as an explanation of some of the NMR results. This phenomenon would be more important in the DPhSO dinuclear compound, since it contains two electronattracting groups located directly on the binding atom. This situation would lead to an increase the electron density on the S atom and its neighbouring atoms. Attempts will be made in the future to study Pt(II) complexes containing other aromatic sulfoxides, such as *para*-substitued phenyl sulfoxides. The symmetric dibenzylsulfoxide complexed dimer is too insoluble for solution NMR studies, but the mixed-TMSO-DBzSO dimer is slightly soluble and its <sup>195</sup>Pt-NMR spectrum was recorded, suggesting a chemical shift of -3059 ppm for the symmetric dimer. Furthermore, the presence of a -CH<sub>2</sub> group between the S bonding atom and the phenyl group seems to have a large influence and our NMR results indicate that the benzyl group behaves more like an alkyl group.

### References

- (1) S. Komeda, G.V. Kalayda, M. Lutz, A.L. Spek, Y. Yamanaka, T. Sato, M. Chikuma, J. Reedijk, *J. Med. Chem.* **2003**, *46*, 1210.
- (2) N.J. Wheate, J.G. Collins, Coord. Chem. Rev. 2003, 241, 133.
- (3) S. Komeda, M. Lutz, A.L. Spek, M. Chikuma, J. Reedijk, *Inorg. Chem.* **2000**, *39*, 4230.
- (4) S. Komeda, M. Lutz, A.L. Spek, Y. Yamanaka, T. Sato, M. Chikuma, J. Reedijk, J. Am. Chem. Soc. 2002, 124, 4738.
- (5) N. Farrell, Met. Ions Bio. Syst. 2004, 42, 251.
- (6) P.M.G. Calvert, A.N. Hughes, E.R. Plummer, A.S.T. Azzabi, M.W. Verrill, M.G. Camboni, E. Verdi, A. Berareggi, M. Zuchetti, A.M. Robinson, J. Carmichael, A.H. Calvert, *Clinical Cancer Res.* 1999, 5, 3796.
- (7) Y. Qu, H. Rauter, A.P.S. Fontes, R. Bandarage, L.R. Kelland, N. Farrell, J. Med. Chem. 2000, 43, 3189.
- (8) A. Hegmans, Y. Qu, L.R. Kelland, J.D. Roberts, N. Farrell, *Inorg. Chem.* **2001**, 40, 6108.
- (9) G.V. Kalayda, S. Fakih, H. Bertram, T. Ludwig, H. Oberleithner, B. Krebs, J. Reedijk, *J. Inorg. Biochem.* **2006**, *100*, 1332.
- (10) M. Caluccia, A. Nassi, F. Loseto, A. Boccarelli, M.A. Mariggio, D. Giordano, F.D. Intini, P. Caputo, G. J. Natile. *Med. Chem.* 1993, 36, 510.
- (11) K. J. Barnham, M. I. Djuran, P.S. Murdoch, J.D. Ranford, P.J. Sadler, *Inorg. Chem.* 1996, 35, 1065.
- (12) N. Farrell, D.M. Kiley, W. Schmidt, M.P. Hacker, *Inorg. Chem.* **1990**, 29, 397.

- (13) M. van Beusichem, N. Farrell, *Inorg. Chem.* **1992**, *31*, 634.
- (14) J.H. Price, A.N. Williamson, R.F. Schram, B.B. Wayland, *Inorg. Chem.* 1972, 11, 1280.
- (15) L. I. Elding, A. Oskarsson, Inorg. Chim. Acta. 1987, 130, 209.
- (16) N. Nédélec, F.D. Rochon, *Inorg. Chim. Acta.* **2001**, *319*, 95.
- (17) N. Nédélec, F.D. Rochon, Inorg. Chem. 2001, 40, 5236.
- (18) F.D. Rochon, J.R.L. Priqueler, Can. J Chem. 2004, 82, 649.
- (19) J.R.L. Priqueler, F.D. Rochon. *Inorg. Chim. Acta.* **2004**, *357*, 2167.
- (20) G. A. Foulds, D.A. Thorton, *Spectrochim. Acta 37A.* **1981**, *10*, 917.
- (21) A. Albinati, F. Isaia, W. Kaufmann, C. Sorato, L.M. Venanzi, *Inorg. Chem.* **1989**, 28, 1112.
- (22) P.S. Hall, D.A. Thornton, G.A. Foulds, *Polyhedron*. **1987**, *6*, 85.
- (23) A.R. Siedle, K.R. Mann, D.A. Bohling, G. Filipovich, P.E. Toren, F.J. Palensky, R.A. Newmark, R.W. Duerst, W.L. Stebbings, H.E. Mishmash, K. Melancon, *Inorg. Chem.* **1985**, *24*, 2216.
- (24) Yu.N. Kukushkin, Yu.E. Vyaz'menskii, L.I. Zorina, Russ. J. Inorg. Chem. 1968, 13, 1573.
- (25) F.D. Rochon, C. Bensimon, C. Tessier, *Inorg. Chim. Acta*, **2008**, *361*, 16.
- (26) J.D. Simmons, K.K. Innes, G.M. Begun. J. Mol. Spectrosc. 1964, 14, 190.
- (27) F.D. Rochon, P-C. Kong, L. Girard, Can. J. Chem. 1986, 64, 1897.
- (28) S. Breda, I.D. Reva, L. Lapinski, M.J. Nowak, R. Fausto, J. Mol. Struct. 2006, 786, 193.

- (29) S. Gama de Almeida, J.L. Hubbard, N. Farrell, *Inorg. Chim. Acta.* **1992**, *193*, 149.
- (30) V.Yu. Kukushkin, V.K. Belsky, V.E. Konovalov, G.A. Kirakosyan, L.V. Konovalov, A.I. Moiseev, V.M. Tkachuk, *Inorg. Chim. Acta.* **1991**, *185*, 143.
- (31) Yu.N. Kukushkin, I.V. Pakhomova, Russ. J. Inorg. Chem. 1971, 16, 226.
- (32) Yu.N. Kukushkin, V.N. Spevak, Russ. J. Inorg. Chem. 1973, 18, 240.
- (33) B.F.G. Johnson, R.A. Walton, Spectrochim. Acta. 1966, 22, 1853.
- (34) K. Nakamoto, P.J. McCarthy, J. Fujita, R.A. Condrate, G.T. Behnke, *Inorg. Chem.* **1965**, *4*, 36.
- (35) Yu.N. Kukushkin, N.V. Ivannikova, K.A. Khokhryakov, *Russ. J. Inorg. Chem.* 1970, 15, 1595.
- (36) T.P.E. Auf der Heyde, G.A. Foulds, D.A. Thorthon, H.O. Desseyn, B.J. Van der Veken, *J. Mol. Struct.* **1983**, 98, 11.
- (37) P.D. Harvey, K.D. Truong, K.T. Aye, M. Drouin, A.D. Bandrauk, *Inor. Chem.* **1994**, *33*, 2347.
- (38) N.T. Tam, R.P. Cooney, J. Chem. Soc., Faraday Trans. 1976, 72, 2598.
- (39) R.C. Lord, A.L. Marston, F.A. Miller, Spectrochim. Acta. 1957, 9, 113.
- (40) R. Foglizzo, A. Novak, *Appl. Spectroscopy.* **1970**, *24*, 601.
- (41) M.T. Forel, M. Tranquille, *Spectrochim. Acta, Part A*, **1970**, *26*, 1023.
- (42) J.R. Durig, C.M. Player Jr, J.J. Bragin, Chem. Phys. 1970, 52, 4224.
- (43) F.D. Rochon, R. Boughzala, R. Melanson, Can. J. Chem. 1992, 70, 2476.
- (44) F.D. Rochon, S. Boutin, P.C. Kong, R. Melanson, *Inorg. Chim. Acta.* 1997, 264, 89.

- (45) P.S. Pregosin, Coord. Chem. Rev. 1982, 44, 247.
- (46) F.D. Rochon, M. Doyon, I.S. Butler, Inorg. Chem. 1993, 32, 2717.
- (47) D.G. Cooper, J Powell, *Inorg. Chem.* **1977**, *16*, 142.
- (48) F.D. Rochon, L. Gruia, Inorg. Chim. Acta. 2000, 306, 193.

 $\label{eq:table 3.1} \textbf{ Raman spectra of the symmetric dimers } Pt(R_2SO)Cl_2(\mu\text{-pz})Pt(R_2SO)Cl_2 \ (5 \ first \ compounds) \ and \ the \ mixed-ligands \\ dimers Pt(TMSO)Cl_2(\mu\text{-pz}) Pt(R_2SO)Cl_2 \ (assignments \ based \ on \ (38,39)).$ 

assignment	free pz	DMSO	DEtSO	DPrSO	DBuSO	DBzSO	DMSO	DEtSO	DPrSO	DBuSO	DBzSO	DPhSO
	3822m											
	3581w	3580w	3579w	3581w	3581w	3581w	3579w		3579w	3580w	3579w	3579w
$ u_2 A_g $	3048w				3108w	3059w					3061w	3068w
ν <sub>7b</sub> <i>B</i> <sub>2g</sub>	3032w	3005w	2984w	2945w	2971w	2969w	2926w	2935w	2942w	2935w	2935w	2940w
$2v_{19a(ring)} A_g$	2967w	2920w	2929w	2917w	2921w	2913w			2918w		2917w	
		2909w					2873w		2873w	2873w		2873w
	2303w	2344w	2350w	2350w	2339w							
								1794wbr	1781wbr	1798wbr	1785wbr	1793wbr
	1615w						1610w	1611s	1612s	1610m	1609m	1612s
$v_{8a(ring)} A_g$	1580m	1607m	1612m	1611s	1610s				1517w		1586w	1580m
V <sub>8b(ring)</sub> B <sub>2g</sub>	1520w	1515w	1514w	1522w	1516w	1514w	1453w	1444w	1445w	1441w		1445w
	1358w	1408w	1414w	1400w	1407w	1411w	1404w	1408w	1403w	1406w	1405w	1402w

$v_{9a( ext{Hbend})}A_g$	1248m			1248w	1306w	1265m	1318w		1299w	1307w	1266w	
$2v_{6a}-A_g$	1226	1217m	1225m	1226m	1217m	1225m		1222w	1224m	1223w	1226w	1225m
Su g				_		1207m					1208w	1178w
v(S-O)		1140w	1138w	1133w	1138w	1136w	1125v	1139w	1139w	1140w	1150w	1142w
			1075w	1082w	1109w		1097w		1084w	1080w		
$v_{1(\mathrm{ring})} A_g$	1013vs	1048s	1048vs	1053s	1048s	1043vs	1067w	1047s	1050s	1050m	1044m	1048s
		1028m	1026m	1032s	1037m	1002vs	1034w		1033m	1033w	1033w	1023m
	976w	985vw	969vw	897vw	899w	831w	985w	961w		957w	1003m	998s
$V_{10a({ m Hbend})}B_{Ig}$	754w	742w		758w	747w	778w 762w	881w	870w	867w	877w	876w	868w
		705w		706w			736w				779w	
$v_{4(\text{ring})} B_{3g}$	699s	694m	694m		692w	693m	694m	694m	694m	692m	693w	694m
			681w		671w	676w						
$ u_{6a(\mathrm{ring})} A_g $	596w		651w			617w	658w	680w	662w	661m	661w	662w
γ(ring)								560w		560w	555w	566w
ν(Pt-N)		521w	508w	522w	523w	525w	521w	507w	523w	520w		533w

			473w	456w		484w						
ν(Pt-S)		445w	428w		436w	417m	447w	426w		440w	418m	
δ(C-S-O)		384w	395w		364m	355w	376m			373w	356w	
ν(Pt-Cl)		335vs	335vs	337vs	336vs	333vs	329vs	332vs	335vs	338vs	335s	334vs
δ(N-Pt-S)		290w	282w	288m	271w	298w	302m		289w	303m		
		253m	255m	257m	253m	258m	277m		259w	248m	244w	261m
π(Pt-N)	202w	208w	241m	216m	221w	207m	231m	228w	218m	211w	210w	205m

**Table 3.2**  $\nu(Pt\text{-Cl})$  and  $\nu(Pt\text{-S})$  (cm<sup>-1</sup>) (1<sup>st</sup> line IR, 2<sup>nd</sup> line Raman and symmetric dimer in parentheses (19))

R <sub>2</sub> SO	ν(Ρ	t-Cl)	ν(Pt-	-S)
TMSO	(3	(347)		(3)
	(3	35)	(45	(4)
DMSO	349	(349)	442	(443)
	329	(335)	447	(445)
DEtSO	351	(351)	419	(419)
	332	(335)	426	(428)
DPrSO	352	(351)	447	(450)
	335	(337)		
DBuSO	355	(354)	457	(458)
	338	(336)	440	(436)
DBzSO	352	(349)	416	(478)
	335	(333)	418	(417)
DPhSO	350	(351)	446	(448)
	334			
	334			

$R_2SO$	$\delta(^{195}\text{Pt}_1)$	$\delta(^{195}\text{Pt}_2)$	δ( <sup>195</sup> Pt) symmetric
R <sub>2</sub> SO	0(11)	0(112)	dimer
TMSO			-3041 (19)
DMSO	-3043	-3061	-3049 <sup>a</sup> (19)
DEtSO	-3043	-3077	-3076
DPrSO	-3042	-3048	-3048 (19)
DBuSO	-3043	-3050	-3051 (19)
DBzSO	-3044	-3059	Not soluble
DPhSO	-3041	-3112	-3113 (19)

<sup>&</sup>lt;sup>a</sup> in DMF-d<sub>7</sub>

 $\begin{table}{llll} \textbf{Table 3.4} & $\delta(^1H)$ and $\delta(^{13}C)$ (ppm) of pyrazine in $Pt(TMSO)Cl_2(\mu-pz)Pt(R_2SO)Cl_2$ and in the symmetric dimer $Pt(R_2SO)Cl_2(\mu-pz)Pt(R_2SO)Cl_2$ (in $CDCl_3)$ \\ \end{table}$ 

R <sub>2</sub> SO	$\delta(^{1}\text{H})$	$\delta(^{1}\text{H})$ sym. dimer	$\delta(^{13}C)$	$\delta(^{13}C)$ sym. dimer
TMSO		9.105 (19)		148.25 (19)
DMSO	9.091	9.100 (19)	148.26	148.03 <sup>a</sup> (19)
DEtSO	9.106	9.106	148.26	148.18
			148.18	
DPrSO	9.097	9.098 (19)	148.31	148.20 (19)
			148.21	
DBuSO	9.107	9.104 (19)	148.21	148.21 (19)
			148.10	
DBzSO	9.104		148.26	
DPhSO	9.106	9.134 (19)	148.26	148.41 (19)
	9.137		148.53	

<sup>&</sup>lt;sup>a</sup> In DMF-d<sub>7</sub>

 $\begin{table}{llll} \textbf{Table 3.5} & ^1H & NMR & \Delta\delta & (\delta_{complex}\text{-}\delta_{sulfoxide}) & (ppm) & of the sulfoxide ligands in the \\ complexes & Pt(TMSO)Cl_2(\mu-pz)Pt(R_2SO)Cl_2 & (1^{st} line,TMSO, 2^{nd} line R_2SO) \\ \end{table}$ 

R <sub>2</sub> SO	$H_{\alpha}$	$\mathbf{H}_{eta}$	$\mathbf{H}_{\gamma}$	$H_{\delta}$	
TMSO (19)	1.20, 0.84	0.01, 0.25			
DMSO	1.22, 0.87	-0.01, 0.23			
	1.04, 1.02				
DEtSO	1.19, 0.84	0.00, 0.23			
	1.06, 0.73	0.34			
DPrSO	1.19, 0.82	0.00, 0.23			
	1.09, 0.68	0.47	0.19		
DBuSO	1.20, 0.84	0.00, 0.23			
	0.86, 0.59	0.43, 0.33	0.13	0.07	
DBzSO	1.22, 0.82	-0.01, 0.23			
	1.18, 0.70		0.38 (ortho)	0.11 ( <i>meta</i> )	0.11 (para)
DPhSO	1.20, 0.82	0.00, 0.23			
		0.29 (ortho)	0.12 (meta)	0.12 ( <i>para</i> )	

**Table 3.6**  $^{13}C$  NMR  $\Delta\delta$   $(\delta_{complex}\text{-}\delta_{sulfoxide})$  (ppm) of the TMSO (1st line) and  $R_2SO$  (2nd line) in the complexes (TMSO)Cl2Pt( $\mu\text{-}pz$ )Pt( $R_2SO$ )Cl2

R <sub>2</sub> SO	$C_{\alpha}$	$\mathbf{C}_{eta}$	$\mathbf{C}_{\gamma}$	$\mathbf{C}_{\delta}$	
TMSO (19)	2.97	-1.11			
DMSO	2.98	-1.11			
	4.04				
DEtSO	2.96	-1.12			
	4.79, 4.60	0.64			
DPrSO	2.93	-1.12			
	2.77	0.52	-0.40		
DBuSO	2.93	-1.08			
	3.50	0.03	-0.49	0.00	
DBzSO	5.29	-0.41			
	2.46	0.94	2.13 (ortho)	2.78 (meta)	0.75 (para)
DPhSO	2.96	-1.12			
	-4.74	2.85 (ortho)	-0.24 (meta)	2.35 (para)	

### **CHAPTER IV**

 $Trans-trans-\{Pt(R_2SO)Cl_2\}_2(\mu-Me_2pyrazine)$ 

 $R_2SO = DMSO$ , TMSO, DEtSO, DPrSO, DBuSO, DBzSO, DPhSO and MeBzSO

This chapter reports the synthesis and characterization of new dimeric platinum(II) complexes, with sulfoxide and 2,5-dimethylpyrazine ligands. A series of sulfoxide ligands with different steric hindrance and chemical behavior has been chosen. They include dimethylsulfoxide (DMSO), tetramethylenesulfoxide (TMSO), diethylsulfoxide (DEtSO), di-*n*-propylsulfoxide (DPrSO), di-*n*-butylsulfoxide (DBuSO), dibenzylsulfoxide (DBzSO), diphenylsulfoxide (DPhSO) and methylbenzylsulfoxide (MeBzSO). Previous research projects of platinum chemistry in our laboratory have involved the use of pyrazine ligand as a bridging ligand. It has

been judged interesting to study other bidentate bridging ligands, pyrazine derivatives. They include 2,5-dimethylpyrazine, quinoxaline and phenazine. Only the work on the first one is presented here. The complexes are characterized by multinuclear NMR spectroscopy (<sup>1</sup>H, <sup>13</sup>C and <sup>195</sup>Pt) and vibrational spectroscopy (Raman and IR). Crystals are isolated and two structures are resolved using X-Rays diffraction.

### 4.1 Preparation

### **4.1.1 Starting materials**

The salt, K<sub>2</sub>[PtCl<sub>4</sub>], was obtained from Johnson Matthey Inc. and was purified by recrystallization from water before use. Deuterochlorofrom, CDCl<sub>3</sub>, was purchased from CDN Isotopes. Dimethylpyrazine and most of the sulfoxide ligands were obtained from Aldrich Chemical Co. Dimethylsulfoxide was purchased from Anachemia Chemicals Ltd, diethylsulfoxide from Narchem Corp. and di-*n*-propylsulfoxide from Phillips Petroleum Co. The latter was purified by distillation before use.

#### 4.1.2 Synthesis of the complexes K[Pt(R<sub>2</sub>SO)Cl<sub>3</sub>]

The new complexes were synthesized with the following ligands: dimethylsulfoxide (DMSO), diethylsulfoxide (DEtSO), tetramethylenesulfoxide (TMSO), di-*n*-propylsulfoxide (DPrSO), di-*n*-butylsulfoxide (DBuSO), diphenylsulfoxide (DPhSO), dibenzylsulfoxide (DBzSO) and methylbenzylsulfoxide (MeBzSO). The synthetic method used was that of Kukushkin *et al.* (1), slightly modified for the different sulfoxide ligands.

### 4.1.2.1 K[Pt( $R_2SO$ )Cl<sub>3</sub>] ( $R_2SO$ = DMSO, DEtSO, TMSO and DPrSO)

Crystals of K<sub>2</sub>[PtCl<sub>4</sub>] (0.8304 g, 2.0 mmol) were crushed and dissolved in a minimum of water (15 mL). The sulfoxide ligand, 0.1565 g, (2.0 mmol) for DMSO, 0.2228 g (2.1 mmol) for DEtSO, 0.2688 g (2.6 mmol) for TMSO and 0.2947 g (2.2 mmol) for DPrSO), mixed with about 5 mL of water was added to the K<sub>2</sub>[PtCl<sub>4</sub>] solution. The mixture was closed from air with a watch glass and vigorously stirred magnetically for about 2 h 15 min for DMSO, 6 h for DEtSO, 24 h for TMSO and 21 h for DPrSO. The precipitate obtained (disubstituted complex) was separated by filtration and washed with water (3 x 10 mL). The filtrate obtained from the DMSO reaction was poured into a large watch glass and then left to evaporate in air. Once completely dry, the white KCl salt, which appeared on the extremities of the watch glass, could be easily get scratched off from the yellow crystals. While still on the watch glass, the latter were mixed with a minimum of water and allowed to evaporate. The procedure was repeated until all the KCl had been removed. The filtrates obtained with the other sulfoxide ligands were left to evaporate and the yellow crystals were dissolved in acetone (about 40 mL). The mixtures were stirred for about 30 min, and then filtered. The purified filtrates, following separation from KCl and from any remaining  $K_2[PtCl_4]$  starting material, were left to evaporate. The new complexes produced, K[Pt(DMSO)Cl<sub>3</sub>], K[Pt(DEtSO)Cl<sub>3</sub>], K[Pt(TMSO)Cl<sub>3</sub>] and K[Pt(DPrSO)Cl<sub>3</sub>], were dried under vacuum in the dessicator The yields were 91, 89, 73 and 86%, respectively.

### 4.1.2.2 K[Pt( $R_2SO$ )Cl<sub>3</sub>] ( $R_2SO$ = DBuSO, DBzSO, MeBzSO and DPhSO)

Since the sulfoxide ligands are insoluble in water, a water:methanol (1:2) mixture was used to dissolve di-n-butylsulfoxide and dibenzylsulfoxide, whereas a water:ethanol (1:3) mixture was preferred for diphenylsulfoxide. The crystals of K<sub>2</sub>[PtCl<sub>4</sub>] (0.8264 g, 2.0 mmol) were ground up and dissolved in a minimum of water (10 mL)/alcohol (5 mL) mixture in a small beaker. The sulfoxide ligand, 0.3408 g (2.1 mmol) for DBuSO, 0.4837 g (2.1 mmol) for DBzSO and 0.4047 g (2.0 mmol) for DPhSO) dissolved in 15 mL of the 2:2 water: alcohol mixture (10 mL for DPhSO) was added to the solution. The top of the beaker was closed with a watch glass and the mixture was vigorously stirred with the aid of a magnetic stirrer for about 24 h for DBuSO, 18 h for DBzSO and 72 h for DPhSO. The precipitate obtained in each case (disubstituted complex) was separated by filtration and then washed with alcohol (3 x 10 mL). The precipitate was then put back into a 5 mL water/15 mL alcohol mixture and stirred for about 15 h in a closed beaker. Following filtration, the precipitate was washed with alcohol, dried and set aside. All the successive filtrates were combined and then left to evaporate slowly in air. The yellow crystals obtained were redissolved in acetone (about 40 mL). The mixture was agitated for about 30 min and filtered. The purified filtrate, separated from KCl and any remaining  $K_2[PtCl_4]$  starting material, was left to evaporate. The complexes obtained were recrystallized from alcohol (20 mL), dried, and then washed with diethylether in order to remove any trace of sulfoxide ligands. Finally, the products were dried under vacuum in the desiccator. The preparative yields of K[Pt(DBuSO)Cl<sub>3</sub>], K[Pt(DBzSO)Cl<sub>3</sub>] and K[Pt(DPhSO)Cl<sub>3</sub>] were 29, 49 and 25%, respectively.

# 4.1.3 Synthesis of the dimeric complexes trans-trans-{Pt(R<sub>2</sub>SO)Cl<sub>2</sub>}<sub>2</sub>( $\mu$ -Me<sub>2</sub>pyrazine)

The main experimental conditions employed for the syntheses of the new dimeric complexes of the type  $\textit{trans-trans-}\{Pt(R_2SO)Cl_2\}_2(\mu\text{-Me}_2pyrazine)$  are given in the Table 4.1.

## 4.1.3.1 $trans-trans-\{Pt(R_2SO)Cl_2\}_2(\mu-Me_2pyrazine)$ (R<sub>2</sub>SO = DMSO, DEtSO, TMSO and DPrSO)

Crystals of K[Pt(R<sub>2</sub>SO)Cl<sub>3</sub>], 0.0992 g (0.24 mmol) for DMSO, 0.0703 g (0.16 mmol) for DEtSO, 0.102 g (0.23 mmol) for TMSO and 0.0950 g (0.20 mmol) for DPrSO were ground up and dissolved in a minimum of distilled water (4-5 mL). 2,5-dimethylpyrazine, 0.0122 g (0.11 mmol) for K[Pt(DMSO)Cl<sub>3</sub>], 0.0080 g (0.07 mmol) for K[Pt(DEtSO)Cl<sub>3</sub>], 0.0108 g (0.10 mmol) for K[Pt(TMSO)Cl<sub>3</sub>] and 0.0103 g (0.10 mmol) for K[Pt(DPrSO)Cl<sub>3</sub>]) were mixed with 1-2 mL of water in a second beaker. The 2,5-dimethylpyrazine solution was added slowly to the platinum salt solution while stirring constantly. The beaker containing 2,5-dimethylpyrazine was rinsed with water (2 x 1 mL) and the washings were added to the reaction mixture. A lemon-yellow precipitate (whitish-yellow in the case of the reaction with K[Pt(DMSO)Cl<sub>3</sub>]) appeared rapidly. The mixture was stirred for about 1 h, filtered and the resulting precipitate was washed with distilled water (3 x 3 mL) in order to remove any remaining traces of the two water-soluble starting materials. The crystals obtained were dried to air and then washed with diethylether. Finally, they

were dried under vacuum in a dessiccator. The products were obtained as a yellow powder. trans-trans-{Pt(DMSO)Cl<sub>2</sub>}<sub>2</sub>(μ-Me<sub>2</sub>pyrazine): yield, 91%; decomp. pt. 172-196 °C, the compound turned whitish and then white; IR (cm<sup>-1</sup>): 3736.9m, 3125.6w, 3046.6msh, 3016.2w, 2917.9m, 2821.3vw, 2242.9vw, 1990.1vw, 1639.4vw, 1505.0m, 1480.2w, 1444.0vw, 1430.6vw, 1400.7vw, 1382.8w, 1373.1vw, 1347.1w, 1320.2w, 1305.2w, 1270.7vw, 1248.8vw, 1163.1mbr, 1138.0sbr, 1094.5w, 1032.7s, 990.9w, 944.5w, 928.0wsh, 889.6m, 759.6vw, 735.4m, 695.6m, 573.7vw, 443.4s, 376.6m, 353.0vs, 302.9w. trans-trans- $\{Pt(DEtSO)Cl_2\}_2(\mu-Me_2pyrazine): yield, 81\%; decomp. pt.176-190 °C, the$ compound tended to melt; IR (cm<sup>-1</sup>): 3738.0m, 3121.5w, 3033.8wsh, 2971.4w, 2927.6w, 2868.1w, 2790.5vw, 2647.4vw, 2359.5w, 2336.2w, 1992.7w, 1733.6vw, 1652.6vw, 1539.0vw, 1499.4w, 1485.9w, 1449.8mbr, 1422.9w, 1408.5w, 1379.8m, 1345.1m, 1279.0m, 1251.2w, 1146.9vsbr, 1094.2w, 1071.0w, 1031.7m, 979.8mbr, 894.0m, 786.2s, 684.8vs, 654.8m, 506.8m, 472.7m, 451.8m, 429.2s, 348.9vs, 332.9msh, 303.2w. *trans-trans*-{Pt(TMSO)Cl<sub>2</sub>}<sub>2</sub>(μ-Me<sub>2</sub>pyrazine): yield, 89%; decomp. pt. 208-215 °C, the compound turned whitish and then white; IR (cm<sup>-1</sup>): 3736.8m, 3125.0vw, 3045.8msh, 2997.7vw, 2934.4m, 2873.5m, 2361.4w, 2334.1w, 1992.0w, 1733.9vw, 1652.8vw, 1539.2w, 1503.4s, 1482.7w, 1455.9w, 1442.0vw, 1426.3wbr, 1400.1m, 1384.3w, 1373.2w, 1346.1m, 1305.6w, 1265.2wbr, 1250.7vw, 1163.4m, 1140.6sbr, 1098.1vw, 1077.6s, 1032.0m, 990.5m, 958.5w, 889.8mbr, 757.6wsh, 674.2m, 594.8s, 512.8vw, 454.7m, 352.2vs, 301.w. trans-trans- $\{Pt(DPrSO)Cl_2\}_2(\mu-Me_2pyrazine): yield, 87\%; decomp. pt. 183-195 °C, the$ compound tends to melt; IR (cm<sup>-1</sup>): 3736.9m, 3117.4w, 3048.7msh, 2961.4s, 2937.4m, 2874.2m, 2735.6vw, 2361.1w, 2332.8w, 1972.7w, 1651.6vw, 1540.3w, 1502.0m, 1457.0m, 1424.4w, 1403.9w, 1375.0w, 1346.1m, 1300.8w, 1259.7w, 1225.7vw, 1161.4m, 1134.3vsbr, 1096.9w, 1073.7m, 1033.0w, 986.1w, 884.6w, 869.4w, 760.5msh, 739.9m, 667.7w, 593.1vw, 511.8s, 450.3s, 353.4vs, 302.1w.

## 4.1.3.2 $trans-trans-\{Pt(R_2SO)Cl_2\}_2(\mu-Me_2pyrazine)$ (R<sub>2</sub>SO = DBuSO, DBzSO, DPhSO and MeBzSO)

A 1:2 water:methanol mixture (1:3 in the case of K[Pt(DPhSO)Cl<sub>3</sub>]) was prepared. Crystalline K[Pt(R<sub>2</sub>SO)Cl<sub>3</sub>], 0.110 g (0.22 mmol) for DBuSO, 0.0732 g (0.13 mmol) for DBzSO, 0.0473 g (0.10 mmol) for MeBzSO and 0.0961 g (0.18 mmol) for DPhSO) was ground and dissolved in a minimum quantity of the water:alcohol mixture (6-8 mL). Vigourous magnetic stirring was necessary for complete dissolution of the crystals. 2,5-Dimethylpyrazine, 0.0113 g (0.10 mmol) for K[Pt(DBuSO)Cl<sub>3</sub>], 0.0066 g (0.06 mmol) for K[Pt(DBzSO)Cl<sub>3</sub>], 0.0047 g (0.04 mmol) for K[Pt(MeBzSO)Cl<sub>3</sub>] and 0.0087 g (0.08 mmol) for K[Pt(DPhSO)Cl<sub>3</sub>]) was mixed with 2-3 mL of alcohol in a second beaker. The 2,5-dimethylpyrazine was slowly added to the platinum salt solution while stirring constantly. The beaker containing 2,5-dimethylpyrazine was rinsed thoroughly with a 1:1 water:alcohol mixture (2 x 1 mL) and the washings were added to the reaction mixture. An orangeyellow precipitate appeared after several minutes. The reaction mixture was stirred for about 3 h, filtered and the resulting precipitate was washed with a 1:1 water: alcohol mixture (3 x 3 mL) in order to remove any traces of the two starting materials, which are soluble in alcohol. The products were obtained as a yellow powder. trans-trans-{Pt(DBuSO)Cl<sub>2</sub>}<sub>2</sub>(μ-Me<sub>2</sub>pyrazine): yield, 89%; decomp. pt.

174-185 °C, the compound turned whitish and then white; IR (cm<sup>-1</sup>): 3736.7m, 3123.0m, 3042.1msh, 2958.8s, 2933.1m, 2871.9m, 2361.6w, 2332.9w, 1985.8vw, 1818.7vw, 1651.6vw, 1505.9m, 1489.1m, 1467.4m, 1423.9w, 1402.3m, 1385.3w, 1345.4m, 1314.2w, 1284.5w, 1234.8w, 1202.1w, 1143.0vsbr, 1108.8w, 1093.1w, 1080.0m, 1041.4w, 989.6w, 922.5msh, 900.2w, 792.0w, 758.3vw, 743.1m, 728.5m, 667.8w, 519.7w, 498.6m, 455.2m, 425.8w, 353.2vs, 303.2w. trans-trans- $\{Pt(DBzSO)Cl_2\}_2(\mu-Me_2pyrazine): yield, 80\%; decomp. point = 153-162 °C, the$ compound tends to melt; IR (cm<sup>-1</sup>): 3738.0m, 3104.2vw, 3056.1wsh, 3031.2w, 2982.8w, 2923.9w, 2787.1vw, 2632.8vw, 2255.2vw, 1961.0vw, 1600.7w, 1537.2vw, 1492.5msh, 1454.5msh, 1426.2w, 1405.8w, 1339.7w, 1299.7vw, 1250.3vw, 1167.1mbr, 1117.3mbr, 1072.6wsh, 1029.8w, 972.7vw, 921.2w, 882.0w, 764.9s, 696.7vs, 579.6m, 482.7s, 414.1m, 350.5m, 318.9m, 301.8vw. trans-trans- $\{Pt(MeBzSO)Cl_2\}_2(\mu-Me_2pyrazine): yield, 75\%; decomp. pt. 191-205 °C, the$ compound turned yellow-whitish and then white; IR (cm<sup>-1</sup>): 3737.4m, 3121.5vw, 3044.3m, 3007.0w, 2973.1w, 2920.5m, 2851.8vw, 2361.8w, 2332.8w, 1962.7w, 1891.5vw, 1652.6wsh, 1538.6vw, 1495.0m, 1455.3m, 1427.5wbr, 1394.8wbr, 1345.7m, 1303.2w, 1268.8vw, 1251.5w, 1165.6s, 1124.9s, 1097.4vw, 1074.6w, 1029.8w, 969.0s, 922.2w, 887.7wsh, 811.0w, 766.7ssh, 719.9w, 698.3vs, 590.5m, 484.4s, 449.3s, 378.w, 346.6vs, 301.8msh. *trans-trans*-{Pt(DPhSO)Cl<sub>2</sub>}<sub>2</sub>(μ-Me<sub>2</sub>pyrazine): yield, 79%; decomp. pt. 207-221 °C, the compound turned whitish and then white; IR (cm<sup>-1</sup>): 3738.3m, 3054.2m, 2962.1vw, 2915.6w, 2851.8vw, 2649.9w, 2259.3vw, 1981.5w, 1593.2vw, 1578.7w, 1488.7w, 1472.8w, 1442.7m, 1426.2w, 1385.3w, 1375.4w, 1345.1w, 1307.8w, 1245.4vw, 1147.4mbr, 1094.7w, 1069.7m, 1020.1w, 997.8w, 922.2vw, 901.3w, 756.2w, 746.4m, 713.2w, 698.2m, 682.7m, 613.9w, 562.6vs, 524.8vs, 439.6m, 351.7s, 327.8w, 307.0w.

**Table 4.1** Experimental conditions and synthesis yields for the *trans-trans*- ${Pt(R_2SO)Cl_2}_2(\mu-Me_2pyrazine)$  complexes.

R <sub>2</sub> SO	Solvent	Reaction time	Ratio Pt/pz	Yield
DMSO	$H_2O$	1 h	2.2/1.0	91%
DEtSO	$H_2O$	1 h	2.3/1.0	81%
TMSO	H <sub>2</sub> O	1 h	2.3/1.0	89%
DPrSO	H <sub>2</sub> O	1 h	2.0/1.0	87%
DBuSO	H <sub>2</sub> O:MeOH (1:2)	3 h	2.2/1.0	89%
DBzSO	H <sub>2</sub> O:MeOH (1:2)	3 h	2.2/1.0	80%
MeBzSO	H <sub>2</sub> O:MeOH (1:2)	3 h	2.5/1.0	75%
DPhSO	H <sub>2</sub> O:EtOH (1:3)	3 h	2.3/1.0	79%

The prepared dimeric compounds were obtained with satisfactory experimental yields, ranging from 75% for  $trans-trans-\{Pt(MeBzSO)Cl_2\}_2(\mu-Me_2pyrazine)$  to 91% to  $trans-trans-\{Pt(DMSO)Cl_2\}_2(\mu-Me_2pyrazine)$ . The steric

hindrance seems to play a role in the observed yields. Multinuclear NMR spectroscopy (<sup>1</sup>H, <sup>13</sup>C and <sup>195</sup>Pt), discussed in the next section, is a good probe of purity for the complexes. The IR spectra of the compounds were also pretty clear, showing they were relatively pure (section 4.3).

Attempts were also made to synthesize the monomeric analogues, but all efforts were unsuccessful. For example, even when varying the experimental conditions (ratio of the starting materials, time of reaction, temperature) for the reaction between K[Pt(DPhSO)Cl<sub>3</sub>] and 2,5-dimethylpyrazine, the only product formed was the dimeric complex. This result illustrates that the reactivity of 2,5dimethylpyrazine is different from that of pyrazine. In the case of the latter, the products formed in good yield when the Pt/pz ratio was changed from 2:1 to 1:1. went from the dimeric compounds, trans-trans- $\{Pt(R_2SO)Cl_2\}_2(\mu-pz)$ , to their monomeric analogues, cis- and trans-Pt(R<sub>2</sub>SO)(pz)Cl<sub>2</sub> (2,3). Previous research work has shown that incorporation of methyl groups into heteroaromatic rings significantly affects the electronic distribution as well as the self-association behaviour (4-7). In the case of the 1:1 stochiometry for 2,5-dimethylpyrazine, it is possible that the monomeric compound is produced first when the initial molecule of the platinum compound reacts with a molecule of 2,5-dimethylpyrazine. But the hypothetical molecule, 'Pt(R<sub>2</sub>SO)(Me<sub>2</sub>pyrazine)Cl<sub>2</sub>', is probably so unstable that it attracts another ligand molecule immediately to form the final dimeric compound,  $trans-trans-\{Pt(R_2SO)Cl_2\}_2(\mu-Me_2pyrazine).$ 

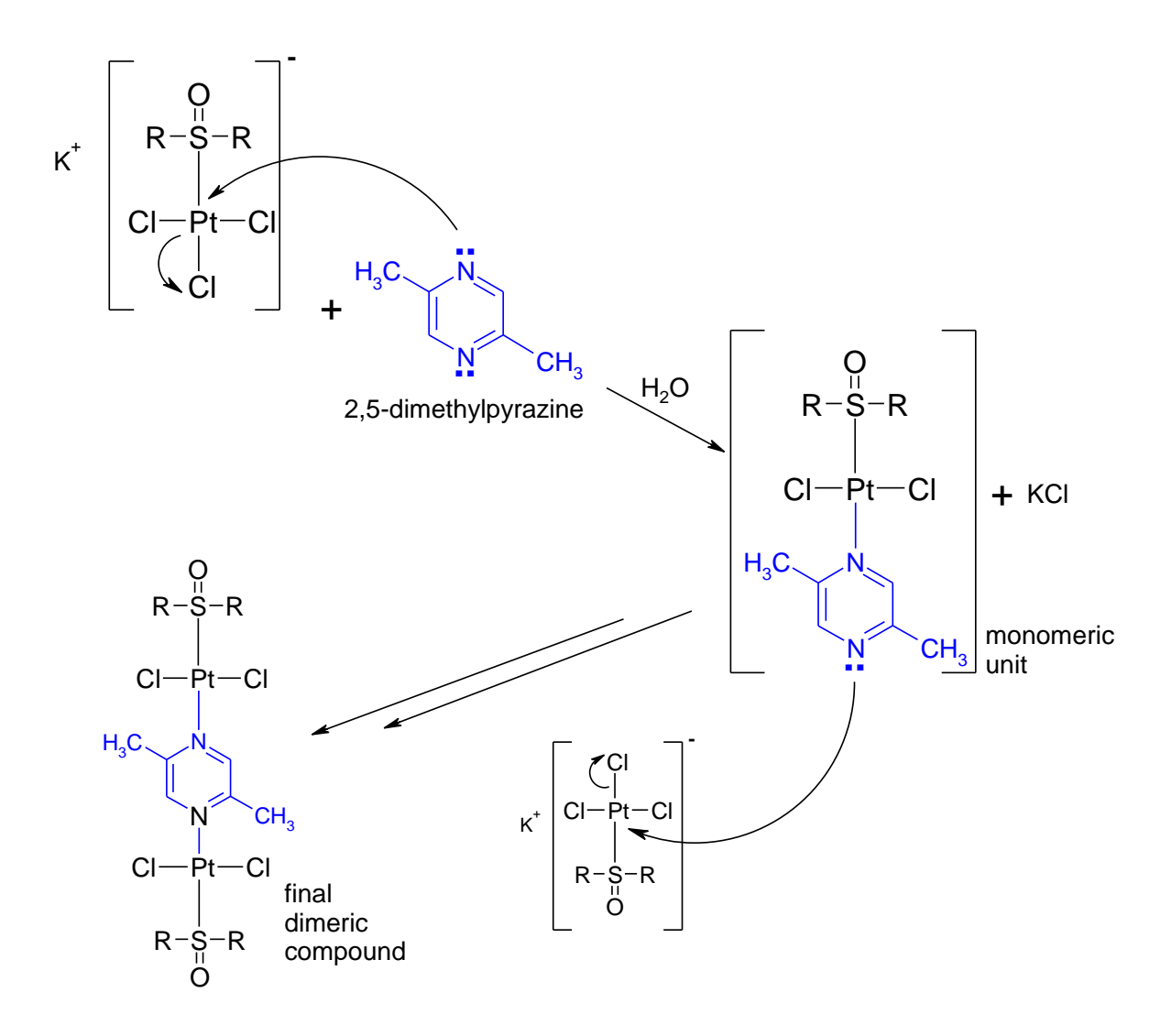


**Figure 4.1** Mechanism for the possible formation of the monomeric compound.

## 4.2 Analysis of the complexes by multinuclear NMR spectroscopy

All the NMR spectra were measured in CDCl<sub>3</sub> solution on a Varian Gemini 300BB spectrometer operating at 300.069, 75.460 and 64.326 MHz for  $^{1}$ H,  $^{13}$ C and  $^{195}$ Pt, respectively. The standard recording conditions used in this thesis work were the following: SW = 4500.5 Hz, AT = 1.998 s., FB = 2600 Hz, PW = 7.0  $\mu$ s., NT = 500 to 2000 for proton NMR, SW = 18761.7 Hz, AT = 1.815 s, FB = 10400 Hz, PW

= 8.7  $\mu$ s, NT = 100000 to 300000 for carbon-13 NMR and SW = 100000 Hz, AT = 0.150 s., FB = 51200 Hz, PW = 8.7  $\mu$ s, TOF = 0, NT = 60000 to 300000 for platinum-195 NMR. The chloroform peaks were used as an internal standard for the  $^{1}$ H (7.24 ppm) and  $^{13}$ C (77.00 ppm) NMR spectra. For  $^{195}$ Pt, the external reference was K[Pt(DMSO)Cl<sub>3</sub>] in D<sub>2</sub>O, adjusted to -2998 ppm from K<sub>2</sub>[PtCl<sub>6</sub>] ( $\delta$ (Pt) = 0 ppm). The  $^{195}$ Pt-NMR spectra were measured between approximately -2500 and -4000 ppm.

## 4.2.1 2,5-Dimethylpyrazine

The spectra of 2,5-dimethylpyrazine were taken in CDCl<sub>3</sub> solution. In  $^{1}$ H-NMR spectroscopy, two singlets were observed. The first singlet, observed at 8.218 ppm (intensity = 2) can be assigned to the ring protons, H<sub>3</sub> and H<sub>6</sub>. The second singlet, observed at 2.395 ppm (intensity = 6) can be attributed to the methyl protons.

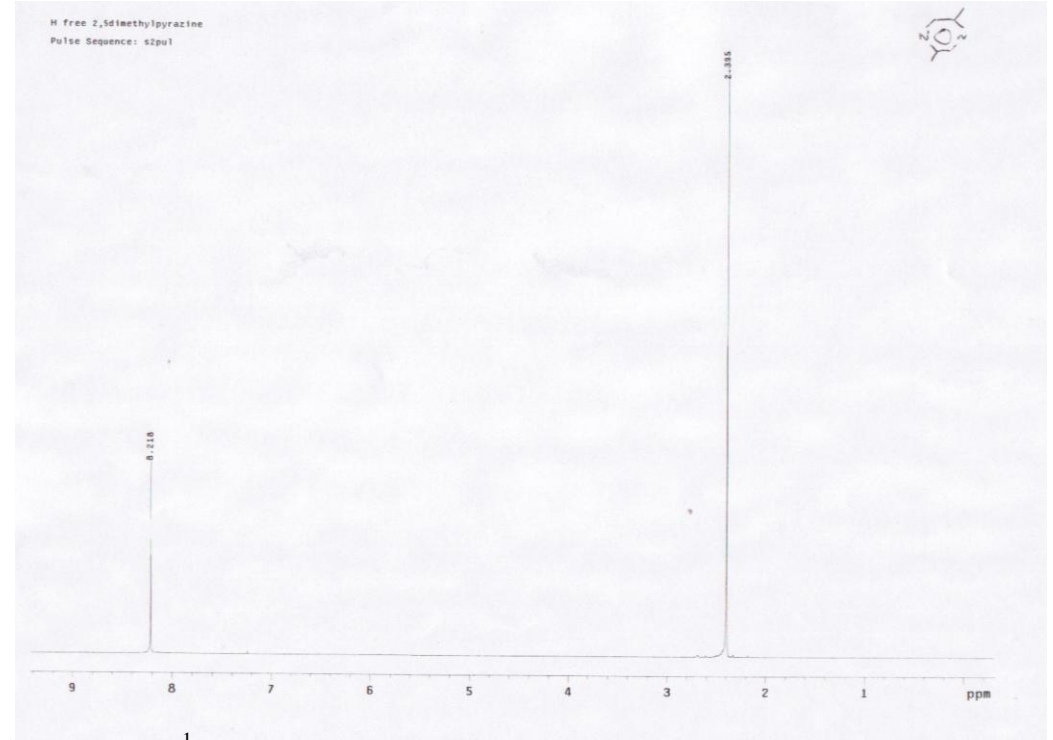


**Figure 4.2.1.1** <sup>1</sup>H-NMR spectrum of free 2,5-dimethylpyrazine.

In the  $^{13}$ C-NMR spectrum, two signals were observed. The first one, observed at 150.32 ppm, can be assigned to the two carbon atoms on which the methyl groups are attached,  $C_2$  and  $C_5$ . They are more deshielded than are the other carbons and the signal is weaker. The second signal, observed at 143.28 ppm, is assigned to the two other ring carbon atoms,  $C_3$  and  $C_6$ . Finally, the signal observed at 20.81 ppm is due to the carbon atoms of the two methyl groups.

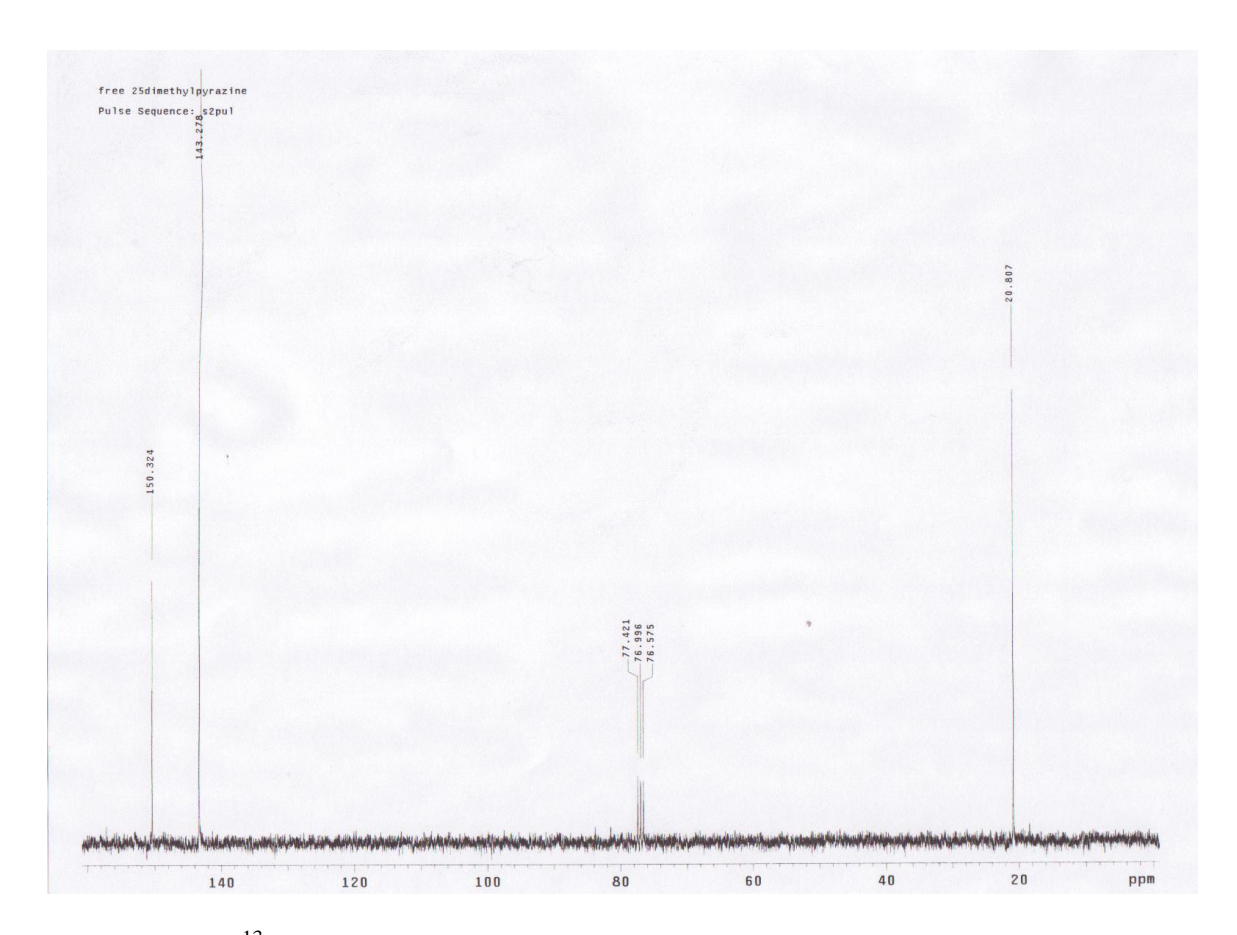


**Figure 4.2.1.2**  $^{13}$ C-NMR spectrum of free 2,5-dimethylpyrazine.

### 4.2.2 Sulfoxide ligands

The free sulfoxide ligands have been analyzed by <sup>1</sup>H- and <sup>13</sup>C-NMR spectroscopy, and the results are summarized in the Tables 4.2.2.1 and 4.2.2.2. The

multiplicities are also indicated beside the chemical shift values. The coupling constants for the signals, when it has been possible to identify them, are indicated on the second line. The earlier work of Gottlied and Nudelman allowed us to identify the signals of the solvents (CHCl<sub>3</sub>, CH<sub>2</sub>Cl<sub>2</sub>, H<sub>2</sub>O, CH<sub>3</sub>COCH<sub>3</sub>, ethers) (6).

**Table 4.2.2.1** <sup>1</sup>H-NMR signals (ppm) and coupling constants (Hz) of the free sulfoxide molecules in CDCl<sub>3</sub> (2)

R <sub>2</sub> SO	$\mathbf{H}_{\alpha}$	$\mathbf{H}_{eta}$	$\mathbf{H}_{\gamma}$	$\mathbf{H}_{\delta}$	
TMSO	2.83m	2.40m, 1.98m			
DMSO	2.48s				
DEtSO	2.625dq	1.256t			
DEISO	7.7, 3.0	7.7			
DPrSO	2.56m	1.74 tq	1.01t		
21100	2.30111	6.9, 6.9	6.9		
DBuSO	2.81m	2.67m	1.75m	1.47m	
DBzSO	3.88m		7.27m( <i>ortho</i> )	7.34m ( <i>meta</i> )	7.34m ( <i>para</i> )
DPhSO		7.63m	7.44m ( <i>meta</i> )	7.44m ( <i>para</i> )	
211150		(ortho)	, iii (meta)	, , , im (parti)	

The free dimethylsulfoxide ligand shows only one singlet signal, because the two methyl groups are chemically and magnetically equivalent. The chemical shift is strongly deshielded in comparison to methane ( $\delta$  = -2.3 ppm), the reference compound for the methyl group. This difference illustrates the inductive effect of the sulfoxide group. The further the protons are away from the sulfur atom, the more their signals are shielded. In fact, because of the inductive effect of the sulfur atom,

the near protons are deshielded. The effect decreases when the length of the carbon chain increases, which explains the increase of the chemical shift values,  $\delta(H\alpha) > \delta(H\beta) > \delta(H\gamma) > \delta(H\delta)$ , for the carbon chains.

In comparison with the di-n-propylsulfoxide ligand, the H $\beta$  and H $\gamma$  protons of the di-n-butylsulfoxide ligand are more deshielded ( $\Delta_{\beta}=0.93$ ppm and  $\Delta_{\gamma}=0.74$ ppm). This is due to the fact that a hydrogen atom on the C $\gamma$  carbon atom is replaced by another carbon atom. This effect is also observed on the  $\alpha$  position, where the H $\alpha$  protons are more deshielded the longer is the carbon chain.

In the DBuSO spectrum, one would expect to observe a triplet for the protons located in  $\alpha$  position. However, a multiplet is observed. This could be due to the fact that rotation around the S-C axis is slowed down and so the protons are then non-equivalent. This effect could diminish further we are from the sulfur atom.In the dibenzylsulfoxide ligand spectrum, the two protons of the  $CH_2$  group appear as an AB system; they are not equivalent due to the anisotropic effect of the benzene rings.

For the tetramethylenesulfoxide ligand, the geminal protons are non-equivalent because they are influenced by the presence of the oxygen atom. Some are closer to the oxygen atom, and two series of signals are observed for the  $H\beta$  protons, whereas only one series is obtained for the  $H\alpha$  protons. It is also possible,

however, that two series are obtained for the  $\alpha$  position, but the chemical shifts are so close to each other that it is difficult to distinguish between them with the spectrometer used in our experiments (300 MHz).

Table 4.2.2.2 <sup>13</sup>C NMR (ppm) of the free sulfoxide molecules in CDCl<sub>3</sub> (2)

R <sub>2</sub> SO	$\mathbf{H}_{lpha}$	$\mathbf{H}_{eta}$	$\mathbf{H}_{\gamma}$	$\mathbf{H}_{\delta}$
TMSO	54.39	25.42		
DMSO	40.70			
DEtSO	44.68	6.61		
DPrSO	54.20	16.14	13.27	
DBuSO	51.62	24.64	22.04	13.66
DBzSO	57.22		128.34, 128.93,130.10	
DPhSO	145.41	124.57 (ortho)	129.10 (meta)	130.83 (para)

The same observations can be made for the  $^{13}\text{C-NMR}$  spectra as for the  $^{1}\text{H-NMR}$  spectra. The inductive effect of the sulfoxide function diminishes with the distance to the function:  $\delta(C \alpha) > \delta(C\beta) > \delta(C\gamma) > \delta(C\delta)$  for the carbon chains.

The carbon atoms in the  $\beta$  and  $\gamma$  positions in di-*n*-butylsulfoxide are more deshielded than are the analogous carbons in di-*n*-propylsulfoxide, because the hydrogen atom on the carbon  $C\gamma$  is replaced by another carbon atom. This effect is also observed for the  $\alpha$  position. The longer is the carbon chain, the more the  $C\alpha$  carbon is deshielded. The same effect is observed for the next carbon atoms. The

spectrum of the diphenylsulfoxide ligand shows a strong deshielding of the  $C\alpha$  carbon atom, because it is subject to the inductive effects of both the sulfoxide function and the phenyl rings. The influence of the sulfoxide group diminishes on the next carbon atoms.

## 4.2.3 Complexes of the type *trans-trans*- $\{Pt(R_2SO)Cl_2\}_2(\mu-Me_2pyrazine)$

All the compounds have been analysed by multinuclear NMR spectroscopy using chloroform-d as the solvent. The observed chemical shifts are given in the Tables 4.2.3.1 to 4.2.3.4. The differences from the chemical shifts of the free ligands (2,5-dimethylpyrazine and the series of the sulfoxide ligands) are also listed here.

**Table 4.2.3.1** <sup>195</sup>Pt- and <sup>1</sup>H-NMR chemical shifts and  $\Delta\delta$  ( $\delta_{complex}$ - $\delta_{dmpz}$ ) (ppm) of dmpz in the complexes {Pt(R<sub>2</sub>SO)Cl<sub>2</sub>}<sub>2</sub>( $\mu$ -Me<sub>2</sub>pz) (in CDCl<sub>3</sub>)

$R_2SO$	$\delta(^{195}\text{Pt})$	$\delta(^{1}H_{3-6})$	$\delta(^{1}H_{3}C)$	$^{3}J(^{195}\text{Pt-H}_{3-6})$
		Δδ	$\Delta\delta$	
TMSO	-3059	8.73	3.13	38
		$\Delta \delta = 0.51$	$\Delta \delta = 0.73$	
DMSO	too insoluble			
DEtSO	-3103	8.71	3.13	25
		$\Delta \delta = 0.49$	$\Delta \delta = 0.73$	
DPrSO	-3073	8.70	3.13	26
		$\Delta \delta = 0.48$	$\Delta \delta = 0.73$	
DBuSO	-3075	8.70	3.13	29
		$\Delta \delta = 0.48$	$\Delta \delta = 0.73$	
MeBzSO	-3097	8.67	3.19	31
		$\Delta \delta = 0.45$	$\Delta \delta = 0.79$	
DBzSO	-3093	8.40	2.77	
		$\Delta \delta = 0.18$	$\Delta \delta = 0.37$	
DPhSO	-3135	8.51,8.53	3.10,3.17	
		$\Delta \delta = 0.29, 0.31$	$\Delta \delta = 0.70, 0.77$	

The  $^{195}$ Pt-NMR spectra of the compounds show a single signal between -3159 and -3035 ppm. This is comparable to the results obtained for the pyrazine analogues, trans, trans-{Pt(R<sub>2</sub>SO)Cl<sub>2</sub>}<sub>2</sub>( $\mu$ -pz), with a difference of ca. 22ppm (2). For instance, the tetramethylenesulfoxide compound showed a chemical shift at -3041 ppm ( $\Delta_{pz-dmpz} = 18$  ppm), the dipropylsulfoxide compound showed a shift at -3048 ppm ( $\Delta = 25$  ppm), the dibutylsulfoxide compound showed a shift at -3051 ppm ( $\Delta = 24$ ppm) and the diphenylsulfoxide compound showed a shift at -3113 ppm ( $\Delta = 22$ ppm). The compound trans, trans-{Pt(diethylsulfoxide)Cl<sub>2</sub>}<sub>2</sub>( $\mu$ -pz), prepared in this project, also showed a similar shift, at -3076 ppm ( $\Delta = 27$  ppm) (section 5.2). The solvent and the spectrometer used for analyzing all of these compounds were the same. So, we can deduce that the two extra methyl groups present on the bridging ligand in the {Pt(R<sub>2</sub>SO)Cl<sub>2</sub>}<sub>2</sub>( $\mu$ -Me<sub>2</sub>pz) complexes are responsible for the slight shielding observed when compared to their {Pt(R<sub>2</sub>SO)Cl<sub>2</sub>}<sub>2</sub>( $\mu$ -pz) analogues.

All the platinum(II) complexes in the literature, with the identical coordination sphere [PtNSCl<sub>2</sub>], showed chemical shifts in the same spectral window, from -3150 to 2800 ppm. Farrell *et al.* observed unique signals at -3023 and -3014 ppm, respectively, for *trans*-Pt(Me<sub>2</sub>SO)(picoline)Cl<sub>2</sub> and *trans*-Pt(Me<sub>2</sub>SO)(pyridine)Cl<sub>2</sub> (7). And, for our mixed ligand compounds, {*trans*-Pt(tetramethylenesulfoxyde)Cl<sub>2</sub>}(μ-pz){*trans*-Pt'(dibenzyl-sulfoxyde)Cl<sub>2</sub>}, we observed shifts at -3044 ppm for the TMSO unit and at -3059 ppm for the DBzSO unit (section 3.2).

Most of the research done on complexes with dimethylpyrazine ligands has been with the two methyl groups located in positions 2 and 6 or in positions 2 and 3 (8-21). Fewer studies have been published on the 2,5-dimethylpyrazine ligand (19-25). This latter is more sterically hindered and generally is not favored for the reactions when a 1:1 Pt:dmpz ratio is used. However, we thought it could be an interesting bridging ligand with a central symmetry. The goal was to obtain dimeric compounds first, in which we succeeded, and then to try to synthesize the monomeric analogues, in which, unfortunately, we ultimately failed.

The <sup>1</sup>H-NMR chemical shifts observed for the 2,5-dimethylpyrazine ligand in our complexes consist of two singlets. The first singlet, observed in the window 2.7-3.2ppm corresponds to the methyl protons. The second singlet, observed in the window 8.4-8.8ppm, can be identified as the signal of the aromatic protons. The dimethylpyrazine peaks of our complexes are all shifted to the left upon coordination. The aromatic protons,  $H_3$  and  $H_6$ , are deshielded by about 0.4 ppm and the methyl protons are deshielded by about 0.7 ppm. This situation is due to the  $\sigma$ bond that diminishes the electronic density on the dimethylpyrazine unit. The observed values are comparable to those in the litterature. Venanzi et al. detected signals at 2.55 and 2.98 ppm for the methyl protons and at 8.47 and 8.49ppm for the aromatic protons in the monomeric compound trans-Pt(2,5-Me<sub>2</sub>pz)(PEt<sub>3</sub>)Cl<sub>2</sub> (21). The dimeric analogue, trans, trans- $\{Pt(PEt_3)Cl_2\}_2(\mu-2,5-Me_2pz)$ , showed shifts in the same region, at 3.05 and 8.69 ppm, respectively, for the methyl and for the aromatic protons. This last case is very similar to our compounds and so it is quite normal to find a very small shielding differences, 0.04 ppm for the methyl protons and 0.06 ppm for the aromatic protons. Three other dimeric complexes showed similar chemical shifts. First at all, the  $trans, trans = \{Pt(PMe_2Ph)Cl_2\}_2(\mu-2, 5-Me_2pz)$  compound displays signals at 3.05 and 8.75 ppm. And the complexes trans, trans-{Pt(PMePh<sub>2</sub>)Cl<sub>2</sub>}<sub>2</sub>( $\mu$ -2,5-Me<sub>2</sub>pz) and trans, trans-{Pt(H<sub>2</sub>C=CH<sub>2</sub>)Cl<sub>2</sub>}<sub>2</sub>( $\mu$ -2,5-Me<sub>2</sub>pz) showed pairs of signals at 3.12/8.77 and 3.08/8.71ppm for the methyl and aromatic protons, respectively.

There has not been much research reported on complexes containing both platinum(II) and the 2,5-dimethylpyrazine ligand. It is possible, however, to notice a similarity between our compounds and the complexes in which a non-branched pyrazine unit is involved as a bridging ligand. There are numerous examples known (2,26,27). We identified a shift of ca. 0.52 ppm for the *trans,trans*-{Pt(R<sub>2</sub>SO)Cl<sub>2</sub>}<sub>2</sub>(μ-pz) complexes (2), whereas Komeda *et al.* found a shift of 0.45 ppm for [*cis,cis*-{Pt(NH<sub>3</sub>)<sub>2</sub>Cl}<sub>2</sub>(μ-pz)](NO<sub>3</sub>)<sub>2</sub> (26). Hall and Thornton have reported a shift of 0.65 ppm for the compound *trans,trans*-{Pt(CO)Cl<sub>2</sub>}<sub>2</sub>(μ-pz) (27). This slightly higher value can be viewed as the consequence of the larger electronic contribution of the carbonyl group.

The signals of the aromatic protons, H<sub>3</sub> and H<sub>6</sub>, for the dimeric compounds with diphenylsulfoxide and dibenzylsulfoxide ligands are observed at higher field than are those for the other compounds. This difference can be attributed to the electron density associated with the phenyl rings. It is interesting to note that the compound {Pt(DPhSO)Cl<sub>2</sub>}<sub>2</sub>(μ-2,5-Me<sub>2</sub>pz) shows two signals for both the aromatic protons, at 8.51 and 8.53 ppm, and for the methyl protons, at 3.10 and 3.17 ppm. This observation could mean that the two platinum units are not branched in the same geometry to the bridging ligand. It could result in a *cis/trans* dimeric complex.

However, this is only a hypothesis. Only one compound has been found to show such a cis, trans-{Pt(DPrSO)Cl<sub>2</sub>}<sub>2</sub>( $\mu$ -pz) geometry (Chap VI).

In the <sup>1</sup>H-NMR spectra, coupling constants have been detected on the aromatic singlet. These are <sup>3</sup>J(<sup>195</sup>Pt-H<sub>3-6</sub>) and are observed, except for the complex containing the tetramethylenesulfoxide ligand, between 25 and 31Hz. Similar coupling constants have been reported by Albinati *et al.* for *trans,trans*-{Pt(PH<sub>2</sub>C=CH<sub>2</sub>)Cl<sub>2</sub>}<sub>2</sub>(μ-2,5-Me<sub>2</sub>pz) at 22 Hz, for *trans,trans*-{Pt(PMePh<sub>2</sub>)Cl<sub>2</sub>}<sub>2</sub>(μ-2,5-Me<sub>2</sub>pz) and *trans,trans*-{Pt(PMe<sub>2</sub>Ph)Cl<sub>2</sub>}<sub>2</sub>(μ-2,5-Me<sub>2</sub>pz) at 21 Hz and for *trans,trans*-{Pt(PEt<sub>3</sub>)Cl<sub>2</sub>}<sub>2</sub>(μ-2,5-Me<sub>2</sub>pz) at 20Hz (21). The coupling constants are a good tool to suggest the geometry of the platinum(II) complexes (28). Our compounds are believed to be of *trans,trans* geometry since the coupling constants are so low. Coupling constants are generally included in the window 25-35 Hz for *trans* complexes, but about 10 Hz higher for their *cis* analogues (29-32). The case of {Pt(TMSO)Cl<sub>2</sub>}<sub>2</sub>(μ-Me<sub>2</sub>pz) is not so clear, since its coupling constant has a higher value, i.e., 38 Hz. This could be due to a *cis,cis* complex.

**Table 4.2.3.2**  $^{13}$ C NMR chemical shifts and  $\Delta\delta$  ( $\delta_{complex}$ - $\delta_{dmpz}$ ) (ppm) of dmpz in  $\{Pt(R_2SO)Cl_2\}_2(\mu\text{-Me}_2pz) \text{ (in CDCl}_3)$ 

D. 00	$\delta(^{13}C_{2-5})$	$\delta(^{13}C_{3-6})$	$\delta(^{13}\text{CH}_3)$
$R_2SO$	$\Delta\delta$	Δδ	Δδ
TMSO	not	148.84	26.29
TWISO	observed	$\Delta\delta = 5.56$	$\Delta \delta = 5.48$
DMSO	too	_	_
DIVISO	insoluble		
DEtSO	154.93	148.66	23.05
DEISO	$\Delta \delta = 4.61$	$\Delta \delta = 5.38$	$\Delta \delta = 2.24$
DPrSO	154.91	148.71	23.06
DFISO	$\Delta \delta = 4.59$	$\Delta \delta = 5.43$	$\Delta \delta = 2.25$
DBuSO	154.91	148.74	23.05
DBuSO	$\Delta \delta = 4.59$	$\Delta \delta = 5.46$	$\Delta \delta = 2.24$
MeBzSO	154.87	148.76	23.19
MEDZSO	$\Delta \delta = 4.55$	$\Delta \delta = 5.48$	$\Delta \delta = 2.38$
DBzSO	154.82	148.37	22.78
DBZSO	$\Delta \delta = 4.50$	$\Delta \delta = 5.09$	$\Delta \delta = 1.97$
DDFCO	not	148.96	29.69
DPhSO	observed	$\Delta\delta = 5.68$	$\Delta \delta = 8.88$

The <sup>13</sup>C -NMR spectra show three signals for the bridging ligand, 2,5-dimethylpyrazine. An example is given in Figure 4.2.3. for the dimeric compound containing the diethylsulfoxide ligand. In the series of complexes, the aromatic carbons are observed at around 155 ppm for C<sub>2</sub> and C<sub>5</sub>, and at about around 149 ppm for the C<sub>3</sub> and C<sub>6</sub>. This difference represents a shielding of ca.4.6 ppm for the first pair and ca. 5.4ppm for the latter pair. The methyl carbons are observed in the window 23-30 ppm, with a highly variable shielding depending on the sulfoxide ligand present in the complex. The compound *trans,trans*-{Pt(DMSO)Cl<sub>2</sub>}<sub>2</sub>(μ-Me<sub>2</sub>pz) proved to be too insoluble in the different solvents tested, *viz.*, chloroform-d, DMF, hot D<sub>2</sub>O and dichloromethane, to give a satisfactory spectrum. In the series of

the compounds trans, trans-{Pt(DMSO)Cl<sub>2</sub>}<sub>2</sub>( $\mu$ -pz), the DMSO complex was the one that was too insoluble to give good results (2). In general, the longer is the sulfoxide chain, the greater is the solubility of its complex.

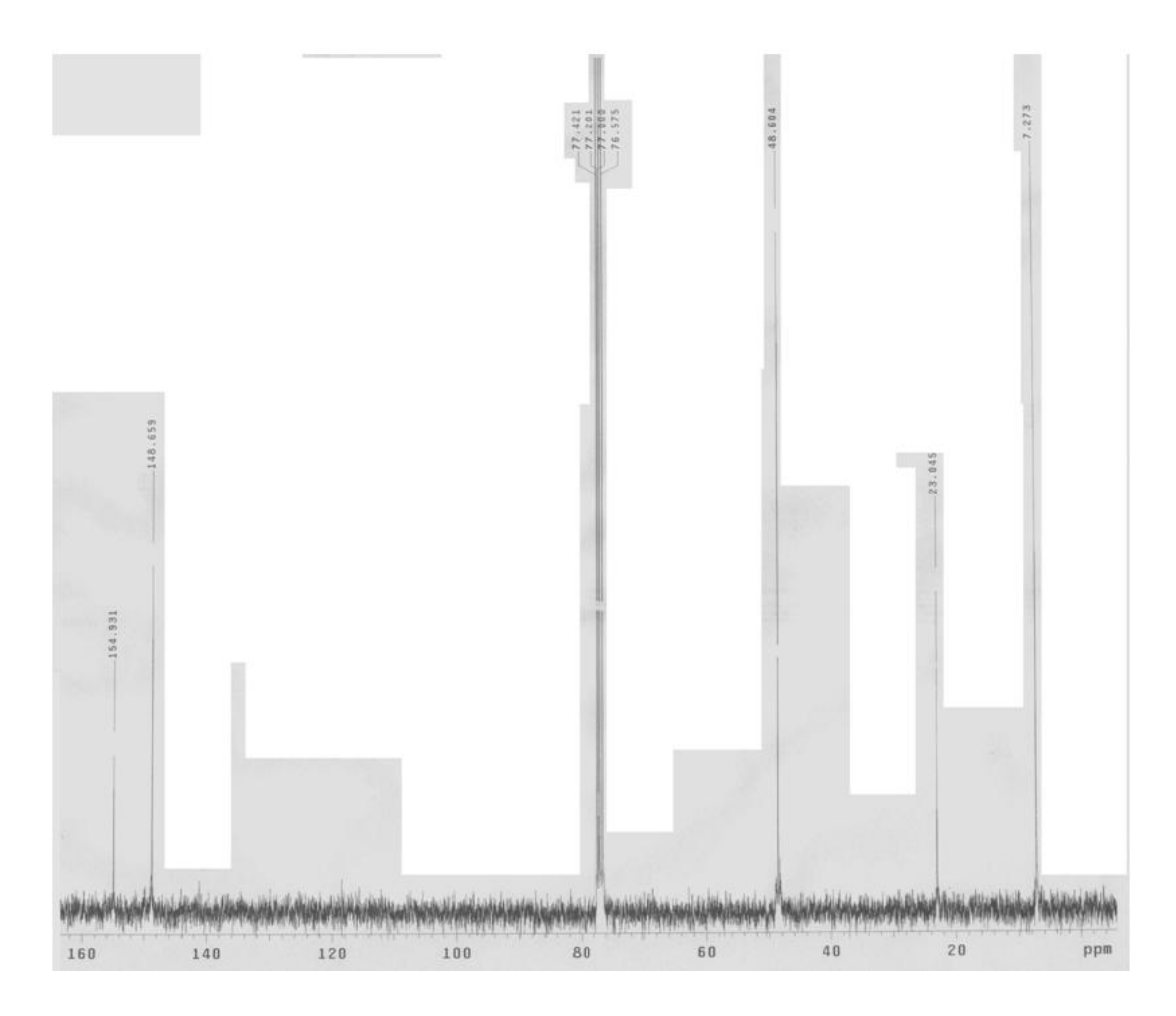


Figure 4.2.3  $^{13}$ C NMR spectrum of the  $\{Pt(DEtSO)Cl_2\}_2(\mu\text{-Me}_2pz)$  taken in CDCl3.

Similar chemical shifts have been obtained for trans, trans-{Pt(PEt<sub>3</sub>)Cl<sub>2</sub>}<sub>2</sub>( $\mu$ -2,5-Me<sub>2</sub>pz) (21). The aromatic carbons are observed at 147.7 and 153.9 ppm, respectively for the carbon atoms C<sub>3</sub>-C<sub>6</sub> and C<sub>2</sub>-C<sub>5</sub>. And the methyl carbon atoms are observed at 22.3ppm. The two other compounds trans, trans-{Pt(R)Cl<sub>2</sub>}<sub>2</sub>( $\mu$ -2,5-

Me<sub>2</sub>pz) ( $R = PMe_2Ph$  and  $PMePh_2$ ) showed similar chemical shifts, respectively at 148.0/154.0ppm and 148.1/154.0ppm and for the aromatic protons and at 22.6ppm and 22.7ppm for the methyl protons.

**Table 4.2.3.3**  $\delta(^1H)$ ,  $\Delta\delta$  ( $\delta_{complex}$ - $\delta_{sulfoxide}$ ) (ppm) of the sulfoxide ligands in the complexes  $\{Pt(R_2SO)Cl_2\}_2(\mu\text{-Me}_2pz)$ .

R <sub>2</sub> SO	$\mathbf{H}_{\alpha}$	$\mathbf{H}_{eta}$	$\mathbf{H}_{\gamma}$	$\mathbf{H}_{\delta}$	CH <sub>3</sub>
DMSO (in CD <sub>3</sub> COCD <sub>3</sub> )	$3.44$ $\Delta \delta = 0.96$				
TMSO	4.02, 3.61 $\Delta \delta = 1.19, 0.78$	2.40, 2.20 $\Delta \delta = 0.00, 0.22$			
DEtSO	3.70, 3.24 $\Delta \delta = 1.07, 0.61$	$1.63$ $\Delta \delta = 0.37$			
DPrSO	3.65, 3.21 $\Delta \delta = 1.09, 0.65$	$2.23$ $\Delta \delta = 0.49$	$1.23$ $\Delta \delta = 0.22$		
DBuSO	3.67, 3.24 $\Delta \delta = 0.86, 0.43$	2.21, 2.11 $\Delta \delta = -0.46, -0.56$	$1.62$ $\Delta \delta = -0.13$	$1.03$ $\Delta \delta = 0.44$	
MeBzSO	4.98, 4.76	7.53 (ortho)	7.47 ( <i>meta</i> )	7.47 (para)	3.05
DBzSO	4.91, 4.58 $\Delta \delta = 1.03, 0.70$	$7.59 (ortho)$ $\Delta \delta = 0.32$	7.47 (meta) $\Delta \delta = 0.13$	$7.47 (para)$ $\Delta \delta = 0.13$	
DPhSO		7.95 (ortho) $\Delta \delta = 0.32$	7.55 (meta) $\Delta \delta = 0.11$	7.55 ( $para$ ) $\Delta \delta = 0.11$	

The chemical shifts of the bonded sulfoxide ligands are more deshielded than are those of the free molecules (table 4.2.2.1). For the compound containing the tetramethylenesulfoxide ligands (TMSO), two signals are observed for the protons  $H_{\alpha}$  and two for the protons  $H_{\beta}$ . The protons closer to the oxygen atom are

the most deshielded upon coordination. For the other sulfoxide ligands, all being non-cyclic, two series of signals are also observed due to limited or slow rotation of the S-C bonds. The separation between the peaks of the geminal protons gets smaller as the distance from the coordination increases. Ultimately, the chemical shifts become superimposable ( $\delta(^{1}H_{\beta})$  for the DEtSO compound,  $\delta(^{1}H_{\beta})$  and  $^{1}H_{\gamma}$ ) for the DPrSO compound or  $\delta(^1H_{\nu}$  and  $^1H_{\delta})$  for the DBuSO compound). Similar observations were reported for the pyrimidine-bridged dimeric complexes,  $trans, trans = \{Pt(R_2SO)Cl_2\}_2(\mu-pyrimidine) (31)$  and their pyrazine analogues (2). The  $\Delta\delta$  values for protons in alpha position seem to increase for less bulky sulfoxide ligands. The angle C-S-C in TMSO is relatively small (95°), which makes the ligand the least sterically hindered and its  $\Delta\delta$  value the largest. No coupling of the sulfoxide protons with the <sup>195</sup>Pt core is observed. It can be explained by the fact that the sulfoxide signals are multiplets of low intensity, and consequently the <sup>195</sup>Pt satellites are very weak and overlap with the main signals. Furthermore, the poor solubility of the complexes results in important background noise.

**Table 4.2.3.4**  $^{13}$ C NMR  $\Delta\delta$  ( $\delta_{complex}$ - $\delta_{sulfoxide}$ ) (ppm) of the sulfoxide ligands in the complexes {Pt(R<sub>2</sub>SO)Cl<sub>2</sub>}<sub>2</sub>( $\mu$ -2,5-Me<sub>2</sub>pz).

R <sub>2</sub> SO	$C_{lpha}$	$\mathbf{C}_{oldsymbol{eta}}$	$\mathbf{C}_{\gamma}$	$C_{\delta}$	CH <sub>3</sub>
TMSO	$56.75$ $\Delta \delta = 2.36$	$24.71$ $\Delta \delta = -1.05$			
DEtSO	$48.60$ $\Delta \delta = 3.92$	$7.27$ $\Delta \delta = 0.66$			
DPrSO	$56.31$ $\Delta \delta = 2.11$	$16.67$ $\Delta \delta = 0.53$	$12.98$ $\Delta \delta = -0.29$		
DBuSO	$54.39$ $\Delta \delta = 2.77$	$24.69$ $\Delta \delta = 0.05$	$21.60$ $\Delta \delta = -0.44$	$13.74$ $\Delta \delta = 0.08$	
MeBzSO	62.02	131.63 ( <i>ortho</i> ), 129.79(C <sub>β</sub> )	129.19(meta)	129.05(para)	39.72
DBzSO	$60.09,$ $\Delta \delta = 2.87$	131.93 ( <i>ortho</i> ), 129.32(C <sub>β</sub> )	129.43( <i>meta</i> )	128.93( <i>para</i> )	
DPhSO	133.08, $\Delta \delta = -12.33$	131.93 (ortho), $\Delta \delta = 2.81$	$128.76(meta)$ $\Delta \delta = -0.34$	$128.85(para)$ $\Delta \delta = -1.98$	

The signals of the carbon atoms in an alpha position are observed at lower field than in the free molecules (table 4.2.2.2.). The difference in chemical shifts is ca. 2.8 ppm. An exception can be noticed for the complex containing the diphenylsulfoxide ligands, which is observed at very high field,  $\Delta\delta$  = -12.33 ppm. Comparable results were already noted for the Pt(R<sub>2</sub>SO)(pyrimidine)Cl<sub>2</sub> (30) and their pyrimidine-bridged dimeric analogues (31). The diphenylsulfoxide ligand is the most sterically hindered, but it is also different than the other sulfoxide ligands since it carries aromatic groups directly bridged on the bonding atom. This could be the

cause of the specific electronic effects of its complex. Actually, it undergoes the inductive effect of both the sulfoxide function and the phenyl rings. For the sulfoxide ligands, usually all the signals of the carbon atoms are less deshielded upon coordination than other types of ligands. The presence of the  $\pi$  (Pt  $\rightarrow$  S) bond increases the electronic density on the sulfoxide ligands. Furthermore, the presence of inverse polarization of the  $\pi$  (S=O) bond would also explain the results observed in the platinum-sulfoxide ligands complexes. Bonding to the platinum atom would reduce the  $\pi$  electron density on the oxygen atom ( $^{\delta}$ -S  $\leftarrow$  O $^{\delta+}$ ) and increase it on the sulfur atom and its neighbouring atoms, including the Pt atom as mentioned above. The chemical shifts in  $^{13}$ C-MR spectroscopy are particularly sensitive to such mesomeric affects. The inverse polarization of the  $\pi$  electrons in the S=O bond would be more important in the complex containing the diphenylsulfoxide ligands since the two electron attracting groups are bonded directly on the sulfur atom.

No work of this project has been done on solid-state NMR spectroscopy, but it would have been interesting to test it at least. This technique is not necessarily useful in coordination chemistry and more industrially oriented. It is particularly common to study solid metallic particles. It is also capable of providing information about the motional heterogeneity in polymer systems. This type of information can in turn be used to elucidate information about morphology in semi-crystalline and bi-amorphous systems. The solid-state NMR techniques for studying molecular motion are Inversion Recovery T1, Rotating Frame T1, Line Broadening and Cross Polarization Techniques. However, the potentials of these techniques remain largely untapped; at this point, the relationships among molecular motions, morphology, and

physical properties are still qualitative at best. Though NMR spectroscopy is used to study solids, extensive atomic-level molecular structural detail is especially challenging to obtain in the solid state. There is little signal averaging by thermal motion in the solid state. At room temperature, most molecules can only undergo restricted vibrations and rotations, each in a slightly different electronic environment, therefore exhibiting a different NMR absorption peak. Such a variation in the electronic environment of the resonating nuclei results in a blurring of the observed spectra, which is often only a broad Gaussian band for non-quadrupolar spins in a solid. It makes, thus, the interpretation of such broadened spectra either very difficult or impossible.

### 4.3 Infrared and Raman spectra

### **4.3.1 IR spectra of the complexes**

The vibrational spectra of the complexes were measured in the solid state between 4000 and about 280 cm<sup>-1</sup> and are summarized in the Table 4.3.1. In each spectrum, bands characteristic of the ligands are present. The IR spectrum of the free 2,5-dimethylpyrazine ligand has been reported by Arenas *et al.* (33) and our assignments for the bridging ligand are based on this study. The assignments are made on a basis of  $C_{2h}$  molecular geometry. The vibrations of coordinated 2,5-dimethylpyrazine are generally observed at higher energies than are those of the free ligand. For instance, the (v(CH),  $B_u$ ) vibration appears at 3080.8 cm<sup>-1</sup> in the free ligand and at around 3120 cm<sup>-1</sup> in the coordinated pyrazine derivative. The sharp and characteristic  $8a + \delta_{as}(CH_3)$  ( $A_u$  or  $B_u$ ) vibration is observed at 3031 and around

 $3046~\text{cm}^{-1}$ , respectively in the free and coordinated ligand. The band observed at  $1487.6~\text{cm}^{-1}$  in the uncoordinated 2,5-dimethylpyrazine is assigned to the  $19a~(v_{ring}, B_u)$  vibration and is found at around  $1499~\text{cm}^{-1}$  in our complexes. The very strong  $r(CH_3)~(B_u)$  vibrations is observed at  $1036.9~\text{cm}^{-1}$  in the free ligand and is displaced to around  $1074~\text{cm}^{-1}$  when the ligand is coordinated.

Table 4.3.1 Infrared assignments (cm $^{-1}$ ) of the complexes  $\{Pt(R_2SO)Cl_2\}_2(\mu-2,5-Me_2pz)$ .

assignment	TMSO	DPrSO	DBuSO	DMSO	DBzSO	DPhSO	DEtSO	MeBzSO
code	B1	B2	B3	B4	B5	B6	B7	B8
	3736.8	3736.9	3736.7 m	3736.9	3738.0	3738.3	3738.0	3737.4 m
	m	m		m	m	m	m	
ν(CH), B <sub>u</sub>	3125.0	3117.4	3123.0 m	3125.6	3104.2		3121.5	3121.5 vw
	vw	W		W	vw		W	
8a +	3045.8	3048.7	3042.1	3046.6	3056.1	3054.2	3033.8	3044.3 m
$\delta_{as}(CH_3), A_u$	msh	msh	msh	msh	wsh	m	wsh	
or B <sub>u</sub>								
$v_{as}(CH_3), A_u$				3016.2	3031.2 w			3007.0 w
or B <sub>u</sub>				W				
$v_{as}(CH_3), A_u$	2997.7	2961.4 s	2958.8 s		2982.8 w	2962.1	2971.4	2973.1 w
or B <sub>u</sub>	vw					vw	W	
$v_s(CH_3), B_u$	2934.4	2937.4	2933.1 m	2917.9	2923.9 w	2915.6	2927.6	2920.5 m
	m	m		m		W	W	
$2 \text{ X } \delta_{as}(\text{CH}_3),$	2873.5	2874.2	2871.9 m	2821.3		2851.8	2868.1	2851.8 vw
$B_{u}$	m	m		vw		vw	W	
$2 \text{ X } \delta_{\text{s}}(\text{CH}_3),$		2735.6			2787.1		2790.5	
$A_u$ or $B_u$		vw			vw		vw	
$8a + r(CH_3),$					2632.8	2649.9	2647.4	
$B_u$					vw	w	vw	
	2361.4	2361.1	2361.6 w				2359.5	2361.8 w
	w	W					W	
	2334.1	2332.8	2332.9 w	2242.9	2255.2	2259.3	2336.2	2332.8 w
	w	W		vw	vw	vw	W	
v(CX) + 12,	1992.0	1972.7	1985.8	1990.1	1961.0	1981.5	1992.7	1962.7 w
$B_{u}$	w	W	VW	vw	vw	W	W	
	1733.9		1818.7				1733.6	1891.5 vw
	vw		vw				vw	
14 + 6a, B <sub>u</sub>	1652.8	1651.6	1651.6	1639.4	1600.7 w	1593.2	1652.6	1652.6
	vw	vw	vw	vw		vw	vw	wsh
$r(CH_3) + 6a,$	1539.2	1540.3			1537.2	1578.7	1539.0	1538.6 vw
$\mathbf{B}_{\mathbf{u}}$	w	W			vw	w	vw	
$19a, v_{ring}, B_u$	1503.4	1502.0	1505.9 m	1505.0	1492.5	1488.7	1499.4	1495.0 m
,g, u	S	m		m	msh	w	w	
	1482.7 w		1489.1 m	1480.2 w			1485.9 w	

$\delta_{as}(CH_3), A_u$	1455.9	1457.0	1467.4 m	1444.0	1454.5	1472.8	1449.8	1455.3 m
or B <sub>u</sub>	w	m		vw	msh	w	mbr	
<u>u</u>	1442.0					1442.7		
	vw					m		
19b, $v_{ring}$ , $B_u$	1426.3	1424.4	1423.9 w	1430.6	1426.2 w	1426.2	1422.9	1427.5
170, Ting, 2u	wbr	W	1.201,	vw	1 .20.2	W	W	wbr
$\delta_{\rm s}({\rm CH_3}),{\rm B_u}$	1400.1	1403.9	1402.3 m	1400.7	1405.8 w	1385.3	1408.5	1394.8
og(0113), Du	m	W	110210 111	vw	1.00.0	W	W	wbr
	1384.3		1385.3 w	1382.8			,,,	,,,,,,
	w		1303.3 11	W				
	1373.2	1375.0		1373.1		1375.4	1379.8	
	w	W		vw		w	m	
δ(CH), B <sub>u</sub>	1346.1	1346.1	1345.4 m	1347.1	1339.7 w	1345.1	1345.1	1345.7 m
o(CII), <b>B</b> <sub>u</sub>	m	m	13 13.1 111	W	1337.7 W	w	m	13 13.7 111
	111	111		1320.2		• • • • • • • • • • • • • • • • • • • •	111	
				W				
r(CH <sub>3</sub> ) +	1305.6	1300.8	1314.2 w	1305.2	1299.7	1307.8		1303.2 w
$\gamma(CX)$ , $B_u$	W	W	1317.2 W	W	1299.7 VW	W		1303.2 W
$\frac{\gamma(CX), B_u}{\nu(CX), B_u}$	1265.2	1259.7	1284.5 w	1270.7	V VV	VV	1279.0	1268.8 vw
ν(CA), <b>D</b> <sub>ll</sub>	wbr	W	1207.J W	1270.7 VW			m	1200.0 VW
12 + 6a, B <sub>u</sub>	1250.7	1225.7	1234.8 w	1248.8	1250.3	1245.4	1251.2	1251.5 w
$12 \pm 0a$ , $D_{\rm u}$	1230.7 VW	VW	1234.0 W	1240.0 VW	1230.3 VW	1243.4 VW	W	1231.3 W
14, ν <sub>ring</sub> , B <sub>u</sub>	1163.4	1161.4	1202.1 w	1163.1	1167.1	VVV	VV	1165.6 s
14, V <sub>ring</sub> , D <sub>u</sub>	m		1202.1 W	mbr	mbr			1105.0 8
ν(S-O)	1140.6	m 1134.3	1143.0	1138.0	1117.3	1147.4	1146.9	1124.9 s
v(3-O)	sbr	vsbr	vsbr	sbr	mbr	mbr	vsbr	1124.98
	501	V S U 1	1108.8 w	301	11101	11101	VSUI	
$1 + \delta(CX)$ ,	1009 1	1006.0		1094.5		1004.7	1004.2	1097.4 vw
	1098.1	1096.9	1093.1 w			1094.7	1094.2	1097.4 VW
B <sub>u</sub>	VW	W	1000 0	W	1072.6	w 1069.7	W	1074 6
$r(CH_3), B_u$	1077.6	1073.7	1080.0 m		wsh		1071.0	1074.6 w
	s 1032.0	m	1041 4	10227.0		m 1020 1	1031.7	1029.8 w
		1033.0	1041.4 w	1032.7 s	1029.8 w	1020.1		1029.8 W
(CII ) A	m	W	000 6	000 0	072.7	W	m 070.9	060.0 =
$r(CH_3), A_g$	990.5 m	986.1 w	989.6 w	990.9 w	972.7 vw	997.8 w	979.8	969.0 s
				044.5			mbr	
d S(GW)	050.5		022.5	944.5 w	001.0	0000		022.2
$6b + \delta(CX)$ ,	958.5 w		922.5	928.0	921.2 w	922.2		922.2 w
B <sub>u</sub>	000.0	004.6	msh	wsh	002.0	VW	0040	007.7
$\gamma$ (CH), $A_u$	889.8	884.6 w	900.2 w	889.6 m	882.0 w	901.3 w	894.0 m	887.7 wsh
	msh	0.10.1						
1.01 (077)		869.4 w	792.0 w					811.0 w
16b + v(CX),	757.6	760.5	758.3 vw	759.6	764.9 s	756.2 w	786.2 s	766.7 ssh
Bu	wsh	msh		VW				
12, $\delta_{\text{ring}}$ , $B_{\text{u}}$		739.9 m	743.1 m	735.4 m		746.4 m		719.9 w
			728.5 m			713.2 w		
$r(CH_3)$ -	674.2 m	667.7 w	667.8 w	695.6 m	696.7 vs	698.2 m	684.8 vs	698.3 vs
$\gamma(CX), A_{u}$								
						682.7 m	654.8 m	
						613.9 w		
	594.8 s	593.1		573.7	579.6 m	562.6 vs		590.5 m
		vw		vw				
ν(Pt-N)	512.8	511.8 s	519.7 w	not	not	524.8 vs	506.8 m	not
	vw			observed	observed			observed
			498.6 m				472.7 m	484.4 s

ν(Pt-S)	454.7 m	450.3 s	455.2 m	443.4 s	482.7 s	439.6 m	451.8 m	449.3 s
16b, γ <sub>ring</sub> , A <sub>u</sub>			425.8 w		414.1 m		429.2 s	
				376.6 m				378.9 w
ν(Pt-Cl)	353.2	353.4 vs	353.2 vs	353.0 vs	350.5 m	351.7 s	348.9 vs	346.6 vs
	VS							
					318.9 m	327.8 w	332.9	
							msh	
$\delta(CX), B_u$	301.4 w	302.1 w	303.2 w	302.9 w	301.8 vw	307.0 w	303.2 w	301.8 msh

The v(S–O) vibrations of our complexes absorb between 1124 and 1147 cm<sup>-1</sup>. This broad and intense characteristic vibration has more energy than in the free sulfoxide ligands. For instance, free dimethylsulfoxide shows a vibration at 1050 cm<sup>-1</sup>, whereas the coordinated ligand absorbs at 1138 cm<sup>-1</sup>. The average displacement for the v(S–O) vibration in the sulfoxide ligands is around 106 cm<sup>-1</sup>. This is what is expected when the ligands are bonded to the platinum center by the sulfur atom. The S–O d $\pi$ –p $\pi$  bond is strengthened upon coordination to the metal, since mesomer-III is favored (section 1.5). It is interesting to notice that the starting material, the monosubstitued complexes K[Pt(R<sub>2</sub>SO)Cl<sub>3</sub>], already show this energy displacement compared to the free sulfoxide ligands (34). The band is less displaced, however, than in our disubstituted complexes, viz., by about 30 cm<sup>-1</sup>. For instance, the band observed for K[Pt(DMSO)Cl<sub>3</sub>] is at 1101 cm<sup>-1</sup>. The phenomenon is probably amplified by the kinematic coupling occurring between the v(S-O) and v(M-S) vibrational modes.

The IR spectra show only one stretching v(Pt-Cl) vibration between 346 and 354 cm<sup>-1</sup>, suggesting a *trans* geometry, since two bands are usually observed for *cis* complexes (30,35-37). These predictions are expected for the  $C_{2v}$  and  $D_{2h}$  geometries for this type of complex (structural framework  $Cl_2LLPtNNPtLL'Cl_2$ ), respectively, and provide another argument in favor of the geometry suspected from

the  ${}^3J(^{195}\text{Pt-H}_{3-6})$  coupling constants observed in the  ${}^1\text{H-NMR}$  spectroscopy study. A comparison can be made with the compound,  $trans, trans-\{\text{Pt(CO)Cl}_2\}_2(\mu-\text{pz})$ , where the stretching vibration was observed at 357 cm $^{-1}$ , i.e., slightly higher than for our compounds (27).

One absorption band is observed around 450 cm<sup>-1</sup> and can be assigned to a v(Pt-S) stretching mode, as suggested in the literature (38-42). A band between 506 and 525 cm<sup>-1</sup> is assigned to the v(Pt-N) stretching vibration, based also on some earlier published results (43,44). The chief difference among our complexes, viz., the nature of the coordinated sulfoxide ligand, does not seem to influence either the v(Pt-S) or the v(Pt-N) vibrations. Only the v(Pt-S) vibration of trans, trans- $Pt(DBzSO)Cl_2\}_2(\mu-Me_2pz)$  is observed at higher energy than for the other complexes, at 483 cm<sup>-1</sup>. A similar difference was also noted for the pyrazine analogues, where the v(Pt-S) mode was observed at 478 cm<sup>-1</sup> for trans, trans- $Pt(DBzSO)Cl_2\}_2(\mu-pz)$  (2), as well as for the associated monomeric complex, where this vibration was observed at 483 cm<sup>-1</sup>, for trans- $Pt(pz)(DBzSO)Cl_2$  (3).

### **4.3.2** Raman spectroscopy of the complexes

The Raman spectra of the complexes were measured between 4000 and about 200 cm<sup>-1</sup> and the data are summarized in Table 4.3.2. In each spectrum, there are bands characteristic of the ligands present. The Raman spectrum of the free 2,5-dimethylpyrazine ligand has been reported by Arenas *et al.* (33) and our assignments for the bridging ligand are based on this study. The vibrations of coordinated 2,5-dimethylpyrazine are almost all observed at higher energies than are those of the free ligand.

Table 4.3.2 Raman assignments (cm  $^{\text{-}1}$  ) of the complexes  $\{Pt(R_2SO)Cl_2\}_2(\mu\text{-}2,5\text{-}Me_2pz).$ 

assignment	free Me <sub>2</sub> pz	DMSO	DEtSO	TMSO	DPrSO	DBuSO	DBzSO	DPhSO	MeBzSO
code	•	B4	В7	B1	B2	В3	B5	В6	B8
		3578.8 msh	3579.0 msh	3579.0 wsh	3579.1 ms	3578.2 msh	3579.2 msh	3578.7 msł	3579.2 m
ν(CH), A <sub>g</sub>	3030 s	3019.6 vw				3070.5 vw	3058.9 w	3067.6 w	3069.2 vw
$v_{as}(CH_3), B_g$	2980 sh	3009.3 vw		2996.5 vv					
$v_{as}(CH_3), A_g$	2960 m		2975.8 vw		2971.3 vv	2971.1 vw			
$v_{as}(CH_3), A_g$				2937.1 w	2941.9 vv				
$v_s(CH_3), A_g$	2921vvs	2920.4 m	2928.7 m		2919.2 m	2923.5 m	2927.8 w	2923.3 w	2920.2 w
$\begin{array}{c} 2 \ X \ \delta_{as}(CH_3), \\ A_g \end{array}$	2875 sh	2872.6 wsh	2872.4 w	2872.3 vv	2872.6 ws	2872.4 w	2872.4 msh	2871.2 msł	2872.4 w
$8a, v_{ring}, A_g$	1583 s	1620.4 m	1615.6 m	1612.8 m	1610.5 m	1613.3 m	1603.1 s	1607.4 m	1605.7 m
	-		-		-		-	1579.6 s	
$8b, v_{ring}, A_g$	1526 w	1517.4 w	1514.3 w	15168 w	1520.1 w	1515.2 w		1512.6 w	1516.8 w
$\delta_{as}(CH_3), A_g$ or $B_g$	1442 b	1425.7 vwbr	1443.3 w		1448.7 w	1440.9 m		1440.0 w	1426.8 vw
			1408.5 w		1410.4 vv	1405.6 w	1402.0 w		
$\delta_s(CH_3), A_g$	1378 m	1371.5 w	1382.0 m	1372.7 w	1374.0 w	1383.3 w	1379.1 vw	1374.2 w	1372.2 w
$\delta$ (CH), A <sub>g</sub>	1304 w	1324.1 w	1279.7 w	1321.3 vv	1295.9 w	1308.0 w		1308.4 w	1312.0 vw
$\nu(CX), A_g$	1231 s	1271.5 s	1240.6 s	1240.0 s	1242.0 s	1239.7 s	1267.0 m		1241.2 m
							1205.4 w	1207.6 w	1199.8 w
v(S-O)	-	1136.1 mbr	1146.2 wbr	1140.0 w	1132.7 mb	1140.0 m	1158.8 wbr	1145.2 mb	1161.1 wbr
			1076.0 w	1078.3 w		1110.1 w		1072.5 w	
$r(CH_3), B_g$	1039 vw		1053.3 w	1051.9 vv		1051.5 w		1052.0 w	
$12 + \delta(CX),$ $A_g$	1020 w	1032.6 vw	1018.8 vw	1034.5 w			1031.1 m	1021.8 m	1029.0 w
r(CH <sub>3</sub> ), A <sub>g</sub>	980 vw	982.5 vw	968.6 vw				1002.7 s	998.4 s	1003.3 s
				959.6 vw			942.7 vw		
γ(CH), B <sub>g</sub>	931 vw	913.8 w	907.0 w	914.6 vw					911.4 vw
$1, \nu_{\rm ring}, A_{\rm g}$	860 vs	891.0 m	886.1 m	890.3 m	887.6 w	886.7 s		888.4 w	890.1 w
2 x 16b, A <sub>g</sub>	822 vw			869.3 w			832.7 w	865.1 vw	811.2 vw
$4, \gamma_{\rm ring}, A_{\rm g}$	750 vw	733.3 w			761.2 w	748.0 w	763.5 w	747.7 w	769.0 w
$r(CH_3)$ - $\gamma(CX)$ , $A_g$	708 vw	716.2 w	714.6 vw	715.0 w	716.1 m	712.7 m		716.2 m	717.2 m
6b, $\delta_{ring}$ , $A_g$	650 w	696.0 s	684.2 m	674.1 w		675.8 vw	689.9 m	698.6 s	654.9 s
		650.0 vw					659.3 w		
							618.5 w	611.7 m	619.1 w
6a, $\delta_{ring}$ , $A_g$	499 m	505.7 m	507.9 m	505.3 m	502.3 m	506.7 m	507.9 w	503.1 m	505.9 m
		460.6 w	476.4 w			12 : =			
v(Pt-S)	-	437.8 m	426.9 m		• • •	424.7 vw	413.9 m	425.9 w	444.1 w
$\delta(CH_3), A_g$	387 w	385.6 w	373.9 vw	381.8 m	397.4 vw	373.1 w		390.2 w	387.1 w
(D) (C!)		225.2	345.8 m	2242	222.1	226.0	222.5.1	224.2	222.5
v(Pt-Cl)	-	335.2 vs	330.5 vs	334.2 vs		336.0 vs	333.5 sbr		332.5 vs
		315.8 w	273.7 w		293.4 m			302.4 w	

ν(Pt-N)	248.7 vs	246.0 m	241.7 m	265.0 m	259.6 m	274.4 w	267.0 m	280.3 vw
	219.1 w		212.5 m	226.0 m	229.3 m	239.3 w	236.1 w	237.9 w
						206.4 m	207.8 m	220.4 vw

In 2,5-dimethylpyrazine, the hydrogen atom of each methyl group lying in the aromatic plane is in a *trans* conformation with respect to the closest nitrogen atom. Therefore, 2,5-dimethylpyrazine shows an inversion center. According to the mutual exclusion principle, the Raman-active modes are inactive in the IR. Then, the 42 normal vibrations are divided into  $14A_g + 8\ A_u + 7B_g + 13B_u$ .

Platinum-halogen stretching vibrations are always observed in the region 600-200 cm<sup>-1</sup>. The stretching Pt-Cl band is undoubtedly observed at 336-330 cm<sup>-1</sup>, as it is for similar compounds, trans, trans-{Pt(R<sub>2</sub>SO)Cl<sub>2</sub>}<sub>2</sub>( $\mu$ -pz) (337-33 cm<sup>-1</sup>), trans, trans-{Pt(TMSO)Cl<sub>2</sub>}( $\mu$ -pz){Pt(R<sub>2</sub>SO)Cl<sub>2</sub>} (338-329cm<sup>-1</sup>) (Chapter III). The peak is always clear and intense. These observations are also in agreement with almost all the published work to date, suc as [Pt<sup>IV</sup>(CN)<sub>5</sub>Cl]<sup>2-</sup>, 330 cm<sup>-1</sup> (45), trans-Pt(di(1-naphthyl)methylarsine)<sub>2</sub>Cl<sub>2</sub>, 316 cm<sup>-1</sup> (46) or trans-Pt(n-hydroxypyridine)<sub>2</sub>Cl<sub>2</sub> (n = 3,4), 328 and 336 cm<sup>-1</sup> (47).

The Pt-S stretching mode is generally observed in the 480-400 cm<sup>-1</sup> window. For our compounds, this band is detected at 444-414 cm<sup>-1</sup>. This result is in agreement with what was observed for Pt(2,2'-bipyridine)(4-CN-C<sub>6</sub>F<sub>4</sub>S)<sub>2</sub>, 405 cm<sup>-1</sup>, and Pt(1,10-phenanthroline)(4-CN-C<sub>6</sub>F<sub>4</sub>S)<sub>2</sub>, 414 cm<sup>-1</sup> (48), for the K[Pt(R<sub>2</sub>SO)Cl<sub>3</sub>] series of compounds, between 427 and 447 cm<sup>-1</sup>, and for the *cis*-Pt(R<sub>2</sub>SO)(pz)I<sub>2</sub> compounds, between 484 and 448 cm<sup>-1</sup> (section 7.3).

Assignment of the Pt-N stretching mode it is not as straightforward. Some researchers have placed this mode in the 570-530 cm<sup>-1</sup> region, while others have

located it in the 270-230 cm<sup>-1</sup> region, depending of whether or not it is a ring nitrogen. For instance, Pfennig et al. have assigned this Pt-N stretching modes to the bands at 475 and 508 cm<sup>-1</sup> in  $(NH_3)_5Pt^{IV}(\mu-NC)Fe^{II}(CN)_5$  and at 472 and 506 cm<sup>-1</sup> in the  $[(NC)_5Fe^{II}(\mu-CN)Pt^{IV}(NH_3)_4(\mu-NC)Fe^{II}(CN)_5]^{4-}$  ion (49). Hegmans *et al.* have attributed bands at 529 and 541 cm<sup>-1</sup> to v(Pt-N) modes in trans-Pt(9cm<sup>-1</sup> methyladenine)(NH<sub>3</sub>)I<sub>2</sub> 541 and 575 trans-Pt(9and at ethylguanine)(NH3)Cl<sub>2</sub> (50). On the other hand, Chowdhury et al. have assigned them between 249 and 170 cm<sup>-1</sup> in trans-Pt(n-hydroxypyridine)<sub>2</sub>Cl<sub>2</sub> (n = 3 or 4) and at 199 cm<sup>-1</sup> in Pt(3-hydroxypyridine)<sub>3</sub>Cl (47). Michalska and Wysokiński have assigned the  $v(Pt-N_{ring})/v(Pt-NH_3)$  modes at 256/544, 253/485, 241/492 and 252/494for cis-[Pt(2-picoline)(H<sub>2</sub>O)<sub>2</sub>(NH<sub>3</sub>)<sub>2</sub>]<sup>2+</sup>, cis-[Pt(2-picoline)(H<sub>2</sub>O)-524 (NH<sub>3</sub>)<sub>2</sub>Cl<sub>1</sub><sup>+</sup>, cis-Pt(2-picoline)(NH<sub>3</sub>)<sub>2</sub>Cl<sub>2</sub> and cis-Pt(orotato)(NH<sub>3</sub>)<sub>2</sub>, respectively (51). For the above reasons, the bands observed for our compounds between 280 and 241 cm<sup>-1</sup> are assigned to v(Pt-N) modes.

It has been shown that substitution of hydrogen atoms by methyl groups in any aromatic ring generally causes vibrational modes to shift to lower wavenumbers (52). For instance, the ring breathing mode for pyrazine,  $v_{1(ring)}$  ( $A_g$ ), which is observed at 860 cm<sup>-1</sup> for the free molecule and in the 886-891 cm<sup>-1</sup> window for *trans,trans*-{Pt(R<sub>2</sub>SO)Cl<sub>2</sub>}<sub>2</sub>( $\mu$ -dmpz), occurs at 1013 cm<sup>-1</sup> in free pyrazine and between 1047 and 1067 cm<sup>-1</sup> in *trans,trans*-{Pt(TMSO)Cl<sub>2</sub>}( $\mu$ -pz){Pt(R<sub>2</sub>SO)Cl<sub>2</sub>}. The same situation exists for the mode 6a ( $A_g$ ) for which bands are observed at 502-508 cm<sup>-1</sup> for *trans*-{Pt(R<sub>2</sub>SO)Cl<sub>2</sub>}<sub>2</sub>( $\mu$ -Me<sub>2</sub>pz) (free Me<sub>2</sub>pz: 499 cm<sup>-1</sup>) and in the 658-680 cm<sup>-1</sup> window for *trans,trans*-{Pt(TMSO)Cl<sub>2</sub>}( $\mu$ -pz){Pt(R<sub>2</sub>SO)Cl<sub>2</sub>} (free pz: 596

cm<sup>-1</sup>).On the other hand, the fundamental ring modes, 8a and 8b, are observed at similar positions in both cases, in the 1500 cm<sup>-1</sup> region. This behaviour has also been noticed for other similar molecules by Arenas *et al.* (53,54).

The CH stretching vibrations are observed in the usual 3000 cm<sup>-1</sup> region for aromatic molecules. The CH bending vibrations appear in the 1324-1280 cm<sup>-1</sup> window, which is similar to that observed for the *trans,trans*-{Pt(R<sub>2</sub>SO)Cl<sub>2</sub>}<sub>2</sub>( $\mu$ -pz) compounds (1226-1217 cm<sup>-1</sup>). The asymmetric bending modes of the methyl groups,  $\delta_{as}$ (CH<sub>3</sub>) (A<sub>g</sub>/B<sub>g</sub>), are observed in the 1449-1425 cm<sup>-1</sup>. These modes are of low intensity, except for *trans*-{Pt(DBuSO)Cl<sub>2</sub>}<sub>2</sub>( $\mu$ -Me<sub>2</sub>pz). The analogous symmetric modes,  $\delta_{s}$ (CH<sub>3</sub>) (A<sub>g</sub>), are observed at lower energy, 1393-1371 cm<sup>-1</sup>.

# 4.4. Single-crystal X-ray diffraction studies of trans,trans-{Pt(DEtSO)Cl<sub>2</sub>}<sub>2</sub>(μ-Me<sub>2</sub>pyrazine) (I) and trans,trans-{Pt(DBuSO)Cl<sub>2</sub>}<sub>2</sub>(μ-Me<sub>2</sub>pyrazine) (II)

The structural results obtained from the multinuclear NMR and infrared spectroscopic analyses can be further confirmed by single-crystal X-ray diffraction of (I) and (II).

# 4.4.1 Crystal structure of the dimeric species ( $\{Pt(DEtSO)Cl_2\}_2(\mu\text{-Me}_2pyrazine)$

A suitable crystal of (**I**) was obtained by recrystallization of about 4 mg of the complex from a 20-mL chloroform:methanol (2:1) mixture. The solvent mixture, enclosed with protective parafilm into which a few holes had been pierced, was allowed to evaporate slowly in a refrigerator at about 5°C. The crystal obtained had a yellow rectangular shape of approximate dimensions 0.31 x 0.07 x 0.07 mm. It was mounted on a glass fiber using Paratone N hydrocarbon oil. The collection of the

crystallographic data  $(2\theta/\theta)$  was performed at low temperature (173(2) K) in order to minimize the background noise.

The crystal data and structure refinement details are included in Table 4.4.1.1. The measurements were made on a Bruker APEX II area detector diffractometer equipped with graphite-monochromated MoKα radiation. Frames corresponding to an arbitrary hemisphere of data were collected using  $\omega$  scans of 0.5° counted for a total of 10 s per frame. An orientation matrix, corresponding to cell constants listed in Table 4.4.1.1., was obtained from a least-squares refinement using the measured positions of 4909 centered reflections in the range  $2.38^{\circ} < \theta <$ 28.08°. The program used for retrieving cell parameters and data collection was APEX II (55). Data were integrated using the program SAINT (56). The data were then corrected for Lorentz and polarization effects. Face-indexed and multiscan absorption corrections were both performed, using the XPREP (57) and SADABS (58) programs, respectively. The structure was solved and refined using SHELXS-97 and SHELXL-97 (59). All non-H atoms were refined anisotropically. The hydrogen atoms were placed at idealized positions. Neutral atom scattering factors were taken from the International Tables for X-Ray Crystallography (60,61). All calculations and drawings were performed using the SHELXTL package (62). The final model was checked for missed symmetry or voids in the crystal structure using the PLATON software (63,64). None was found. This crystal structure gave a satisfactory chekcif report.

Table 4.4.1.1 Crystal data and structure refinement for (I)

Identification code fdr005 (B7)

Formula weight 852.48
Temperature 173(2) K
Wavelength 0.71073 Å
Crystal system Monoclinic

Space group C2/m

Unit cell dimensions a = 13.069(6) Å  $\alpha = 90^{\circ}$ .

b = 11.309(5) Å  $\beta = 91.567(5)^{\circ}.$ 

c = 8.292(4) Å  $\gamma = 90^{\circ}$ .

Volume  $1225.1(10) \text{ Å}^3$ 

 $\mathbf{Z}$ 

Density (calculated) 2.311 Mg/m<sup>3</sup>
Absorption coefficient 12.025 mm<sup>-1</sup>

F(000) 796

Crystal size  $0.31 \times 0.07 \times 0.07 \text{ mm}^3$ 

 $\theta$  range for data collection 2.38 to 25.99°.

Index ranges -16 <= h <= 16, -13 <= k <= 13, -10 <= l <= 10

Reflections collected 6213

Independent reflections 1270 [R(int) = 0.0560]

Observed Reflections 1180 [I> $2\sigma(I)$ ]

Completeness to  $\theta = 25.99^{\circ}$  99.7 %

Absorption correction Semi-empirical from equivalents

Max. and min. transmission 0.4330 and 0.1052

Refinement method Full-matrix least-squares on F<sup>2</sup>

Data / restraints / parameters 1270 / 6 / 112

Goodness-of-fit on  $F^2$  1.213

Final R indices [I>2 $\sigma$ (I)] R1 = 0.0385, wR2 = 0.0975 R indices (all data) R1 = 0.0421, wR2 = 0.1029 Largest diff. peak and hole 3.814 and -3.218 e.Å<sup>-3</sup> The compound crystallizes in the space group C2/m. Two disordered conformations were present in a 50:50 ratio. Some atoms are common to both conformations (Table 4.4.1.2.). Although no atom is actually located on it, the compound is situated on a specific equipoint - the 2a equipoint of local symmetry 2/m, in the center of the cycle. The mirror plane is a bisector of the *cis* Cl-Pt-Cl angles (Fig. 4.4.1.1.) and contains the atoms Pt1, S1 and N1, as well as their equivalent atoms by symmetry, Pt1B, S1B and N1B. These atoms are located on the specific equipoint 4i, of local symmetry m. The other atoms are on the general equipoint, but they all have an occupancy level of 0.5. The 2-fold axis is located in the center of the cycle, orthogonal to the mirror plane. The table below gives the atomic partitioning for the two conformations.

**Table 4.4.1.2** Atomic partitioning for the two possible conformations in the crystal framework of (**I**).

Conformation 1	Belong to both	Conformation 2
	conformations	
Cl1, Cl2	Pt1	
C1, C2, C3, C1B, C2B C3B	N1, N1B	C1A, C2A, C3A, C1C, C2C, C3C
O1, C4, C5, C6, C7	<b>S</b> 1	O1A, C4A, C5A, C6A, C7A
Cl1B, Cl2B	Pt1B	C11C, C12C
O1B, C4B, C5B, C6B, C7B	S1B	O1C, C4C, C5C, C6C, C7C

Equipoints: A: x, -y, z; B: -x, -y, -z+2; C: -x, y, -z+2

It is possible to assign the atoms to their respective conformations and eliminating conformations with contacts too short within non bonded atoms. For instance, the atomic distance between the C3 atom from a conformation and the C12 atom from another conformation is 1.93(2) Å. However, the sum of the Van der Waals radii is 3.45 Å. For the sulfoxide ligands, the distance between the H5A and C11 of two different conformations is 1.69 Å, whereas the sum of the Van der Waals radii is 2.95 Å (1).

**Table 4.4.1.3** Atomic coordinates  $(x10^4)$  and equivalent isotropic displacement parameters  $(\mathring{A}^2 \ x \ 10^3)$  for (**I**). U(eq) is defined as one third of the trace of the orthogonalized  $U^{ij}$  tensor.

	Occ.	X	у	Z	U(eq)
Pt(1)	1	2097(1)	0	7603(1)	29(1)
S(1)	1	3485(2)	0	6156(4)	54(1)
Cl(1)	0.50	2731(3)	-1597(4)	9006(6)	48(1)
Cl(2)	0.50	1348(4)	1601(5)	6345(6)	49(1)
O(1)	0.50	4199(9)	-811(11)	6121(15)	42(3)
N(1)	1	808(6)	0	9010(10)	27(2)
C(1)	0.50	760(11)	769(11)	10188(15)	28(3)
C(2)	0.50	62(10)	-816(12)	8821(17)	29(3)
C(3)	0.50	104(13)	-1765(18)	7520(20)	50(4)
C(4)	0.50	4104(14)	1382(11)	6810(20)	63(6)

C(5)	0.50	4547(18)	1260(20)	8540(20)	74(7)
C(6)	0.50	3214(12)	570(15)	4131(13)	50(4)
C(7)	0.50	2528(18)	-339(19)	3230(20)	73(8)

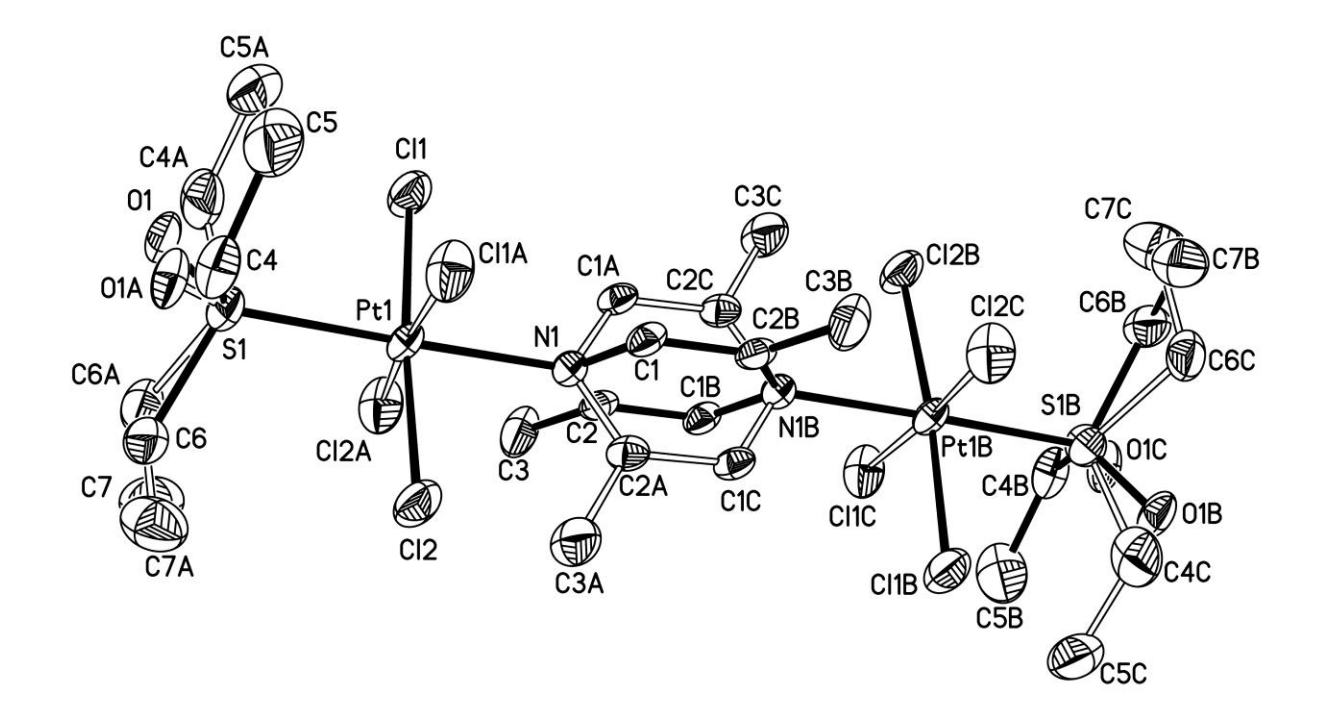


**Figure 4.4.1.1** ORTEP view of (**I**). (disorder, 2 orientations) showing the numbering scheme adopted. Anisotropic atomic displacement ellipsoids are shown at the 40% probability level. The symmetry transformations used to generate the atoms are labelled A (x, -y, z), B (-x, -y, -z+2) and C (-x, y, -z+2).

The bond lengths and angles for the complex are summarized in Table 4.4.1.4. The symmetry transformations used to generate the equivalent points are -x,-y,-z+2. The torsion angles are summarized in Table 4.4.1.5.

**Table 4.4.1.4** Bond lengths  $[\mathring{A}]$  and angles  $[^{\circ}]$  for (I).

Pt(1)-N(1)	2.075(9)	N(1)-C(1)	1.310(12
Pt(1)-S(1)	2.202(3)	N(1)-C(2)	1.348(14
Pt(1)-Cl(1)	2.291(4)	C(1)-C(2)#1	1.37(2)
Pt(1)-Cl(2)	2.295(4)	C(2)-C(1)#1	1.37(2)
S(1)-O(1)	1.309(11)	C(2)-C(3)	1.52(2)
S(1)-C(6)	1.825(8)	C(4)-C(5)	1.53(2)
S(1)-C(4)	1.836(9)	C(6)-C(7)	1.54(2)
N(1)-Pt(1)-S(1)	178.8(2)	C(1)-N(1)-C(2)	119.5(11)
N(1)-Pt(1)-Cl(1)	90.14(17)	C(1)-N(1)-Pt(1)	118.4(7)
S(1)-Pt(1)-Cl(1)	89.11(12)	C(2)-N(1)-Pt(1)	122.0(8)
N(1)-Pt(1)-Cl(2)	85.01(18)	N(1)-C(1)-C(2)#1	121.8(12)
S(1)-Pt(1)-Cl(2)	95.73(13)	N(1)-C(1)-H(1)	119.1
Cl(1)- $Pt(1)$ - $Cl(2)$	175.14(13)	C(2)#1-C(1)-H(1)	119.1
O(1)-S(1)-C(6)	110.3(8)	N(1)-C(2)-C(1)#1	118.6(12)
O(1)-S(1)-C(4)	107.1(8)	N(1)-C(2)-C(3)	121.7(13)
C(6)-S(1)-C(4)	92.6(9)	C(1)#1-C(2)-C(3)	119.7(12)
O(1)-S(1)-Pt(1)	127.6(6)	C(5)-C(4)-S(1)	110.6(11)
C(6)-S(1)-Pt(1)	111.1(5)	C(7)-C(6)-S(1)	107.8(10)
C(4)-S(1)-Pt(1)	101.6(6)		

Symmetry transformations used to generate equivalent atoms:

<sup>#1 -</sup>x,-y,-z+2

**Table 4.4.1.5** Torsion angles  $[^{\circ}]$  for (I).

Cl(1)-Pt(1)-S(1)-O(1)	10.2(7)
Cl(2)-Pt(1)-S(1)-O(1)	-170.3(7)
Cl(1)-Pt(1)-S(1)-C(6)	150.2(6)
Cl(2)-Pt(1)-S(1)-C(6)	-30.2(6)
Cl(1)-Pt(1)-S(1)-C(4)	-112.4(6)
Cl(2)-Pt(1)-S(1)-C(4)	67.2(6)
Cl(1)-Pt(1)-N(1)-C(1)	101.0(8)
Cl(2)-Pt(1)-N(1)-C(1)	-78.7(8)
Cl(1)-Pt(1)-N(1)-C(2)	-74.2(8)
Cl(2)-Pt(1)-N(1)-C(2)	106.2(8)
C(2)-N(1)-C(1)-C(2)#1	-4(2)
Pt(1)-N(1)-C(1)-C(2)#1	-179.4(10)
C(1)-N(1)-C(2)-C(1)#1	4(2)
Pt(1)-N(1)-C(2)-C(1)#1	179.1(9)
C(1)-N(1)-C(2)-C(3)	-177.2(13)
Pt(1)-N(1)-C(2)-C(3)	-2.1(17)
O(1)#2-S(1)-C(4)-C(5)	-111(3)
O(1)-S(1)-C(4)-C(5)	-63.7(17)
C(6)-S(1)-C(4)-C(5)	-175.9(15)
C(4)#2-S(1)-C(4)-C(5)	-38(2)
Pt(1)-S(1)-C(4)-C(5)	72.0(15)
O(1)-S(1)-C(6)-C(7)	78.5(14)
C(4)-S(1)-C(6)-C(7)	-172.2(13)
Pt(1)-S(1)-C(6)-C(7)	-68.7(13)

Symmetry transformations used to generate equivalent atoms:

#1 -x,-y,-z+2 #2 x,-y,z

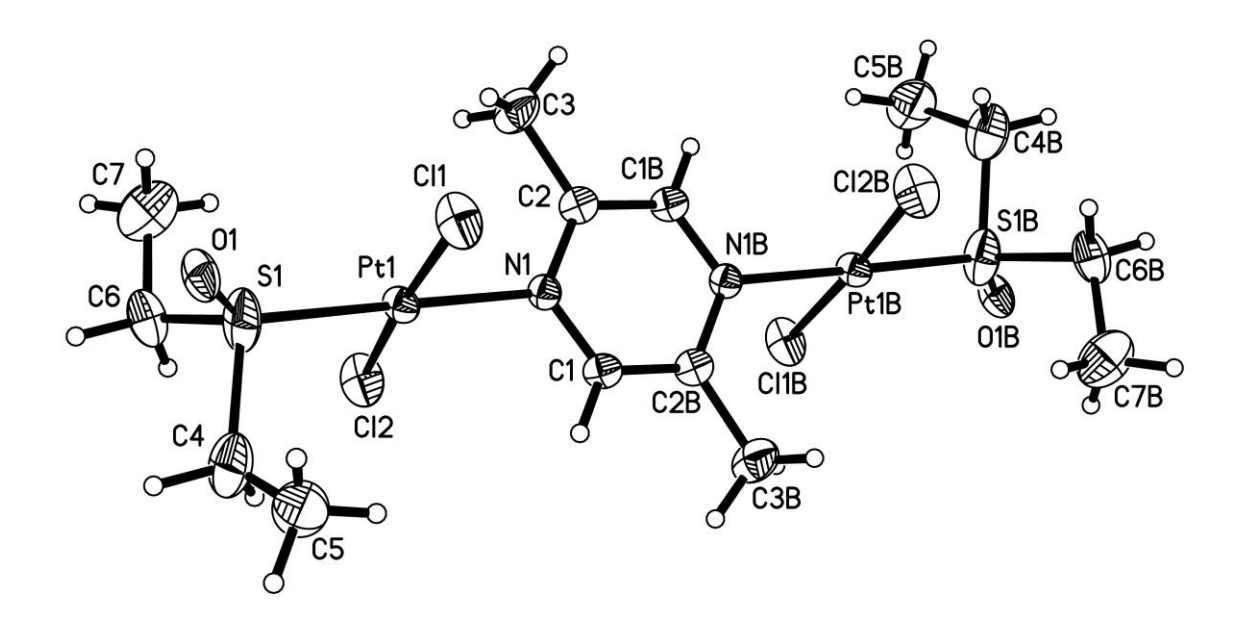


**Figure 4.4.1.2** ORTEP view of (**I**) (conformation 1) showing the numbering scheme adopted. Anisotropic atomic displacement ellipsoids for the non-hydrogen atoms are shown at the 40% probability level. Hydrogen atoms are represented by spheres of arbitrary size. The symmetry transformations used to generate the atoms is labelled B (-x, -y, -z+2).

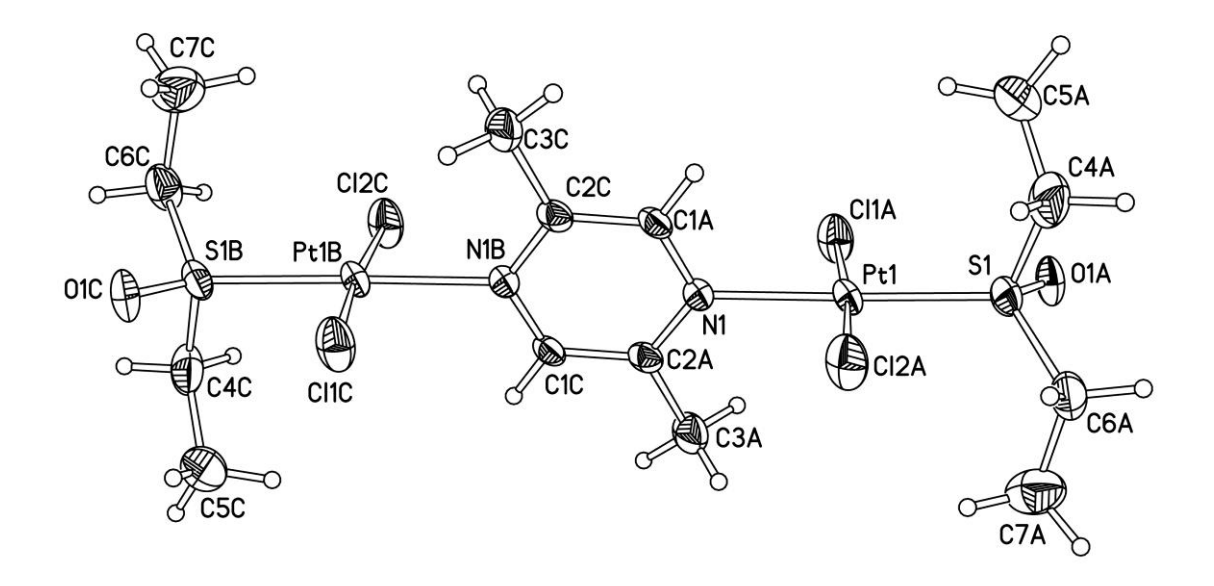
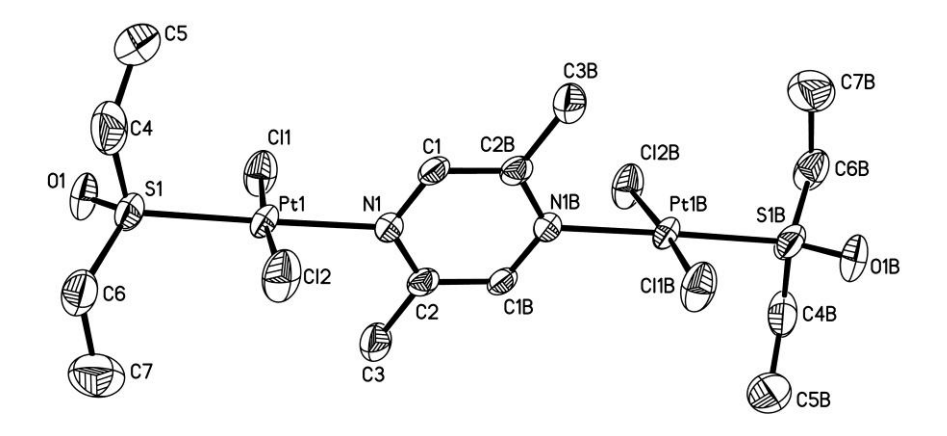


**Figure 4.4.1.3** ORTEP view of (**I**) (conformation 2) showing the numbering scheme adopted. Anisotropic atomic displacement ellipsoids for the non-hydrogen atoms are

shown at the 40% probability level. Hydrogen atoms are represented by spheres of arbitrary size. The symmetry transformations used to generate the atoms are labelled A (x, -y, z), B (-x, -y, -z+2) and C (-x, y, -z+2).

```
Least-squares planes (x,y,z) in crystal coordinates) and deviations from them
```

```
(* indicates atom used to define plane)
 5.7109 (0.0206) \times + 6.9292 (0.0188) \text{ y} + 5.3592 (0.0123) \text{ z} = 5.2821
(0.0092)
    -0.0102 (0.0017)
                        Pt1
    -0.0026 (0.0023)
                        C11
    -0.0026 (0.0022)
                        C12
     0.0074 (0.0021)
                        S1
     0.0081 (0.0024)
                        N1
     -0.1658 (0.0130)
                        01
Rms deviation of fitted atoms =
 6.0733 (0.0708) x - 7.0645 (0.0720) y + 5.0963 (0.0438) z = 5.0963
(0.0438)
Angle to previous plane (with approximate esd) = 76.50 ( 0.35 )
     -0.0137 (0.0069)
                        N1
      0.0138 (0.0069)
     -0.0133 (0.0067)
                        C2 $2
                        N1 $2
     0.0137 (0.0068)
    -0.0138 (0.0069)
                        C1 $2
     0.0133 (0.0067)
                        C2
     0.0466 (0.0295)
                        C3
     -0.0466 (0.0295)
                       C3 $2
```



Rms deviation of fitted atoms =

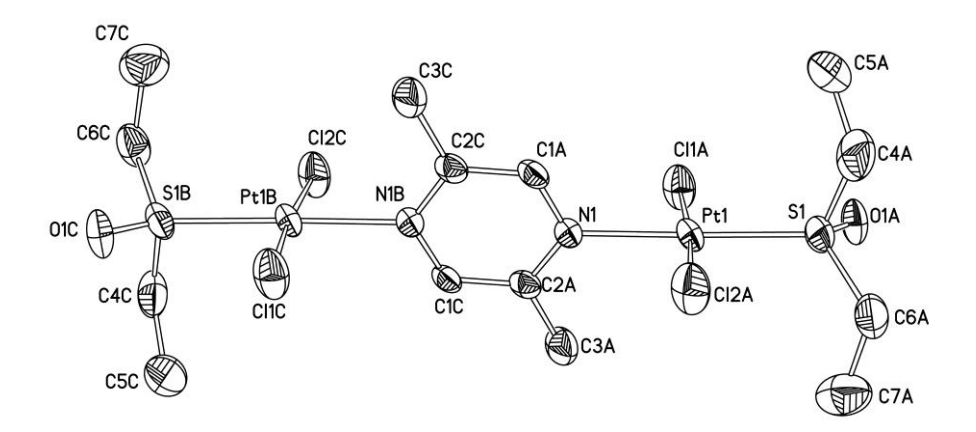


**Figure 4.4.1.4** ORTEP view of (**I**) (conformations 1, top and 2, bottom) showing the numbering scheme adopted. Anisotropic atomic displacement ellipsoids are shown at the 50% probability level. The symmetry transformations are A (x, -y, z), B (-x, -y, -z+2) and C (-x, y, -z+2).

The reliability factor  $R_1$  obtained for (I) is low, 0.0385, and this shows that the crystal structure is relatively well refined. No structure of a platinum(II) complex containing the diethylsulfoxyde ligand has been published so far. Our complex shows a *trans,trans* geometry, confirming what was suggested by the coupling constant  ${}^3J({}^{195}\text{Pt}^{-1}\text{H})$ , 25Hz, in the signal of the bridging ligand in the proton- NMR spectrum (section 4.2.3). The four donor atoms, two Cl atoms which are *trans* to each other, the S atom of the DEtSO molecule and the N atom of the 2,5-dmpz, are almost exactly coplanar with the metal, as expected.

The angles around the metal centers are all almost orthogonal, in agreement with what is usually obtained with the  $D_{4h}$  square-planar geometry. The largest angular deviation from the regular values involves the Cl(1)—Pt(1)—Cl(2) angle. The two Cl atoms bend away from the bulky DEtSO group, closing the Cl—Pt—Cl angle to

175.14(13)°. Similarly, the orthogonal N(1)—Pt(1)—Cl(2) angle, 85.01(18)°, is much lower than the expected 90°. The consequence of this is to increase substantially the adjacent S(1)—Pt(1)—Cl(2) angle to 95.73(13)°. To a lesser extent, a similar situation has already been reported for *trans*-Pt(TMSO)(pz)Cl<sub>2</sub> (3) and *trans*, *trans*-{Pt(DPrSO)Cl<sub>2</sub>}<sub>2</sub>(μ-pz) (2), where the S—Pt—Cl angles in the solid state are 92.13(11)° and 93.44(13)°, respectively. Actually, for all similar *trans* structures containing sulfoxide ligands, the two chlorine atoms are located closer to the nitrogen atom than to the sulfur atom. This situation arises from a combination of steric hindrance and some intermolecular hydrogen bonds. In the fig. 4.4.1.2., it appears that the two chlorine atom, Cl(2) and Cl(2)B, are drastically displaced from the normal orthogonality because the DEtSO aliphatic chains are located on their side.

The Pt—S bond length, 2.202(3) Å, is in the range of that normally observed for similar *trans* compounds. Our monomeric compound, *trans*-Pt(TMSO)(pz)Cl<sub>2</sub>, has a Pt—S bond length of 2.217(3) Å (3), whereas Nédélec *et al.* have reported values of 2.224(7) Å and 2.218(3) Å for the dimeric *trans*, *trans*-{Pt(DMSO)Cl<sub>2</sub>}<sub>2</sub>(μ-pm) and *trans*, *trans*-{Pt(DPrSO)Cl<sub>2</sub>}<sub>2</sub>(μ-pm) complexes, respectively (31). The Pt—S length could be influenced by the geometry of the platinum complexes. For instance, in the *cis*, *cis*-{Pt(DBuSO)Cl<sub>2</sub>}<sub>2</sub>(μ-pm) compound (31), the length is somewhat shorter, *viz*., 2.171(7) Å. The sulfur atom in the DEtSO molecule is in approximate tetrahedral environment with angles ranging from 92.6(9) to 127.6(6)°.

The Pt—Cl bond lengths, measured at 2.291(4) and 2.295(4) Å, are also in the same range that is normally observed for two chlorine atoms in a *trans* position to one another. The observed bond lengths are 2.294(9) Å for *trans*-Pt(PEt<sub>3</sub>)Cl<sub>2</sub> (65),

2.289(3)/2.310(4) Å for *trans*, *trans*-{Pt(PEt<sub>3</sub>)Cl<sub>2</sub>}<sub>2</sub>(μ-Me<sub>2</sub>pz) (21), 2.2953(13) Å for [*cis*-{Pt(NH<sub>3</sub>)<sub>2</sub>Cl}<sub>2</sub>(μ-pz)](NO<sub>3</sub>)<sub>2</sub> (26) and an average of 2.290(4) Å for *trans*, *trans*-{Pt(R<sub>2</sub>SO)Cl<sub>2</sub>}<sub>2</sub>(μ-pz) (R<sub>2</sub>SO = TMSO, DPrSO and DBuSO) (2). These values can also be compared to those situations in which a chlorine atom is located *trans* to a nitrogen atom, as in *trans*-PtCl(NH(4-Cl,2-NO<sub>2</sub>-C<sub>6</sub>H<sub>3</sub>))(PEt<sub>3</sub>)<sub>2</sub> [2.297(6) Å] (66), *cis*-Pt(DMSO)(thiazole)Cl<sub>2</sub> [2.295(3) Å] (67) and *cis*-Pt(DPrSO)(pz)Cl<sub>2</sub> [2.292(5) Å], whereas the chlorine atom in a *trans* position to the sulfoxide ligand is located at 2.316(5) Å from the metal (3). In our compounds *cis*-Pt(DMSO)(C<sub>2</sub>H<sub>3</sub>CN)Cl<sub>2</sub> (68) and *cis*-Pt(DMSO)(CH<sub>3</sub>CN)Cl<sub>2</sub> (69), where the Pt—Cl group is in a *trans* position to the sulfoxide ligand, the lengths are 2.337(5) and 2.324(2) Å, respectively. These X-ray results confirm the suggestion that the *trans* influences of Cl and the N atoms are similar, whereas that of the sulfoxide ligand is greater.

The same conclusion can be reached on the basis of the Pt—N bond lengths. In our compound, the bond length is 2.075(9) Å. This value is similar to those observed for the pyrazine analogues, *trans*, *trans*-{Pt(R<sub>2</sub>SO)Cl<sub>2</sub>}<sub>2</sub>(μ-pz) (R<sub>2</sub>SO = TMSO, DPrSO and DBuSO), which have values of 2.067(12) Å, 2.059(9) Å and 2.067(6) Å (2), respectively, and also the 2,5-dimethylpyrazine compounds, *trans*, *trans*-{Pt(L)Cl<sub>2</sub>}<sub>2</sub> (μ-2,5-Me<sub>2</sub>pz) (L = PEt<sub>3</sub> and C<sub>2</sub>H<sub>4</sub>), which have values of 2.116(7) and 2.059(8) Å (21), respectively. These Pt—N bond lengths are clearly longer than that measured for *cis*-Pt(DPrSO)(pz)Cl<sub>2</sub>, 2.004(14) Å (3), *cis*-Pt(py)<sub>2</sub>Cl<sub>2</sub>, 2.02(2) Å (70), or {Pt(DMSO)Cl}<sub>2</sub>(μ-N(CH<sub>3</sub>)CHO)<sub>2</sub>, 2.019(9) Å (68). In the two last cases, the nitrogen atom is located in a position *trans* to a chlorine atom.

The S—O bond distance in the coordinated diethylsulfoxide ligand, 1.309(11) Å, is very short compared to that for some other sulfoxide ligands. These distances are respectively 1.474(10), 1.463(9) and 1.456(6) Å in *trans,trans*-{Pt(R<sub>2</sub>SO)Cl<sub>2</sub>}<sub>2</sub>(μ-pz) (R<sub>2</sub>SO = TMSO, DPrSO and DBuSO) (2). It is 1.488(10) Å for *trans*-Pt(TMSO)(pz)Cl<sub>2</sub> and 1.45(2) Å for *cis*-Pt(DPrSO)(pz)Cl<sub>2</sub> (3). This is the first time that a so short bond length has been observed, but there is no comparison in the literature for the structure of a platinum(II) complex with a coordinated diethylsulfoxide ligand. The S—C bond distances are longer than in the expected 1.76-1.84 Å range, even if in our sulfoxide complexes these bonds are usually shorter than what is observed in *trans,trans*-{Pt(DEtSO)Cl<sub>2</sub>}<sub>2</sub>(μ-Me<sub>2</sub>pz) (4,5,35,73). The sulfur atom is in an approximate tetrahedral environment. The C—S—C angle, 92.6(9)°, is much smaller than are the other angles observed for similar compounds (67,68,71-80). Once again, it seems that the diethylsulfoxide ligand is structurally different than are the other sulfoxide ligands previously used by our research group.

For the bridging 2,5-dimethylpyrazine ligand, the average N—C bond length is 1.329(14) Å, while the average aromatic C—C bond length is 1.37(2) Å. These distances are in agreement with the corresponding distances determined for the free ligand, 1.320 and 1.390 Å, respectively (81). The average methyl C—C bond length is 1.53(2) Å, which corresponds to the 1.505 Å distance in the free 2,5-dimethylpyrazine ligand. The binding of the ligand to platinum(II) through the N atom slightly increases the internal C—N—C angles to 119.5(11)°. In free dimethylpyrazine, these angles are 117.8° (81). The other internal aromatic angles, C—C—N, are identical, 118.6(12) and 121.8(12)° in

our crystal and 119.7 and 122.5° in free 2,5-dimethylpyrazine (81). The same observations can be made for the C—C—N, C—C—C and C—C—H methyl angles.

Planar ligands such as pyridine derivatives are often located orthogonal to the platinum plane in order to reduce the steric hindrance, especially for crowded ligands. The dihedral angles between the platinum and the ring of the dimethylpyrazine plane are calculated to be  $76.5(8)^{\circ}$ . We observed smaller values for the pyrazine and pyrimidine-bridged dimers, viz.,  $53.7(5)^{\circ}$  and  $53.2(6)^{\circ}$  (2,31). This illustrates how much more hindered ligands, such as 2,5-dimethylpyrazine, tend to crystallize in a structural position closer to orthogonality. Packing forces are also important factors in determining the orientation of the pyridine derivative rings.

# 4.4.2 Crystal structure of the dimeric species ({Pt(DBuSO)Cl<sub>2</sub>}<sub>2</sub>(μ-Me<sub>2</sub>pyrazine)

A crystal of (II) was obtained by recrystallization of about 6 mg the complex from a 40-mL chloroform:methanol (1:1), mixture maintained at a temperature of 45 °C. Slow evaporation was achieved in a fridge at about 5 °C. The medium was closed with protective parafilm in which a few holes had been punched. The crystal obtained had an orange platlet shape with approximate dimensions of 0.20 x 0.06 x 0.06 mm. It was mounted on a glass fiber using Paratone N hydrocarbon oil. The collection of the crystallographic data  $(2\theta/\theta)$  was done at medium temperature [200(2) K] for the compound in order to minimize the background noise.

The measurements were made on a Bruker APEX II area detector diffractometer equipped with graphite monochromated MoK $\alpha$  radiation. Frames corresponding to an arbitrary hemisphere of data were collected using  $\omega$  scans of 0.5° counted for a total of 10 s per frame. An orientation matrix corresponding to cell constants listed in Table 4.4.2.1.

was obtained from a least-squares refinement using the measured positions of 5414 centered reflections in the range  $2.46^{\circ} < \theta < 27.97^{\circ}$ . The program used for retrieving cell parameters and data collection was APEX II (55). Data were integrated using the program SAINT (56) and were corrected for Lorentz and polarization effects. Face-indexed and multiscan absorption corrections were both performed xusing the XPREP (57) and SADABS (58) programs, respectively. The structure was solved and refined using SHELXS-97 and SHELXL-97 (59). All non-H atoms were refined anisotropically. The hydrogen atoms were placed at idealized positions. Neutral atom scattering factors are taken from the International Tables for X-Ray Crystallography (60,61). All calculations and drawings were performed using the SHELXTL package (62). The final model was checked for either missed symmetry or voids in the crystal structure using the PLATON software (63,64). None was found. This crystal structure gave a satisfactory chekcif report.

Table 4.4.2.1 Crystal data and structure refinement for (II)

Identification code fdr006 (B3)

Empirical formula  $C_{22}H_{44}Cl_4N_2O_2Pt_2S_2$  Moiety formula  $C_{22}H_{44}Cl_4N_2O_2Pt_2S_2$ 

Formula weight 964.69
Temperature 200(2) K
Wavelength 0.71073 Å
Crystal system Hexagonal

Space group R-3

Unit cell dimensions a = 26.9935(9) Å  $\alpha = 90^{\circ}$ .

b = 26.9935(9) Å  $\beta$ = 90°. c = 11.7575(7) Å  $\gamma$  = 120°.

Volume 7419.3(6) Å<sup>3</sup>

Z 9

Density (calculated) 1.943 Mg/m<sup>3</sup>
Absorption coefficient 8.948 mm<sup>-1</sup>

F(000) 4158

Crystal size  $0.20 \times 0.06 \times 0.06 \text{ mm}^3$ 

 $\theta$  range for data collection 1.51 to 26.00°.

Index ranges -33 <= h <= 33, -33 <= k <= 33, -14 <= l <= 14

Reflections collected 26918

Independent reflections 3244 [R(int) = 0.0331]

Observed Reflections 2839 [I>2 $\sigma$ (I)]

Completeness to  $\theta = 26.00^{\circ}$  99.8 %

Absorption correction Semi-empirical from equivalents

Max. and min. transmission 0.5850 and 0.2543

Refinement method Full-matrix least-squares on F<sup>2</sup>

Data / restraints / parameters 3244 / 12 / 157

Goodness-of-fit on  $F^2$  1.379

Final R indices [I>2 $\sigma$ I)] R1 = 0.0245, wR2 = 0.0599 R indices (all data) R1 = 0.0312, wR2 = 0.0618 Largest diff. peak and hole 2.181 and -0.821 e.Å<sup>-3</sup>

**Table 4.4.2.2** Atomic coordinates  $(x10^4)$  and equivalent isotropic displacement parameters  $(\mathring{A}^2 \ x \ 10^3)$  for  $(\mathbf{H})$ . U(eq) is defined as one third of the trace of the orthogonalized  $U^{ij}$  tensor.

6409(1)	915(1)	2500(4)	1
	713(1)	5680(1)	28(1)
7321(1)	1436(1)	6188(1)	37(1)
6095(1)	1127(1)	7322(1)	49(1)
6653(1)	654(1)		54(1)
7761(1)	1617(1)	5304(3)	42(1)
5562(1)	388(2)	5257(3)	26(1)
5259(2)	-90(2)	5873(4)	31(1)
5300(2)	487(2)	4375(4)	30(1)
5605(2)	1042(2)	3754(4)	52(1)
7451(2)	1024(2)	7228(4)	49(1)
7444(2)	517(2)	6685(4)	48(1)
7592(3)	170(3)	7505(5)	64(2)
7573(3)	-337(3)	6948(6)	77(2)
7450(2)	2055(2)	6962(5)	54(2)
7389(3)	2463(3)	6208(6)	67(2)
7511(4)	2999(3)	6851(8)	99(3)
7540(5)	3437(5)	6048(11)	160(5)
	6653(1) 7761(1) 5562(1) 5259(2) 5300(2) 5605(2) 7451(2) 7444(2) 7592(3) 7573(3) 7450(2) 7389(3) 7511(4)	6653(1) 654(1) 7761(1) 1617(1) 5562(1) 388(2) 5259(2) -90(2) 5300(2) 487(2) 5605(2) 1042(2) 7451(2) 1024(2) 7444(2) 517(2) 7592(3) 170(3) 7573(3) -337(3) 7450(2) 2055(2) 7389(3) 2463(3) 7511(4) 2999(3)	6653(1)       654(1)       4014(1)         7761(1)       1617(1)       5304(3)         5562(1)       388(2)       5257(3)         5259(2)       -90(2)       5873(4)         5300(2)       487(2)       4375(4)         5605(2)       1042(2)       3754(4)         7451(2)       1024(2)       7228(4)         7444(2)       517(2)       6685(4)         7592(3)       170(3)       7505(5)         7573(3)       -337(3)       6948(6)         7450(2)       2055(2)       6962(5)         7389(3)       2463(3)       6208(6)         7511(4)       2999(3)       6851(8)

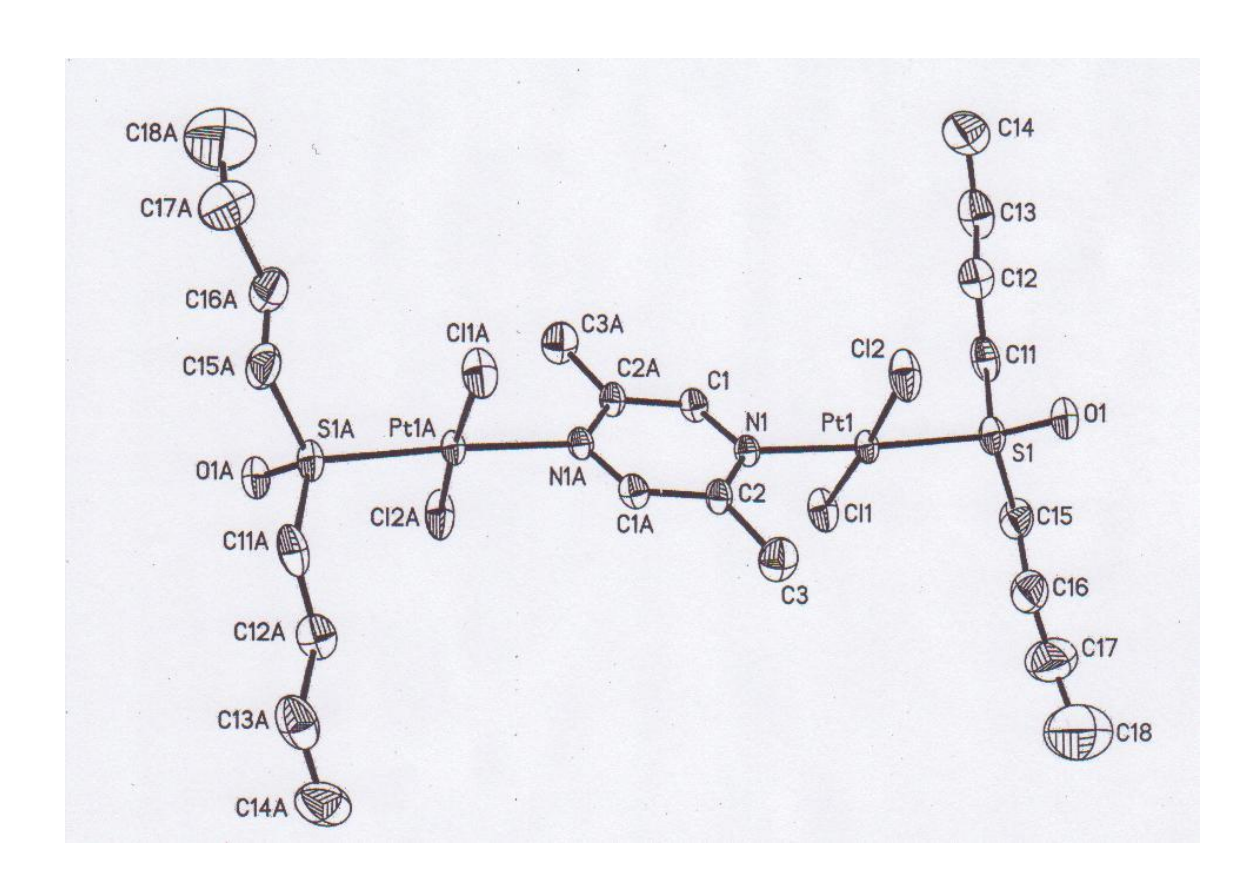


**Figure 4.4.2.1** ORTEP view of (**II**) compound showing the numbering scheme adopted. Anisotropic atomic displacement ellipsoids for the non-hydrogen atoms are shown at the 40% probability level. The symmetry transformation used to generate the atoms labelled A is -x+1, -y, -z+1.

Table 4.4.2.3 Bond lengths  $[\mathring{A}]$  and angles  $[^{\circ}]$  for (II).

Pt(1)-N(1)	2.059(3)	C(1)-C(2)#1	1.377(6)
Pt(1)-S(1)	2.2210(11)	C(2)-C(1)#1	1.377(6)
Pt(1)-Cl(2)	2.2880(12)	C(2)-C(3)	1.490(7)
Pt(1)-Cl(1)	2.2926(12)	C(11)-C(12)	1.503(8)
S(1)-O(1)	1.466(3)	C(12)-C(13)	1.530(7)
S(1)-C(15)	1.779(5)	C(13)-C(14)	1.494(9)
S(1)-C(11)	1.801(5)	C(15)-C(16)	1.486(9)
N(1)-C(1)	1.342(5)	C(16)-C(17)	1.516(9)
N(1)-C(2)	1.356(5)	C(17)-C(18)	1.483(12)
N(1)-Pt(1)-S(1)	176.34(10)	C(1)-N(1)-Pt(1)	117.8(3)
N(1)-Pt(1)-Cl(2)	88.40(10)	C(2)-N(1)-Pt(1)	123.8(3)
S(1)-Pt(1)-Cl(2)	91.48(4)	N(1)-C(1)-C(2)#1	122.6(4)
N(1)-Pt(1)-Cl(1)	87.43(10)	N(1)-C(2)-C(1)#1	119.0(4)
S(1)-Pt(1)-Cl(1)	92.65(4)	N(1)-C(2)-C(3)	119.5(4)
Cl(2)-Pt(1)-Cl(1)	175.79(4)	C(1)#1-C(2)-C(3)	121.2(4)
O(1)-S(1)-C(15)	107.7(2)	C(12)-C(11)-S(1)	110.9(3)
O(1)-S(1)-C(11)	108.2(2)	C(11)-C(12)-C(13)	113.7(5)
C(15)-S(1)-C(11)	103.0(3)	C(14)-C(13)-C(12)	112.6(5)
O(1)-S(1)-Pt(1)	118.50(14)	C(16)-C(15)-S(1)	110.4(4)
C(15)-S(1)-Pt(1)	111.54(19)	C(15)-C(16)-C(17)	111.0(6)
C(11)-S(1)-Pt(1)	106.79(17)	C(18)-C(17)-C(16)	110.0(8)
C(1)-N(1)-C(2)	118.4(3)		

#1 -x+1,-y,-z+1

Table 4.4.2.4 Torsion angles  $[^{\circ}]$  for (II).

Cl(2)-Pt(1)-S(1)-O(1)	19.70(18)	Pt(1)-N(1)-C(2)-C(1)#1	176.3(3)
Cl(1)-Pt(1)-S(1)-O(1)	-161.12(18)	C(1)-N(1)-C(2)-C(3)	173.4(4)
Cl(2)-Pt(1)-S(1)-C(15)	145.6(2)	Pt(1)-N(1)-C(2)-C(3)	-8.6(6)
Cl(1)-Pt(1)-S(1)-C(15)	-35.2(2)	O(1)-S(1)-C(11)-C(12)	-58.0(4)
Cl(2)-Pt(1)-S(1)-C(11)	-102.6(2)	C(15)-S(1)-C(11)-C(12)	-171.9(4)
Cl(1)-Pt(1)-S(1)-C(11)	76.6(2)	Pt(1)-S(1)-C(11)-C(12)	70.5(4)
Cl(2)-Pt(1)-N(1)-C(1)	110.5(3)	S(1)-C(11)-C(12)-C(13)	176.1(4)
Cl(1)-Pt(1)-N(1)-C(1)	-68.9(3)	C(11)-C(12)-C(13)-C(14)	179.1(5)
Cl(2)-Pt(1)-N(1)-C(2)	-67.4(3)	O(1)-S(1)-C(15)-C(16)	63.1(5)
Cl(1)-Pt(1)-N(1)-C(2)	113.2(3)	C(11)-S(1)-C(15)-C(16)	177.3(4)
C(2)-N(1)-C(1)-C(2)#1	1.7(7)	Pt(1)-S(1)-C(15)-C(16)	-68.5(4)
Pt(1)-N(1)-C(1)-C(2)#1	-176.4(3)	S(1)-C(15)-C(16)-C(17)	-178.7(5)
C(1)-N(1)-C(2)-C(1)#1	-1.6(7)	C(15)-C(16)-C(17)-C(18)	170.8(7)

#1 -x+1,-y,-z+1

The structure of (II) was solved by the heavy-atom method and refined by least squares to a final reliability factor  $R_1$  of 0.0245 (w $R_2$  = 0.0599). This R value is low and shows that our crystal structure is well refined. This structure is particularly interesting to compare with two other crystals we obtained in the recent years: trans,trans-{Pt(DBuSO)Cl<sub>2</sub>}( $\mu$ -pz) (2) and trans,trans geometry, confirming what was suggested by the coupling constant trans,trans geometry, confirming what was suggested by the coupling constant trans,trans-{Pt(DBuSO)Cl<sub>2</sub>}<sub>2</sub>(trans,trans-{Pt(DBuSO)Cl<sub>2</sub>}<sub>2</sub>(trans,trans-{Pt(DBuSO)Cl<sub>2</sub>}<sub>2</sub>(trans,trans-{Pt(DBuSO)Cl<sub>2</sub>}<sub>2</sub>(trans,trans-{Pt(DBuSO)Cl<sub>2</sub>}<sub>2</sub>(trans,trans-{Pt(DBuSO)Cl<sub>2</sub>}<sub>2</sub>(trans,trans-{Pt(DBuSO)Cl<sub>2</sub>}<sub>2</sub>(trans,trans-{Pt(DBuSO)Cl<sub>2</sub>}<sub>2</sub>(trans,trans-{Pt(DBuSO)Cl<sub>2</sub>}<sub>2</sub>(trans,trans-{Pt(DBuSO)Cl<sub>2</sub>}<sub>2</sub>(trans,trans-{Pt(DBuSO)Cl<sub>2</sub>}<sub>2</sub>(trans,trans-{Pt(DBuSO)Cl<sub>2</sub>}<sub>2</sub>(trans,trans-{Pt(DBuSO)Cl<sub>2</sub>}<sub>2</sub>(trans,trans-{Pt(DBuSO)Cl<sub>2</sub>}<sub>2</sub>(trans,trans-{Pt(DBuSO)Cl<sub>2</sub>}<sub>2</sub>(trans,trans-{Pt(DBuSO)Cl<sub>2</sub>}<sub>2</sub>(trans,trans-{Pt(DBuSO)Cl<sub>2</sub>}<sub>2</sub>(trans,trans-{Pt(DBuSO)Cl<sub>2</sub>}<sub>2</sub>(trans,trans-{Pt(DBuSO)Cl<sub>2</sub>}<sub>2</sub>(trans,trans-{Pt(DBuSO)Cl<sub>2</sub>}<sub>2</sub>(trans,trans-{Pt(DBuSO)Cl<sub>2</sub>}<sub>2</sub>(trans,trans-{Pt(DBuSO)Cl<sub>2</sub>}<sub>2</sub>(trans,trans-{Pt(DBuSO)Cl<sub>2</sub>}<sub>2</sub>(trans,trans-{Pt(DBuSO)Cl<sub>2</sub>}<sub>2</sub>(trans,trans-{Pt(DBuSO)Cl<sub>2</sub>}<sub>2</sub>(trans,trans-{Pt(DBuSO)Cl<sub>2</sub>}<sub>2</sub>(trans,trans-{Pt(DBuSO)Cl<sub>2</sub>}<sub>2</sub>(trans,trans-{Pt(DBuSO)Cl<sub>2</sub>}<sub>2</sub>(trans,trans-{Pt(DBuSO)Cl<sub>2</sub>}<sub>2</sub>(trans,trans-{Pt(DBuSO)Cl<sub>2</sub>}<sub>2</sub>(trans,trans-{Pt(DBuSO)Cl<sub>2</sub>}<sub>2</sub>(trans,trans-{Pt(DBuSO)Cl<sub>2</sub>}<sub>2</sub>(trans,trans-{Pt(DBuSO)Cl<sub>2</sub>}<sub>2</sub>(trans,trans-{Pt(DBuSO)Cl<sub>2</sub>}<sub>2</sub>(trans,trans-{Pt(DBuSO)Cl<sub>2</sub>}<sub>2</sub>(trans,trans-{Pt(DBuSO)Cl<sub>2</sub>}<sub>2</sub>(trans,trans-{Pt(DBuSO)Cl<sub>2</sub>}<sub>2</sub>(trans,trans-{Pt(DBuSO)Cl<sub>2</sub>}<sub>2</sub>(trans,trans,trans-{Pt(DBuSO)Cl<sub>2</sub>}<sub>2</sub>(trans,tr

Like for trans, trans-{Pt(DEtSO)Cl<sub>2</sub>}( $\mu$ -2,5-Me<sub>2</sub>pz), the angles around the metal centers are all almost orthogonal, in agreement with the D<sub>4h</sub> square planar geometry. The angle N(1)—Pt(1)—Cl(1), 87.43(10)° is lower than the expected 90°. The consequence is to increase the adjacent angle S(1)—Pt(1)—Cl(1), 92.65(4)°. The two chlorine atoms are, as expected, located closer to the nitrogen atom than to the sulfur atom, probably due to some intermolecular hydrogen bonds. The expected plane angle Cl(1)—Pt(1)—Cl(2) has a value of 175.79(4)°. To a smaller extend, Cl(2) is also displaced toward the metallic center since the angle N(1)—Pt(1)—Cl(2) also has a value below orthogonality, 88.40(10)°.

The Pt—S length, 2.2210(11) Å, is in the range for *trans*-platinum (II) complexes. Our monomeric compound *trans*-Pt(TMSO)(pz)Cl<sub>2</sub> showed a bond length of 2.217(3) Å (3), and our dimeric compounds, *trans*, *trans*-{Pt(DMSO)Cl<sub>2</sub>}<sub>2</sub>(μ-pm), *trans*, *trans*, *trans*-

 ${Pt(DPrSO)Cl_2}_2(\mu-pm)$ (31), $trans, trans - \{Pt(TMSO)Cl_2\}_2(\mu-pz),$ trans, trans- $\{Pt(DPrSO)Cl_2\}_2(\mu-pz)$  and  $trans, trans-\{Pt(DBuSO)Cl_2\}_2(\mu-pz)$  (2) had lengths of, respectively, 2.224(7), 2.218(3), 2.221(4), 2.223(3) and 2.221(2) Å. The sulfur atom in the DBuSO molecule is in approximate tetrahedral environment with angles ranging from 103.0(3) to 118.50(14)°. The Pt—Cl bond lengths, measured at 2.2880(12) and 2.2926(12) Å, are also in agreement with the *trans* influence of chloride in platinum(II) complexes. The bond lengths were observed at 2.294(9) Å for trans-Pt(PEt<sub>3</sub>)Cl<sub>2</sub> (65), at 2.289(3)/2.310(4) Å for trans, trans-{Pt(PEt<sub>3</sub>)Cl<sub>2</sub>}<sub>2</sub>( $\mu$ -Me<sub>2</sub>pz) (21), at 2.2953(13) Å for  $[cis-{Pt(NH_3)_2Cl}_2(\mu-pz)](NO_3)_2$  (26) and at ave. 2.290(4) Å for trans, trans- $\{Pt(R_2SO)Cl_2\}_2(\mu-pz)$  (R<sub>2</sub>SO = TMSO, DPrSO and DBuSO) (2). The Pt—N bond length is measured at 2.059(3) Å. This is in fair agreement with trans geometry complexes, such  $\{Pt(R_2SO)Cl_2\}_2(\mu-pz)$   $(R_2SO = TMSO, DPrSO and DBuSO)$  (2) and  $\{Pt(C_2H_4)Cl_2\}_2(\mu-2,5-Me_2pz)$  (21), for which the bonds were measured, respectively, at 2.067(12), 2.059(9), 2.067(6) and 2.059(8) Å.

The S—O bond distance in the coordinated diethylsulfoxide ligand, 1.466(3) Å, is in the range of what was measured in *trans*, *trans*-{Pt(R<sub>2</sub>SO)Cl<sub>2</sub>}<sub>2</sub>( $\mu$ -pz) (R<sub>2</sub>SO = TMSO, DPrSO and DBuSO), respectively, 1.474(10), 1.463(9) and 1.456(6) Å (2), in *trans*-Pt(TMSO)(pz)Cl<sub>2</sub>, 1.488(10) Å and in *cis*-Pt(DPrSO)(pz)Cl<sub>2</sub>, 1.45(2) Å (3). The S—C bond distances are measured at 1.779(5) and 1.801(5) Å. The C—S—C angle, 103.0(3)°, is in the range of similar compounds (2,31,67,68,71-80).

In the coordinated 2,5-dimethylpyrazine ligand, the ave. N—C bonds are 1.349(5) Å, while the ave. aromatic C—C bond lengths are 1.377(6) Å. These distances are in agreement with the corresponding distances determined for the free ligand, 1.320 and

1.390 Å respectively (81) and with what is measured for the diethylsulfoxide analogues, 1.349(5) Å and 1.329(14) Å (section 4.4.1). The binding of the ligand to platinum through the N atom slightly modify the internal structure. The C—N—C angles are measured at 119.5(11)°, the ave. methyl C—C bond lengths are 1.490(7) Å. In the free ligand, it corresponds to 117.8° and 1.505 Å (81). The internal aromatic angles, C—C—N, are identical, 119.0(4) and 122.6(4)°, compared to 119.7 and 122.5° (81). The same observations can be made on the methyl angles, C—C—N, C—C—C and C—C—H. The 2,5-dimethylpyrazine plane tends to be orthogonal to the platinum plane, in order to reduce the steric hindrance. The dihedral angles between the two planes are calculated and they are ave. 68.2(3)°, which is comparable to what is observed with the diethylsulfoxide analogue, 76.5(8)° (section 4.4.1). Packing forces are playing a role in the orientation of the pyridine derivatives rings.

# 4.5 Preparation and analysis of the $\{Pt(R_2SO)Cl_2\}_2(\mu$ -quinoxaline) complexes

The method used for the {Pt(R<sub>2</sub>SO)Cl<sub>2</sub>}<sub>2</sub>(μ-quinoxaline) series is based on the one used for the {Pt(R<sub>2</sub>SO)Cl<sub>2</sub>}<sub>2</sub>(μ-2,5-Me<sub>2</sub>pz) series, described in section 4.1. Complexes with the following sulfoxide ligands are prepared: DMSO, DEtSO, TMSO, DPrSO, DBuSO, DBzSO, DPhSO and MeBzSO. The compounds are analyzed by multinuclear (<sup>1</sup>H, <sup>13</sup>C and <sup>195</sup>Pt) NMR spectroscopy and by vibrational (IR and Raman) spectroscopies. No discussion on the quinoxaline complexes seems really relevant, since replacing the bridging ligand from 2,5-dimethylpyrazine did not change any chemical behavior of the products. As for 2,5-dimethylpyrazine, attempts to prepare the

hypothetical monomeric 'Pt(R<sub>2</sub>SO)(quinoxaline)Cl<sub>2</sub>' compounds fail, the dimeric complexes are predominant.

### Conclusion

So, new dimeric compounds were prepared using 2,5-dimethylpyrazine, as the bridging ligand.  $Trans, trans - \{Pt(R_2SO)Cl_2\}_2(\mu-Me_2pz)$ synthesized were and characterized by multinuclear (<sup>1</sup>H, <sup>13</sup>C and <sup>195</sup>Pt), IR and Raman spectroscopy. The observed <sup>3</sup>J(<sup>1</sup>Ha-<sup>195</sup>Pt) coupling constants suggested the trans geometry. Most of the literature dealing on Me<sub>2</sub>pz complexes are with the two methyl groups located in positions 2/6 and 2/3. Fewer studies have been published on the 2,5-Me<sub>2</sub>pz ligand, which is more sterically hindered and generally not favored for the reactions with a 1:1 Pt:Me<sub>2</sub>pz ratio. Suitable crystals of {Pt(DEtSO)Cl<sub>2</sub>}<sub>2</sub>(µ-Me<sub>2</sub>pz) and {Pt(DBuSO)Cl<sub>2</sub>}<sub>2</sub>(µ-Me<sub>2</sub>pz) Me<sub>2</sub>pz) complexes were obtained by recrystallization. X-rays diffraction at low temperature (173 K) helped to resolve their structure with good refinement (R1 = 0.0385and 0.0245). They recrystallized in the C2/m and R-3 space groups, respectively. The short S—O bond distance, 1.31 Å, in the coordinated DEtSO ligand showed a bond order close to 3, which is rare for such coordination complexes. These X-ray results confirm that the trans influences of the Cl and N atoms are similar, whereas that of the sulfoxide ligand is greater. No structure of a Pt(II) complex containing the DEtSO ligand has been published so far.

### References

- (1) Y. N. Kukushkin, Y. E. Vyaz'menskii et L. I. Zorina. *Russ. J. Inorg. Chem.* **1968**, *13*, 1573.
- (2) Priqueler, J.R.L.; Rochon, F.D. Inorg. Chim. Acta. 2004, 357, 2167.
- (3) Priqueler, J.R.L.; Rochon, F.D. Can. J. Chem. 2004, 82, 649.
- (4) F. Peral, E. Gallego, J. Mol. Struct. **1995**, 372, 101.
- (5) F. Peral, E. Gallego, Spectrochim. Acta Part A. 2000, 56.
- (6) H. E. Gottlieb, V. Kotlyar et A. Nudelman. J. Org. Chem. 1997, 62, 7512.
- (7) Fontes, A.P.S.; Oskarsson, Å.; Lövqvist, K.; Farrell, N. *Inorg. Chem.* **2001**, *40*, 1745.
- (8) A. Pawlukojć, L. Sobczyk, M. Prager, G. Bator, E. Grech, J. Nowicka-Scheibe. J. Mol. Struct. 2008, 892, 261.
- (9) M. Prager, W. Sawka-Dobrowolska, L. Sobczyk, A. Pawlukojć, E. Grech, A. Wischnewski, M. Zamponi. *Chem. Phys.* 2007, 332, 1.
- (10) Y. Chen, R.E. Shepherd. *Inorg. Chim. Acta.* **1998**, 268, 279.
- (11) J.M. Gilaberte, C. López, S. Alvarez. J. Organometall. Chem. 1988, 342, C13.
- (12) S.J. Miles, J.D. Wilkins. J. Inorg. Nucl. Chem. 1975, 37, 2271.
- (13) Y.-C. Tsai, C.C. Cummins. Inorg. Chim. Acta, 345, 2003, 63-69.
- (14) T.W. Stringfield, Y. Chen, R.E. Shepherd. *Inorg. Chim. Acta.* **1999**, 285, 157.
- (15) F. Peral, E. Gallego. Spectrochim. Acta A: Mol. Biomol. Spect. 2003, 59, 1223.
- (16) N. Begum, A.C. Ghosh, S.E. Kabir, A. Miah, G. Hossain. *Polyhedron.* 2005, 24, 3074.
- (17) D.R. Martin, C.M. Merkel, C.B. Drake, J.U. Mondal, J.B. Iwamoto. *Inorg. Chim. Acta.* 1985, 97, 189.

- (18) J.M. de la Rosa Arranz, F.J. González-Vila, E. López-Capel, D.A.C. Manning, H. Knicker, J.A. González-Pérez. J. Anal. Appl. Pyrolysis. 2009, 85, 399.
- (19) D.R. Martin, C.M. Merkel, J.U. Mondal, C.R. Rushing Jr. *Inorg. Chim. Acta.* 1985, 99, 81.
- (20) J.W. Wheeler, J. Avery, O. Olubajo, M.T. Shamin, C.B. Storm, R.M. Duffield. Tetrahedron. 1982, 38, 1939.
- (21) A. Albinati, F. Isaia, W. Kaufmann, C. Sorato, L.M. Venanzi. *Inorg. Chem.* **1989**, 28, 1112.
- (22) H. Kuramoto, M. Inoue, S. Emori, S. Sugiyama. *Inorg. Chim. Acta.* **1979**, *32*, 209.
- (23) M.A.M. Abu-Youssef, V. Langer, L. Öhrstrom, Dalton Trans. 2006, 2542.
- (24) U. Eiermann, C. Krieger, F.A. Neugebauer, H.A. Staab. *Tetrahedron Lett.* **1988**, 29, 3655.
- (25) A.H. Shipar. *Food Chem.* **2006**, 98, 403.
- (26) S. Komeda, G. V. Kalayda, M. Lutz, A. L. Spek, Y. Yamanaka, T. Sato, M. Chikuma, J. Reedjik. *J. Med. Chem.* **2003**, *46*, 1210.
- (27) P. S. Hall and D. A. Thornton, G. A. Foulds. *Polyhedron*, **1987**, *6*, 85.
- (28) W. McFarlane. J. Chem. Soc., Dalton Trans. 1974, 324.
- (29) T. B. T. Ha, J. P. Souchard, F. L. Wimmer and N. P. Johnson. *Polyhedron.* **1990**, *9*, 2647.
- (30) N. Nédélec and F. D. Rochon. *Inorg. Chim. Acta.* **2001**, *319*, 95.
- (31) N. Nédélec and F. D. Rochon. *Inorg. Chem.* **2001**, *40*, 5236.
- (32) C. Tessier and F. D. Rochon. *Inorg. Chim. Acta.* **1999**, 295, 25.

- (33) Arenas, J.F.; Lopez-Navarrete, J.T.; Marcos, J.I. and Otero, J.C. *J.Mol.Struct.* **1987**, *162*, 263.
- (34) K. Nakamoto. Infrared and Raman spectra of inorganic and coordination compounds. Wiley and Son, 3<sup>rd</sup> ed.(1978), New-York.
- (35) V. N. Spevak, V. I. Lobadyuk and D. M. Batueva. J. Gen. Chem. Of the USSR. 1990, 60, 1178.
- (36) G. A. Foulds and D. A. Thornton. Spectrochim. Acta. 1981, 37A, 917.
- (37) M. van Beusichem and N. Farrell. *Inorg. Chem.* **1992**, *31*, 634.
- (38) J.H. Price, A.N. Williamson, R.F. Schramm, B.B. Wayland, *Inorg. Chem.* **1972**, *11*, 1280.
- (39) V.Yu. Kukushkin, V.K. Belsky, V.E. Konovalov, G.A. Kirakosyan, L.V. Konovalov, A.I. Moiseev, V.M. Tkachuk, *Inorg. Chim. Acta.* **1991**, *185*, 143.
- (40) Yu.N.Kukushkin, V.N. Spevak, Russ. J. Inorg. Chem. 1973, 18, 240.
- (41) Yu.N. Kukushkin, I.V. Pakhomova, Russ. J. Inorg. Chem. 1971, 16, 226.
- (42) B.F.G. Johnson, R.A. Walton, Spectrochim. Acta. 1966, 22, 1853.
- (43) Yu.N. Kukushkin, N.V. Ivannikova, K.A. Khokhryakov, Russ. J. Inorg. Chem. 1970, 15, 1595.
- (44) K. Nakamoto, P.J. McCarthy, J. Fujita, R.A. Condrate, G.T.Behnke, *Inorg. Chem.* **1965**, *4*, 36.
- (45) Inorg. Chem. **1998**, 37, 5452.
- (46) Inorg. Chim. Acta. **2005**, 358, 2609.
- (47) J. Inorg. Biochem. **2005**, 99, 1098.
- (48) *Inorg. Chem.* **2003**, *42*, 7077.

- (49) Inorg. Chem. 1999, 38, 2941.
- (50) Inorg. Chem. 1998, 37, 4921.
- (51) Chem. Phys. Lett. 2005, 403, 211.
- (52) Arenas, J.F.; Lopez-Tocon, I.; Otero, J.C.; Marcos, J.I. J. Phys. Chem. 1995, 99, 11392.
- (53) Arenas, J.F.; Lopez-Tocon, I.; Otero, J.C.; Marcos, J.I. J. Mol. Struct. 1999, 476, 139.
- (54) Arenas, J.F.; Woolley, M.S.; Lopez-Tocon, I.; Otero, J.C.; Marcos, J.I. J. Chem. Phys. 2000, 112, 7669.
- (55) Bruker (2005b). APEX 2 Version 2.0.2. Bruker AXS Inc., Madison, Wisconsin, USA.
- (56) Bruker (2003). SAINT Version 7.07a. Bruker AXS Inc., Madison, Wisconsin, USA.
- (57) Bruker (2005a). XPREP Version 2005/2. Bruker AXS Inc., Madison, Wisconsin, USA.
- (58) Sheldrick, G.M. (2004). SADABS Version 2004/1. Bruker AXS Inc., Madison, Wisconsin, USA.
- (59) Sheldrick, G.M. (1997). SHELXS-97 and SHELXL-97. Programs for the refinement of crystal structures. University of Gottingen, Germany.
- (60) International Tables for Crystallography (1983). Vol. A. Space-group symmetry, edited by T. Hahn. Dordrecht: Reidel. (Present distributor Kluwer Academic Publishers, Dordrecht).

- (61) International Tables for Crystallography, Vol C. (1992), Ed. A.J.C. Wilson, Kluwer Academic Publishers, Dordecht: Tables 4.2.6.8 (pp 219-222) and 6.1.1.4 (pp. 500-502).
- (62) Bruker (2001). SHELXTL Version 6.12. Bruker AXS, Madison, Wisconsin, USA.
- (63) Spek, A. L. Acta Cryst. 1990, A46, C-34.
- (64) Spek, A. L. (2005). PLATON, A Multipurpose Crystallographic Tool. University of Utrecht, Utrecht, The Netherlands.
- (65) G. G. Messmer and E. L. Amma, *Inorg Chem.* **1966**, *5*, 1775.
- (66) A. C. Albéniz, V. Calle, P. Espinet, S. Gómez. *Inorg. Chem.* **2001**, 40, 4211.
- (67) A. Cornia, A. C. Fabretti, M. Bonivento and L. Cattalini. *Inorg. Chim. Acta.* 1997, 255, 405.
- (68) F. D. Rochon, P. C. Kong and R. Melanson. *Inorg. Chim. Acta.* **1994**, 216, 163.
- (69) F. D. Rochon, P. C. Kong and R. Melanson. *Inorg. Chem.* **1990**, 29, 1352.
- (70) P. Colamarino and P. L. Orioli. J. Chem. Soc., Dalton Trans. 1975, 1656.
- (71) R. Melanson, F.D. Rochon, Can. J. Chem. 1975, 53, 2371.
- (72) R. Melanson, F.D. Rochon, Acta Cryst. 1978, B34, 1125.
- (73) F. Caruso, R. Spagna, L. Zambonelli, *Acta Cryst.* **1980**, *B36*, 713.
- (74) B. Viossat, P. Khodadad, N. Rodier, *Acta Cryst.* **1991**, *C47*, 1316.
- (75) V.K. Belsky, V.E. Konovalov, V.Yu. Kukushkin, *Acta Cryst.* **1991**, *C47*, 292.
- (76) R. Melanson, F.D. Rochon, *Acta Cryst.* **1977**, *B33*, 3571.
- (77) K. Lövqvist, Å. Oskarsson, *Acta Cryst.* **1992**, *C48*, 2073.
- (78) V.K. Belsky, V.E. Konovalov, V.Yu. Kukushkin, A.I. Moiseev, *Inorg. Chim. Acta.* 1990, 169, 101.

- (79) R. Melanson, F.D. Rochon, Acta Cryst. 1984, C40, 793.
- (80) R. Melanson, C. de la Chevrotière, F.D. Rochon, Acta Cryst. 1985, C41, 1428.
- (81) M. A. V. Ribeiro da Silva, V. M. F. Morais, M. A. R. Matos, C. M. A. Rio and C. M. G. S. Piedade, *Struct. Chem.* 1996, 7, 329.

#### **CHAPTER V**

*Trans-trans*-{ $Pt(DEtSO)Cl_2$ }<sub>2</sub>( $\mu$ -pyrazine)

and trans-Pt(pyrazine)(DEtSO)Cl<sub>2</sub>

This chapter presents the synthesis and characterization of two new platinum(II) complexes, with diethylsulfoxide (DEtSO) ligands. A few years ago, two series of compounds,  $Pt(R_2SO)(pz)Cl_2$  and  $\{Pt(R_2SO)Cl_2\}(\mu-pz)\{Pt(R_2SO)Cl_2\}$ , were prepared and characterized in our research laboratory. The first series includes pyrazine as a ligand and the second series as a bridging bidentate ligand. Diethylsulfoxide ligand, not available on the market at that time, has been specifically prepared for this project. Comparison with the two previous series is presented and the geometry of the complexes is studied.

# **5.1 Preparation**

# 5.1.1 Starting material

The salt K<sub>2</sub>[PtCl<sub>4</sub>] was obtained from Johnson Matthey Inc. and was purified by recrystallization in water before use. The solvent CDCl<sub>3</sub> was purchased from CDN Isotopes. Diethylsulfoxide is not available on the market, so we had to request a special micro production of this compound from Narchem Corp.

#### 5.1.2 Synthesis of the complexes K[Pt(DEtSO)Cl<sub>3</sub>]

The method used was that of Kukushkin *et al.* (1), slightly modified. Crystalline K<sub>2</sub>[PtCl<sub>4</sub>] (0.8304 g, 2,.0 mmol) was ground and dissolved in a minimum of water (15 mL). The sulfoxide ligand (0.2228 g, 2.1 mmol), mixed with about 5 mL of water, was added to the K<sub>2</sub>[PtCl<sub>4</sub>] solution. The resulting mixture was closed from air with a watch glass, and stirred vigorously for about 6 h. The precipitate obtained (disubstituted complex) was separated by filtration and washed with water (3 x 10 mL). The filtrate obtained was set aside for evaporation and the resulting yellow crystals were redissolved in acetone (about 40mL). The mixture was stirred for 30 min and then filtered. The purified filtrate, separated from potassium chloride and any remaining K<sub>2</sub>[PtCl<sub>4</sub>] starting material, was left to evaporate. The product obtained was recrystallized from water, dried, and then washed with diethylether to remove any trace of sulfoxide ligand. The crystals were then dried under vacuum in the desiccator. The complex K[Pt(DEtSO)Cl<sub>3</sub>] was prepared in a 89% yield.

#### 5.1.3 Synthesis of the monomeric complex trans-Pt(DEtSO)(pyrazine)Cl<sub>2</sub>

Crystals of K[Pt(DEtSO)Cl<sub>3</sub>] (0.211 g, 0.48 mmol) were crushed and dissolved in a minimum of distilled water (10 mL). Pyrazine (0.0425 g, 0.53 mmol) was mixed with

about 5 mL of water in a second beaker. The platinum mixture was slowly added to the pyrazine solution under constant stirring. The beaker containing K[Pt(DEtSO)Cl<sub>3</sub>] was rinsed with water (2 x 3 mL) and the washings were incorporated into the reaction mixture. An apple-yellow precipitate rapidly appeared. The mixture was stirred for about 30 min, filtered and the residue obtained was washed with distilled water (3 x 3 mL) to remove any traces of the two water-soluble starting materials. The yellow crystals obtained were dried to air, washed with diethylether, and finally dried again in a vacuum dessiccator. *trans*-Pt(DEtSO)(pyrazine)Cl<sub>2</sub>: yield, 92%; decomp. pt. = 179-191 °C, the compound turns whitish and then white; IR (cm<sup>-1</sup>) 3748w, 3102w [ $v_{13}$  ( $B_{1u}$ )], 2910w, 1450w [ $v_{19a}$  ( $B_{1u}$ )], 1416s [ $v_{19b}$  ( $B_{3u}$ )], 1394w [ $v_{19b}$  ( $B_{3u}$ )], 1143s [ $v_{18a}$  ( $B_{1u}$ ))] 1112s [ $v_{3}$  ( $B_{2g}$ )], 1076m [ $v_{14}$  ( $B_{3u}$ )], 1060m [ $v_{1}$  ( $A_{g}$ )], 807m [ $v_{11}$  ( $B_{2u}$ )]; v(S-O) 1159m, v(Pt-N) 516w, v(Pt-S) 479m, v(Pt-Cl) 348s.

#### 5.1.4 Synthesis of the dimeric complexes *trans-trans*-{Pt(DEtSO)Cl<sub>2</sub>}<sub>2</sub>(μ-pyrazine)

Crystals of K[Pt(DEtSO)Cl<sub>3</sub>] (0.274 g (0.62 mmol) were ground up and dissolved in a minimum of distilled water (12 mL). Pyrazine (0.0241 g, 0.30 mmol) was mixed with about 3 mL of water in a second beaker. The pyrazine solution was added slowly to the platinum mixture while stirring constantly. The beaker containing pyazine was rinsed with water (2 x 3 mL) and the washings were added to the reaction mixture. An apple-yellow precipitate rapidly appeared. The mixture was stirred for about 15 min, filtered and the residue obtained was washed with distilled water (3 x 3 mL) to remove any traces of the two water-soluble starting materials. The yellow crystals obtained were dried in air and then washed with diethylether, prior to the final drying under vaccum in a dessiccator. trans, trans-{Pt(DEtSO)Cl<sub>2</sub>}<sub>2</sub>( $\mu$ -pyrazine): yield, 94%; decomp. pt. = 190-

206 °C, the compound turns whitish and then white; IR (cm<sup>-1</sup>): 3762w, 3098m [ $v_{13}$  ( $B_{1u}$ )], 2915w, 1457 m [ $v_{19a}$  ( $B_{1u}$ )], 1415s [ $v_{19b}$  ( $B_{3u}$ )], 1383w [ $v_{19b}$  ( $B_{3u}$ )], 1128s [ $v_{18a}$  ( $B_{1u}$ )], 1102s [ $v_{3}$  ( $B_{2g}$ )], 1072m [ $v_{14}$  ( $B_{3u}$ )], 1059w [ $v_{1}$  ( $A_{g}$ )], 810 w [ $v_{11}$  ( $B_{2u}$ )]; v(S-O) 1164s, v(Pt-N) 519m, v(Pt-S) 468w, v(Pt-Cl) 351m.

# 5.2 Analysis of the compounds by multinuclear (<sup>195</sup>Pt, <sup>13</sup>C and <sup>1</sup>H) NMR spectroscopy

All the NMR spectra were measured in CDCl<sub>3</sub> solutions on a Varian Gemini 300BB spectrometer operating at 300.021, 75.454 and 64.321 MHz for  $^{1}$ H,  $^{13}$ C and  $^{195}$ Pt nuclei, respectively. The chloroform peaks were used as an internal standard for the  $^{1}$ H (7.24 ppm) and  $^{13}$ C (77.00 ppm) NMR spectra. For  $^{195}$ Pt, the external reference was K[Pt(DMSO)Cl<sub>3</sub>] in D<sub>2</sub>O, adjusted to -2998 ppm from K<sub>2</sub>[PtCl<sub>6</sub>] ( $\delta$ (Pt) = 0 ppm). The  $^{195}$ Pt NMR spectra were measured between approximately -2500 and -4000 ppm.

# 5.2.1 <sup>195</sup>Pt NMR spectroscopy

The <sup>195</sup>Pt-NMR chemical shifts of both compounds are given in Table 5.2.1. For comparative purposes, similar data for other monomeric and dimeric analogues are also presented in this table.

**Table 5.2.1** <sup>195</sup>Pt-NMR chemical shifts (ppm) of the  $Pt(R_2SO)(pz)Cl_2$  and  $\{Pt(R_2SO)Cl_2\}(\mu-pz)\{Pt(R_2SO)Cl_2\}$  complexes (in CDCl<sub>3</sub>)

D. S.O.	δ( <sup>195</sup> Pt) monomeric	δ( <sup>195</sup> Pt) dimeric
$R_2SO$	compound	compound
DMSO	-3045	-3049 <sup>a</sup>
TMSO	-3042	-3041
<b>DEtSO</b>	-3079	-3076
DPrSO	-3046	-3048
DBuSO	not isolated	-3051
DPhSO	-3121	-3113
a · .	DI CE 1	

<sup>a</sup> in DMF-d<sub>7</sub>

The spectra obtained for both DEtSO compounds are very similar. One unique peak, very well defined, was observed at -3079 and -3076 ppm for Pt(DEtSO)(pz)Cl<sub>2</sub> and {Pt(DEtSO)Cl<sub>2</sub>}{(μ-pz){Pt(DEtSO)Cl<sub>2</sub>}, respectively. These values are comparable to those observed for the monomeric and dimeric platinum analogues (see Table 5.2.1). This observation is in agreement with the literature (2-9). Chemical shifts are observed between -3139 and -2851ppm for a [NSCl<sub>2</sub>] coordination sphere (Chapter 2 – Appendix A). It is also interesting to notice that the monomeric and dimeric compounds exhibit similar shieldings. The chemical shifts are only slightly influenced by the length of the sulfoxide carbon chain.

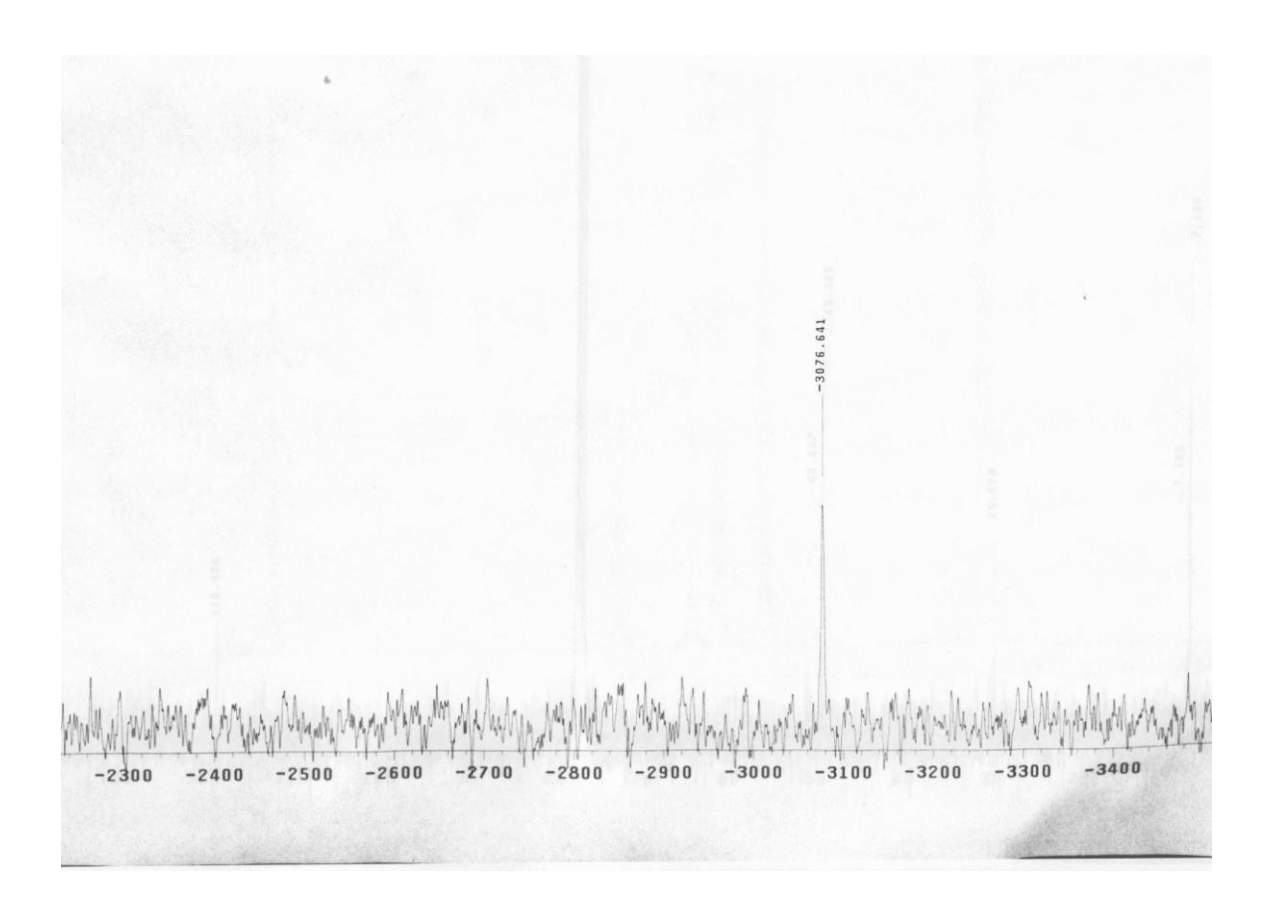


**Figure 5.2.1**  $^{195}$ Pt NMR spectrum of the  $\{Pt(DEtSO)Cl_2\}(\mu-pz)\{Pt(DEtSO)Cl_2\}$  compound (in CDCl<sub>3</sub>)

# 5.2.2 $^{1}\mathrm{H}$ and $^{13}\mathrm{C}$ NMR spectroscopy of the dimeric compound

The pyrazine chemical shifts observed in the proton and carbon-13 NMR spectra are shown in Table 5.2.2.1. The  ${}^{3}J({}^{1}H-{}^{195}Pt)$  coupling constants are added to the table. For the purposes of comparison, the chemical shifts and coupling constants for other dimeric analogues are also given in the table.

**Table 5.2.2.1**  $\delta(^{1}\text{H})$  (ppm),  $^{3}J(^{1}\text{H}-^{195}\text{Pt})$  (Hz) and  $\delta(^{13}\text{C})$  (ppm) of pyrazine in the symmetrical  $\{\text{Pt}(R_{2}\text{SO})\text{Cl}_{2}\}(\mu\text{-pz})\{\text{Pt}(R_{2}\text{SO})\text{Cl}_{2}\}$  dimeric compounds (in CDCl<sub>3</sub>)

$R_2SO$	$\delta(^{1}\text{H})$	$^{3}J(^{1}\text{H}-^{195}\text{Pt})$	$\delta(^{13}C)$
DMSO	9.100s	-	148.03 <sup>a</sup>
TMSO	9.105s	34	148.25
DEtSO	9.106s	29	148.18
DPrSO	9.098s	28	148.20
DBuSO	9.104s	29	148.21
DPhSO	9.134s	35	148.41
a	in DME-da		

<sup>a</sup> in DMF-d<sub>7</sub>

In both the proton and carbon-13 NMR spectra, the pyrazinic chemical shifts appear as two singlets. The values, 9.106 and 148.18 ppm, are in agreement with what has been observed for other *trans,trans*-{Pt(R<sub>2</sub>SO)Cl<sub>2</sub>}( $\mu$ -pz){Pt(R<sub>2</sub>SO)Cl<sub>2</sub>} compounds (2). The nature of the sulfoxide ligand within the complex does not seem to influence the shielding. Only the diphenylsulfoxide ligand does influence slightly because of the presence of the aromatic phenyl rings. In the <sup>1</sup>H-NMR spectra, satellites arising from the coupling of the protons with the platinum-195 isotope are observed. The <sup>3</sup>J(<sup>1</sup>H-<sup>195</sup>Pt) coupling constant in {Pt(DEtSO)Cl<sub>2</sub>}<sub>2</sub>( $\mu$ -pz) has a value of 29Hz. This value can be compared to those observed with other sulfoxide ligands. It confirms the *trans* geometry of the complex, since such coupling constants are generally observed between 20 and 35Hz for the *trans* complexes and between 35 and 50Hz for the *cis* analogues (Section

8.2.2., 2-9). The values of the pyrazine signals in *trans,trans*-{Pt(DEtSO)Cl<sub>2</sub>}(μ-pz){Pt(DEtSO)Cl<sub>2</sub>}, 9.106 and 148.18 ppm, show a deshielding in comparison with the free ligand (8.595 and 145.07 ppm).

The chemical shifts of the sulfoxide ligands observed in the proton and carbon-13 NMR spectra are presented in the Tables 5.2.2.2. and 5.2.2.3. For comparison purpose, similar data for other dimeric analogues are included.

**Table 5.2.2.2** <sup>1</sup>H NMR  $\Delta\delta$  ( $\delta_{complex}$ - $\delta_{sulfoxide}$ ) (ppm) of the sulfoxide ligands in the trans,trans-{Pt(R<sub>2</sub>SO)Cl<sub>2</sub>}( $\mu$ -pz){Pt(R<sub>2</sub>SO)Cl<sub>2</sub>} complexes

R <sub>2</sub> SO	$H_{\alpha}$	$H_{\beta}$	$H_{\gamma}$	$H_{\delta}$
DMSO	1.02, 0.99			
TMSO	1.20, 0.84	0.01, 0.25		
DEtSO	1.09, 0.73	0.34		
DPrSO	1.09, 0.69	0.50, 0.42	0.20	
DBuSO	0.86, 0.58	0.43, 0.33	0.12	0.07
DPhSO		0.28 (ortho)	0.11 (meta)	0.11 (para)

The chemical shifts of the bonded sulfoxide ligands are more deshielded than are those of the free molecules. The protons closer to the O atom are the most deshielded upon coordination, and the  $\Delta\delta$  values become negligible as the distance from the binding site increases. Two series of signals are observed for the  $H_{\alpha}$  proton because of limited

rotation about the S–C bonds. The separation between the signals of the geminal protons decreases as the distance from the coordination site increases, when the chemical shifts become superimposible.

**Table 5.2.2.3** <sup>13</sup>C NMR  $\Delta\delta$  ( $\delta_{complex}$ - $\delta_{sulfoxide}$ ) (ppm) of the sulfoxide ligands in the trans,trans-{Pt(R<sub>2</sub>SO)Cl<sub>2</sub>}( $\mu$ -pz){Pt(R<sub>2</sub>SO)Cl<sub>2</sub>} complexes

R <sub>2</sub> SO	$C_{\alpha}$	$C_{eta}$	$\mathbf{C}_{\gamma}$	$C_{\delta}$
DMSO	3.61			
TMSO	2.97	-1.11		
DEtSO	4.60	0.64		
DPrSO	2.77	0.52	-0.40	
DBuSO	3.49	0.03	-0.50	0.00
DPhSO	-6.61	2.85 (ortho)	-0.24 (meta)	2.34 ( <i>para</i> )

The signals for the C atoms in the  $\alpha$  position are observed at lower field than for the free molecules ( $\Delta\delta \approx 3.5$  ppm), except for the DPhSO complex, which appears at very high field ( $\Delta\delta \approx -6.6$  ppm). Similar results have already been noted for the Pt(R<sub>2</sub>SO)(pm)Cl<sub>2</sub> and pyrimidine-bridged complexes (10,11). The presence of the  $\pi$  (Pt $\rightarrow$ S) bond increases the electronic density on the sulfoxide ligand. Back polarization of the  $\pi$ (S=O) bond would explain the results observed for the Pt-sulfoxide complexes (fig 5.2.2). Bonding to Pt would reduce the  $\pi$ -electron density on the O atom ( $^{\delta}$ -S $\leftarrow$ O $^{\delta+}$ )

and increase it on the S atom and its neighbouring atoms, including the Pt atom as mentioned above. The chemical shifts in the  $^{13}$ C-NMR spectra are particularly sensitive to such mesomeric effects. The back polarization of the  $\pi$ -electrons in the S=O bond would be more important in the DPhSO complex, since the two electron-attracting groups are bonded directly on the S atom.

$$O = \begin{cases} R & CI \\ S & Pt - N \end{cases} N - Pt - S = O$$

$$CI & R$$

**Figure 5.2.2** Sketch of the electronic inverse polarization of the S-O  $\pi$  bond in  $trans, trans-\{Pt(R_2SO)Cl_2\}(\mu-pz)\{Pt(R_2SO)Cl_2\}$  complexes.

# 5.2.3 $^{1}\mathrm{H}\text{-}$ and $^{13}\mathrm{C}\text{-}\mathrm{NMR}$ spectra of the monomeric compound

The pyrazine chemical shifts observed by proton and carbon-13 NMR spectroscopy are listed in Table 5.2.3.1. The  ${}^3J({}^1H_a{}^{-1}H_b)$  coupling constants are included to the table. For comparison purposes, the chemical shifts and coupling constants of other monomeric analogues are also shown

**Table 5.2.3.1**  $\delta(^{1}\text{H})$  (ppm),  $^{3}J(^{1}\text{H}_{a}\text{-}^{1}\text{H}_{b})$  (Hz) and  $\delta(^{13}\text{C})$  (ppm) of pyrazine carbon atoms in the *trans*-Pt(R<sub>2</sub>SO)(pz)Cl<sub>2</sub> monomeric compounds (in CDCl<sub>3</sub>)

R <sub>2</sub> SO	$\delta(^1H_a)$	$\delta(^{1}H_{a})$	$\delta(^{13}C_a)$	$\delta(^{13}C_a)$
DMSO	8.811dd	8.764dd	147.01	145.33
	[3.0, 1.2]	[3.0, 1.2]		
TMSO	8.780d [3.0]	8.770d [3.0]	147.42	145.70
DEtSO	8.820d [3.1]	8.790d [3.1]	147.28	145.63
DPrSO (cis)	8.707d [3.3]	8.685d [3.3]	147.59	147.40
DPhSO	8.896m	8.896m	147.32	145.93

The pyrazine protons are more deshielded in the *trans*-Pt(DEtSO)(pz)Cl<sub>2</sub> complex than in the free ligand ( $\delta = 8.595$  ppm in  $^1\text{H-NMR}$  and 145.07 ppm in  $^{13}\text{C-NMR}$ ). Similar observations have previously been made for other compounds, and  $\Delta\delta(\delta_{complex} - \delta_{pyrazine})$  varies from 0.10 to 0.31 ppm in the  $^1\text{H-NMR}$  spectra. The (N $\rightarrow$ Pt)  $\sigma$  bond diminishes the electronic density on the ligand and the  $\delta(^1\text{H})$  shifts are observed at lower field for the ligands bonded to the metallic center. Unlike the dimeric compounds,  $C_a$  and  $C_b$  are not equivalent so two pyrazine signals are observed in both the proton and carbon-13 spectra. The positions of the  $C_a$  carbons atoms are the most influenced by the Pt $\leftarrow$ N bond. Actually, coordination reduces the electron density on the bonded nitrogen atom and this density reduction is more important on the closer atoms. So, the  $C_a$  atoms would be more deshielded,  $\Delta\delta \sim 2$  ppm, than the  $C_b$  atoms. As in the cases of DMSO, TMSO and DPhSO, the DEtSO complex showed this spectroscopic behavior. This observation

helped in concluding that new DEtSO complex has a *trans* geometry. Rotation of the pyrazine ligand around the Pt-N bond is less limited in the *trans* compounds, probably due to the fact that the  $\pi$ -link is not that strong. In the *cis* compounds, such as the DPrSO complex, steric hindrance becomes a factor to be considered. The rotation meets some constraints and the pyrazine ring goes to the orthogonal position to the platinum plane. A stronger  $\pi$  Pt $\rightarrow$ S bond in the *cis* compounds reduces the electron density on the Pt(II) and increases it on the ligand. This phenomenon has also been observed for the Pt(R<sub>2</sub>SO)(pm)Cl<sub>2</sub> compounds by Rochon *et al.* (10) and for the Pt(PEt<sub>3</sub>)(pz)Cl<sub>2</sub> and Pt(PMePh<sub>2</sub>)(pz)Cl<sub>2</sub> compounds by Venanzi *et al.* (12). In the proton NMR,  $^3J(^1\text{H}_a\text{-}^1\text{H}_b)$  coupling constants are observed (3.1Hz), which is in the range expected.

The chemical shifts of the sulfoxide ligands observed in the proton and carbon-13 NMR spectra are presented in Tables 5.2.3.2. and 5.2.3.3. The chemical shifts and coupling constants of other monomeric analogues are included for comparison purposes.

**Table 5.2.3.2**  $^{1}$ H-NMR  $\Delta\delta$  ( $\delta_{complex}$ - $\delta_{sulfoxide}$ ) (ppm) of the sulfoxide ligands in the  $Pt(R_{2}SO)(pz)Cl_{2}$  complexes

R <sub>2</sub> SO	$H_{\alpha}$	$H_{eta}$	$H_{\gamma}$	$H_{\delta}$
DMSO	1.00			
	$^{3}J(^{195}\text{Pt-}^{1}\text{H}) = 23$			
TMSO	1.17, 0.82	-0.01, 0.25		
DEtSO	1.14, 0.70	0.32		
DPrSO (cis)	1.20, 0.56	0.62, 0.29	0.17 [7.5]	
DPhSO		0.66 [7.8],	0.14 ( <i>meta</i> )	0.14 ( <i>para</i> )
DI IISO		0.30 [7.4] (ortho)	0.1 <del>1</del> (mem)	0.14 (риги)

As for the dimeric compounds, the chemical shifts of the bonded sulfoxide ligands are more deshielded than are those of the free molecules. Two series of signals are observed for the  $H_{\alpha}$  proton - this is due to limited rotation of the S–C bonds. For the  $\beta$  position, the two series of signals become so close that they are superimposible for the  $Pt(DEtSO)(pz)Cl_2$  complex.

**Table 5.2.3.3**  $^{13}$ C NMR  $\Delta\delta$  ( $\delta_{complex}$ - $\delta_{sulfoxide}$ ) (ppm) of the sulfoxide ligands in the  $Pt(R_2SO)(pz)Cl_2$  complexes

R <sub>2</sub> SO	$C_{\alpha}$	$\mathbf{C}_{eta}$	$\mathbf{C}_{\gamma}$	$C_{\delta}$
DMSO	3.76			
TMSO	2.66	-0.75		
DEtSO	4.52	0.69		
DPrSO (cis)	2.31	0.54	-0.52	
DPhSO	-6.99	2.86 (ortho)	-0.34 (meta)	2.12 (para)

As for the other sulfoxide ligands, except for the aromatic DPhSO, the *trans*-Pt(DEtSO)(pz)Cl<sub>2</sub> complex shows a signal at lower field for the carbon atom in  $\alpha$  position ( $\Delta\delta$  ( $\delta_{complex}$ - $\delta_{sulfoxide}$ ) = 4.5 ppm). This is due to the  $\pi$  (Pt $\rightarrow$ L) bond increasing the electronic density on the ligand, and then to the  ${}^{\delta}$ -S $\leftarrow$ O $^{\delta+}$  back-polarization of the sulfoxide function increasing the electronic density on the carbon atoms located in the  $\alpha$  position. As can be seen from the table, the  $\Delta\delta$  values decrease with the length of the sulfoxide ligand chain to become even negative for some of them.

# 5.3 Analysis of the complexes by vibrational spectroscopy

## **5.3.1 IR spectroscopy**

The IR spectra were recorded in the solid state (KBr pellets) on a FTIR Nicolet 4700 spectrometer between 4000 and 280 cm<sup>-1</sup>. The observed vibrations are listed in table 5.3.1. below. The assignments for the pyrazine ligand are based on those reported for the

IR spectrum of pyrazine by Simmons and Innes (13). A recent study of the IR vibrational spectrum of pyrazine in solid argon (10°K) has also been published (14).

**Table 5.3.1.** Infrared spectra observed for the coordinated pyrazine and sulfoxide ligands in the DEtSO compounds (cm<sup>-1</sup>) and assignment of the bands. The Pt-Cl, Pt-N and Pt-S vibrations are also indicated

assignment	free pz	trans-Pt(DEtSO)(pz)Cl <sub>2</sub>	$\textit{trans-}\{Pt(R_2SO)Cl_2\}_2(\mu\text{-pz})$
ν <sub>13</sub> (Β <sub>1u</sub> )	3070	3102 w	3098 m
ν (C-H)	2918	2910 w	2915 w
$\nu_{19a}\left(B_{1u}\right)$	1485	1450 w	1457 m
$\nu_{19b}\left(B_{3u}\right)$	1407	1416 s	1415 s
$\nu_{19b}\left(B_{3u}\right)$	1378	1394 w	1383 w
ν(S	-O)	1159 m	1164 s
$\nu_{18a}\left(B_{1u}\right)$	1134	1143 s	1128 s
$\nu_3$ (B <sub>2g</sub> )	1120	1112 s	1102 s
$\nu_{14}\left(B_{3u}\right)$	1065	1076 m	1072 m
$\nu_1  (A_g)$	1015	1060 m	1059 w
$v_{11}\left(B_{2u}\right)$	788	807 m	810 w
ν(P	t-N)	516 w	519 m
v(P	rt-S)	479 m	468 w
ν(Ρι	t-Cl)	348 s	351 m

Pyrazine has a  $D_{2h}$  point symmetry with 24 vibrations. 10 of which are active in the IR. This corresponds to what is observed on the spectra of the DEtSO complexes. The symmetry of the pyrazine-bridged ligand in the symmetric trans-trans dimer is not changed compared to the free ligand. The results on the monomeric compound are almost identical, as well as to what was observed for other monomeric and dimeric analogues (2,7). All the pyrazine vibrations in the complexes are observed at identical or at slightly higher energies than are those of free pyrazine. As expected, the v(S-O) vibrations absorb at higher energy (~100 cm<sup>-1</sup>) than in the free sulfoxide ligand. This broad and intense characteristic vibration has more energy than in the free sulfoxide ligand, since it is bonded to Pt by the S atom and has been reported in the literature (2,7,10,11,15-18). The sulfoxide S-O p $\pi$ -d $\pi$  bond is stronger when coordinated to the metal atom through the S atom than in the free sulfoxide or when there is a Pt-O coordination bond. The sulfoxide mesomer-III is favored (section 1.5). The  $\nu(Pt-S)$  and  $\nu(Pt-N)$  bands are more difficult to assign, since they usually have low intensity and the  $\nu(Pt-N)$  vibrations often couple with other vibrations of the molecule. The absorption band observed around 520 cm<sup>-1</sup> is assigned to v(Pt-N) vibrations based on the literature (2,7,19,20). The absorption band observed between 460 and 480  $\text{cm}^{-1}$  is assigned to a  $\nu(\text{Pt-S})$  vibration based on data in the literature (15,21-24). The  $\nu$ (Pt-Cl) vibration mode is usually easier to assign since it is strong and stable. The values for our two compounds and the fact there is only one unique signal for both compounds confirms they have the *trans* geometry. Two stretching bands are usually observed for *cis*-dichloro Pt(II) complexes (7).

# **5.3.2** Raman spectroscopy

There is no Raman study on Pt(II) compounds containing Pt-pyrazine bonds in the literature. The Raman spectra of the free pyrazine ligand and our complexes were measured in the solid state between 4000 and about 200 cm<sup>-1</sup> on a Renishaw inVia spectrometer equipped with a microscope. A near-infrared laser (785 nm) was used to excite the spectra and the operating power was 10 %. Five spectral accumulations were made for each sample. The data are summarized in Table 5.3.2. In each spectrum, there are bands characteristic of the ligands present.

**Table 5.3.2.** Raman vibrations observed in the *trans*, trans-{Pt(DEtSO)Cl<sub>2</sub>}<sub>2</sub>( $\mu$ -pz) and trans-Pt(DEtSO)(pz)Cl<sub>2</sub> compounds (cm<sup>-1</sup>)

assignment	Free pyrazine	Dimeric complex	Monomeric complex
	3581 vw	3579 vw	3581 vw
v <sub>7b</sub> (H-stretch) B2g	3032 vw	2984 vw	2989 vw
$2v_{19a}$ (ring) $Ag$	2967 vw	2929 w	2927 w
	2303 vw	2350 vw	2346 vw
$v_{8a}$ (ring) $Ag$	1580 m	1612 m	1608 s
ν <sub>8b</sub> (ring) <i>B2g</i>	1520 w	1514 w	1518 w
	1358 w	1414 vw	1402 w
$v_{9a}$ (H-bend) $Ag$	1248 m	1225 m	1224 m
v(S-O)		1138 m	1134 m
v <sub>1</sub> (ring) Ag	1013 vs	1048 vs	1056 vs

		1026 m	1030 s
$v_{10a}$ (H-bend) $B1g$	754vw	742 vw	738 vw
ν <sub>4</sub> (ring) <i>B3g</i>	699 s	694 m	692 m
v <sub>6a</sub> Ag	596 w	651 w	653 w
ν(Pt-N)		508 vw	503 w
ν(Pt-S)		428 w	428 s
v(Pt-Cl)		335 vs	334 vs
δ(N-Pt-S)		282 vw	284 w
π(Pt-N)		241 m	240 s

The Raman spectrum of the free pyrazine ligand has been reported by Tam and Cooney (25) and our assignments for the ligand are based on this study. The well accepted convention of Lord *et al.* (26) has been used in numbering the vibration modes with the z-axis through the two nitrogen atoms. The symmetry of pyrazine is the same as in the free molecule. Most of the bands of the Pt(II) complexes are very weak in intensity, partly because of the low laser power that has to be used, since the compounds decompose in the laser radiation (785 nm). The green laser (514.5 nm) was tested, but the decomposition proved to be much faster.

The vibrations of coordinated pyrazine are almost all observed at equal or slightly higher energies than are those of the free ligand. For free pyrazine, we observe 9 of the 10 bands reported by Tam and Conney. We do not observe the very weak band at 1226 cm<sup>-1</sup> ( $2v_{6a}$ ) with our spectrometer. This is probably due to the low intensity of the laser radiation. We also observe the two missing bands from the work of Tam and Conney at 1358 and 596 cm<sup>-1</sup>. The band at 1358 cm<sup>-1</sup> is assigned to the  $v_{14}$  mode, as suggested by

Foglizzo and Novak in a Raman study of the chloro and bromo pyrazinium salt (27). In our complexes, this vibration is found at about 1410 cm<sup>-1</sup>. The band at 596 cm<sup>-1</sup> in the free ligand can be assigned to the  $v_{6a(ring)} - Ag$  mode, based on the work of Simmons et al. (13) who reported this vibration at 598 cm<sup>-1</sup>. This vibration is shifted to slightly higher energy ( $\sim 60 \text{ cm}^{-1}$ ) in the Pt(II) complexes. The  $\square$ (S-O) bands are observed in Raman spectroscopy between 1130 and 1140 cm<sup>-1</sup> as expected for Pt(II)-S-bonded sulfoxides. The vibrations involving the Pt(II) atom are usually observed in the region below 550 cm<sup>-1</sup>. The v(Pt-Cl) modes are easily identified, since they are strong vibrations in both the IR and Raman spectra. These modes were observed in the Raman as a intense single band at 335 cm<sup>-1</sup>. They appear at slightly lower energies than those observed by IR spectroscopy (around 350 cm<sup>-1</sup>). The symmetric stretching vibration is probably observed in Raman, while the nonsymmetric stretching mode would be seen in IR only. For comparison, the v(Pt-Cl) vibration mode in trans-Pt(C<sub>2</sub>H<sub>4</sub>)(py)Cl<sub>2</sub> was observed in IR at 345 cm<sup>-1</sup> and at 335 cm<sup>-1</sup> in Raman (28). Since there is only one stretching band for each compound, the complexes are assumed to have the *trans-trans* configuration. The v(Pt-N) and  $\nu(Pt-S)$  vibrational modes are more difficult to observe, since they appear as less intense bands. In our study, one vibration, observed between 500 and 510 cm<sup>-1</sup>, could be tentatively assigned to a v(Pt-N) vibration mode. This assignment seems more popular in the Pt(II)-amine chemistry field. The other stretching vibrational mode involving the Pt(II) atom, v(Pt-S), is believed to be that observed at 428 cm<sup>-1</sup>, as suggested by the literature (18). The Raman bands observed around 285 and 240 cm<sup>-1</sup> in our complexes can be assigned to  $\delta(N-Pt-S)$  and  $\pi(Pt-N)$  vibrations, respectively, based on the literature (29-31).

## Conclusion

This research project required a new sulfoxide ligand, DEtSO, not available on the market, so it has been specially prepared for this study. The aliphatic length of the sulfoxide chain influences Pt(II) complexes, so it was interesting to compare with previous studies. Reaction of K[Pt(DEtSO)Cl<sub>3</sub>] with pz in stochiometric ratio gave the *trans*-Pt(DEtSO)(pz)Cl<sub>2</sub> complex. With a 2:1 ratio, the *trans*, *trans*-{Pt(DEtSO)Cl<sub>2</sub>}<sub>2</sub>(µ-pz) dimeric compound was obtained, with good purity. These results were confirmed by IR, Raman and multinuclear (<sup>1</sup>H, <sup>13</sup>C and <sup>195</sup>Pt) NMR spectroscopy. Even if *cis* geometry is thermodynamically more stable, both *trans* species do not isomerize in organic solvents. This is in contradiction with what was observed with their pyrimidine analogues.

#### References

- Y. N. Kukushkin, Y. E. Vyaz'menskii, L. I. Zorina. Russ. J. Inorg. Chem. 1968, 13, 1573.
- (2) J.R.L. Priqueler, F.D. Rochon. *Inorg. Chim. Acta.* **2004**, *357*, 2167.
- (3) Wagner, G.; Pakhomova, T.B.; Bokach, N.A.; Fraústo da Silva, J.J.R.; Vicente, J.; Pombeiro, A.J.L.; Kukushkin, V.Y. *Inorg. Chem.* **2001**, *40*, 1683.
- (4) Lakomska, I.; Golankiewicz, B.; Wietrzyk, J.; Pelczynska, M.; Nasulewicz, A.; Opolski, A.; Sitkowski, J.; Kozerski, L.; Szlyk, E. *Inorg. Chim. Acta.* 2005, 358, 1911.
- (5) Fontes, A.P.S.; Oskarsson, Å.; Lövqvist, K.; Farrell, N. *Inorg. Chem.* **2001**, *40*, 1745.
- (6) Qu, Y.; Farrell, N. Inorg. Chem. 1992, 31, 930.
- (7) Priqueler, J.R.L.; Rochon, F.D. Can. J. Chem. 2004, 82, 649.
- (8) Appleton, T.G.; Hall, J.R.; Ralph, S.F. Inorg. Chem. 1985, 24, 4685.
- (9) Rochon, F.D.; Buculei, V. Inorg. Chim. Acta. 2005, 358, 2040.
- (10) N. Nédélec, F.D. Rochon, Inorg. Chim. Acta. 2001, 319, 95.
- (11) N. Nédélec, F.D. Rochon, Inorg. Chem. 2001, 40, 5236.
- (12) A. Albinati, F. Isaia, W. Kaufmann, C. Sorato and L. M. Venanzi. *Inorg. Chem.* 1989, 28, 1112.
- (13) J.D. Simmons, K.K. Innes, G.M. Begun. J. Mol. Spectrosc. 1964, 14, 190.
- (14) S. Breda, I.D. Reva, L. Lapinski, M.J. Nowak, R. Fausto, J. Mol. Struct. 2006, 786, 193.

- (15) J.H. Price, A.N. Williamson, R.F. Schram, B.B. Wayland, *Inorg. Chem.* 1972, 11, 1280.
- (16) G. A. Foulds, D.A. Thorton, *Spectrochim. Acta.* **1981**, *37A*, 917.
- (17) F.D. Rochon, C. Bensimon, C. Tessier, *Inorg. Chim. Acta.* **2008**, *361*, 16.
- (18) S. Gama de Almeida, J.L. Hubbard, N. Farrell, Inorg. Chim. Acta. 1992, 193, 149.
- (19) K. Nakamoto, P.J. McCarthy, J. Fujita, R.A. Condrate, G.T. Behnke, *Inorg. Chem.* **1965**, *4*, 36.
- (20) Yu.N. Kukushkin, N.V. Ivannikova, K.A. Khokhryakov, Russ. J. Inorg. Chem. 1970, 15, 1595.
- (21) V.Yu. Kukushkin, V.K. Belsky, V.E. Konovalov, G.A. Kirakosyan, L.V. Konovalov, A.I. Moiseev, V.M. Tkachuk, *Inorg. Chim. Acta.* **1991**, *185*, 143.
- (22) Yu.N. Kukushkin, I.V. Pakhomova, Russ. J. Inorg. Chem. 1971, 16, 226.
- (23) Yu.N. Kukushkin, V.N. Spevak, Russ. J. Inorg. Chem. 1973, 18, 240.
- (24) B.F.G. Johnson, R.A. Walton, *Spectrochim. Acta.* **1966**, 22, 1853.
- (25) Tam, N.T.; Cooney, R.P. J. Chem. Soc., Faraday Trans. 1976, 72, 2598.
- (26) R.C. Lord, A.L. Marston, F.A. Miller, *Spectrochim. Acta.* **1957**, 9, 113.
- (27) R. Foglizzo, A. Novak, *Appl. Spectroscopy.* **1970**, *24*, 601.
- (28) T.P.E. Auf der Heyde, G.A. Foulds, D.A. Thorthon, H.O. Desseyn, B.J. Van der Veken, J. Mol. Struct. 1983, 98, 11.
- (29) P.D. Harvey, K.D. Truong, K.T. Aye, M. Drouin, A.D. Bandrauk, *Inorg. Chem.* 1994, 33, 2347.
- (30) M.T. Forel, M. Tranquille, *Spectrochim. Acta, Part A.* **1970**, 26, 1023.
- (31) J.R. Durig, C.M. Player Jr, J.J. Bragin, *Chem. Phys.* **1970**, *52*, 4224.

#### **CHAPTER VI**

Synthesis of cis- and trans-Pt(R<sub>2</sub>SO)(pz)I<sub>2</sub>

 $(R_2SO = DMSO, TMSO, DPrSO, DBuSO, DBzSO and DPhSO)$ 

This chapter reports the synthesis and characterization of new monomeric platinum(II) complexes, with pyrazine and iodo ligands. A series of sulfoxide ligands with different steric hindrance and chemical behavior has been used. They include dimethylsulfoxide (DMSO), tetramethylenesulfoxide (TMSO), di-*n*-propylsulfoxide (DPrSO), di-*n*-butylsulfoxide (DBuSO), dibenzylsulfoxide (DBzSO) and diphenylsulfoxide (DPhSO). A series of monomeric complexes with pyrazine, sulfoxide and chloro ligands were studied a few years ago. It appeared interesting to study compounds prepared with bulkier halogen ligands, such as iodine. The metallic coordination is quite different and expected to be more shielded. A comparison with the chloro analogues is added as it is relevant.

#### 6.1 Preparation

# 6.1.1 Starting material

The K<sub>2</sub>[PtCl<sub>4</sub>] compound was obtained from Johnson Matthey Inc. and was purified by recrystallization in water before use. Acetone-d<sub>6</sub> was purchased from CDN Isotopes. KI and pyrazine were obtained from Aldrich Chemical Company Inc. Most of the sulfoxide ligands were also bought from Aldrich. Dimethylsulfoxide was supplied by Anachemia Chemicals Ltd and di-*n*-propylsulfoxide by Phillips Petroleum Company. The latter was purified by distillation before use.

#### 6.1.2 Synthesis of the complexes $\{Pt(R_2SO)I\}_2(\mu-I)_2$

The method used for the synthesis of these products is that of Nédélec et *al.* (1), which was based on the method of Rochon et *al.* (2).

# 6.1.2.1 { $Pt(R_2SO)I$ }<sub>2</sub>( $\mu$ -I)<sub>2</sub> (R2SO = DMSO, TMSO, DPrSO)

Crystalline K<sub>2</sub>[PtCl<sub>4</sub>] (0.4211 g, 1.0 mmol) was ground up and dissolved in about 20 mL of distilled water. Similarly, KI (1.328g, 8.0 mmol) was crushed and dissolved in a minimum of distilled water, and the solution was then added in the platinum solution. The mixture was stirred for about 15 min. An excess of the sulfoxide ligand (0.1956 g (2.5 mmol) for DMSO, 0.2683 g (2.6 mmol) for TMSO and 0.3346 g (2.5 mmol) for DPrSO) mixed with about 5 mL of water was added to the resulting K<sub>2</sub>[PtI<sub>4</sub>] solution. The solution was stirred for 40 min for {Pt(DMSO)I}<sub>2</sub>(μ-I)<sub>2</sub>, for 50 min for {Pt(TMSO)I}<sub>2</sub>(μ-I)<sub>2</sub> and for one hour for {Pt(DPrSO)I}<sub>2</sub>(μ-I)<sub>2</sub>. The precipitates obtained were filtered off and washed well with distilled water, in order to remove mainly the excess of salt (KI) as well as any remaining sulfoxide ligand. After allowing the precipitates to dry in air, they were rinsed with diethylether. The DMSO compound was

obtained with a 44% yield, the TMSO compound with a 89% yield and the DPrSO compound with a 80% yield.

#### 6.1.2.2 $\{Pt(R_2SO)I\}_2(\mu-I)_2$ $\{R2SO = DBuSO, DBzSO\}$

Crystals of  $K_2[PtCl_4]$  (0.4213 g, 1.0 mmol) were ground up and dissolved in about 20 mL of a 2:1 methanol/water solution. Potassium iodide crystals (1.326g, 8.0 mmol) were also ground up and dissolved in a minimum of distilled water, and then added to the platinum solution. The mixture was stirred for about 15 min. An excess of the sulfoxide ligand [0.4216 g (2.6 mmol) for DBuSO and 0.5989 g (2.6 mmol) for DBzSO] mixed with about 15 mL of a 2:1 methanol/water solution was added to the the  $K_2[PtI_4]$  solution. This solution was stirred for 2 hours in the case of  $\{Pt(DBuSO)I\}_2(\mu-I)_2$  and for 200 min for  $\{Pt(DBzSO)I\}_2(\mu-I)_2$ . The precipitates thus obtained were filtered off and were washed thoroughly with methanol (3 x 5 mL), in order to remove any excess of KI and the sulfoxide ligand. Once dried out, the precipitate was rinsed with diethylether. The DBuSO compound was obtained with a 81% yield and the DBzSO compound with a 86% yield.

# 6.1.3 Synthesis of the complexes Pt(R<sub>2</sub>SO)(pz)I<sub>2</sub>

# 6.1.3.1 $Pt(R_2SO)(pz)I_2$ (R2SO = DMSO, DPrSO, DBuSO)

Crystals of  $\{Pt(R_2SO)I\}_2(\mu-I)_2$  [0.1054 g, 0.1 mmol for the DMSO compound, 0.1166 g, 0.1 mmol for the DPrSO compound, 0.1222 g, 0.1 mmol for the DBuSO compound and 0.1495 g, 0.1 mmol for the DBzSO compound] were ground up and dissolved in a minimum of dichloromethane. An excess of pyrazine (0.0160 g, 0.2 mmol) was dissolved in a minimum quantity of dichloromethane and this solution was added to the platinum solution. The reaction mixture was closed off from air and was stirred for 15

min in the case of DMSO, for 40 min for DPrSO, for 120 min DBuSO and for 180 min for DBzSO. The resulting solutions were allowed to dry in air. Once dry, the residues were rinsed with diethylether (2 x 3 mL) and dried again in a vacuum desiccator. The products obtained were light red. The Pt(DMSO)(pz)I<sub>2</sub> compound was obtained with a 88% yield, Pt(DPrSO)(pz)I<sub>2</sub> with a 75% yield, Pt(DBuSO)(pz)I<sub>2</sub> with a 79% yield and  $Pt(DBzSO)(pz)I_2$  with a 79% yield. This latter seemed not to be as pure as the other three compounds. cis-Pt(DMSO)(pyrazine)I<sub>2</sub>: decomp. point = 216-253 °C, the compound turns whitish and then white: IR (cm<sup>-1</sup>): 3072w, 3009w, 2909w, 1463w, 1417m, 1379w, 1139s, 1107w, 1072m, 1021m, 817m, 729m, 690m, 512w, 481w, 440s, 380s, 272w. cis-Pt(DPrSO)(pyrazine)I<sub>2</sub>: decomp. point = 197-219 °C, the compound tends to melt; IR (cm<sup>-1</sup>): 3089w, 3064w, 3040w, 2958m, 2932w, 2872w, 1460m, 1417s, 1378w, 1259w, 1125s, 1111w. 1023w, 868w. 808m, 739m, 513m, 475m. 449s. cis- $Pt(DBuSO)(pyrazine)I_2$ : decomp. point = 169-195 °C, the compound tends to melt; IR (cm<sup>-1</sup>): 3086m, 3031w, 2953m, 2919m, 1453m, 1408m, 1379w, 1214w, 1129s, 1109s, 1069w, 908m, 816m, 787m, 727m, 516s, 448m, 402m.

## 6.1.3.2 $Pt(TMSO)(pz)I_2$

Crystalline  $\{Pt(TMSO)I\}_2(\mu-I)_2$  (0.1327 g, 0.12 mmol) was ground up and dissolved in a minimum of dichloromethane, but since its solubility proved to be quite low (about 30%), the mixture was filtered. The solid residue was retained and the filtrate was used to pursue the reaction. An excess of pyrazine (0.0162 g, 0.2 mmol) was dissolved in a minimum of dichloromethane and then added to the platinum solution. The medium was closed to air and the mixture was stirred for 1 h. The resulting solution was allowed to evaporate in air. The dry residue obtained was rinsed with diethylether (2 x 3

mL) and then dried in a vacuum desiccator. The light red  $Pt(TMSO)(pz)I_2$  compound was obtained with a 22% yield. cis- $Pt(TMSO)(pyrazine)I_2$ : decomp. point = 192-226 °C, the compound tends to melt; IR (cm<sup>-1</sup>): 3079w, 2979w, 2944w, 2923w, 1469w, 1415s, 1380w, 1145s, 1117m, 1071s, 1020w, 846w, 804s, 670w, 600s, 479m, 366m, 285m.

#### 6.2 Analysis of the complexes by multinuclear NMR spectroscopy

## **6.2.1** Experimental section

In earlier work, chloroform-d or dichloromethane- $d_2$  were the solvents used for the NMR analyses. It was noticed that for iodo complexes, the solutions were turning pink rapidly, indicating the formation if I<sub>2</sub> (1). There appear to be replacement of the iodine atoms of the compounds with chlorine atoms from the solvents, i.e., halogen exchange. For instance, when Pt(DMSO)(pz)I<sub>2</sub> was put in chloroform-d and the <sup>1</sup>H-NMR spectrum of the solution was recorded, a peak at 3.479 ppm was observed, which corresponds to the chlorinated monomeric compound, Pt(DMSO)(pz)Cl<sub>2</sub> (3). For this reason, acetone- $d_6$  was chosen as the NMR solvent for the analysis of the five complexes in solution. Unfortunately, however, the compounds were not appreciably soluble in acetone but NMR spectra could be obtained. All the NMR spectra are measured on a Varian Gemini 300BB spectrometer operating at 300.021, 75.454 and 64.321 MHz for <sup>1</sup>H, <sup>13</sup>C and <sup>195</sup>Pt respectively. The standard recording conditions used in this project are the following: SW = 4500.5 Hz, AT = 1.998 sec., FB = 2600 Hz,  $PW = 7.0 \mu \text{sec.}$ , NT =200 to 500 for proton NMR, SW = 18761.7 Hz, AT = 1.815 sec., FB = 10400 Hz, PW = 8.7  $\mu$ sec., NT = 100 000 to 300 000 for carbon-13 NMR and SW = 100 000 Hz, AT = 0.150 sec., FB = 51200 Hz, PW =  $8.7 \text{ }\mu\text{sec.}$ , TOF = -900 p, NT = 100 000 to 300 000 for platinum-195 NMR. The acetone peaks are used as an internal standard for the  $^{1}$ H (2.04 ppm for the central peak of the CH<sub>3</sub> quintuplet signal) and  $^{13}$ C (29.80 ppm for the central peak of the CH<sub>3</sub> septuplet signal) NMR spectra. For  $^{195}$ Pt, an external reference is used, Pt(TMSO)<sub>2</sub>(CN)<sub>2</sub> in CDCl<sub>3</sub>, adjusted at -3450 ppm from K<sub>2</sub>[PtCl<sub>6</sub>] ( $\delta$  (Pt) = 0 ppm). When the TOF was set at -900 p, the  $^{195}$ Pt NMR spectra were measured between approximately between -4900 and -3400 ppm.

# 6.2.2 <sup>195</sup>Pt NMR spectroscopy

The cis-Pt(R<sub>2</sub>SO)(pz)I<sub>2</sub> compounds were analyzed by platinum-195 NMR spectroscopy and the results are summarized in Table 6.2.2.

**Table 6.2.2** <sup>195</sup>Pt NMR chemical shifts (ppm) in the *cis*-Pt(R<sub>2</sub>SO)(pz)I<sub>2</sub> complexes in CD<sub>3</sub>COCD<sub>3</sub>

complex	δ(Ca)
cis-Pt(DMSO)(pz)I <sub>2</sub>	-4356
cis-Pt(TMSO)(pz)I <sub>2</sub>	-4407
cis-Pt(DPrSO)(pz)I <sub>2</sub>	-4373
cis-Pt(DBuSO)(pz)I <sub>2</sub>	-4371
cis-Pt(DBzSO)(pz)I <sub>2</sub>	-4398

The samples proved to be very pure and only one peak was observed in each case. The chemical shifts were about the same (-4410 to -4350 ppm) and corresponded

well to a [PtNSI<sub>2</sub>] coordination sphere. For instance, the *cis*-Pt(DMSO)(pyrimidine)I<sub>2</sub>, *cis*-Pt(TMSO)(pn)I<sub>2</sub>, *cis*-Pt(DPrSO)(pn)I<sub>2</sub> and *cis*-Pt(DBuSO)(pm)I<sub>2</sub> complexes showed unique signals at -4387, -4427, -4404 and -4399ppm, respectively (4). When compared to the chloro compounds, *cis* and *trans*-Pt(R<sub>2</sub>SO)(pz)Cl<sub>2</sub>, which were prepared in our laboratory a few years ago, the peaks were shifted, i.e., chemical shifts of around -3050 to -3040ppm. The 1300 ppm difference between the iodo and the chloro complexes is expected. According to Pregosin, the more one goes down a group in the periodic table, the more the metal attached will be deshielded in NMR spectroscopy (5). The pyrazine ring also has a slight influence in comparison to the pyrimidine ring, since the signals are a somewhat more deshielded (about 30 ppm).

## 6.2.3 Pyrazine

Since the NMR spectra of free ligands (pyrazine, sulfoxide ligands) in acetone- $d_6$  have never been analyzed, we could not use any literature values to base our work on. One singlet is observed in the  $^1H$  NMR spectrum of pyrazine in deuterated acetone at 8.606 ppm, which can been assigned to the 4 equivalent ring protons,  $H_2$ ,  $H_3$ ,  $H_5$  and  $H_6$ . In the  $^{13}C$  NMR spectrum, one singlet is also observed, at 146.098 ppm, which corresponds to the 4 equivalent ring carbon atoms,  $C_2$ ,  $C_3$ ,  $C_5$  and  $C_6$ . The  $^1H$  and  $^{13}C$  chemical shifts of the pyrazine ligand in the complexes are given in the Tables 6.2.3.1. and 6.2.3.2., respectively.

**Table 6.2.3.1** <sup>1</sup>H NMR chemical shifts (ppm) and coupling constants (Hz) of the pyrazine ligand in the complexes cis-Pt(R<sub>2</sub>SO)(pz)I<sub>2</sub> (R<sub>2</sub>SO = DMSO, TMSO, DPrSO, and DBuSO) (in CD<sub>3</sub>COCD<sub>3</sub>). The chemical shift differences ( $\Delta$  ( $\delta$ <sub>complex</sub>-  $\delta$ <sub>free pz</sub>) ) are also indicated.

complex	δ(Ha)	δ(Hb)	Δδ (Ha)	Δδ (Hb)
cis-Pt(DMSO)(pz)I <sub>2</sub>	8.872 dd	8.838 dd	0.273	0.232
	[1.2; 3.0]	[1.4; 2.7]	0.273	0.232
cis-Pt(TMSO)(pz)I <sub>2</sub>	8.899 dd	8.849 dd	0.293	0.243
	[1.2; 2.9]	[1.1; 3.0]	0.293	0.243
ois Dt(DDrCO)(ng)I.	8.907 dd	8.826 dd	0.301	0.220
cis-Pt(DPrSO)(pz)I <sub>2</sub>	[1.2; 3.0]	[1.5; 3.2]	0.301	0.220
cis-Pt(DBuSO)(pz)I <sub>2</sub>	8.899 dd	8.825 dd	0.293	0.219
	[1.4; 3.0]	[1.4; 3.2]	0.293	0.219

As can be seen from the table above, the pyrazine protons are, more deshielded upon coordination [ $\Delta\delta$  (Ha) = 0.29 ppm and  $\Delta\delta$  (Hb) = 0.23 ppm]. Similar observations have been noted for the monomeric and dimeric chloro analogues (3,6). However, the shifts to the left were smaller for *cis* and *trans*-Pt(R<sub>2</sub>SO)(pz)Cl<sub>2</sub>. There was less deshielding for *trans*-Pt(DMSO)(pz)Cl<sub>2</sub>, *trans*-Pt(TMSO)(pz)Cl<sub>2</sub> and *cis*-Pt(DPrSO)(pz)Cl<sub>2</sub>., viz., 0.078/0.047, 0.067/0.064 and 0.179/120ppm, respectively. Since it proved impossible to prepare a monomeric Pt(DBuSO)(pz)Cl<sub>2</sub> complex, the dimeric compound forming instantly, no comparison can be made for the di-*n*-butylsulfoxide complexes.

**Table 6.2.3.2** <sup>13</sup>C NMR chemical shifts (ppm) of the pyrazine ligand in the complexes cis-Pt(R<sub>2</sub>SO)(pz)I<sub>2</sub> (R<sub>2</sub>SO = DMSO, TMSO, DPrSO and DBuSO) (in CD<sub>3</sub>COCD<sub>3</sub>). The chemical shift ( $\Delta$  ( $\delta$ <sub>complex</sub>- $\delta$ <sub>free pz</sub>)) differences are also indicated.

complex	δ(Ca)	δ(Cb)	Δδ (Ca)	Δδ (Cb)
cis-Pt(DMSO)(pz)I <sub>2</sub>		too ir	nsoluble	
cis-Pt(TMSO)(pz)I <sub>2</sub>	148.76	148.48	2.66	2.38
cis-Pt(DPrSO)(pz)I <sub>2</sub>	148.89	148.28	2.80	2.18
cis-Pt(DBuSO)(pz)I <sub>2</sub>	148.91	148.29	2.81	2.19

As expected, since the carbon atoms are non-equivalent, two signals are observed in the spectrum of each complex. The nature of the sulfoxide ligand does not seem to influence the chemical shifts significantly. It is interesting to compare the chemical shifts of the Pt(R<sub>2</sub>SO)(pz)I<sub>2</sub> compounds with those of the chloro analogues (3). All Pt(R<sub>2</sub>SO)(pz)Cl<sub>2</sub> compounds showed pyrazine chemical shifts of ca.147 ppm for Ca and 145 ppm for Cb. They all showed a *trans* geometry. However, in the Pt(R<sub>2</sub>SO)(pz)Cl<sub>2</sub> series, only one compound showed a very different preparation behavior, as well as an unique analytical state, Pt(DPrSO)(pz)Cl<sub>2</sub>. For instance, its <sup>13</sup>C spectrum showed two very close shifts for the pyrazine carbon atoms signals, at 147.6 and 147.4ppm. Further study revealed that this compound had a *cis* geometry. This is what makes us think that our iodo compounds are all of *cis* geometry. In the *trans* compounds, Pt-N rotation is possible, explaining the fact that Ca and Cb have different deshielding upon coordination.

In the *cis* compounds, the rotation is more limited due to steric hindrance. The pyrazine ligand, in order to reduce tension, probably finds a better position being mainly orthogonal to the platinum plane.

# **6.2.4** Sulfoxide ligands

Since the free sulfoxide ligands in acetone- $d_6$  have never been analyzed, we could not use any literature values to base our work on. The spectra of the sulfoxide ligands have then been taken in deuterated acetone prior to synthesize our complexes. The chemical shifts of the  $^1$ H NMR spectra are given in the Table 6.2.4.1. The multiplicity is also indicated beside the chemical shift values. The signals coupling constants, when it has been possible to identify them, are indicated on the second lines. The works of Gottlied and Nudelman allowed us to identify the solvents signals (CHCl<sub>3</sub>, CH<sub>2</sub>Cl<sub>2</sub>, H<sub>2</sub>O, CH<sub>3</sub>COCH<sub>3</sub>, ethers) (7).

**Table 6.2.4.1** <sup>1</sup>H NMR chemical shifts (ppm) and coupling constants (Hz) of the free sulfoxide ligands in CD<sub>3</sub>COCD<sub>3</sub>.

ligand	δ(Ηα)	δ(Ηβ)	δ(Ηγ)	δ(Ηδ)
DMSO	2.511 s			
TMSO	2.812 m	2.295 m		
	2.688 m	1.978 m		
DPrSO	2.610 m	1.728 tq	1.032 t	
	2.010 III	J = 7.2, 6.9	J = 7.4	
DBuSO	2.656 m	1.677 m	1.469 m	0.932 t
				J = 7.2
DBzSO	4.109 d, <i>J</i> = 12.9	7.353 m		
	3.869, J = 12.9			

The chemical shifts of the <sup>13</sup>C NMR spectra are given in the table 6.2.4.2.

**Table 6.2.4.2**  $^{13}$ C NMR chemical shifts (ppm) of the free sulfoxide ligands in  $CD_3COCD_3$ .

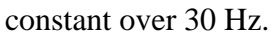
ligand	δ(Cα)	δ(Сβ)	δ(Cγ)	δ(Cδ)	δ(Сε)
DMSO	41.346				
TMSO	54.990	25.843			
DPrSO	54.831	16.930	13.832		
DBuSO	52.668	25.452	22.655	13.959	
DBzSO	58.450	132.776	131.126	129.373	128.644

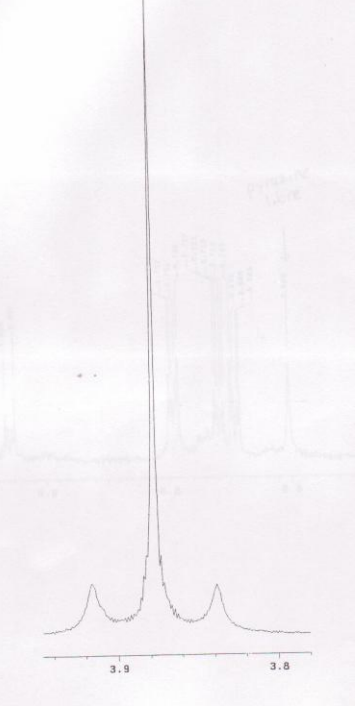
The cis-Pt(R<sub>2</sub>SO)(pz)I<sub>2</sub> compounds were also analyzed by NMR spectroscopy and the spectra were taken in deuterated acetone. The chemical shifts of the <sup>1</sup>H-NMR spectra are given in the Table 6.2.4.3. The multiplicity is also indicated beside the chemical shift values. The coupling constants of the signals, whenever it has been possible to identify them, are indicated on the second lines.

Table 6.2.4.3  $^1$ H-NMR chemical shifts (ppm), coupling constants (Hz) of the sulfoxide ligands in the cis-Pt(R<sub>2</sub>SO)(pz)I<sub>2</sub> complexes. The chemical shift differences ( $\Delta$  ( $\delta_{complex}$ - $\delta_{free\ ligand}$ ) ) are also indicated.

ligand	δ(Ηα)	δ(Ηβ)	δ(Ηγ)	δ(Ηδ)
DMSO	$3.899s$ $(\Delta \delta = 1.388)$ ${}^{3}J({}^{195}Pt-{}^{1}H) =$ $23.4$			
TMSO	$3.987 \text{m}$ $(\Delta \delta = 1.175)$ $3.898 \text{m}$ $(\Delta \delta = 1.210)$	$2.524m$ $(\Delta\delta = 0.229)$ $1.980m$ $(\Delta\delta = 0.002)$		
DPrSO	$4.050m$ $(\Delta\delta = 1.440)$ $3.678m$ $(\Delta\delta = 1.068)$	$2.218m$ $(\Delta\delta=0.490)$	$1.204t$ $(\Delta \delta = 0.002)$ $J = 7.5$	
DBuSO	$4.093m$ $(\Delta\delta = 1.437)$ $3.722m$ $(\Delta\delta = 1.066)$	$2.197m$ $(\Delta\delta = 0.520)$	$1.657m$ $(\Delta\delta=0.188)$	$1.022 t$ $(\Delta \delta = 0.090)$ $J = 7.4$

When the sulfoxide ligands are coordinated, all the chemical shifts of the ligands are observed at higher values than in the free ligands. For the compound containing the tetramethylenesulfoxide (TMSO) ligand, two signals were observed for the  $H_{\alpha}$  protons and two for the  $H_{\beta}$  protons. The protons closer to the oxygen atom are the most deshielded upon coordination. For the other sulfoxide ligands, all of which are non-cyclic, two series of signals were also observed as a result of the limited or slow rotation about the S-C bonds. The separation between the peaks of the geminal protons gets smaller as the distance from the coordination site increases. In addition, it is possible to observe coupling with the metallic atom. For instance the cis-Pt(DMSO)(pz)I<sub>2</sub> complex shows a coupling constant of 23.4Hz (Fig 6.2.4.3.). This value confirms the cis geometry, since it is usually observed around 22-25 Hz, whereas a trans analogue shows a coupling





**Figure 6.2.4.3** <sup>1</sup>H NMR spectrum of the *cis*-Pt(DMSO)(pz)I<sub>2</sub> complex in the sulfoxide region ( ${}^{3}J({}^{195}\text{Pt-}{}^{1}\text{H}) = 23.4\text{Hz}$ ).

The chemical shifts for the <sup>13</sup>C-NMR spectra are given in the Table 6.2.4.4.

**Table 6.2.4.4**  $^{13}$ C-NMR chemical shifts (ppm) of the sulfoxide ligands in the *cis*-Pt(R<sub>2</sub>SO)(pz)I<sub>2</sub> complexes. The chemical shift differences ( $\Delta$  ( $\delta$ <sub>complex</sub>- $\delta$ <sub>free ligand</sub>) ) are also indicated.

ligand	δ(Cα)	δ(Сβ)	δ(Сγ)	δ(Cδ)
DMSO	too insoluble			
TMSO	64.305	25.330		
TMSO	$\Delta\delta = 9.315$	$\Delta\delta = -0513$		
DPrSO	61.846	17.935	12.916	
DITSO	$\Delta \delta = 7.015$	$\Delta \delta = 1.005$	$\Delta \delta = -0.667$	
DBuSO	59.980	26.085	21.938	13.959
DBusO	$\Delta \delta = 7.312$	$\Delta\delta = 0.633$	$\Delta\delta = -0.717$	$\Delta\delta=0.000$

The carbon atoms closer to the platinum center are more deshielded. This is due to the higher electronic density on the Pt brought about by the  $\sigma$  link of the ligands. The signals of the carbon atoms in an alpha position are observed at lower field than in the free molecules. The difference in chemical shifts is ca.7.9 ppm. This is much higher than what was observed for the 2,5-dimethylpyrazine chloro compounds (Chapter IV), where the difference was ca. 2.8ppm. This is also much higher than what was observed for the pyrazine and pyrimidine chloro compounds, by about 5 ppm (3,4,6,8). Most probably, the presence of two iodine atoms brings an extra electronic effect in comparison to chlorine

atoms, which leads to the higher deshielding. The deshielding becomes smaller and smaller the further one is away from the metallic center.

### 6.3 Analysis of the complexes by vibrational spectroscopy

### **6.3.1 IR Spectroscopy**

The vibrational spectra of the complexes were measured in the solid state, as KBr pellets, on a Nicolet Avatar 370 Csl spectrometer. The software used was OMNIC E.S.P. 5.2a. The spectra were recorded from 4000 to 225cm<sup>-1</sup> (300 scans and a resolution of 1 cm<sup>-1</sup>). In each spectrum, characteristic vibrations of the pyrazine and sulfoxide ligands could be observed. Tables 6.3.1.1 and 6.3.1.2 present the observed vibrations for the free pyrazine and the sulfoxide ligands as well as the coordinated ligands. The Pt-N and Pt-S vibrations are also indicated in Table 6.3.1.1. The IR spectrum of pyrazine has been reported by Simmons and Innes and our assignments on the pyrazine ligand are based on this study (9).

**Table 6.3.1.1** Vibrations observed for the coordinated pyrazine ligand in the *cis*-Pt(R<sub>2</sub>SO)(pz)I<sub>2</sub> compounds (cm<sup>-1</sup>) and assignment of the bands. The Pt-N and Pt-S vibrations are also indicated.

Assignment	Free	$Pt(R_2SO)(pz)I_2$						
8	Pyrazine	DMSO	TMSO	DPrSO	DBuSO			
v <sub>13</sub> (B <sub>1u</sub> )	3070	3072	3079	3089	3086			
v (C-H)	2964	3009	2979	2958	2953			
v (C-H)	2918	2909	2923	2932	2919			

$v_{19a} (B_{1u})$	1485	1463	1469	1460	1453
v <sub>19b</sub> (B <sub>3u</sub> )	1407	1417	1415	1417	1408
v <sub>19b</sub> (B <sub>3u</sub> )	1378	1379	1380	1378	1379
v <sub>3</sub> (B <sub>2g</sub> )	1120	1107	1117	1111	1109
v <sub>14</sub> (B <sub>3u</sub> )	1065	1072	1071	-	1069
v <sub>1</sub> (A <sub>g</sub> )	1015	1021	1020	1023	-
v <sub>11</sub> (B <sub>2u</sub> )	788	817	804	808	816
Pt-N		512	-	513	516
Pt-S		440	479	449	448

**Table 6.3.1.2** Comparison between the v(S-O) vibration (cm<sup>-1</sup>) of the free ligands and the  $Pt(R_2SO)(pz)X_2$  complexes (X = Cl, I).

	R <sub>2</sub> SO	Pt(R <sub>2</sub> SO)I <sub>2</sub>	Δν
DMSO	1050	1139	89
TMSO	1020	1145	125
DPrSO	1010	1125	115
DBuSO	1029	1129	100

The pyrazine molecule has  $D_{2h}$  point symmetry and there are 24 fundamental vibrations, 10 of which are IR active and 12 of which are Raman active. The vibrations of coordinated pyrazine were observed at higher or identical energies to those of the free pyrazine ligand. The v(S–O) vibrations absorb between 1125 and 1145 cm<sup>-1</sup>, at higher energies than in the free sulfoxides (ave. 110 cm<sup>-1</sup>), since the ligands are bonded to Pt

through the S atom. The S–O  $d\pi$ – $p\pi$  bond is strengthened upon coordination to the metal. As for similar compounds, one absorption band was observed at around 450 cm<sup>-1</sup> and can be assigned to a v(Pt–S) vibration (10-14, section 4.3.1.). The band observed between 510 and 520 cm<sup>-1</sup> is assigned to the v(Pt–N) stretching vibration, based also on some earlier published results (3,15,16). The only difference among our complexes, i.e., the nature of the coordinated sulfoxide ligand does not seem to influence either the v(Pt–S) or the v(Pt–N) vibrations.

The IR spectrum of the *cis*-Pt(DBzSO)(pz)I<sub>2</sub> compound was not analyzed because it was not pure enough. Even after several recrystallizations, it was still judged to be too impure to be analyzed.

# **6.3.2.** Raman spectroscopy

For the Raman spectroscopic analyses, the spectra were measured on a Renishaw inVia spectrometer, equipped with a microscope. A near-IR laser (785 nm) was used to excite the spectra and the power was less than 10 mW. Five accumulations were made for each sample. The Raman spectra of the complexes were measured between 4000 and about 200 cm<sup>-1</sup> and the data are presented in Table 6.3.2.

**Table 6.3.2** Vibrations observed in the Raman spectra of the coordinated pyrazine ligand in the cis-Pt(R<sub>2</sub>SO)(pz)I<sub>2</sub> compounds (cm<sup>-1</sup>) and assignment of the bands. The Pt-I, Pt-N and Pt-S vibrations are also indicated. (assignments are based on references 17-18).

assignment	free pz	DMSO	TMSO	DPrSO	DBuSO
$\mathbf{v_2} A_g$	3048w	3059w	3082w	3072vw	3062vw
ν <sub>7b</sub> B <sub>2g</sub>	3032w	2989w	2988w	2962w	2962w
$2v_{19a(ring)}A_g$	2967w	2909m	2922w	2912w	2908w
	2303w	2310w	2309vw	2315w	2308w
$ u_{8a(ring)} A_g $	1580m	1598m	1611m	1612s	1608s
$v_{8b(ring)} B_{2g}$	1520w	1516w	1517w	1513w	1512w
				1439w	1432w
	1358w	1404w	1409w	1398w	1401w
		1301w	1298vw	1292w	1302w
$v_{9a(Hbend)}A_g$	1248m		1249w	1242w	1249vw
$2v_{6a}-A_g$	1226m	1216m	1218m	1212m	1210m
v(S-O)		1136m	1139w	1132m	1131w
		1084m	1072w	1075w	1089w
$v_{1(\mathrm{ring})} A_g$	1013vs	1048w	1049vs	1051s	1053s
		1028s	1026vs	1039vs	1040m
	976w	971w	969w	962w	969w
					799m
$v_{10a(Hbend)} B_{Ig}$	754w	731m		754w	743w

$v_{4(ring)} B_{3g}$	699s	693m	692m	693s	692m
$ m v_{6a(ring)}\it A_{g}$	596w	652m	650m		
$\gamma$ (ring)			534w	518m	524w
v(Pt-S)		482w	484w	449w	455w
□(C-S-O)		379w	379w		397w
δ(N-Pt-S)		275m	284w	287m	290m
π(Pt-N)		236w	245vw	252s	253s
v(Pt-N)		219vs	213vs	218vs	218s
v(Pt-I)		152w	148w	151w	153w

There have been no Raman studies reported in the literature on Pt(II) compounds containing Pt-pyrazine bonds and only one on Pt-R<sub>2</sub>SO complexes (19). In each case, there are bands characteristic of the ligands present. The Raman spectrum of the free pyrazine ligand has been reported by Tam and Cooney (17) and our assignments for the bridging ligand are based on this study. The well-accepted convention of Lord *et al.* (18) has been used in numbering the vibration modes with the z-axis being through the two nitrogen atoms. The vibrations of coordinated pyrazine are observed at similar energies than are those of the free ligand. However, some vibrations are slightly shifted in the complexes. The band at 596 cm<sup>-1</sup> in the free ligand can be assigned to the  $v_{6a(ring)} - Ag$  mode, based on the literature (17,18). This vibration is shifted to slightly higher energy (~60 cm<sup>-1</sup>) in the Pt(II) complexes. A very strong band is observed in all the complexes around 1050 cm<sup>-1</sup>, which is consistent with the ring breathing mode ( $v_{1(ring)}$ ) observed at 1013 cm<sup>-1</sup> in free pyrazine. A relatively intense vibration at 1580 cm<sup>-1</sup>, which is assigned

to the  $v_{8a(ring)}$   $A_g$  mode, was also observed at higher energy in the complexes (1598-1612 cm<sup>-1</sup>).

The band detected at around  $1130-1140 \text{ cm}^{-1}$  for each compound is assigned to the S-O stretching mode. This assignment is in full agreement with literature data for the v(S-O) position in platinum-sulfoxide compounds (19) and the IR study in our previous investigation on the coordinated sulfoxide molecules (3,6,8). The S-O stretching frequency of the sulfoxide ligands is known to be strongly affected by coordination. This vibration is shifted to higher energy (by about  $+80 \text{ cm}^{-1}$ ) with respect to the free molecules (20,21). Such an increase is characteristic of the sulfoxide-platinum S-bonding. Coordination via the oxygen atom induces a decrease in energy (22).

The 150-500cm<sup>-1</sup> region is characteristic of the v(Pt-X) bands (23). The bands for the stretching depend essentially on the nature of the anionic ligand, X. The neutral ligand has also an effect, but in a smaller scale. The peaks observed at 482, 484, 449 and  $455\text{cm}^{-1}$ , respectively, for Pt(DMSO)(pz)I<sub>2</sub>, Pt(TMSO)(pz)I<sub>2</sub>, Pt(DPrSO)(pz)I<sub>2</sub> and Pt(DBuSO)(pz)I<sub>2</sub>, are assigned to the Pt-S stretching modes. The observed energies are in good agreement with what was observed for Pt(2,2'-bipyridine)(4-CN-C<sub>6</sub>F<sub>4</sub>S)<sub>2</sub>, 405cm<sup>-1</sup>, and for Pt(1,10-phenanthroline)(4-CN-C<sub>6</sub>F<sub>4</sub>S)<sub>2</sub>, 414cm<sup>-1</sup> (24). The K[Pt(R<sub>2</sub>SO)Cl<sub>3</sub>] (R<sub>2</sub>SO = DMSO, TMSO, DEtSO, DPrSO, DBuSO, DBzSO and DPhSO) complexes also exhibit similar vibrations, with values between 427 and 447cm<sup>-1</sup>. The peak at 236-253 cm<sup>-1</sup> is attributed to a  $\pi$ (Pt-N) mode, in agreement with the literature (25).

The Pt-N stretching mode depends essentially on the neutral ligand, even if the degree of covalent character of the bond Pt-X plays also a role. In the spectra of our complexes, we observed this mode in the 213-219 cm<sup>-1</sup> region, in the form of a very

strong and sharp signal. This is in agreement with the literature. Chowdhury *et al.* has assigned them between 170 and 249cm<sup>-1</sup> for *trans*-Pt(n-hydroxypyridine)<sub>2</sub>Cl<sub>2</sub> (n = 3 or 4) and at 199cm-1 for Pt(3-hydroxypyridine)<sub>3</sub>Cl (26). Michalska and Wysokiński assigned the v(Pt-N<sub>ring</sub>) modes at 256, 253, 241 and 252 for, respectively, *cis*-[Pt(2-picoline)(H<sub>2</sub>O)<sub>2</sub>(NH<sub>3</sub>)<sub>2</sub>]<sup>2+</sup>, *cis*-[Pt(2-picoline)(H<sub>2</sub>O) (NH<sub>3</sub>)<sub>2</sub>Cl]<sup>+</sup>, *cis*-Pt(2-picoline)(NH<sub>3</sub>)<sub>2</sub>Cl<sub>2</sub> and *cis*-Pt(orotato)(NH<sub>3</sub>)<sub>2</sub> (27). Finally, the signal observed at around 150 cm<sup>-1</sup> is assigned to the Pt-I stretching mode, based on what we observed for *cis*-Pt(pz)<sub>2</sub>I<sub>2</sub> where v(Pt-I) vibrates at 151cm<sup>-1</sup>.

# 6.4 Attempts to prepare $Pt(DBzSO)(pz)I_2$ and $Pt(DPhSO)(pz)I_2$

The attempt to prepare the Pt(DBzSO)(pz)I<sub>2</sub> compound seemed to be unsuccessful. When using the same method or a similar one to those used for the other monomeric complexes, a mixture was formed. The NMR analysis of this mixture showed the presence of the free dibenzylsulfoxide ligand and the {Pt(DBzSO)I}<sub>2</sub>(μ-I)<sub>2</sub> intermediate. The <sup>1</sup>H-NMR spectrum exhibited four doublets of doublets in the aromatic region, suggesting the formation of various pyrazinic complexes. It could have been a mixture of the *cis* and *trans* monomeric species, but nothing conclusive could be reached.

In the case of diphenylsulfoxide, the problem was to prepare the  $\{Pt(DBzSO)I\}_2(\mu-I)_2$  intermediate. Using the same method as for other sulfoxide ligands (section 6.1.2.), the final product was a very dark green oil. It does not give anything expected, even varying the time of reaction or the heating temperature and the solvent. The result was always the same. The green/black product appeared to be different from the starting materials, the  $K_2[PtCl_4]$  being pink in solution and the sulfoxide ligand being

colorless in solution. However, the <sup>1</sup>H-NMR spectrum of the product only showed the presence of the starting materials. With the chlorine analogue, the reaction worked well, but for some reason this was not the case with the iodide. It is possible that the PtCl<sub>4</sub><sup>2-</sup> salt has decomposed. Another hypothesis is that the diphenylsulfoxide ligand is too sterically hindered and this prevented the metallic center binding to the iodine atom, this latter being larger than the chlorine atom. We favor the second scenario.

#### Conclusion

So, a series of new  $Pt(R_2SO)(pz)I_2$  compounds were synthesized from the dimeric  $\{Pt(R_2SO)I\}_2(\mu-I)_2$  complexes, prepared a few years ago in our laboratory. The compounds were then characterized by IR, Raman and multinuclear ( $^1H$ ,  $^{13}C$  and  $^{195}Pt$ )NMR spectroscopy. The  $^{195}Pt$  chemical shift values were found shifted by about 1300ppm in comparison to  $Pt(R_2SO)(pz)Cl_2$  chloro analogues. The peaks appeared between -4407 and -4356ppm, corresponding well to a  $[PtNSI_2]$  coordination sphere. The analyses of the compounds seem to show their *cis* geometry, but no final statement can be made at this point.

#### References

- (1) N. Nédélec, G. Masserweh, F.D. Rochon. *Inorg. Chim. Acta.* 2003, 346, 197.
- (2) P.C. Kong, F.D. Rochon. *Inorg. Chim. Acta.* **1979**, *37*, L457.
- (3) Priqueler, J.R.L.; Rochon, F.D. Can. J. Chem. 2004, 82, 649.
- (4) N. Nédélec; F. D. Rochon. *Inorg. Chim. Acta.* **2001**, *319*, 95.
- (5) Pregosin, P.S. Coord. Chem. Rev. 1982, 44, 247.
- (6) Priqueler, J.R.L.; Rochon, F.D. *Inorg. Chim. Acta.* **2004**, *357*, 2167.
- (7) H. E. Gottlieb, V. Kotlyar et A. Nudelman. J. Org. Chem. 1997, 62, 7512.
- (8) N. Nédélec and F. D. Rochon. *Inorg. Chem.* **2001**, *40*, 5236.
- (9) J. D. Simmons and K. K. Innes. J. Mol. Spectrosc. **1964**, 14, 190.
- (10) J.H. Price, A.N. Williamson, R.F. Schramm, B.B. Wayland, *Inorg. Chem.* 1972, 11, 1280.
- (11) V.Yu. Kukushkin, V.K. Belsky, V.E. Konovalov, G.A. Kirakosyan, L.V. Konovalov, A.I. Moiseev, V.M. Tkachuk, *Inorg. Chim. Acta.* **1991**, *185*, 143.
- (12) Yu.N.Kukushkin, V.N. Spevak, Russ. J. Inorg. Chem. 1973, 18, 240.
- (13) Yu.N. Kukushkin, I.V. Pakhomova, Russ. J. Inorg. Chem. **1971**, 16, 226.
- (14) B.F.G. Johnson, R.A. Walton, *Spectrochim. Acta.* **1966**, 22, 1853.
- (15) Yu.N. Kukushkin, N.V. Ivannikova, K.A. Khokhryakov, Russ. J. Inorg. Chem. 1970, 15, 1595.
- (16) K. Nakamoto, P.J. McCarthy, J. Fujita, R.A. Condrate, G.T.Behnke, *Inorg. Chem.* **1965**, *4*, 36.
- (17) N.T. Tam, R.P. Cooney, J. Chem. Soc., Faraday Trans. 1976, 72, 2598.

- (18) R.C. Lord, A.L. Marston, F.A. Miller, Spectrochim. Acta. 1957, 9, 113.
- (19) S. Gama de Almeida, J.L. Hubbard, N. Farrell, *Inorg. Chim. Acta.* 1992, 193, 149.
- (20) Xuan, X.; Wang, J.; Zhang, H. Spectrochim. Acta Part A. 2005, 62, 500.
- (21) Skripkin, M.Y.; Lindqvist-Reis, P.; Abbasi, A.; Mink, J.; Persson, I.; Sandström, M. Dalton Trans. 2004, 4035.
- (22) Molla-Abbassi, A.; Skripkin, M.; Kritikos, M.; Persson, I.; Mink J.; Sandström, M. Dalton Trans. 2003, 1746.
- (23) Baranska, H.; Cacciari, S. J. Raman. Spectrosc. 1997, 28, 1.
- (24) Weinstein, J. A.; Blake, A. J.; Davies, E. S.; Davis, A. L.; George, M. W.; Grills, D. C.; Lileev, I. V.; Maksimov, A. M.; Matousek, P.; Mel'nikov, M. Ya.; Parker, A. W.; Platonov, V. E.; Towrie, M.; Wilson, C.; Zheligovskaya, N. N. *Inorg. Chem.* 2003, 42, 7077.
- (25) Harvey, P.D.; Truong, K.D.; Aye, K.T.; Drouin, M.; Bandrauk, A.D. *Inorg. Chem.* **1994**, *33*, 2347.
- (26) Ashraf Chowdhury, J. Inorg. Biochem. 2005, 99, 1098.
- (27) Chem. Phys. Lett. **2005**, 403, 211.

#### **CHAPTER VII**

cis- and trans- $Pt(pz)_2(X)_2$ (X = Cl, Br, I, NO<sub>2</sub>)

This chapter reports the synthesis and characterization of monomeric platinum(II) complexes, with two pyrazine and two halogen or nitro ligands. Three different halogen atoms have been used, Cl, I and Br, showing different steric hindrance and chemical behavior. Nitro ligand has also been chosen because it has an interesting nature; it can bind to metallic center through the nitrogen atom as well as the oxygen atom. Characterization tends to confirm the presence of the Pt-N bond. Considering the *trans* effect, two different routes had to be used to prepared *cis* and *trans* species.

#### 7.1 Preparation

# 7.1.1 Starting material

The starting compound K<sub>2</sub>[PtCl<sub>4</sub>] was obtained from Johnson Matthey Inc. and was purified by recrystallization in water before use. CDCl<sub>3</sub> was purchased from CDN Isotopes. KBr, KI, NaNO<sub>2</sub> and pyrazine were obtained from Aldrich Chemical Co. Most of the sulfoxide ligands were also obtained from Aldrich. Dimethylsulfoxide was bought from Anachemia Chemicals Ltd and di-*n*-propylsulfoxide from Phillips Petroleum Company. The latter was purified by distillation before use.

# 7.1.2 Synthesis of the complexes cis-Pt(pz)<sub>2</sub>(X)<sub>2</sub>, (X = Cl, Br, I, NO<sub>2</sub>)

The method used was that of Foulds and Thornton (1). It was, however, slightly modified.

#### 7.1.2.1 Step 1

Crystals of K<sub>2</sub>[PtCl<sub>4</sub>] [0.8001 g (1.9 mmol) for the bromo compound, 0.9214 g (2.2 mmol) for the iodo compound and 0.8428 g (2.0 mmol) for the NO<sub>2</sub> compound] were ground and dissolved in about 40 mL of distilled water. Excess amounts of KBr (0.9757 g, 8.2 mmol), KI (1.990 g, 12.0 mmol) and NaNO<sub>2</sub> (1.083 g, 15.7 mmol) were dissolved in water (20 mL) and then added to the platinum(II) solutions. The mixtures were kept in closed beakers under constant stirring for about 4 h. The complexes, K<sub>2</sub>[PtBr<sub>4</sub>], K<sub>2</sub>[PtI<sub>4</sub>] et K<sub>2</sub>[Pt(NO<sub>2</sub>)<sub>4</sub>], thus obtained were kept in solution for use in Step 2. In the case of the chloro compound, crystals of K<sub>2</sub>[PtCl<sub>4</sub>] (0.8420 g, 2.0 mmol) were ground, dissolved in about 60 mL of distilled water and the mixture was stirred for 10 min.

#### 7.1.2.2 Step 2

The pyrazine ligand (0.3920 g (4.9 mmol) for the chloro compound, 0.3760 g (4.7 mmol) for the bromo compound, 0.4483 g (5.6 mmol) for the iodo compound and 0.4009 g (5.0 mmol) for the NO<sub>2</sub> compound) was dissolved in a minimum of water (10 mL). The pyrazine solutions were added to the aqueous platinum solutions. The precipitates obtained were filtered off and well washed with distilled water in order to remove mainly the excesses of the salt (KBr, KI and NaNO<sub>2</sub>), as well as any unreacted pyrazine ligand. Once dry, the precipitates were rinsed with diethylether.

# 7.1.3 Synthesis of the *trans*-Pt(pz)<sub>2</sub>(X)<sub>2</sub>, (X = Cl, Br, I, NO<sub>2</sub>) complexes

The trans-Pt(pz)<sub>2</sub>(X)<sub>2</sub> complexes were prepared by isomerization of the cis compounds. The method used was first described by Foulds and Thornton (1).

# 7.1.3.1 trans-Pt(pz)<sub>2</sub>(X)<sub>2</sub>, (X = Cl, Br)

The appropriate *cis* complex. (0.2541 g (0.59 mmol) for *cis*-Pt(pz)<sub>2</sub>(Cl)<sub>2</sub> and 0.2159 g (0.42 mmol) for *cis*-Pt(pz)<sub>2</sub>(Br)<sub>2</sub>), was put in dimethylformamide solution (30 mL) and the medium was stirred. The solution was heated up to 70°C and kept at that temperature for about 2 h. An excess of 4 eq. of pyrazine ligand [0.1899 g (2.37 mmol) and 0.1339 g (1.67 mmol), respectively] was added to the solution in order to form the tetrasubstitued complex. Then, an excess of HX was added to the solution allowing protonation to occur. Subsequent isolation of the excess pyrazine and addition of NaX induced precipitation of the *trans* compound. The precipitate was filtered off and washed with diethylether. The *trans*-Pt(pz)<sub>2</sub>(Cl)<sub>2</sub> compound was been obtained in a 26% yield, whereas its bromo analogue was obtained in a 22% yield.

# 7.1.3.2 trans-Pt(pz)<sub>2</sub>(I)<sub>2</sub>

The *cis*-Pt(pz)<sub>2</sub>(I)<sub>2</sub> complex (0.1404 g, 0.23 mmol) was put in a test tube and deuterated acetone was added to fill ¾ of the tube. The tube was closed with a rubber cap and agitated in order to dissolve the complex. The tube was placed in a 40°C water bath for 48 h. The resulting solution was poured into a beaker and left to evaporate slowly in air. The resulting solid was then scratched off the sides of the beaker and washed with diethylether. The *trans*-Pt(pz)<sub>2</sub>(I)<sub>2</sub> complex was obtained in a 89% yield.

# 7.1.3.3 $trans-Pt(pz)_2(NO_2)_2$

The *cis*-Pt(pz)<sub>2</sub>(NO<sub>2</sub>)<sub>2</sub> complex (0.2688 g, 0.60 mmol) was mixed with dimethylformamide (40 mL), and the medium was stirred. The solution was heated up to 70°C and kept at that temperature for about 3 h. An excess of 4 eq. of pyrazine ligand (0.1874 g, 2.34 mmol) was added to the solution in order to form the tetrasubstitued complex. An excess of HNO<sub>2</sub> was then added to the solution, allowing protonation to occur. The excess pyrazine was isolated and 12 eq. of NaNO<sub>2</sub> was added. Another excess of pyrazine (0.1458 g, 1.82 mmol) induced precipitation of the *trans* compound after the reaction mixture was left under constant stirring for 24 h. The precipitate was filtered off and washed with diethylether. A yield of 21% was obtained.

#### 7.2 Analysis of the complexes by multinuclear NMR spectroscopy

### 7.2.1 Experimental section

The compound are not very soluble in any solvent except acetone, so deuterated acetone was chosen as NMR solvent for the analysis of the eight complexes in solution.

All the NMR spectra are measured on a Varian Gemini 300BB spectrometer operating at

300.021, 75.454 and 64.321 MHz for  $^{1}$ H,  $^{13}$ C and  $^{195}$ Pt, respectively. The standard recording conditions used in this project were: SW = 4500.5 Hz, AT = 1.998 s., FB = 2600 Hz, PW = 7.0  $\mu$ s., NT = 500 to 2000 for proton NMR, SW = 18761.7 Hz, AT = 1.815 s., FB = 10400 Hz, PW = 8.7  $\mu$ s., NT = 100000 to 300000 for carbon-13 NMR and SW = 100000 Hz, AT = 0.150 s., FB = 51200 Hz, PW = 8.7  $\mu$ s., TOF = 0, NT = 60000 to 300000 for platinum-195 NMR. The acetone peaks were used as an internal standard for the  $^{1}$ H (2.09 ppm for the central peak of the CH<sub>3</sub> quintuplet signal) and  $^{13}$ C (30.60 ppm for the central peak of the CH<sub>3</sub> septuplet signal) NMR spectra (2). For  $^{195}$ Pt, several external references were used. Pt(TMSO)<sub>2</sub>(CN)<sub>2</sub> in CDCl<sub>3</sub>, adjusted at -3450 ppm from K<sub>2</sub>[PtCl<sub>6</sub>] ( $\delta$  (Pt) = 0 ppm), was used for the iodo complexes. K<sub>2</sub>[PtCl<sub>4</sub>] in D<sub>2</sub>O, adjusted at -1628 ppm from Na<sub>2</sub>[PtCl<sub>6</sub>] ( $\delta$  (Pt) = 0 ppm), was used for the chloro, bromo and nitro complexes. The  $^{195}$ Pt-NMR spectra were measured approximately between -4000 and -2500 ppm for Pt(pz)<sub>2</sub>(I)<sub>2</sub>, between -2800 and -1300 ppm for Pt(pz)<sub>2</sub>(CI)<sub>2</sub>.

# 7.2.2 <sup>195</sup>Pt-NMR spectroscopy

The samples proved to be very pure and only one unique peak was observed for each compound (Table 7.2.2). Whatever the geometry is, the platinum coordination sphere is the same, and this is why the cis and the trans compounds for a given complex show a signal in the same region [e.g., -3260 and -3269 ppm, respectively, for cis and trans-Pt(pz)<sub>2</sub>(I)<sub>2</sub>]. It should be noted that the cis compounds are more deshieded than are their trans analogues.

**Table 7.2.2** <sup>195</sup>Pt-NMR chemical shifts (ppm) for *cis*- and *trans*-Pt(pz)<sub>2</sub>(X)<sub>2</sub>, (X = Cl, Br, I, NO<sub>2</sub>) (in CD<sub>3</sub>COCD<sub>3</sub>)

Complex	Geometry	$\delta(^{195}\text{Pt})$	$\Delta\delta_{cis\text{-trans}}$
$Pt(pz)_2(Cl)_2$	cis	-2009	27
$Pt(pz)_2(Cl)_2$	trans	-2036	21
$Pt(pz)_2(Br)_2$	cis	-2355	38
$Pt(pz)_2(Br)_2$	trans	-2393	30
$Pt(pz)_2(I)_2$	cis	-3260	9
$Pt(pz)_2(I)_2$	trans	-3269	,
$Pt(pz)_2(NO_2)_2$	cis	-2255	111
$Pt(pz)_2(NO_2)_2$	trans	-2366	111

The signals observed for the Pt(pz)<sub>2</sub>(Br)<sub>2</sub> complexes are in the expected window, -2355 ppm for the *cis* and -2393 ppm for the *trans* compound. These values can be compared with that obtained for *cis*-Pt(NH<sub>3</sub>)<sub>2</sub>Br<sub>2</sub>, -2459 ppm (3). The peaks for the iodo compounds are observed at -3260 ppm (*cis*) and -3269 ppm (*trans*). The literature confirms the [PtN<sub>2</sub>I<sub>2</sub>] coordination sphere, with values of -3342 and -3360 ppm for *cis* and *trans*-Pt(MeNH<sub>2</sub>)<sub>2</sub>I<sub>2</sub> (4) and -3353 and -3362 ppm for *cis*- and *trans*-Pt(cyclopropylamine)<sub>2</sub>I<sub>2</sub> (5). The peaks for the chloro complexes, observed at -2009 and 2036 ppm, can be compared with those for *cis*- and *trans*-Pt(2-pic)<sub>2</sub>Cl<sub>2</sub>, observed at -2021 and 1973 ppm (6) and with *cis*-Pt(<sup>i</sup>PrOc)<sub>2</sub>Cl<sub>2</sub>, observed at -2052 ppm (7). The peaks for *cis*-Pt(pz)<sub>2</sub>(NO<sub>2</sub>)<sub>2</sub> and *trans*-Pt(pz)<sub>2</sub>(NO<sub>2</sub>)<sub>2</sub> are observed at -2255 and -2366 ppm, respectively. These values are in agreement with what was observed by Kukushkin *et al*.

for  $Pt(\underline{N}H=C(Ph)NC(Ph)=\underline{N}Ph)_2$ , -2270 ppm (8) or by our research group for  $[Pt(iso-PrNH_2)_4]I_2$ , -2724 ppm (9).

The signals observed for the Pt(pz)<sub>2</sub>(NO<sub>2</sub>)<sub>2</sub> compounds are around -2300 ppm (-2255 ppm and -2366 ppm, respectively, for the *cis* and the *trans* geometries), which is what is expected for coordination through a nitrogen atom. The chemical shifts for platinum(II) compounds are observed between -2800 and -2200 ppm when coordinated through a nitrogen atom, whereas they are observed between -2200 and -1500 ppm when coordinated through the oxygen atom.

# 7.2.3 <sup>1</sup>H-NMR spectroscopy

The <sup>1</sup>H-NMR spectrum for the free ligand shows a unique singlet at 8.62 ppm in deuterated acetone. The variation of the chemical shifts between the coordinated pyrazine and the free ligand is positive (Table 7.2.3). The pyrazine signals are more deshielded in the platinum complexes. This is what is expected since S donation towards the platinum atom increases the electronic density around it, disfavoring the pyrazine protons.

**Table 7.2.3** Pyrazine  ${}^{1}$ H-NMR chemical shifts (ppm) and coupling constants (Hz) for the *cis*- and *trans*-Pt(pz)<sub>2</sub>(X)<sub>2</sub>, (X = Cl, Br, I, NO<sub>2</sub>) complexes (in CD<sub>3</sub>COCD<sub>3</sub>).

Complex	Geometry	δ(Ha)	δ(Hb)	<sup>3</sup> J (Ha-Pt)
Pt(pz) <sub>2</sub> (Cl) <sub>2</sub>	a <b>i</b> g	8.909 d	8.733 d	41
	cis	[3.3]	[3.3]	41
D <sub>1</sub> ( ) (Cl)	trans	8.959 dd	8.796 dd	33
$Pt(pz)_2(Cl)_2$		[3.0; 1.5]	[3.0; 1.5]	33
$Dt(nz) \cdot (Dr)$	ais	8.995 d	8.735 d	42
$Pt(pz)_2(Br)_2$	cis	[3.3; 1.2]	[3.3]	42

$Pt(pz)_2(Br)_2$	tuans	9.001 dd	8.763 dd	33
1 t(pz) <sub>2</sub> (D1) <sub>2</sub>	trans	[3.0; 1.5]	[3.0; 1.2]	33
$Pt(pz)_2(I)_2$	cis	9.083 d	8.746 d	42
	Cis	[3.0]	[3.0]	42
D((n-) (I)	4	9.060 d	8.720 d	36
$Pt(pz)_2(I)_2$	trans	[3.3]	[3.3]	30
$D_t(\mathbf{p}_{\mathbf{Z}})_*(\mathbf{N}\Omega_*)_*$	cis	9.092 d	8.958 d	47
$Pt(pz)_2(NO_2)_2$	Cis	[3.0]	[3.0]	
$Pt(pz)_2(NO_2)_2$	trans	9.114 m	8.986 m	-

For the halogenated derivatives, it can also be noticed that the chemical shifts of the pyrazine protons are more deshielded as we go down the halogen group, i.e., the Ha protons of both isomers and for the Hb protons of the *cis* isomers. This observation is in agreement with the results obtained from <sup>195</sup>Pt NMR spectroscopy. Actually, for a higher electronic density on Pt, there will be a decrease on the pyrazine protons. The shielding of Pt being greater for halogen atoms from higher periods, we will notice an increase in the proton deshielding. No rationale can yet be put forward to explain the difference in the shielding of the Hb protons for the *trans* isomers. The *cis* compounds are more shielded than are their *trans* analogues, which is in agreement with what was observed in the <sup>195</sup>Pt-NMR spectroscopy. However, this is not the case for the Pt(pz)<sub>2</sub>(I)<sub>2</sub>, where the *trans* complex is more shielded.

The coupling constants,  ${}^{3}J({}^{1}\text{Ha-}{}^{195}\text{Pt})$ , also provide some information on the geometry of platinum(II) complexes. Often a higher coupling constant is observed for the *cis* compounds. In our case, the *cis* compounds show coupling constants between 41 and 47 Hz, whereas the *trans* compounds show constants between 33 and 36 Hz. The 9 Hz

difference is also about what was observed in the literature for similar complexes (5,10,11).

# 7.2.4 <sup>13</sup>C-NMR spectroscopy

The interpretation of the results for the  $^{13}$ C-NMR spectra is almost identical to that described for the proton-NMR spectra. The carbon atoms closer to the platinum center are more deshielded (Table 7.2.4). This is due to the higher electron density on the Pt because of the  $\sigma$  bonds to the ligands.

**Table 7.2.4** Pyrazine  $^{13}$ C NMR chemical shifts (ippm) in the complexes *cis* and *trans*-Pt(pz)<sub>2</sub>(X)<sub>2</sub>, (X = Cl, Br, I) (in CD<sub>3</sub>COCD<sub>3</sub>)

Complex	Geometry	δ(Ca)	δ(Cb)
$Pt(pz)_2(Cl)_2$	cis	149,08	148,36
$Pt(pz)_2(Cl)_2$	trans	148,65	148,37
$Pt(pz)_2(Br)_2$	cis	149,14	148,57
$Pt(pz)_2(Br)_2$	trans	149,86	148,31
$Pt(pz)_2(I)_2$	cis	150,84	148,94
$Pt(pz)_2(I)_2$	trans	150,84	148,17

For the Ca carbon atoms, the signals appear at higher fields as we go down the halogen group for the *cis* compounds (149.08 ppm for the chloro compound, 149.14 ppm for the bromo compound and 150.84 ppm for the iodo compound). The same observation can be made for the *trans* analogues (148.65 ppm for chloro compound, 149.86 ppm for the bromo compound and 150.84 for iodo compound). No coupling constant of the type  ${}^3J({}^{13}\text{Cb}-{}^{195}\text{Pt})$  or  ${}^2J({}^{13}\text{Ca}-{}^{195}\text{Pt})$  could be observed, probably because of the background noise in the spectra.

# 7.3 Raman spectroscopy

The infrared spectra of this type of complex have already been published by Foulds and Thornton (1) and so this analysis is not included here.

For the analysis of the Raman spectra, measurements were made on a Renishaw inVia spectrometer, equipped with a microscope between 4000 and about 175 cm<sup>-1</sup>. A near-IR CW laser at a wavelength of 785 nm was used to excite the spectra and the power level used was between 10-50% of the available intensity. The laser intensity was usually set at 5mW, because the samples would decompose under higher powers. For this reason, many of the observed peaks are quite weak. Five accumulations were made for each sample. An example of the signals observed between 950 and 175 cm<sup>-1</sup> is shown in Fig. 7.3 for *cis*-Pt(pz)<sub>2</sub>Br<sub>2</sub>.

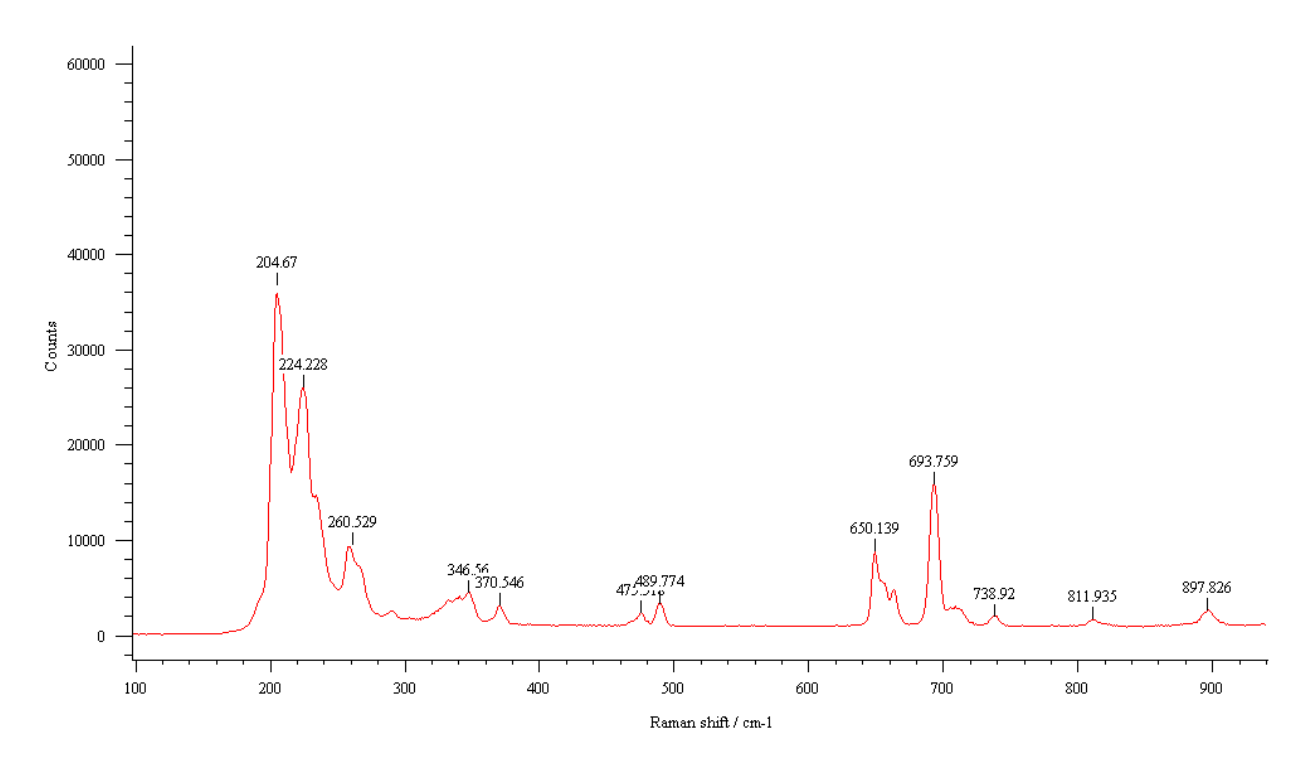


**Figure 7.3** Raman spectra of *cis*-Pt(pz)<sub>2</sub>Br<sub>2</sub> between 950 and 175cm<sup>-1</sup>.

The Raman spectrum of pyrazine was published in 1976 by Tam and Cooney (1). All the bands observed in our work were assigned according to this reference. The results are summarized in the Table 7.3 and a comparison is made with the experimental bands observed for the free ligand.

**Table 7.3** Raman bands (in cm<sup>-1</sup>) of the complexes cis and trans-Pt(pz)<sub>2</sub>(X)<sub>2</sub>, (X = Cl, Br, I, NO<sub>2</sub>).

Assignment	free pz	Cl <sub>trans</sub>	Cl <sub>cis</sub>	Br <sub>trans</sub>	Br <sub>cis</sub>	I <sub>trans</sub>	$I_{cis}$	NO <sub>2trans</sub>	NO <sub>2cis</sub>
$v_{2(\text{H-stretch})} - Ag$		3077w	3077w	3070w	3070vw	3066w	3064w	3078w	3080w
$v_{7b(\text{H-stretch})} - B2g$		3057vw	3060vw			3054vw		3051vw	3048vw
$2v_{19a(ring)} - Ag$	2967w	2931vw	2935vw		2939vw	2939vw	2942vw	2936vw	2934vw
	1615w		1608vs	1606m	1604m	1603s	1602vs		1617w
$v_{8a(ring)} - Ag$	1580m	1595s	1594s	1593m 1585m	1593m	1592s	1591s	1596m	1595m
$v_{8b(ring)} - B2g$	1502w	1516w	1517w 1483vw	1517m 1479w	1516w	1517m	1516m 1484vw	1514w 1490vw	1520w 1490vw
	1358w	1424w	1420vw		1423w	1417w	1417w		
$v_{asym}$ (NO <sub>2</sub> )								1389m	1393m
v <sub>sym</sub> (NO <sub>2</sub> )								1340m	1342m
$v_{9a(H-bend)} - Ag$	1248m	1223s	1224s 1207m	1220m	1220m 1209m	1220s	1217vs	1225m	1224s
		1125m	1124w	1118w	1123w	1120w	1119m	1124w	1124w
		1085vs	1082s	1083m	1083s	1083s	1081vs	1085s	1084s
$v_{1(\mathrm{ring})} - Ag$	1013vs	1021vs	1050m 1016vs	1048w	1050m 1021m	1044m	1042m	1021vs	1020vs

	976w	1009vs		1015vs	1009s	1015vs	1017vs	1007m	1008m
$v_{10a(H-bend)} - Big$	754w	738vw	740vw	739vw	737vw	740w	740vw	828vs	829vs
			713m		715w		711m	742w	743w
$v_{4(\text{ring})} - B_3 g$	699s	691m	694s	694s	692m	693s	694vs	695s	695s
$V_{6a(ring)} - Ag$	596w	664m	665m	650s	664w	663s	662s	665m	665m
			654m			646m	647m		
$\gamma_{(\mathrm{ring})}$		468vw	491vw	490vw	548w	490w	491vw	516m	516m
$v(Pt-\underline{N}O_2)$								305vs 282s	305vs 283s
ν(Pt-Cl)		325vs	328vs 347m						
ν(Pt-Br)				261w	265vw 258w				
ν(Pt-pz)		228m 216m	229m 216m	224s 205vs	226m 204vs	225s	226s	228m	229m
δ(pz-Pt-pz)						199w	197w	195w	195w
ν(Pt-I)						175m	174m 151w		

The abbreviations used are: vs = very strong, s = strong, m = medium, w = weak, vw = very weak.

There are no Raman data in the literature for Pt(II) compounds containing Pt-pyrazine bonds. The only papers dealing with Raman studies on platinum and the pyrazine ligand do not exhibit any Pt-pz bonds (13,14).

All the cis and trans-Pt(pz)<sub>2</sub>(X)<sub>2</sub> are square planar, with pyrazine acting as a monodentate nitrogen donor. The trans-Pt(pz)<sub>2</sub>(X)<sub>2</sub> complexes have  $D_{2h}$  point group symmetry, while the cis complexes have  $C_{2v}$  point group symmetry. Pyrazine exhibits a  $D_{2h}$  point group symmetry, for which there are 24 vibrations expected, 12 being active in Raman. All the vibrational modes of free pyrazine have been assigned (12). The well accepted convention of Lord et al. has been used in numbering the vibrational modes with the z-axis being through the two nitrogen atoms (15). Two bands, with low intensities, are observed for free pyrazine at 1358 and 596 cm<sup>-1</sup>. These bands were not reported by Tam and Cooney (12). The first one can be assigned to the  $v_{14}$  mode by comparison with the frequency observed, around 1350 cm<sup>-1</sup>, by Foglizzo and Novak in another Raman study of pyrazine (16). This mode, however, seems to appear in our compounds at a slightly higher energy, around 1420cm<sup>-1</sup>. The band at 596 cm<sup>-1</sup>, also omitted by Tam and Cooney, is assigned to the mode  $v_{6a(ring)} - Ag$  when compared with the work of Simmons et al., who reported this band at 598 cm<sup>-1</sup> (17). This mode also appears shifted by about 60 cm<sup>-1</sup> in our complexes, comparable with what was observed for mixed sulfoxide dimeric compounds, such as trans-trans- $Pt(TMSO)Cl_2(\mu-pz)Pt(R_2SO)Cl_2$  (section 3.3.2).

The very weak band at 1226 cm<sup>-1</sup>, which was assigned by Tam and Cooney (12) to  $2v_{6a} - Ag$  was not observed in our study, perhaps because of the sensitivity of the spectrometer. It would have certainly been observed with a more intense green laser

(514.5 nm), but our sample burned when using this wavelength. An intense vibration is observed in the complexes around 1050 cm<sup>-1</sup>, which seems consistent with the ring breathing mode for pyrazine ( $v_{1(ring)}$ ) observed at 1013 cm<sup>-1</sup> in free ligand. Adam *et al.* accounted for this shift to lower energy through theoretical calculations using extended Hückel theory (EHT) developed by Hoffmann (18,19). These authors attributed the results to the large polarizibility of the σ-bond contributing to the pyrazine ring backbone. In the complexes, a strong vibration was observed at around 694 cm<sup>-1</sup>, which is consistent with the  $v_{4(ring)}$  ( $B_3g$ ) vibration that was observed around 694 cm<sup>-1</sup> for *trans-trans*-Pt(TMSO)Cl<sub>2</sub>(μ-pz)Pt(R<sub>2</sub>SO)Cl<sub>2</sub> (section 3.3.2.) and at 700 cm<sup>-1</sup> for the free pyrazine (12).

Vibrations involving the Pt(II) atom are usually observed in the region below 550 cm<sup>-1</sup>. A noteworthy feature of the spectra of the *cis* complexes is the additional splitting observed in the Pt-X bands, which clearly provides a diagnostic distinction between the *cis* and the *trans* complexes. The chloro compounds show a very intense Pt-Cl stretching vibration at 325 cm<sup>-1</sup> for the *trans* complex and two intense stretching vibrations at 347 and 328 cm<sup>-1</sup> for the *cis* analogue. The bromo compounds show, respectively, one band at 261 cm<sup>-1</sup> and two bands at 265 and 258 cm<sup>-1</sup> for the Pt-Br stretching modes in the *trans* and the *cis* compounds. And, finally, the *cis* and *trans*-Pt(pz)<sub>2</sub>(I)<sub>2</sub> complexes show Pt-I stretching vibrations at 174 and 151 cm<sup>-1</sup> and 175cm<sup>-1</sup>, respectively. Interestingly enough, a similar observation cannot be made in the nitrito complexes, where two vibrations are observed for both complexes. The □(Pt-Cl) vibrations are observed at slightly lower energies than are those observed in IR spectroscopy (1). These bands are quite broad because of the presence of the two Cl isotopes.

# Conclusion

Complexes of the type *cis*- and *trans*- Pt(pz)<sub>2</sub>X<sub>2</sub> (X = Cl, I, Br and NO<sub>2</sub>) were formed and characterized by Raman and multinuclear NMR spectroscopy (<sup>1</sup>H, <sup>13</sup>C and <sup>195</sup>Pt). The <sup>3</sup>J(<sup>1</sup>Ha-<sup>195</sup>Pt) coupling constants, observed in <sup>1</sup>H NMR spectroscopy, were particularly useful to account for the compounds geometry. They were measured around 40 and 30 Hz, respectively for the *cis* and *trans* compounds. The <sup>195</sup>Pt NMR chemical shifts were observed at -2020, -2300, -2375 and -3265ppm, respectively for the [PtN<sub>2</sub>Cl<sub>2</sub>], [PtN<sub>4</sub>], [PtN<sub>2</sub>Br<sub>2</sub>] and [PtN<sub>2</sub>I<sub>2</sub>] coordination spheres, the *cis* complexes being more deshielded than their *trans* analogues.

#### References

- (1) G.A. Foulds, D.A. Thornton, *Spectrochimica Acta 37A.* **1981**, *10*, 917.
- (2) J. Org. Chem. 1997, 62, 7512.
- (3) Appleton, T.G.; Hall, J.R.; Ralph, S.F. *Inorg. Chem.* **1985**, 24, 4685.
- (4) Rochon, F.D.; Buculei, V. Inorg. Chim. Acta. 2004, 357, 2218.
- (5) Rochon, F.D.; Buculei, V. Inorg. Chim, Acta. 2005, 358, 2040.
- (6) Fontes, A.P.S.; Oskarsson, Å.; Lövqvist, K.; Farrell, N. Inorg. Chem. 2001, 40, 1745.
- (7) Malon, M.; Travnicek, Z.; Strnad, M. J. Inorg. Biochem. 2005, 99, 2127.
- (8) Bokach, N.A.; Kuznetsova, T.V.; Simanova, S.A.; Haukka, M.; Pombeiro, A.J.L.; Kukushkin, V.Y. *Inorg. Chem.* **2005**, *44*, 5152.
- (9) Rochon, F.D.; Tessier, C.; Buculei, V. Inorg. Chim. Acta. 2007, 360, 2255.
- (10) T. B. T. Ha, J. P. Souchard, F. L. Wimmer et N. P. Johnson. *Polyhedron*. **1990**, *9*, 2647.
- (11) N. Nédélec and F. D. Rochon. *Inorg. Chim. Acta.* **2001**, *319*, 95.
- (12) N.T. Tam, R.P. Cooney, J. Chem. Soc., Faraday Trans. 1976, 72, 2598.
- (13) J. Electroanal. Chem. **1991**, 319, 71.
- (14) Angew. Chem. Int. Ed. **2005**, 44, 4069.
- (15) R.C. Lord, A.L. Marston, F.A. Miller, *Spectrochim. Acta.* **1957**, 9, 113.
- (16) R. Foglizzo, A. Novak, Appl. Spectroscopy. 1970, 24, 601.
- (17) J.D. Simmons, K.K. Innes, G.M. Begun. J. Mol. Spectrosc. **1964**, 14, 190.
- (18) W. Adam, A. Grimison, G. Rodrigues. *Tetrahedron*. **1967**, 23, 2513.
- (19) R. Hoffmann. J. Chem. Phys. **1964**, 40, 2745.

#### CONCLUSIONS AND CONTRIBUTIONS

#### TO ORIGINAL KNOWLEDGE

Platinum is a relatively inert metal and has no natural biological role. Nevertheless, platinum complexes are now amongst the most widely used drugs for the treatment of cancer. The first and second generation compounds, *cisplatin* (*cis*-Pt(NH<sub>3</sub>)<sub>2</sub>Cl<sub>2</sub>) and *carboplatin*, are in widespread use to treat a variety of cancers, either as single agents or in combination with other drugs. *Oxaliplatin*, introduced into the clinic in 2002, has also become an important option since. The search for improved platinum-based drugs continues with the goals of reducing toxic side-effects, and particularly their nephrotoxicity, and broadening the spectrum of activity to tumors resistant to *cisplatin* (1). A major focus of current research is in the investigation of "non-classical" platinum antitumor compounds, including *trans*- and polynuclear Pt(II) derivatives, that act by a different mechanism to that of *cisplatin* to achieve a different profile of activity. The use of other sulfur-based ligands, like sulfoxides, could also overcome that problem.

This project consisted of the preparation and the analysis of platinum(II) complexes, containing several pyrazine and sulfoxide ligands. In the literature, numerous compounds with pyrazine ligands are mentioned, but very few are platinum(II) complexes (2-7). In order to obtain more information on the behavior of such a ligand, synthesis and study of novel platinum(II) complexes, containing pyrazine and sulfoxide ligands, have been made. Several sulfoxide ligands, with different size and reactivity, have been used in this project.

1/ First of all, new dimers were prepared, using a derivative of pyrazine, 2,5dimethylpyrazine, as the bridging ligand.  $Trans, trans - \{Pt(R_2SO)Cl_2\}_2(\mu-Me_2pz)$  were synthesized from K[Pt(R<sub>2</sub>SO)Cl<sub>3</sub>] and 2,5-dimethylpyrazine in aqueous/alcoholic solution, and characterized by multinuclear (<sup>1</sup>H, <sup>13</sup>C and <sup>195</sup>Pt), IR and Raman spectroscopy. The observed  ${}^{3}J({}^{1}\text{Ha}{}^{-195}\text{Pt})$  coupling constants, measured around 30Hz, are characteristic of the *trans* geometry. Most of the literature dealing on Me<sub>2</sub>pz complexes are with the two methyl groups located in positions 2/6 and 2/3 (5,8-20). Fewer studies have been published on the 2,5-Me<sub>2</sub>pz ligand (5,19-24), which is more sterically hindered and generally not favored for the reactions with a 1:1 Pt:Me<sub>2</sub>pz ratio. However, we thought it could be an interesting bridging ligand with a central symmetry. Suitable crystals of the DEtSO and the DBuSO complexes were obtained by recrystallization and mounted on glass fibbers. X-rays diffraction at low temperature (173 K) helped us to resolve their structure with good refinement (R1 = 0.0385 and 0.0245). They recrystallized in the C2/m and R-3 space groups, respectively. The S—O bond distance in the coordinated DEtSO ligand, 1.31 Å, is found to be particularly short compared to that for some other sulfoxide ligands (1.44-1.47 Å). This could mean a bond order close to 3 (resonance form III on fig. 1.5.1), which is rare for such coordination complexes. These X-ray results confirm that the *trans* influences of the Cl and N atoms are similar, whereas that of the sulfoxide ligand is greater. No structure of a Pt(II) complex containing the DEtSO ligand has been published so far. After our work on Me<sub>2</sub>pz, we studied quinoxaline in similar reactions and characterizations. In the future, phenazine could also be tested. It has shown some interesting biological properties.

2/ Our research team prepared a *trans*-Pt(TMSO)(pz)Cl<sub>2</sub> monomeric species a few years ago, and an original new method of synthesis was initiated from that starting material. Pyrazine-bridged mixed-sulfoxides Pt(II) complexes have been prepared from the reaction of that monomeric compound with a series of K[Pt(R<sub>2</sub>SO)Cl<sub>3</sub>] monosubstituted ionic compounds. IR and Raman spectroscopy showed only one v(Pt-Cl) band suggesting *trans-trans* isomers, confirmed by the <sup>3</sup>J(<sup>195</sup>Pt-<sup>1</sup>H) coupling constants. The <sup>195</sup>Pt NMR signals of the dinuclear species were observed between -3042 and -3112 ppm. The method used for connecting a second platinum-sulfoxide unit is fairly new and could be extended to other bridging ligand, such as pyrimidine, triazine or phenazine. This procedure could help ultimately to design the 'two units' molecules, one unit being an active medicinal molecule and the other being an inert 'carrying' molecule. Being carried directly to the tumor sides, the side effects of such metal-based complexes would be drastically reduced to the minimum.

3/ This research project required a new sulfoxide ligand, DEtSO, not available on the market, so it has been specially prepared for this study. The aliphatic length of the sulfoxide chain influences Pt(II) complexes, so it was interesting to compare with previous studies (6,7,25,26). Reaction of K[Pt(DEtSO)Cl<sub>3</sub>] with pz in stochiometric ratio gave the *trans*-Pt(DEtSO)(pz)Cl<sub>2</sub> complex. With a 2:1 ratio, the *trans*,*trans*-{Pt(DEtSO)Cl<sub>2</sub>}<sub>2</sub>(μ-pz) dimeric compound was obtained, with good purity. These results were confirmed by IR, Raman and multinuclear NMR spectroscopy. Even if *cis* geometry is thermodynamically more stable, both *trans* species do not isomerize in organic solvents. This is in contradiction with what was observed with their pyrimidine analogues (25,26).

4/ All our past attempts to prepare pyrazine complexes with a *cis* geometry were unsuccessful. One exception can be noticed, the monomeric *cis*-Pt(DPrSO)(pz)Cl<sub>2</sub> complex, prepared from the equimolar reaction between K[Pt(DPrSO)Cl<sub>3</sub>] and pyrazine. So, this compound was tested to prepare new dimers. Amongst them, one compound was isolated and characterized, the mixed-geometry *cis,trans*-{Pt(DPrSO)Cl<sub>2</sub>}<sub>2</sub>(μ-pz) dimer. It was obtained from the reaction in chloroform of our *cis* starting material with the ionic K[Pt(DPrSO)Cl<sub>3</sub>] species. A crystal was isolated and X-ray diffraction allowed determination of the structure, permitting confirmation of the results obtained from the multinuclear-NMR and IR analyses (fig. 8). It is the first Pt(II) mixed-geometry compound, but similar mixed complexes could then on be designed.

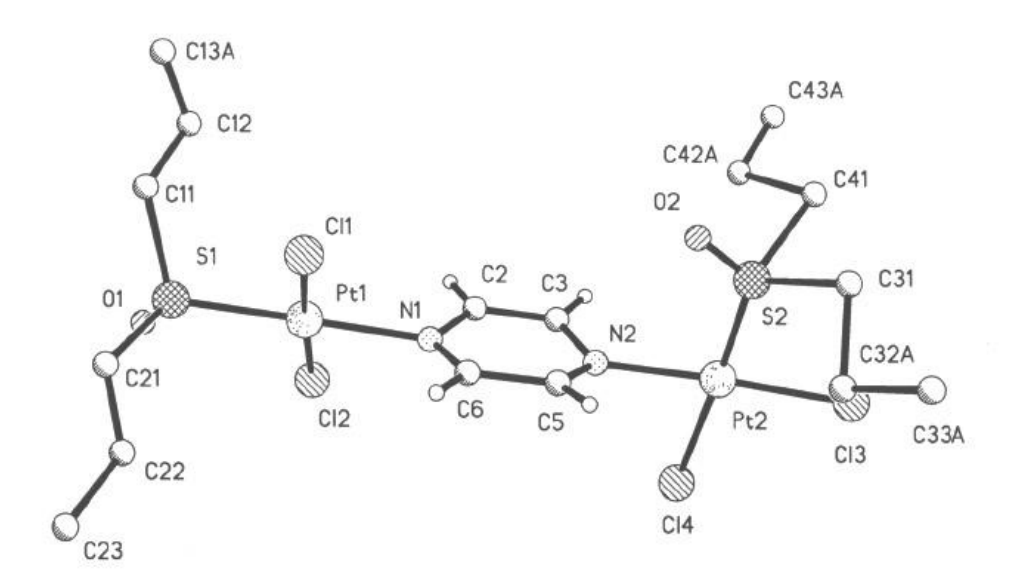


**Figure 8** Sketch of the ORTEP structure of the mixed-geometry dimeric species cis, trans-{Pt(DPrSO)Cl<sub>2</sub>}<sub>2</sub>( $\mu$ -pz). Anisotropic atomic displacement ellipsoids for the non-hydrogen atoms are shown at the 50% probability level.

5/ Complexes of the type cis- and trans-  $Pt(pz)_2X_2$  (X = Cl, I, Br and NO<sub>2</sub>) were formed and characterized by Raman and multinuclear NMR spectroscopy ( ${}^{1}H$ ,  ${}^{13}C$  and  ${}^{195}Pt$ ). The  ${}^{3}J({}^{1}Ha-{}^{195}Pt)$  coupling constants, observed in  ${}^{1}H$  NMR spectroscopy, were particularly useful to account for the compounds geometry. They were measured around 40 and 30 Hz, respectively for the cis and trans compounds.

6/ The {Pt(R<sub>2</sub>SO)I}<sub>2</sub>(μ-I)<sub>2</sub> series was prepared in our laboratory a few years ago (27) and was used as starting material for the synthesis of Pt(R<sub>2</sub>SO)(pz)I<sub>2</sub>. The <sup>195</sup>Pt chemical shift values were found shifted by about 1300ppm in comparison to chloro analogues. The peaks appeared between -4407 and -4356ppm, corresponding well to a [PtNSI<sub>2</sub>] coordination sphere (table 2.3). The analyses of the compounds seem to show their *cis* geometry, but no final statement can be made at this point.

7/ All throughout the project,  $^{195}$ Pt-NMR spectroscopy has been the key tool to monitoring the research line. It is a powerful analytical technique, which encompasses a lot of applications. In this project, it has been widely used to confirm the coordination sphere of prepared complexes, to account for purity and suggest geometry. It was particularly important since many complexes were not very soluble, which was the greatest issue encountered. A large  $\delta(^{195}$ Pt) NMR database was found to be a necessity and we used the summary sketch (table 2.3) we designed on a daily research basis. Our compounds were, moreover, characterized by Raman spectroscopy. There are no Raman data in the literature for Pt(II) compounds containing Pt-pyrazine bonds. The only papers dealing with Raman studies on platinum and the pyrazine ligand do not exhibit any Pt-pz interaction (28).

Transition metals complexes containing electro-attracting ligands can undergo reversible electronic transfers. This is a major research field in metalloenzyme chemistry. However, the electrochemical reduction of Pt(II) complexes is generally a two-electrons irreversible process. But some complexes with pz ligands, and their derivatives, have shown interesting cyclic voltametries, with reversible reductions (2). It was within positive potentials and involved one electron. Thus evaluated, our complexes could show interesting properties in redox chemistry. Our research group could also evaluate the possibility of preparing Pt(II) polymeric complexes, with bridging pz ligands, such as (- $Pt(R_2SO)Cl_{-}(\mu-pz)_n^{n+}$ ,  $(-Pt(R_2SO)Cl_{-}(\mu-Me_2pz)_n^{n+})_n^{n+}$  or  $(-PtCl_2-(\mu-pz)_n^{-})_n^{n+}$ . The method used could be derived from that used for the mixed geometry dimer preparation. The polymeric compounds could bind to DNA in a trans geometry. One of the biggest issues we came across was the low solubility of our products, which did not facilitate their analysis in solution. One way to go around that problem would be to modify the charge. All the complexes of this project, even if they are neutral, could get charged, for instance by the replacement of a halide ligand by an ammine one. The compounds would then be more soluble and their medical administration to be facilitated. As medicines, they could be ingested and not by intravenous injection, as in the case for *cisplatin* and *carboplatin*. Their biological action would be also very different, due to another cellular pharmacology. Targets of ionic complexes are not ovarian, testes, breasts or prostates (hormonal-dependent cancers), but can be intestines or throat, which could extend the action of Pt(II) complexes to the other fields of cancer.

Finally, it would be interesting to really test the biological activity of the novel synthesized complexes. A simple method would be to check their efficiency on murine leukemia, such as P388 and L1210, by the Farrell method (IC<sub>50</sub> test) (29). Their antitumor activity could be tested in cells sensitive to *cisplatin*, but also in other cells, resistant to this latter. Currently, the main problem in chemotherapy is medicinal resistance (30). *Cisplatin* effects seem to diminish with time, pushing medical authorities to increase concentrations administrated to patients, with the negative effects that it implies. The mixed geometry species appears to be a good try since it can bind to DNA from its *cis* unit, and probably show a mode of action similar to *cisplatin*. But it could also connect from its *trans* unit to DNA in a very different way, using interchain binding, and become an interesting candidate for cancers where *cisplatin* is ineffective.

#### References

- A. W. Prestayko, S. T. Crooke et S. K. Carter. Cisplatin Current status and new developments, Eds., Academic Press, New York, 1980.
- (2) A. R. Siedle, K. R. Mann, D. A. Bohling, G. Filipovich, P. E. Toren, F. J. Palensky, R. A. Newmark, R. W. Duerst, W. L. Stebbings, H. E. Mishmash, K. Melancon. *Inorg. Chem.* 1985, 24, 2216.
- (3) S. Komeda, G. V. Kalayda, M. Lutz, A. L. Spek, Y. Yamanaka, T. Sato, M. Chikuma, J. Reedjik. J. Med. Chem. 2003, 46, 1210.
- (4) P. S. Hall, D. A. Thornton, G. A. Foulds. Polyhedron. **1987**, *6*, 85.
- (5) A. Albinati, F. Isaia, W. Kaufmann, C. Sorato et L. M. Venanzi. Inorg. Chem. 1989, 28, 1112.
- (6) Priqueler, J.R.L.; Rochon, F.D. Inorg. Chim. Acta. 2004, 357, 2167.
- (7) Priqueler, J.R.L.; Rochon, F.D. Can. J. Chem. **2004**, 82, 649.
- (8) A. Pawlukojć, L. Sobczyk, M. Prager, G. Bator, E. Grech, J. Nowicka-Scheibe. J. Mol. Struct. 2008, 892, 261.
- (9) M. Prager, W. Sawka-Dobrowolska, L. Sobczyk, A. Pawlukojć, E. Grech, A. Wischnewski, M. Zamponi. *Chem. Phys.* 2007, 332, 1.
- (10) Y. Chen, R.E. Shepherd. *Inorg. Chim. Acta.* **1998**, 268, 279.
- (11) J.M. Gilaberte, C. López, S. Alvarez. J. Organometall. Chem. 1988, 342, C13.
- (12) S.J. Miles, J.D. Wilkins. J. Inorg. Nucl. Chem. **1975**, 37, 2271.
- (13) Y.-C. Tsai, C.C. Cummins. *Inorg. Chim. Acta.* **2003**, *345*, 63.
- (14) T.W. Stringfield, Y. Chen, R.E. Shepherd. *Inorg. Chim. Acta.* **1999**, 285, 157.

- (15) F. Peral, E. Gallego. Spectrochim. Acta A: Mol. Biomol. Spect. 2003, 59, 1223.
- (16) N. Begum, A.C. Ghosh, S.E. Kabir, G. Hossain. *Polyhedron.* **2005**, *24*, 3074.
- (17) D.R. Martin, C.M. Merkel, C.B. Drake, J.U. Mondal, J.B. Iwamoto. *Inorg. Chim. Acta.* 1985, 97, 189.
- (18) J.M. de la Rosa Arranz, F.J. González-Vila, E. López-Capel, D.A.C. Manning, H. Knicker, J.A. González-Pérez. J. Anal. Appl. Pyrolysis. 2009, 85, 399.
- (19) D.R. Martin, C.M. Merkel, J.U. Mondal, C.R. Rushing Jr. *Inorg. Chim. Acta.* 1985, 99, 81.
- (20) J.W. Wheeler, J. Avery, O. Olubajo, M.T. Shamin, C.B. Storm, R.M. Duffield. *Tetrahedron.* **1982**, *38*, 1939.
- (21) A.H. Shipar. Food Chem. 2006, 98, 403.
- (22) H. Kuramoto, M. Inoue, S. Emori, S. Sugiyama. *Inorg. Chim. Acta.* **1979**, *32*, 209.
- (23) M.A.M. Abu-Youssef, V. Langer, L. Öhrstrom. Dalton Trans. 2006, 2542.
- (24) U. Eiermann, C. Krieger, F.A. Neugebauer, H.A. Staab. *Tetrahedron Lett.* **1988**, 29, 3655.
- (25) N. Nédélec, F. D. Rochon. *Inorg. Chim. Acta.* **2001**, *319*, 95.
- (26) N. Nédélec, F. D. Rochon. *Inorg. Chem.* **2001**, 40, 5236.
- (27) N. Nédélec, G. Masserweh, F.D. Rochon. *Inorg. Chim. Acta.* **2003**, 346, 197.
- (28) J. Electroanal. Chem. **1991**, 319, 71. Angew. Chem. Int. Ed. **2005**, 44, 4069.
- (29) N. Farrell, L. R. Kelland, J. D. Roberts, M. van Beusichem. *Cancer Res.* 1992, 52, 5065.
- (30) E. L. M. Lempers, J. Reedijk. J. Adv. Inorg. Chem. 1992, 37, 175.